AD-A111 391 ILLINOIS UNIV AT URBANA F/G 13/2
FUNDAMENTAL STUDY ON THE OZONE POSTTREATMENT OF REVERSE OSMOSIS--ETC(U)
MAR 81 E S CHIAN, P P KUO, B J CHANG DAMD17-75-C-5006
UNCLASSIFIED NL

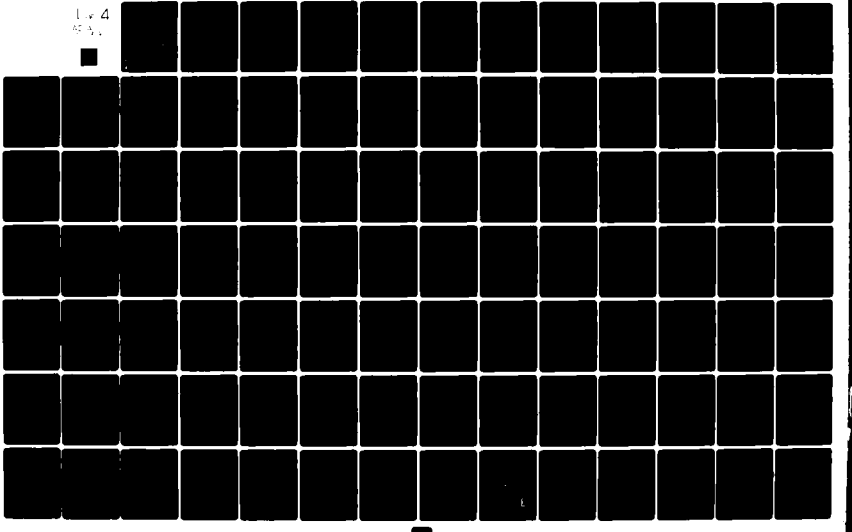

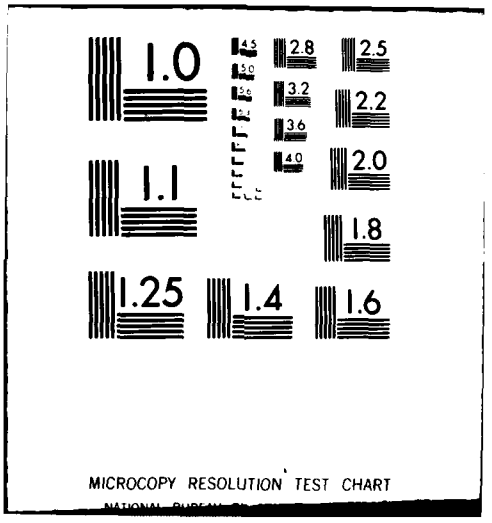
1.0
1.1
1.25
1.4
1.6
1.8
2.0
2.2
2.5
2.8
3.2
3.6
4.0
MICROCOPY RESOLUTION TEST CHART

ADA111391

AD _____

FUNDAMENTAL STUDY ON THE OZONE POSTTREATMENT OF REVERSE OSMOSIS PERMEATES FROM ARMY WASTEWATERS

FINAL REPORT

Edward S.K. Chian[1]

Powell P.K. Kuo

Bei J. Chang

MARCH 1981

Supported by
US ARMY MEDICAL RESEARCH AND DEVELOPMENT COMMAND
Fort Detrick, Frederick, MD 21701

Contract No. DAMD 17-75-C-5006

University of Illinois
Urbana, IL 61801

DTIC
ELECTE
FEB 26 1982
S D
A

Project Officer: William J. Cooper
Environmental Protection Research Division
US Army Medical Bioengineering
Research and Development Laboratory
Fort Detrick, Frederick, MD 21701

Approved for Public Release; Distribution Unlimited

The findings in this report are not to be construed as an official Department of the Army position unless so designated by other authorized documents.

[1]Principal Investigator
Current Affiliation:
Georgia Institute of Technology
Atlanta, Georgia 30332
(404) 894-2265

DTIC FILE COPY

UNCLASSIFIED

SECURITY CLASSIFICATION OF THIS PAGE *(When Data Entered)*

REPORT DOCUMENTATION PAGE		READ INSTRUCTIONS BEFORE COMPLETING FORM
1. REPORT NUMBER	2. GOVT ACCESSION NO. AD-A111 391	3. RECIPIENT'S CATALOG NUMBER
4. TITLE *(and Subtitle)* FUNDAMENTAL STUDY ON THE OZONE POSTTREATMENT OF REVERSE OSMOSIS PERMEATES FROM ARMY WASTEWATERS		5. TYPE OF REPORT & PERIOD COVERED Final Report Sep 1974 - Aug 1977
		6. PERFORMING ORG. REPORT NUMBER
7. AUTHOR(s) Edward S.K. Chian, Sc.D. Powell P.K. Kuo, Ph.D. Bei J. Chang, Ph.D.		8. CONTRACT OR GRANT NUMBER(s) DAMD 17-75-C-5006
9. PERFORMING ORGANIZATION NAME AND ADDRESS University of Illincis Urbana, Illinois 61801		10. PROGRAM ELEMENT, PROJECT, TASK AREA & WORK UNIT NUMBERS 62720A.3E162720A835.00.019
11. CONTROLLING OFFICE NAME AND ADDRESS US Army Medical Research and Development Command ATTN: SGRD-RMS Fort Detrick, Frederick, MD 21701		12. REPORT DATE March 1981
		13. NUMBER OF PAGES 316
14. MONITORING AGENCY NAME & ADDRESS*(if different from Controlling Office)*		15. SECURITY CLASS. *(of this report)* UNCLASSIFIED
		15a. DECLASSIFICATION/DOWNGRADING SCHEDULE

16. DISTRIBUTION STATEMENT *(of this Report)*

Approved for public release; distribution unlimited.

17. DISTRIBUTION STATEMENT *(of the abstract entered in Block 20, if different from Report)*

18. SUPPLEMENTARY NOTES

19. KEY WORDS *(Continue on reverse side if necessary and identify by block number)*

Analysis of purgeable organics
Analysis of trace organics
Organic analysis
Ozonation
Ozone contactor
Scale-up
Water reuse

20. ABSTRACT *(Continue on reverse side if necessary and identify by block number)*

The ozonation process is demonstrated to be an effective means to remove trace amounts of organics that pass through the reverse osmosis (RO) process. The kinetics and the mechanism of the ozonation process have been studied to improve removal of these compounds from RO permeates. An extensive effort was made to develop methodologies for the analysis of trace organics in RO permeates as well as for the intermediates formed during ozonation of RO permeate. This involved the use of distillation, head space, and purge and trap methods

DD FORM 1 JAN 73 1473 EDITION OF 1 NOV 65 IS OBSOLETE

UNCLASSIFIED

SECURITY CLASSIFICATION OF THIS PAGE *(When Data Entered)*

20. Abstract (continued)

for the concentration of volatile organic constituents and of the solvent extraction method for the concentration of intermediately volatile (i.e., GC volatile) and nonvolatile organics. Gas chromatography (GC) was used to determine the volatile and intermediately volatile compounds, whereas high pressure liquid chromatography (HPLC) was used for the nonvolatile compounds.

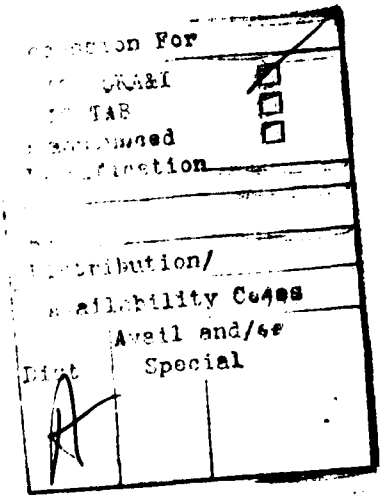

DTIC
COPY
INSPECTED

EXECUTIVE SUMMARY

The ozonation process is demonstrated to be an effective means of removing trace amounts of organics that pass through the reverse osmosis (RO) process. The kinetics and the mechanism of the ozonation process have been studied to improve removal of these compounds from RO permeates. An extensive effort was made to develop methodologies for the analysis of trace organics in RO permeates as well as for the intermediates formed during ozonation of RO permeate. This involved the use of distillation, headspace, and purge and trap methods for the concentration of volatile organic constituents and of the solvent extraction method for the concentration of intermediately volatile (i.e., GC volatile) and nonvolatile organics. Gas chromatography (GC) was used to determine the volatile and intermediately volatile compounds, whereas high pressure liquid chromatography (HPLC) was used for the nonvolatile compounds.

It was found that the organics from synthetic hospital wastewater passing through the reverse osmosis consisted mainly of the low molecular-weight volatile polar organics, such as methanol, ethanol, propanols, acetic and propionic acids, acetone, methyl ethyl ketone, and diether ether. The distillation method in conjunction with the headspace/GC analysis was found to be most effective in analyzing these compounds at ppb levels. The less volatile compounds in RO permeates are mainly phenolics, whereas the nonvolatile ones are N,N-diethyl-m-toluamide and o-toluidine.

Ozonation and ultraviolet (UV) light-catalyzed ozonation of the above compounds were conducted. Formic and oxalic acids were the major intermediates resulting from ozonation of most of the organic compounds tested. These intermediates were removed effectively by ozone in the presence of UV irradiation. In general, under favorable conditions of pH for ozonation of RO permeates, the rates of mass transfer of ozone controlled the initial rate of organic removal and the chemical-rate limitation governed the rate of removal of the resulting intermediates. When UV irradiation was employed after the initial phase of high rate of total organic carbon (TOC) removal, the TOC in ozonated effluents was reduced to less than 3 to 5 mg/L within 1 to 2 hours with hospital RO permeates. Because of the highly oxygenated state of the resulting intermediates, such as formic and oxalic acids, the chemical oxygen demand (COD) to TOC ratios are very close to unity. As such, the ozonated effluents with UV irradiation meet the requirement of less than 5 mg/L of COD for the Medical Unit, Self-contained, Transportable (MUST) hospital water purification system for potable purposes.

The success of using the ozone/UV process to reduce gross organics in the RO permeates prompted our investigation of methods for the scale-up of ozone-sparged vessels. Since it represented the bulk of the organics present in RO permeates, methanol was used as the model compound in the scale-up study. The scale-up method based on the mathematical model developed in this study accurately predicts the superficial gas velocity and the gas phase ozone concentration required for a large vessel to achieve the same level of TOC removal obtained in a small vessel. The vessel configurations under study included a circular and a rectangular cross section. The latter involved a single-stage modified Torricelli ozone contactor.

FOREWORD

Citation of trade names in this report does not constitute an official Department of the Army endorsement or approval of the use of such items.

TABLE OF CONTENTS

EXECUTIVE SUMMARY.....1

FOREWORD.....2

INTRODUCTION.....11

REMOVAL OF ORGANIC MATTER IN RO PERMEATES OF MUST WASTEWATERS.....12

Ozonation of RO Permeates After Pretreatment by Sorptive Processes.....13
Preliminary Evaluation of Activated Carbon and Ion-Exchange Sorptive Processes.....17
Mechanism of Organic Removal by Ozonation.....21
Biological Pretreatment of MUST Wastes.....31

ORGANIC ANALYSIS.....38

Literature Review.....38
Freeze Concentration.....38
Carbon Adsorption.....39
Resin Adsorption.....39
Solvent Extraction.....40
Gas Stripping Technique.....40
High Pressure Liquid Chromatography.....41
Determination of Volatile Organics.....43
Determination of Nonvolatile Organics.....44
Determination of Carboxylic Acids.....45
General.....46
Development of a Distillation Technique for Determining Volatile Organics in RO Permeates.....48
Preliminary Evaluation of Distillation Technique.....49
Concentration of Trace Low Molecular-Weight Volatile Polar Organics in Water by Distillation Method.....51
Determination of Volatile Polar Organics in RO Composite Permeates.....63
Experimental.....69
Results and Discussion.....70
Summary.....73
Determination of Acetic Acid.....74
Distillation of Acetic Acid.....74
Concentration of Acetic Acid with Evaporation Technique.....75
Determination of Acetic Acid in RO Permeate.....75
Evaluation of Headspace Gas Stripping Technique.....76
Evaluation of Bellar's Stripping Technique.....99
Determination of Volatile Organics in RO Permeates.....112
Identification of Volatile Organics by GC/MS.....112
Determination of Nonvolatile Organics by HPLC.....125
Evaluation of Solvent Extraction Technique for Determining Nonvolatile Organics.....132
Solvent Extraction of Phenolic Compounds.....132
Solvent Extraction of o-Toluidine and N,N-Diethyl-m-Toluamide.....137
Determination of Nonvolatile Organics in RO Composite Permeates....139
Summary of Organic Analyses.....142

DETERMINATION OF GLYOXAL, METHYLGLYOXAL, AND DIMETHYLGLYOXAL BY GAS CHROMATOGRAPHY.....144

DETERMINATION OF PYRUVIC AND GLYOXYLIC ACIDS.....146

OZONATION OF MODEL COMPOUNDS.....147

Literature Review.....147
Introduction.....149
Ozonation and UV-Ozonation of 1-Propanol.....151
Ozonation and UV-Ozonation of Propionic Acid.....151
Ozonation and UV-Ozonation of 2-Propanol.....151
Ozonation and UV-Ozonation of Methyl Ethyl Ketone.....161
Ozonation and UV-Ozonation of Acetic Acid.....168
Ozonation and UV-Ozonation of Diethyl Ether.....168
Ozonation and UV-Ozonation of o-Toluidine.....173
Ozonation and UV-Ozonation of Methanol.....183
Ozonation and UV-Ozonation of N,N-Diethyl-m-Toluamide.....183
Summary.....188

OZONATION AND UV-OZONATION OF OXALIC ACID AND pH EFFECT.....191

OZONATION AND CHLORINATION OF ULTRAFILTRATION AND REVERSE OSMOSIS RETENTATES OF SECONDARY EFFLUENT.....196

Introduction.....196
Experimental.....196
Results and Discussion.....197
Ozonation and Chlorination of UF and RO Retentates of Secondary Effluent.....197
Application of Ozonation in Drinking Water Treatment.....201

ULTRAVIOLET-OZONATION OF COMPOSITE REVERSE OSMOSIS PERMEATE.....203

Ultraviolet-Ozonation of Mixture of Methanol and Acetone.....203
UV-Ozonation of Composite RO Permeate.....205

SCALE-UP OF OZONE-SPARGED VESSELS.....205

Introduction.....205
Literature Search.....207
Mass Transfer Characteristics of Gas-Sparged Vessels.....207
Mixing in Gas-Sparged Vessels.....216
Ozone Absorption and Simultaneous Chemical Reactions.....217
Mass Transfer Characteristics of Agitated Vessels.....222
Objectives.....223
Scope of Work.....224
Materials and Methods.....225
Evaluation of Diffuser Materials.....225
Kinetics of Ozonation of Methanol and Its Degradation Products in Aqueous Solution.....227
Mathematical Model for Ozone-Sparged Vessel.....230
Effect of Operational Variables on Performance of Ozone-Sparged Vessel.....234

Scaling-Up of Ozone-Sparged Vessel.....234
Comparison of Ozone-Sparged Vessel with Agitated Vessel.....235

RESULTS AND DISCUSSIONS.....235

Evaluation of Diffuser Materials.....235
Kinetics of Ozonation of Methanol and Its Degradation Products in Aqueous Solution.....237
Mathematical Model for Ozone-Sparged Vessel.....245
Effect of Operational Variables on Performance of Ozone-Sparged Vessel.....258
Scaling-Up of Ozone-Sparged Vessel.....265
Comparison of Ozone-Sparged Vessel with Agitated Vessel.....265

ENGINEERING SIGNIFICANCE.....270

CONCLUSIONS.....271

NOMENCLATURE.....275

RECOMMENDATIONS.....279

REFERENCES.....280

DISTRIBUTION LIST.....319

APPENDIXES

A. List of Publications.....293
B. GC Chromatographs.....295
C. GC Septum Cooler.....303
D. Computer Program for Computations of Kinetics of Semi-Batch Ozonation of Methanol and its Degradation Products.....307
E. Computer Program for Solving Mathematical Models for Ozone-Sparged Vessel Treating an Aqueous Methanol Solution.....311
F. Computer Program for Computations of Concentrations and Concentration Gradients of Ozone and TOC in the Liquid Film.....315

FIGURES

1. Oxygen Stripping for Ethanol in Distilled Water at 30°C and 50°C.....22
2. Log Plot of Oxygen Stripping for Ethanol in Distilled Water at 30°C and 50°C.....24
3. Oxygen Stripping and Ozonation of Permeate of Laboratory Waste.....25
4. Log Plot of Ozonation of RO Permeate of Laboratory Waste after Correction for Stripping Effect.....26
5. Semi-Log Plot of Oxygen Stripping and Ozonation of Permeate of Laboratory Waste.....27
6. Semi-Log Plot of Ozonation of Permeate of Laboratory Waste after Correction for Stripping Effect.....28
7. Oxygen Stripping and Ozonation of Permeate of Hospital Composite.....29

8. Semi-Log Plot of Ozonation of Permeate of Hospital Composite after Correction for Stripping Effect.....30
9. pH Variation of Hospital Composite RO Permeate During Course of Oxygen Stripping and Ozonation.....32
10. Experimental Protocol on Biological Pretreatment of MUST Wastewater Followed by UF-RO-O_3 Runs.....33
11. UV-Ozonation of Composite RO Permeates With or Without (Control) Biological Pretreatment.....37
12. Relation of Concentration of Low Molecular-Weight Volatile Polar Organic Compounds in Distillate and Sample Volume.....55
13. Concentration Profile of Low Molecular-Weight Volatile Polar Organic Compounds in Successively Collected Distillates.....59
14. Headspace Gas Chromatogram of Distillate from 0.08 mg/L Standard Mixture of Volatile Compounds.....72
15. Removal of Organic Matter by Stripping.....79
16. Effect of Stripping Temperature on Removal of 3-Pentanone and Adsorption Efficiency of Tenax-GC Precolumns.....82
17. Effect of Stripping Temperature on Removal of Butanal and Adsorption Efficiency of Tenax-GC Precolumns.....83
18. Effect of Stripping Temperature on Removal of Ethanol and Adsorption Efficiency of Tenax-GC Precolumns.....84
19. Conventional Gas Scrubber (Bubbler 1).....86
20. Stripping Bubbler (Bubbler 2).....87
21. Stripping Flask.....88
22. Stripping Apparatus.....89
23. Stripping Time Profile at Different Helium Flow Rates for n-Butanol.....90
24. Stripping Efficiency at Different Helium Flow Rates for n-Butanol.....91
25. Stripping Time Profile for Three Different Stripping Vessels.....92
26. Diagram of 4-Way Valve Gas Injection System for GC Injection.....94
27. GC Chromatogram of n-Butanol Obtained by Use of 4-Way Valve Injection System.....95
28. Dimension of Bellar's Purging Device.....100
29. Desorber.....104
30. Block Diagram of Gas Chromatographic Injection System.....106
31. Mass Chromatogram of Acetone Solution.....116
32. Mass Spectrum of Acetone Peak.....117
33. Mass Chromatogram of Ethanol Solution Spiked with Acetone.....118
34. Mass Spectrum of Methanol Peak.....119
35. Mass Spectrum of Acetone Peak.....120
36. Mass Chromatogram of Simulated Unknown.....121
37. Mass Spectrum of Second Peak Appearing in Figure 35.....122
38. Mass Spectrum of Third Peak Appearing in Figure 35.....123
39. Peak Area Ratio Calibration Curves for o-Toluidine and N,N-Diethyl-m-Toluamide.....129
40. Peak Height Ratio Calibration Curves for o-Toluidine and N,N-Diethyl-m-Toluamide.....130
41. Calibration Curves for o-Toluidine and N,N-Diethyl-m-toluamide.....133
42. LC Chromatograms of 1x Composite RO Permeate after Treatment Extraction and Concentration, and Its Spiked Solution.....134
43. Gas Chromatogram of K-D Concentrate Obtained from a 100 mg/L Standard Aqueous Mixture of Glyoxal, Methylglyoxal, and Dimethylglyoxal after Their Reaction with o-Phenylenediamine Followed by Benzene Extraction and K-D Evaporation.....145

44. Ozonation of 1-Propanol.....152
45. Yields of Ozonation Products from 1-Propanol.....153
46. UV-Ozonation of 1-Propanol.....154
47. Yields of UV-Ozonation Products from 1-Propanol.....155
48. Ozonation of Propionic Acid.....156
49. UV-Ozonation of Propionic Acid.....157
50. Percent Carbon Contributed by Propionic Acid in Ozonated Propionic Acid Solution.....158
51. Removal of 1-Propanol by Ozonation.....159
52. Removal of Propionic Acid by Ozonation.....160
53. Ozonation of 2-Propanol.....162
54. UV-Ozonation of 2-Propanol.....163
55. Oxygen Stripping of 2-Propanol.....165
56. Ozonation of Methyl Ethyl Ketone.....166
57. UV-Ozonation of Methyl Ethyl Ketone.....167
58. Ozonation of Sodium Acetate.....169
59. UV-Ozonation of Sodium Acetate.....170
60. Observed TOC and Calculated TOC in UV-Ozonation of Sodium Acetate.....171
61. Ozonation of Diethyl Ether.....172
62. Observed TOC and Calculated TOC in Ozonation of Diethyl Ether.....175
63. UV-Ozonation of Diethyl Ether.....176
64. Observed TOC and Calculated TOC in UV-Ozonation of Diethyl Ether.....178
65. Ozonation of o-Toluidine.....179
66. UV-Ozonation of o-Toluidine.....181
67. Ozonation of Methanol.....184
68. UV-Ozonation of Methanol.....185
69. Ozonation of N,N-Diethyl-m-Toluamide.....186
70. UV-Ozonation of N,N-Diethyl-m-Toluamide.....187
71. UV-Ozonation of Oxalic Acid.....192
72. UV-Ozonation of Oxalic Acid.....193
73. Inorganic Carbon in Reaction.....195
74. Reconstructed Gas Chromatogram of Chlorinated RO Retentate Stored for 7 Days.....199
75. Reconstructed Gas Chromatogram of Nonchlorinated RO Retentate Stored for 7 Days (Control).....200
76. UV-Ozonation of Mixture of Methanol and Acetone.....204
77. Schematic of Torricelli Ozone Contactor.....206
78. Variation of First-Order (K_1) and Second-Order (K_2) Reaction Rate Constants Calculated from COD Data for Lime-Clarified Raw Wastewater at a pH of 9.0±0.3.....220
79. Ozone Decomposition as Function of Time.....239
80. Determination of Reaction Order with Respect to Ozone for Ozone-Methanol Reaction.....240
81. Determination of Reaction Order with Respect to Methanol.....241
82. Determination of Reaction Order with Respect to Oozne for Ozone-Formaldehyde Reaction.....242
83. Determination of Reaction Order with Respect to Formaldehyde.....243
84. Semi-Batch Ozonation of Formic Acid in Aqueous Solution.....244
85. Semi-Batch Ozonation of Methanol in Aqueous Solution.....246
86. Response to Step-Tracer Input.....247
87. Response to Pulse-Tracer Input.....248
88. Determination of Steady State.....250
89. Percent TOC Removal vs. Methanol Concentration in Feed.....251
90. Percent Ozone Absorption vs. Methanol Concentration in Feed.....252

91. Dissolved Ozone vs. Methanol Concentration in Feed.....253
92. Performance of 22.09-Liter Vessel.....254
93. Percent TOC Removal vs. Partial Pressure of Ozone.....259
94. Percent Ozone Absorption vs. Partial Pressure of Ozone.....260
95. Overall Mass Transfer Coefficient vs. Superficial Gas Velocity.....261
96. Percent TOC Removal vs. Superficial Gas Velocity.....262
97. Percent Ozone Absorption vs. Superficial Gas Velocity.....263
98. Predicted Effect of Liquid Residence Time on Performance of Sparged Vessel.....264
99. Percent TOC Removal vs. Impeller Speed for Agitated Vessel.....269

TABLES

1. Ozonation of MUST RO Permeates.....14
2. Ozonation of MUST RO Permeates, Variations of TOC and pH.....15
3. TOC Removal by Activated Carbon and Ion-Exchange Pretreatments.....16
4. Composition of Laundry Waste Type II.....18
5. Composition of Shower Waste.....18
6. Composition of Laboratory Waste.....19
7. Composition of Composite Waste.....20
8. Effect of Biological Pretreatment of Composite Waste on Performance of Membrane Processes.....35
9. Concentrations of Methanol and Ethanol in RO Permeates of Wastewaters.....48
10. Recovery of Volatiles by Distillation Technique.....50
11. Concentration of Volatile Polar Organic Compounds in First 10 mL of Distillate.....54
12. Relative Volatility of Volatile Polar Organic Compounds in Dilute Aqueous Solution.....56
13. Two-Stage Distillation.....58
14. Effect of Salting Out.....61
15. Identification of RO Permeates Analyzed for Volatile Compounds by Distillation/GC Technique.....64
16. Concentration Factors of Model Compounds.....65
17. Concentration of Volatile Organic Compounds in MUST Hospital RO Permeates.....66
18. Percent TOC of Identified Compounds in RO Permeates and in Their Distillates Using Volatile Organic Analysis.....67
19. Concentrations of Volatile Compounds Determined in RO Permeates.....68
20. Quantitative Analyses of MUST Hospital Synthetic Wastewater Samples by DHGC Technique.....73
21. Distillation of 100 mL of 200 µL/L Acetic Acid.....74
22. Concentration of Acetic Acid by Evaporation Technique.....76
23. Stripping Efficiency for Model Compounds.....78
24. Stripping of MUST Wastewaters.....80
25. Characteristics of GC Packings Used as Adsorption Material in Stripping Method.....96
26. Adsorption and Desorption Efficiency of n-Butanol with Three Different Adsorbents.....97
27. Comparison of Stripping Efficiencies of Several Model Compounds with Large Stripping Flask and Bellar and Lichtenberg Apparatus at Room Temperature.....101

28. Stripping of Volatile Polar Water-Soluble Organics with Bellar and Lichtenberg Apparatus at Room and Elevated Temperatures.....102
29. Components of Gas Chromatographic Injection System.....107
30. Adsorption and Desorption Efficiencies for Model Compounds.....109
31. Concentrations of Volatile Polar Water-Soluble Organics Determined in RO Permeates.....113
32. Concentrations of Volatile Nonpolar Water-Insoluble Organics Determined in RO Permeates.....114
33. Identification of Ethanol and Acetone by Comparing Mass Ion Intensity Ratio of Major M/E Species.....124
34. Volatile Organics Identified by GC/MS.....125
35. Separation of o-Toluidine, p-Toluidine, and N,N-Diethyl-m-Toluamide by Liquid Chromatography.....127
36. Results of Qualitative and Quantitative Study on o-Toluidine and N,N-Diethyl-m-Toluamide with Methyl Benzoate as the Internal Standard.....128
37. Retention Time and Relative Retention Time of o-Toluidine and N,N-Diethyl-m-Toluamide.....135
38. Extraction and K-D Concentration Efficiencies for Phenolic Compounds.....136
39. Percent Recoveries of Phenolic Compounds by Different Extraction/Concentration Methods.....138
40. Extraction and K-D Concentration Efficiencies for Methyl Benzoate, o-Toluidine, and N,N-Diethyl-m-Toluamide.....139
41. Extraction and Concentration Procedures.....140
42. Concentrations of Nonvolatile Organics Identified in RO Permeates.....141
43. TOC and Percent TOC of Accounted Organics.....143
44. Concentration of Determined Organic Compounds in UV-Ozonated Acetone Mixtures.....164
45. Degradation Products Other than Ethyl Acetate and Acetate in Ozonation of Diethyl Ether.....174
46. Degradation Products Other than Ethyl Acetate, Acetate, and Oxalate in UV-Ozonation of Diethyl Ether.....177
47. Glyoxylate in Ozonation and UV-Ozonation of o-Toluidine.....180
48. Nitrate-Nitrogen in Ozonation and UV-Ozonation of o-Toluidine.....182
49. Ozonation Products.....189
50. Organic Removal by Ozonation.....190
51. Organic Removal by Ozonation and UV-Ozonation of Oxalic Acid at Various pH.....194
52. Chlorination of UF and RO Retentates Upon Storage.....198
53. Concentrations of Volatile Halogenated Organics in Chlorinated UF and RO Retentates.....198
54. Summary of Research on Ozone Decomposition in Water.....218
55. Comparison of Absolute Method and Iodometric Method.....236
56. Comparison of Fritted Gas-Washing Bottle and Dreschel Gas-Washing Bottle Using Iodometric Method.....237
57. Results of Evaluation of Stainless Steel, Teflon, and Fused Alumina Diffusers at High Ozone Concentration.....238
58. Concentration Profiles and Gradients of Dissolved Ozone and TOC in Liquid Film.....255
59. Comparison of $K_L\alpha$ Determined from Experiment and Correlations.....257
60. Computer Code Used to Calculate Required Superficial Gas Velocity in Large Ozone-Sparged Vessel Treating Methanol Solution.....266
61. Computer Code for Scale-Up of Ozone-Sparged Vessel.....272

INTRODUCTION

The U.S. Army is interested in having the capability to use direct recycled and reused wastewater for both field and fixed installations. Reuse of wastewater under combat conditions provides greater tactical flexibility and reduces the logistical burden of hauling water. Offsetting water shortages and pollution abatement are the principal driving forces for reuse at fixed installations. The U.S. Army Medical Research and Development Command has research contracts addressing these two objectives underway at various research facilities.

These studies involve the development of a mission-oriented medical treatment system known as the Medical Unit, Self-Contained, Transportable (MUST) program. The basic requirements for the MUST hospital unit specify that all waste materials generated therein be rendered inert or nontoxic prior to disposal. The ultimate goal for the MUST hospital system is to comply with the zero discharge of pollutants by 1985 called for by the U.S. Water Quality Act Amendments of 1972 (PL-92-500). Therefore, a prototype water and waste management system was developed for the MUST hospital, composed of three principal elements: a utility room, a water processing element, and a mobile incinerator. The emphasis of this study is on the water processing element.

The water processing element consists of a water treatment unit (WTU) and a water purification unit (WPU). This element is designed to treat all wastewaters, such as from the kitchen, laboratory, shower, operating room, and X-ray wastes, generated within the functional areas of the hospital. However, treatment of human wastes will not be included in these units. A portable incinerator attached to the toilet unit is used solely for the disposal of human wastes. The WTU and WPU are each housed in a specially modified MUST service ward container that can be transported by standard cargo trucks, external helicopter loads, or railroad, ship, or cargo aircraft. These units can be operated independently or in combination.

The requirements of WTU are to provide surge capacity for continued operation during periods of low waste input and for stabilizing the chemical and physical characteristics prior to treatment, and to produce an effluent free from biological contamination as well as turbidity or suspended solids. Raw wastes discharged by the hospital are first treated by the WTU. Its effluent may be discharged directly into receiving streams or pumped to the WPU for further treatment. Normally the WPU is used to produce a water of potable quality from the WTU effluent. However, it also has the capability to produce a potable water from a brackish water source.

The design criteria for the WPU are such that it should be capable of processing MUST wastewaters after treatment by WTU, except human wastes from the toilet sanitizer function, and clarified fresh or desalted brackish water as obtained from natural sources for potable purposes. The

PRECEDING PAGE BLANK-NOT FILMED

potable water produced by WPU must meet the water quality standards established by the responsible Surgeon General in terms of both chemical and bacteriological characteristics. A residual chlorine content of not less than 4 mg/L is also required. Whereas the maximum concentrations of heavy metals in potable water are comparable to that of the U.S. drinking water standards, the maximum total dissolved solids (TDS) and chemical oxygen demand (COD) are 1,500 and 5 mg/L, respectively.

The latest water processing element consists of a WTU utilizing membrane ultrafiltration for suspended solids removal and a WPU utilizing reverse osmosis (RO) for TDS and organic removals and ozonation for final polishing of organics. The purpose of this study was to conduct a fundamental study on the kinetics, mechanisms, and scale-up of the ozonation process to improve removal of the trace amount of organics that pass through the reverse osmosis system. In addition, an extensive effort was made to develop methodologies for the analysis of trace organics resulting from both MUST hospital wastewaters and ozone degradation products. It is anticipated that the results obtained from a complete analysis of ozonated effluent would aid in assessing the suitability of the ozone-polished water for potable purposes.

REMOVAL OF ORGANIC MATTER IN RO PERMEATES OF MUST WASTEWATERS

An investigation was conducted to study the removal of organic matter in MUST hospital wastewaters after the reverse osmosis process followed by treatment with ozone, activated carbon, and ion-exchange resins. Biological pretreatment of MUST wastes in the stabilization tank was investigated for possible reduction of the gross organic loading to the ozonation process. In general, the entire study consisted of: (1) ozonation of RO permeates of MUST wastewaters, pretreated with sorptive processes; (2) treatment of ozonated RO permeates with sorptive processes; (3) understanding of the mechanism of organic removal by ozonation; and (4) biological pretreatment of MUST wastes followed by membrane and ozonation processes.

It was found that pretreatment of RO permeates with activated carbon enhanced total organic carbon (TOC) removal upon ozonation, whereas ion-exchange pretreatment had little or no effect. Separate studies revealed that organic removals from different RO permeates of MUST wastes were less than 20% with either of the two sorptive processes. However, the removal of organics with these sorptive processes was enhanced when the RO permeates were pretreated by ozone. This was especially true with the MUST shower wastewater. In the case of RO permeate of composite waste, the enhancement was observed only for the ion-exchange process. During the ozonation process, removal of organics was attributed to both oxidation and stripping in the early stages. However, in the later stage, TOC removal was mainly due to the stripping effect, which tapered off asymptotically. It was concluded that the advantage of using biological pretreatment of MUST wastewaters to reduce the power requirements for the ozonation step might be offset by the additional power requirement for the membrane ultrafiltration process due to resulting poor membrane flux.

Ozonation of RO Permeates After Pretreatment by Sorptive Processes

Preliminary studies on the removal of organics with ozonation were carried out. RO permeates of MUST hospital composite, shower, and laboratory wastewaters, with or without pretreatment with activated carbon and ion-exchange sorptive processes, were evaluated.

Pretreatment with sorptive processes was conducted in packed columns. The activated carbon and ion-exchange resins used were granular Filtrasorb 400, 40/48 mesh (Calgon, Pittsburgh, PA) and weak base Duolite A-7 resins, 40/80 mesh (Diamond Shamrock, Redwood City, CA), respectively. The ozone generator was a Welsbach T-408 ozonator (Welsbach, Philadelphia, PA). Two liters of permeates were ozonated in a batch reactor at 25°C and an initial pH of 7.0. The entire ozonation period was 2 hours. TOC was determined by a Beckman Model 915 TOC Analyzer (Fullerton, CA) having a detection limit of about 4 to 5 ppm of TOC.

Table 1 shows the results of these studies. The final TOC, percent removal of TOC, and the TOC removal constant (k1) with the ozonation process are listed in the fourth, fifth, and seventh columns, respectively. In all three cases, activated carbon pretreatment enhances the final TOC removal as well as the removal rate constant, while ion-exchange pretreatment has little or no effect on the total percent removal of TOC. It is also noted that laboratory RO permeates (prepared according to Table 6) are the most reactive to ozonation in terms of total percentage of TOC removal or TOC removal rate constant. Table 2 lists the changes of TOC and pH of the RO permeates during the 2-hour ozonation. The results of TOC removal and pH of the ozonated effluents are shown in Tables 1 and 2.

It can be concluded that the rate of TOC removal is enhanced when solution has a higher value of pH. This pH effect is supported by the theories of Hewes and Davison (1971) and Stumm (1958). They proposed that the decomposition rate of ozone in aqueous solution was accelerated by the concentration of the hydroxyl ion, i.e., at a higher pH (Stumm, 1958), and the rate of TOC removed by ozonation was in turn proportional to the ozone decomposition rate (Hewes and Davison, 1971). This pH effect on the rate of TOC removal by ozonation was also observed by Sierka (1974). In view of this, the efficient removal of TOC from the laboratory RO permeates may be attributed to the small decrease of pH from the initial pH of 7 after ozonation. However, it may also be attributable to the nature of the organic constituents in this RO permeate that are most subject to degradation by ozone.

Table 3 shows the TOC removal of various RO permeates with the activated carbon and ion-exchange pretreatment processes. The activated carbon pretreatment removes approximately one-third of the TOC from the RO permeates studied. It is more effective for shower and laboratory RO permeates than the composite RO permeate (Table 3). In the case of ion-exchange pretreatment, the removal is more effective for shower RO permeate than for laboratory RO permeate. This indicates that the RO permeates contain organic

TABLE 1. OZONATION OF MUST RO PERMEATES ($T = 25°C$, $pH_{initial} = 7.0$)

	Sample and Pretreatment	Initial TOC (ppm)	Final TOC (ppm) 2 hrs	Total % Removal of TOC[a]	Final pH 2 hrs	k_1 (hr^{-1})
Composite (10x)[b]	Initial	415	233.6	43.7	5.20	0.27
	Ion-Exchange Pretreatment	364	220.3	46.9	4.80	0.43
	Carbon Pretreatment	299	139.0	66.5	5.25	0.38
Shower (2x)[b]	Initial	30.6	17.7	42.2	5.40	0.37
	Ion-Exchange Pretreatment	25.6	17.5	42.8	4.45	0.27
	Carbon Pretreatment	19.6	10.6	64.7	6.00	0.47
Laboratory (2x)[b]	Initial	20.5	1.6	92.2	7.30	3.75
	Ion-Exchange Pretreatment	20.1	2.2	89.3	6.90	5.39
	Carbon Pretreatment	13.0	0.9	95.6	6.80	3.93

a. Based on initial TOC, i.e., TOC of feed prior to pretreatment.

b. 10x and 2x indicate the strength of the specific wastewaters used was 10 and 2 times that of the normal ones.

TABLE 2. OZONATION OF MUST RO PERMEATES, VARIATIONS OF TOC AND pH
($T = 25°C$, $pH_i = 7.0$)

		Minutes						
		0	15	30	45	60	90	120
Comp. Initial	TOC	414.7	358.7	347.1	322.9	307.1	265.2	233.6
	pH	7.0	5.4	5.3	--	5.35	5.30	5.20
IXC[a]	TOC	364.0	324.7	294.6	275.5	260.1	242.0	220.3
	pH	7.0	5.9	5.6	5.2	5.05	5.0	4.80
ACC[b]	TOC	298.7	277.8	249.6	230.3	202.4	165.8	139.1
	pH	7.0	6.70	6.25	5.95	5.75	5.45	5.25
Shower Initial	TOC	30.6	28.51	26.5	24.2	21.2	19.7	17.7
	pH	7.0	6.80	6.70	6.70	6.40	5.45	5.40
IXC	TOC	25.6	24.9	22.1	21.1	21.2	19.0	17.5
	pH	7.0	6.1	5.20	4.85	4.70	4.60	4.45
ACC	TOC	19.6	19.8	17.5	15.7	13.8	11.8	10.8
	pH	7.0	6.70	6.55	6.65	6.40	6.25	6.0
LaL Initial	TOC	20.5	6.7	3.7	2.5	2.3	2.1	1.8
	pH	7.0	6.60	7.20	7.30	7.50	7.35	7.30
IXC	TOC	20.1	2.7	3.6	2.4	2.3	1.3	2.2
	pH	7.0	6.70	6.70	6.70	6.70	6.85	6.90
ACC	TOC	13.0	1.40	1.26	0.93	0.82	0.88	0.94
	pH	7.0	6.50	6.65	6.85	6.75	6.80	6.80

Supplying an overdose of 50 mg/L/min O_3. Sample Volume = 2 L. Gas Flow rate = 4 L/min.

a. IXC = RO permeates pretreated with ion-exchange column.
b. ACC = RO permeates pretreated with activated carbon column.

TABLE 3. TOC REMOVAL BY ACTIVATED CARBON AND ION-EXCHANGE PRETREATMENTS

	Sample	Initial TOC (ppm)	TOC Removal (%)
Composite	Initial	415	--
	Ion-exchange	364	12.29
	Activated carbon	299	27.95
Shower	Initial	30.6	--
	Ion-exchange	25.6	16.34
	Activated carbon	19.6	35.95
Laboratory	Initial	20.5	--
	Ion-exchange	20.1	1.95
	Activated carbon	13.0	36.59

compounds that are relatively polar and low in molecular weight. As such, the London-van der Waals forces between the resin and these compounds are relatively weak to effect the removal by sorptive mechanism. This is especially true with the organics in the laboratory RO permeates, which show almost no removal by resins. Unsatisfactory results of removing organics in RO permeates by activated carbon also indicate the presence of an appreciable amount of low molecular weight polar organic compounds. A parallel study was also conducted by Sierka (1974) with no pretreatment. A detailed comparisor of these two studies showed that pH had, indeed, a pronounced effect on TOC removal with ozonation.

In summary, activated carbon pretreatment not only removes approximately one-third of the TOC from most of the RO permeates, but also enhances the rate of TOC removal by ozonation. On the other hand, ion-exchange pretreatment has little or no effect on ozonation of organics and, in some cases, is detrimental to the removal rate by ozone. The effect of pretreatment on the rate of TOC removal by ozonation is closely related to the removal of certain organic species that are present in RO permeates. These species will otherwise hinder or enhance the rate of ozonation. It is also observed experimentally that the rate of TOC removal by ozonation is accelerated by the concentration of hydroxyl ion. These effects imply that organic species present in the RO permeates play important roles in controlling the rate of TOC removal by ozonation or the rate of ozone decomposition through a complicated process mediated by pH of the solution. To elucidate the mechanism of ozonation of a complex wastewater, ozonation of model compounds commonly found in the RO permeates of the MUST hospital wastewaters was the major focus of study for the second year of this project.

Preliminary Evaluation of Activated Carbon and Ion-Exchange Sorptive Processes

Both activated carbon and ion-exchange sorptive processes were evaluated using RO permeates of different MUST hospital wastewaters. The RO permeates were either pretreated with ozone or not. When using ozone-pretreated RO permeates, all samples were ozonated for 2 hours prior to both sorptive processes. Tables 4, 5, 6, and 7 give the formulas of various MUST hospital wastewaters employed in this study.

For RO permeate of laundry waste, an average of only 20% removal of TOC was attained by passing through either the activated carbon or ion-exchange columns. Further treatment of the RO permeate from laundry waste is unnecessary because TOC of the RO permeates is down to 4 ppm, which is lower than the reuse criteria, i.e., 5 ppm TOC. For RO permeates of shower waste, only about 10 to 15% TOC removal was observed by both sorptive processes. However, the removal improved to 30% when ozonated RO permeate of shower waste was tested. Further treatment of the RO permeate, even from ozonated permeate followed by sorptive processes, is needed to meet the reuse criteria because the effluent still has a TOC of 14 ppm. In the case of RO permeates of laboratory waste, the TOC removal with both sorptive processes was negligible. The poor removal of TOC with these sorptive processes is attributable to the presence of the low molecular-weight polar compounds, such as methanol and acetone, used in formulating the laboratory waste. However, after ozonation of the RO permeate of laboratory waste, the TOC

TABLE 4. COMPOSITION OF LAUNDRY WASTE
TYPE II (25-gallon batch 2x)

Items	Grams
Group 1	
Detergent (Tide)	98.1
Kaolinite	18.9
Na_2CO_3	94.7
Group 2	
Sour (Downey)	21.95
Vegetable Oil (Wessor)	18.895

Mix items in groups 1 and 2 separately, then add to 25 gallons of water.

TABLE 5. COMPOSITION OF SHOWER WASTE
(25-gallon batch 2x)

Items	Grams
Group 1	
Soap	6.26
NaCl	7.54
Urea	0.0917
Kaolin	1.725
Talc	1.783
Shower Cleaner	9.06
Group 2	
Hail Oil	14.18
Hail Gel	3.36
Shampoo	0.456
Toothpaste	3.36
Deodorant	0.0917
DEET (N,N-diethyl toluamide)	0.0917
Mouthwash	0.178
Phisohex	0.2723
Hair Dye	0.0917
Hair Coloring	0.0917

Mix items in groups 1 and 2 separately, then add to 25 gallons of water.

TABLE 6. COMPOSITION OF LABORATORY WASTE (25-gallon batch 2x)

Group 1 Items			
Alconox	5.0 grams		
Group 2 Items			
Lysol	0.625 grams		
Group 3 Items			
Acetone	1.25 mL		
Dichromate Cleaning Solution	12.5 mL		
Group 5 Items			
Wright Stain	1.37 mL	Safranin	0.25 mL
Giemsa Stain	1.5 mL	Immersion Oil	0.125 mL
Crystal Violet Stain	0.25 mL		
Group 6 Items			
Ether	0.125 mL	Diazo Blank	0.189 mL
$ZnSO_4$ Solution	0.125 mL	Hypochlorite Reagent	0.25 mL
KI-I Solution	0.125 mL	Bilirubin Standard	0.125 mL
1.5% Thiolglycolate	4.125 mL	0.85% NaCl	6.97 mL
5.0% Phenol	3.125 mL	o-Toluidine	0.69 mL
22.2% Na_2SO_4	0.25 mL	Diazo Reagent	0.125 mL
1% Formaldehyde	0.25 mL	Biuret Reagent	0.375 mL
3% Sulfosalicylic Acid	0.25 mL	DNPH Reagent	0.125 mL
0.1 N NaOH	4.5 mL	Phenol Reagent	0.314 mL
3% Trichloroacetic Acid	0.189 mL	2% Sodium Citrate	0.125 mL
		Methyl Alcohol	4.0 mL
Group 7 Items			
Blood	17.5 mL		
Spinal Fluid	0.125 mL		
Urine	42.36 mL		
Agar	10.56 mL		
LMB Agar	4.125 mL		

Items in groups 1, 2, and 3 are weighed, mixed, and stored separately until use.

Items in groups 5 and 6 are weighed and stored in separate containers and added to the waste mix in the order shown.

TABLE 7. COMPOSITION OF COMPOSITE WASTE
(100-liter batch prepared, 10x)[a]

Chemical	Grams 10x Conc.	Use
A. Nontoxic		
Acetic acid	38.2	99.9% $HC_2H_3O_2$
Ammonium chloride	40.7	NH_4Cl
Chloroform	0.68	$CHCl_3$
Ethanol	1.85	95% EtOH
Triton X-100	48.5	(in Bethadine)
Potassium alum[a]	6.70	$Alk(SO_4)_2.12H_2O$
Potassium hydroxide	81.2	KOH
Sodium bicarbonate	81.6	$NaHCO_3$
Sodium dichromate	35.0	$Na_2Cr_2O_7.2H_2O$
Sodium hydroxide	137.3	NaOH
Sodium LAS	35.0	Conoco C-560
Sodium sulfite	324.0	Na_2SO_3
Sodium thiosulfate	188.0	$Na_2S_2O_3.5H_2O$
Soap	221.0	Ivory Flakes
Sodium chloride	163.0	NaCl
Sulfuric acid	90.9	H_2SO_4
B. Toxic		
Boric acid	6.11	H_3BO_3
Copper sulfate	0.0595	$CuSO_4.5H_2O$
Formaldehyde	12.0	40% HCHO
Lithium (as Li)	0.0013	LiCl
Methanol	18.0	CH_3OH
Optical brighteners	2.18	Blancophor CN
Iodine	0.0864	I_2
Nonylphenyl...Iodine	3.05	Wescodyne 8.7% NI
Polyethoxy...Iodine	3.19	Wescodyne 9.1% PI
Potassium Iodide	0.0682	KI
Tripolyphosphate	261.5	$Na_5P_3O_{10}$
Phosphates	5.07	$Na_3PO_4.12H_2O$
Phosphoric acid	P	(in Wescodyne)
Povidone iodine	14.5	Betadine
Sodium hexametaphosphate	197.0	$(NaPO_3)_6$
Silicate	44.2	$Na_2SiO_3.9H_2O$
Silica	29.4	SiO_2
Silver chloride	8.53	AgCl
Silver nitrate	0.437	$AgNO_3$
Sodium nitrate	0.00009	$NaNO_3$
o-Toluidine	0.204	p-Toluidine
Zinc sulfate	0.204	$ZnSO_4.7H_2O$
C. Suspect		
Chemical	ppm 1X Conc.	Use
Ammonium oxalate	0.0431	$(NH_4)_2C_2O_4.h_2O$
o-Benzyl-p-chlorophenol	0.0835	Santophen
2,4-Dinitrophenylhydrazine	0.0062	2,4-DNPH (10% h_2O)
Entsulfon	4.28	pHisoderm
Hydroquinone	162.0	Hydroquinone
Isopropyl myristate	79.4	Emerest 2314
N,N-Diethyl-m-toluamide	0.379	N,N-DE-m-Toluamide
Oleic acid (0.895 g/mL)	0.432	Oleic acid
Pyrogallol	0.0294	Pyrogallol
Sodium thioglycollate	0.348	$HSCH_2COONa$
Xylenols	0.0463	2,4-Xylenol

a. The composite waste was formulated according to the listing compiled by the University of Cincinnati, Third Quarterly Report, FY 1974, Table 2. Due to delays in receipt of chemicals, the following changes were made:

$Na_3PO_4.12H_2O$ instead of Tripolyphosphate, m-cresol instead of 2,4-Xylenol, N,N-Diethylaniline instead of N,N-Diethyl-m-toluamide, o-benzyl-p-chlorophenol was not replaced.

was brought down to 2 ppm, which was lower than the criteria for reuse. Because of the low TOC, which is subject to appreciable analytical errors, the ozonated laboratory RO permeate cannot be studied with carbon and ion-exchange sorptive processes. For composite RO permeate, an average of 20% TOC removal with carbon column and 10% removal with ion-exchange column was obtained after about 80 to 90 column bed volumes. For the ozonated composite RO permeate, an additional 40% removal of TOC was observed with the ion-exchange column. However, the average removal of TOC with the carbon column does not seem to be affected by the ozonation process. DeWalle and Chian (1974) reported that the ion-exchange resin is preferable for the removal of higher molecular-weight fractions in the secondary effluent. Therefore, the increase in TOC removal after ozonation by ion-exchange column may have been contributed by the increase in the molecular weight of the TOC material as a result of ozonation. This, however, needs to be confirmed experimentally, and work is presently underway to verify such a postulation. If this is indeed the case, then RO treatment of ozonated wastes should be explored in the treatment of the MUST hospital wastewater for complete reuse.

Mechanism of Organic Removal by Ozonation

Based on the experience of stripping the volatile organic compounds from aqueous solutions, it is conceivable that the same volatile fractions present in the RO permeates may also be stripped during the course of ozonation experiments. Therefore, the kinetic expression obtained for TOC removal may not be representative of the true chemical reaction by ozone. Rather, it is a combination of physical removal by stripping and chemical oxidation by ozone. As such, the kinetic equation developed for TOC removal cannot be used for the design of an ozone contactor. This is especially true when a multi-stage contactor is to be used in series. The volatile fractions that are stripped from the first vessel can either be reabsorbed by the second vessel or retard the rate of stripping due to the increased partial pressure of the volatile compounds in the gas phase when a cocurrent process is employed. Eventually a point will be reached in the succeeding vessels where the physical stripping will come to a halt. Beyond that vessel, reabsorption of the volatile organics may occur. The later process of reabsorption would tend to impair the effluent quality, especially when ozone is exhausted, in both gas and liquid phases, in the last vessel. If this were the case, counter-current flow of gas and liquid might be advantageous, because the volatile compounds that are highest in concentration in the first vessel would simply be stripped off along with the effluent gas.

In a recent report on "Oxidation of Refractory Organic Materials by Ozone and UV Light" by Hewes et al. (1974), kinetic reactions of a number of organic compounds, e.g., acetic acid, ethanol, palmitic acid, and glycine, were studied extensively at different temperatures with and without UV irradiation. Since ethanol was found to be stripped effectively by the helium gas sparging method as discussed later, experiments on stripping of ethanol at 30°C and 50°C were conducted. Figure 1 shows that an appreciable fraction of ethanol can be stripped under experimental conditions similar to those employed by Hewes et al., i.e., at an oxygen flow rate of 1 v/vm

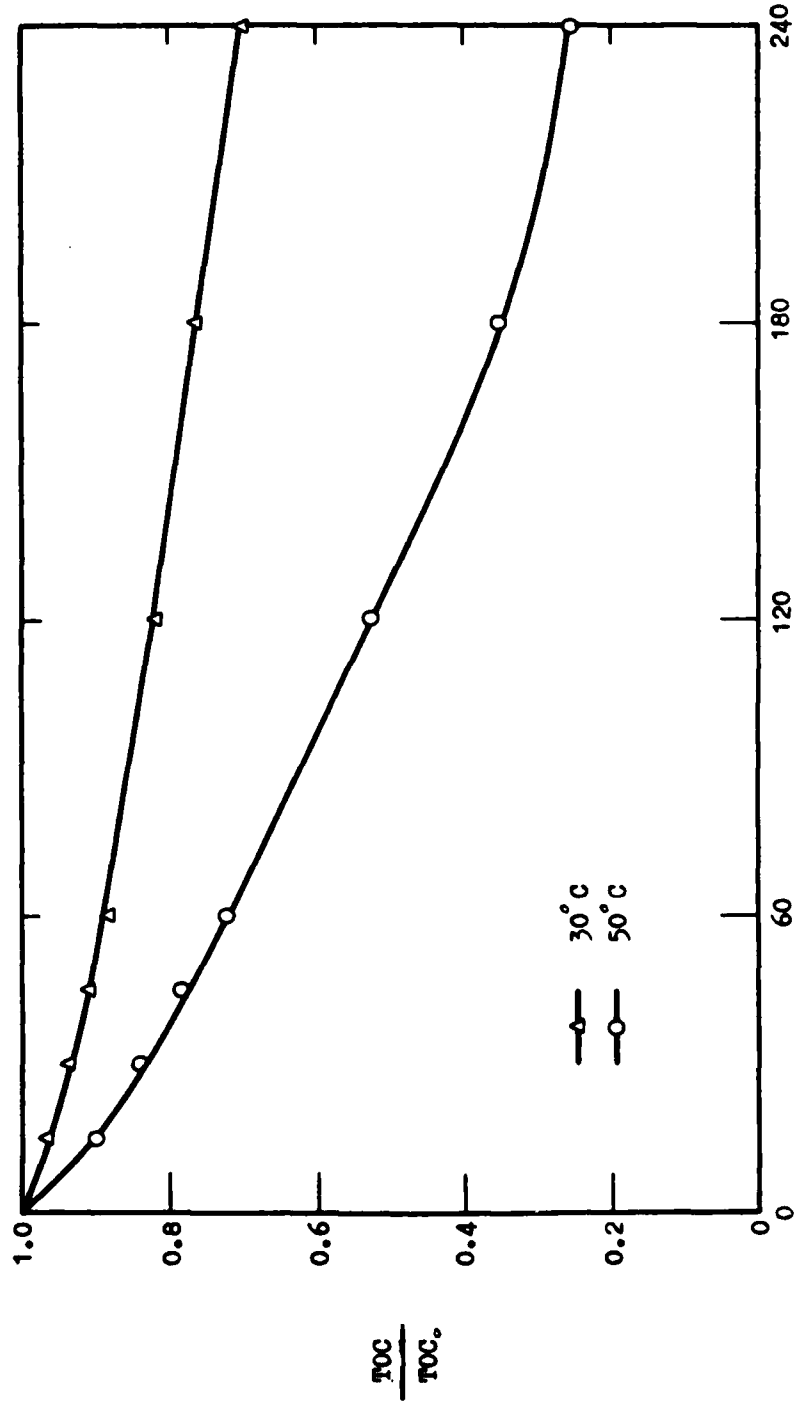

Figure 1. Oxygen Stripping for Ethanol in Distilled Water at 30°C and 50°C.

(volume of gas per unit volume of liquid per minute) with a vessel having a $k_L a$ (overall, or volumetric, mass transfer coefficient based on liquid phase concentration) of approximately 160 hr^{-1} for oxygen transfer. As much as 50% of ethanol can be removed within 2 hours by stripping at 50°C (see Fig. 2). The rate of stripping of ethanol was also found to follow the same logarithmic decrease versus time as shown in Figure 2. Therefore, the higher rate of ethanol removal while ozonating at an elevated temperature is actually contributed partially by the higher rate of stripping. Hewes et al. (1974) have also shown that the rate of removal of the intermediate products of ethanol is the rate limiting step rather than that of ethanol itself during ozonation with UV. Under such circumstances, stripping of ethanol may also enhance the overall rate of removal of TOC by ozone due to production of smaller amounts of intermediate products.

Oxygen stripping and ozonation of RO permeates of laboratory and composite wastes received from Walden Research Laboratory were conducted at an optimum temperature of 40°C as reported by Walden on their ozonation studies. Figure 3 shows the percentage of TOC removal versus time for the laboratory RO permeate, and Figure 4 shows the removal of TOC by ozonation on a semilogarithmic scale after correction for the stripping effect. It is also seen from Figure 3 that the volatile fraction consists of approximately 40 to 50% of TOC. Figures 3 and 4 show that during the latter stage of the ozonation process, TOC removal appears to be contributed mainly by the stripping process, as the rate of TOC removal by ozonation after correction for the stripping effect starts leveling off toward the end of the ozonation study. The early stage of the ozonation process follows pseudo first-order reaction kinetics. Similar curves of TOC removal by ozone as reported by Walden were obtained while plotting their data on the semilog paper (see Fig. 5). The same logarithmic decrease in TOC by oxygen stripping is also seen from Figure 5 with the laboratory waste. Figure 6 shows the kinetics of TOC removal from the laboratory waste after correction for stripping effect. Figure 6 indicates similar pseudo first-order reaction kinetics to Figure 4, which is based on results obtained in our laboratory.

Figure 7 shows the results of ozonation and oxygen stripping of the RO permeate of the composite waste. Results of the ozonation study agree well with those obtained by Walden, i.e., TOC can be removed rather effectively by ozone. However, after approximately 45 minutes of ozonation, further decrease in TOC appears to be contributed solely by stripping up to 120 minutes. The nonvolatile organics were found to be the major fraction of TOC in the RO permeate of the composite waste. Figure 7 shows that approximately 80% of the TOC is nonvolatile, which agrees well with the value of 72% derived from data in Table 24 and based on the helium stripping study using the RO permeate of 10x composite waste prepared at the University of Illinois. Figure 8 shows the kinetic data of TOC removal by ozone after correction for the stripping effect.

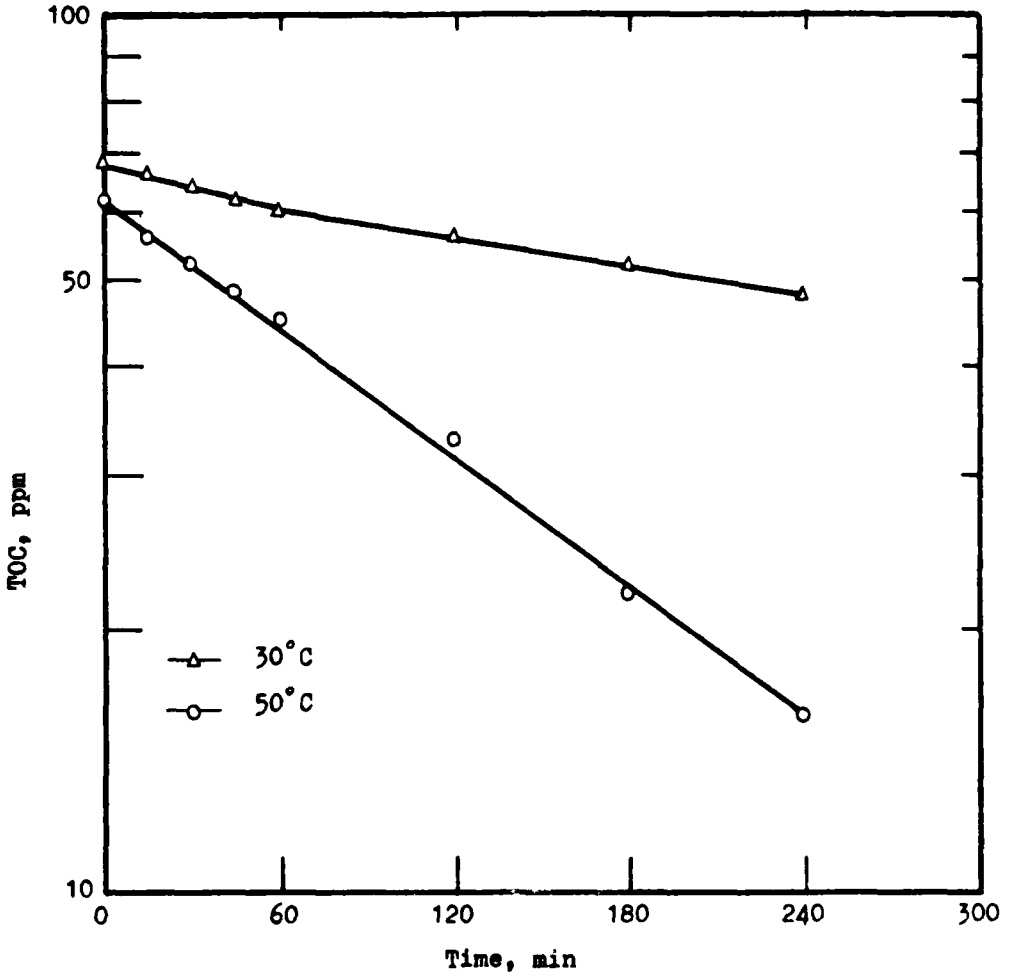

Figure 2. Log Plot of Oxygen Stripping for Ethanol in Distilled Water at 30°C and 50°C.

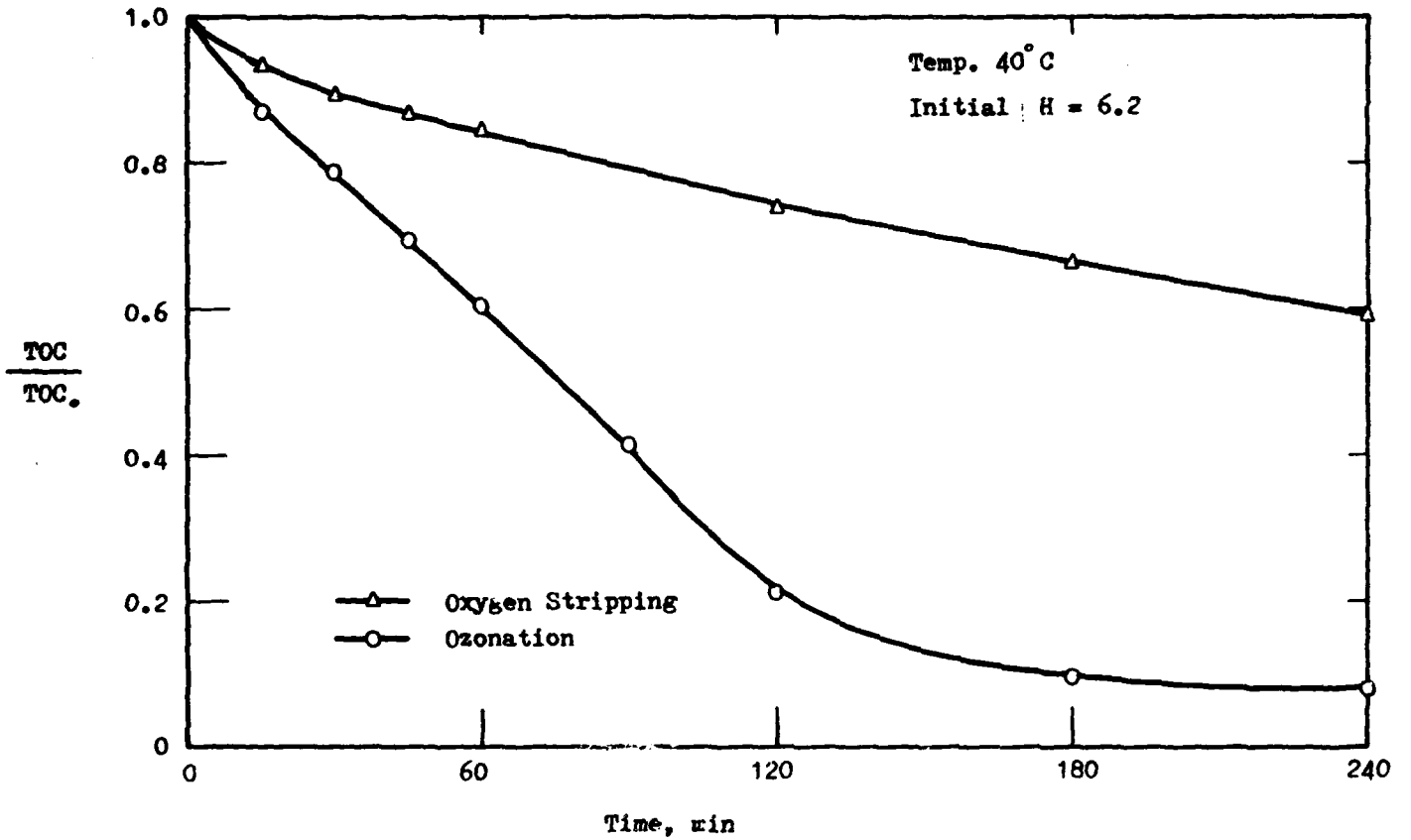

Figure 3. Oxygen Stripping and Ozonation of Permeate of Laboratory Waste.

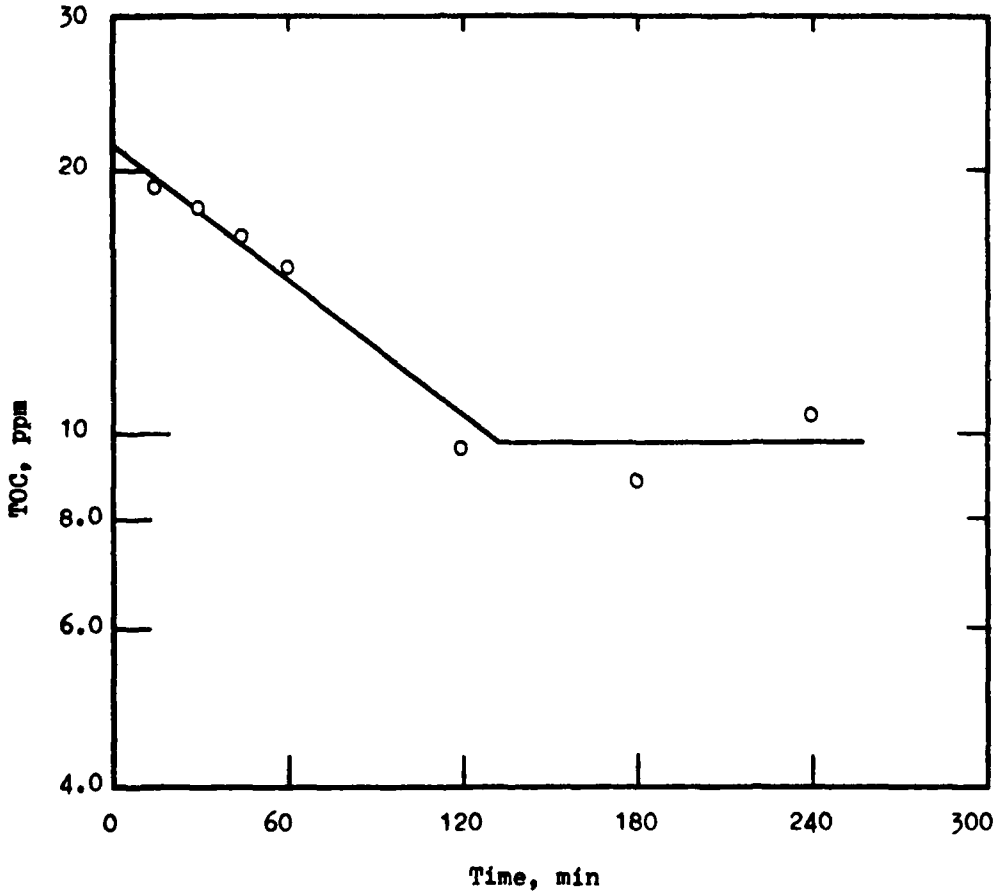

Figure 4. Log Plot of Ozonation of RO Permeate of Laboratory Waste After Correction for Stripping Effect.

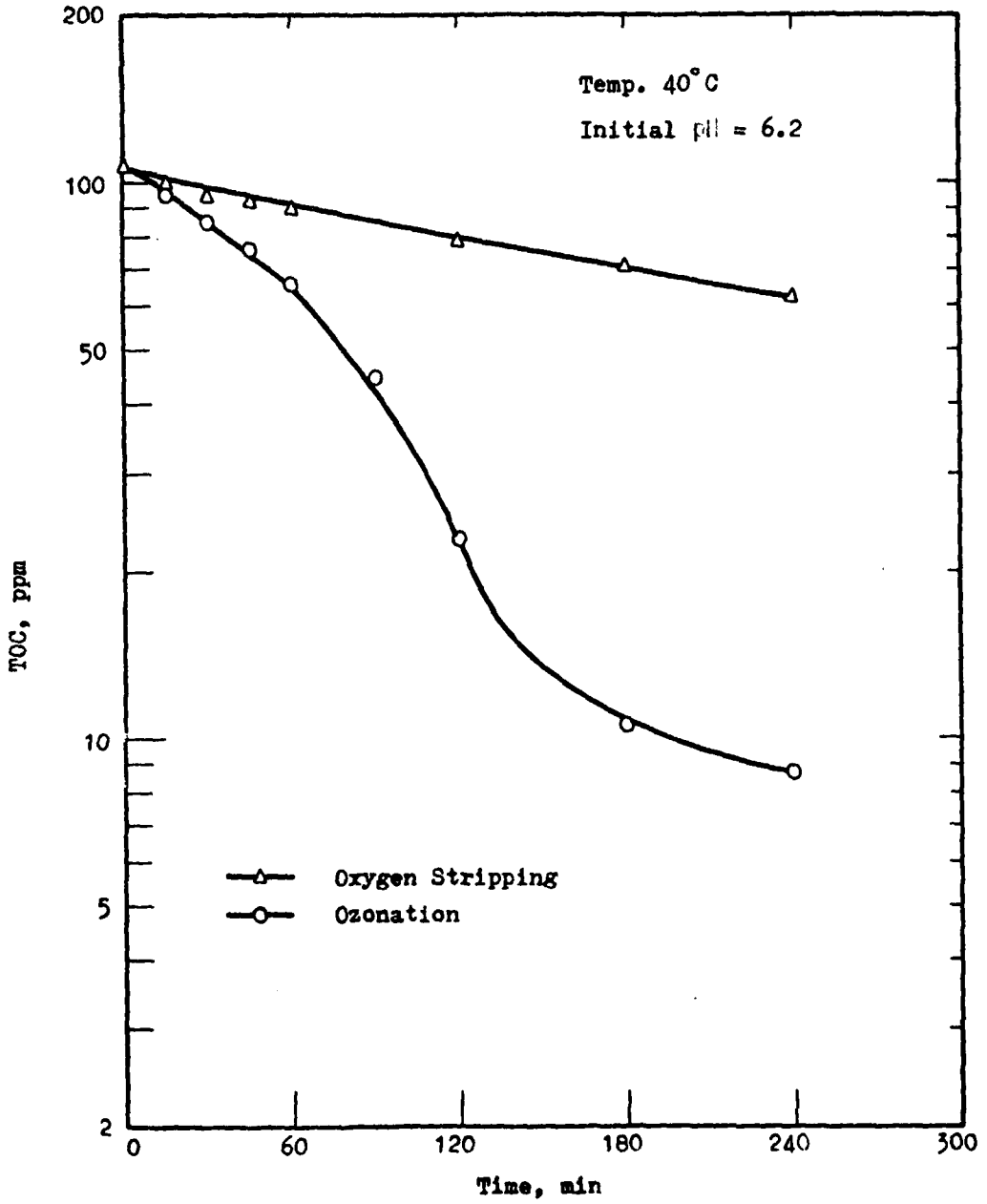

Figure 5. Semi-Log Plot of Oxygen Stripping and Ozonation of Permeate of Laboratory Waste.

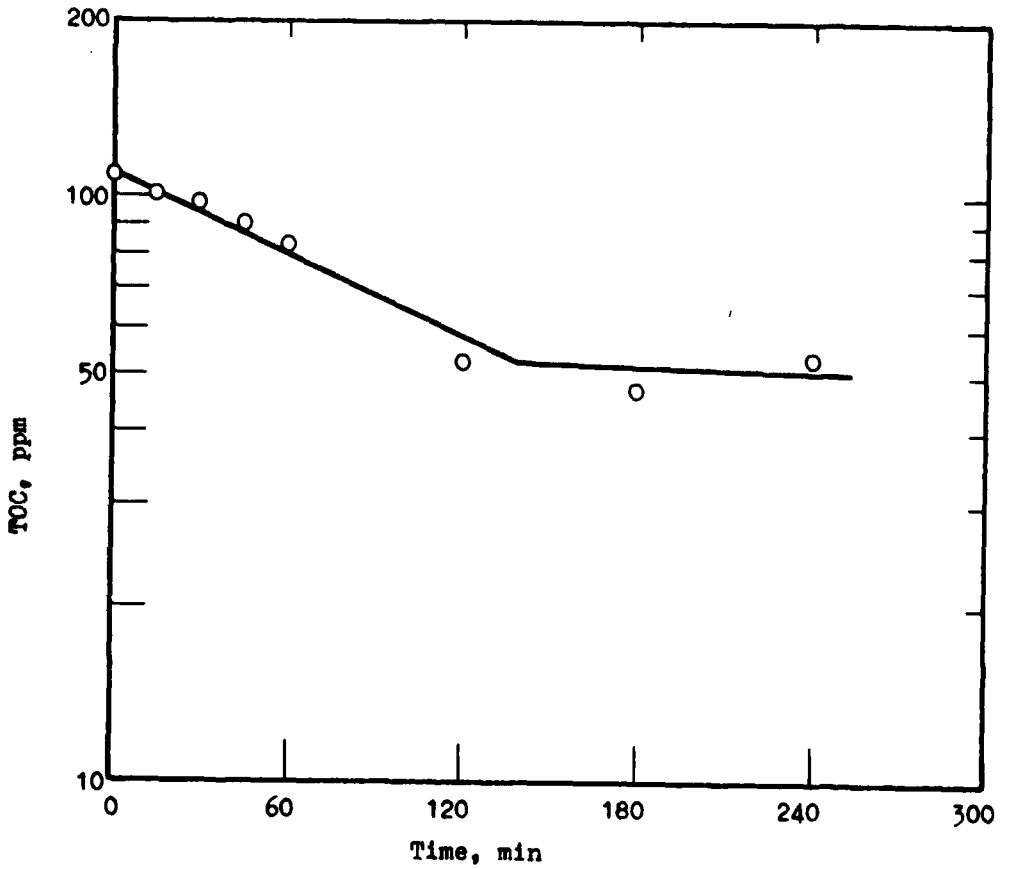

Figure 6. Semi-Log Plot of Ozonation of Permeate of Laboratory Waste After Correction for Stripping Effect.

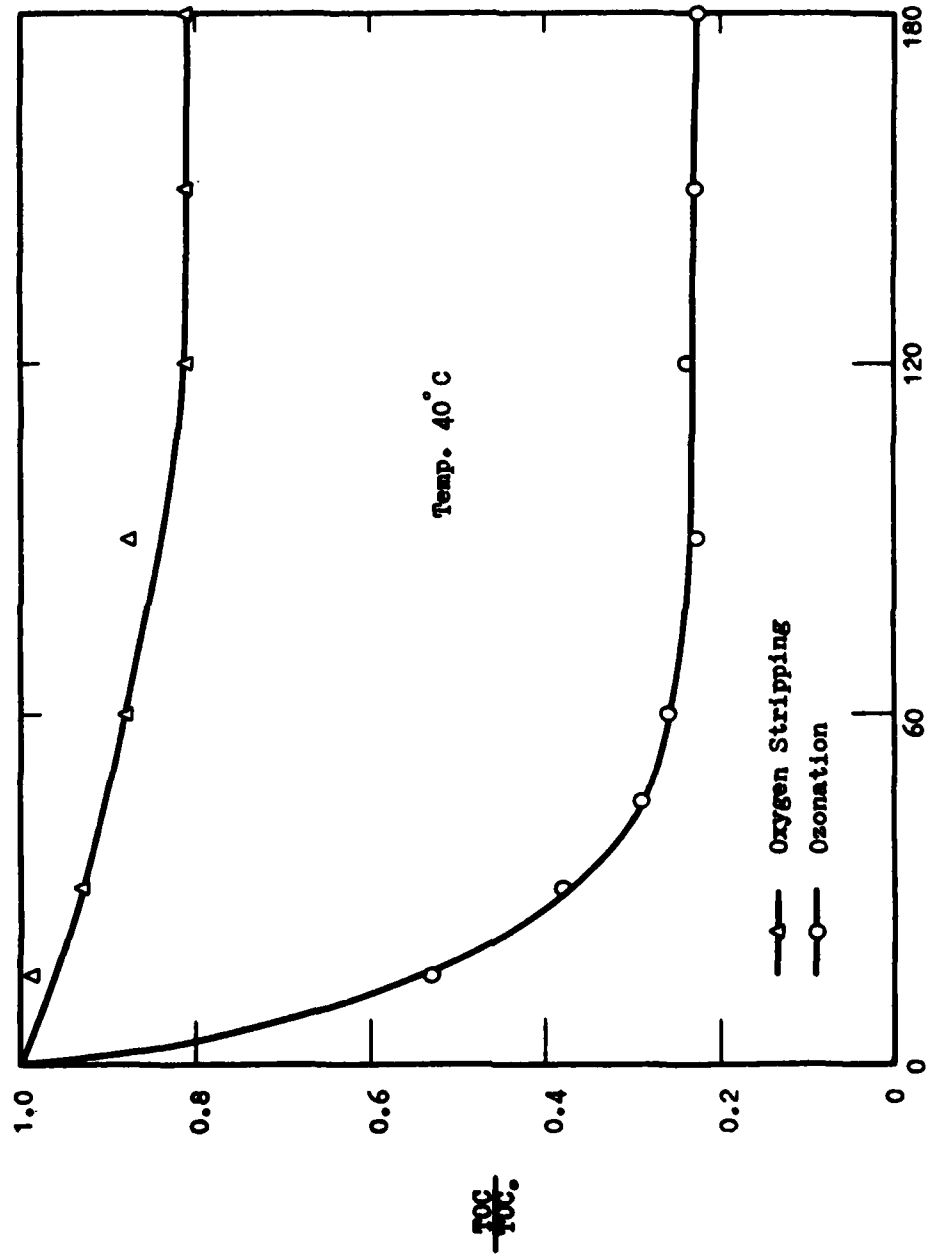

Figure 7. Oxygen Stripping and Ozonation of Permeate of Hospital Composite.

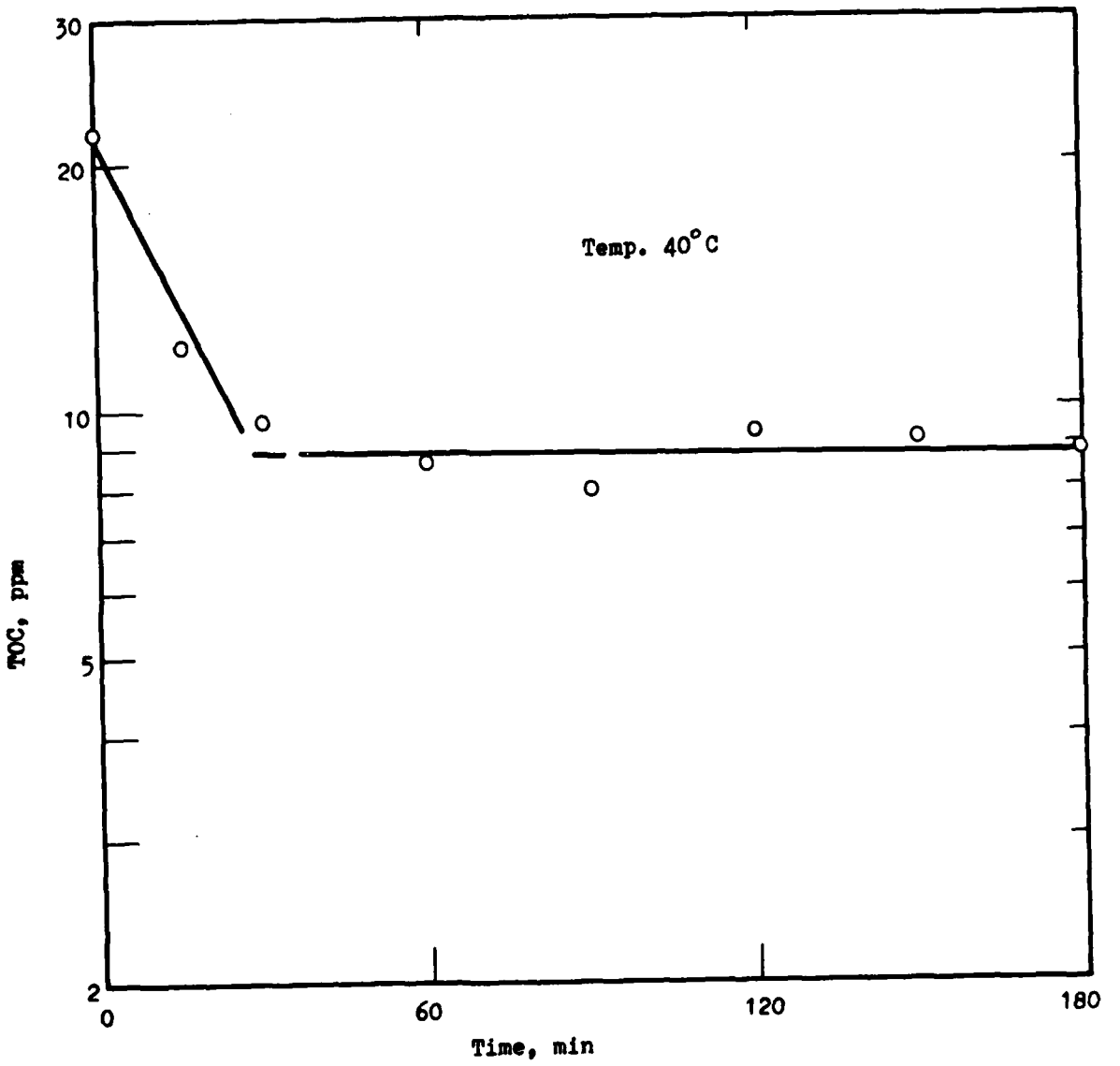

Figure 8. Semi-Log Plot of Ozonation of Permeate of Hospital Composite After Correction for Stripping Effect.

Oxygen stripping of the composite waste also resulted in a decrease of pH as was observed during ozonation of the same waste (see Figure 9). The decrease in TOC (see Fig. 7), along with a similar pattern of decrease in pH during oxygen stripping (see Fig. 9), suggests that the volatile organic compounds in the composite waste that are stripped are weak base in nature. However, the trace amount of CO_2 that might be in the oxygen gas tank may also contribute to a slight decrease in pH.

Biological Pretreatment of MUST Wastes

Because of the intense energy required to final polish residual organics in RO permeates with ozonation to an acceptable level, i.e., 5 ppm TOC, it was proposed that the biological pretreatment of MUST wastes in the stabilization tank be investigated for possible reduction of gross organic compounds that were poorly removed by the membrane processes. Experimental protocol on the biological pretreatment of MUST wastes was set up based on the discussion with LTC Reuter during his visit in early April 1975. Figure 10 shows the schedule as well as the testing program conducted in April.

Prior to biological treatment studies, acclimation of sludge was carried out using the RO permeates of both composite and laboratory wastes. The ratios of RO permeates to municipal sewage were increased gradually according to the schedule given in Figure 10. After it was acclimated with the full-strength RO permeates of composite and laboratory wastes, the sludge was fed with untreated MUST raw wastes. Preweighed MUST composite and laboratory wastes were provided by Walden Research Laboratory to ensure consistency in the composition of these synthetic wastes. Enough ingredients to make 100 gallons of raw wastes were received. Nutrients were added to ensure a TOC:N:P ratio of 40:5:1. Since phosphate is in excess in the MUST raw wastes, only nitrogen was added. The amount of nitrogen addition was based on the TOC of the wastes using the ratio of TOC to N of 40:5 (or 8:1). Ammonium sulfate was used as the nitrogen source. The TOC of MUST composite and laboratory wastes was 204 and 240 mg/L, respectively.

Two 1-liter graduated cylinders were used to acclimate the sludge. Each was fed with 500 mL of the composite and the laboratory wastes daily. Aeration was made through a small aquarium air stone located at the bottom of the cylinders. The dissolved oxygen level was maintained above 2 mg/L throughout the runs. There was excessive foaming while aerating the wastes, especially the laboratory wastes. Foam separation accounted for the bulk of the removal of organics during aeration of these units. By taking into account TOC removal through foam separation, little or no removal of organics was observed in batch culture fed with raw laboratory waste after seeding with sludge acclimated to RO permeate of the same waste. This was also confirmed by little or no growth of sludge in the laboratory waste. However, growth was observed in batch culture fed with raw composite waste. Approximately 30% TOC removal was observed after 24 hours of aeration.

Studies on the continuous culture with no cell recycle were carried out to simulate the growth conditions in the stabilization tank. Two hydraulic

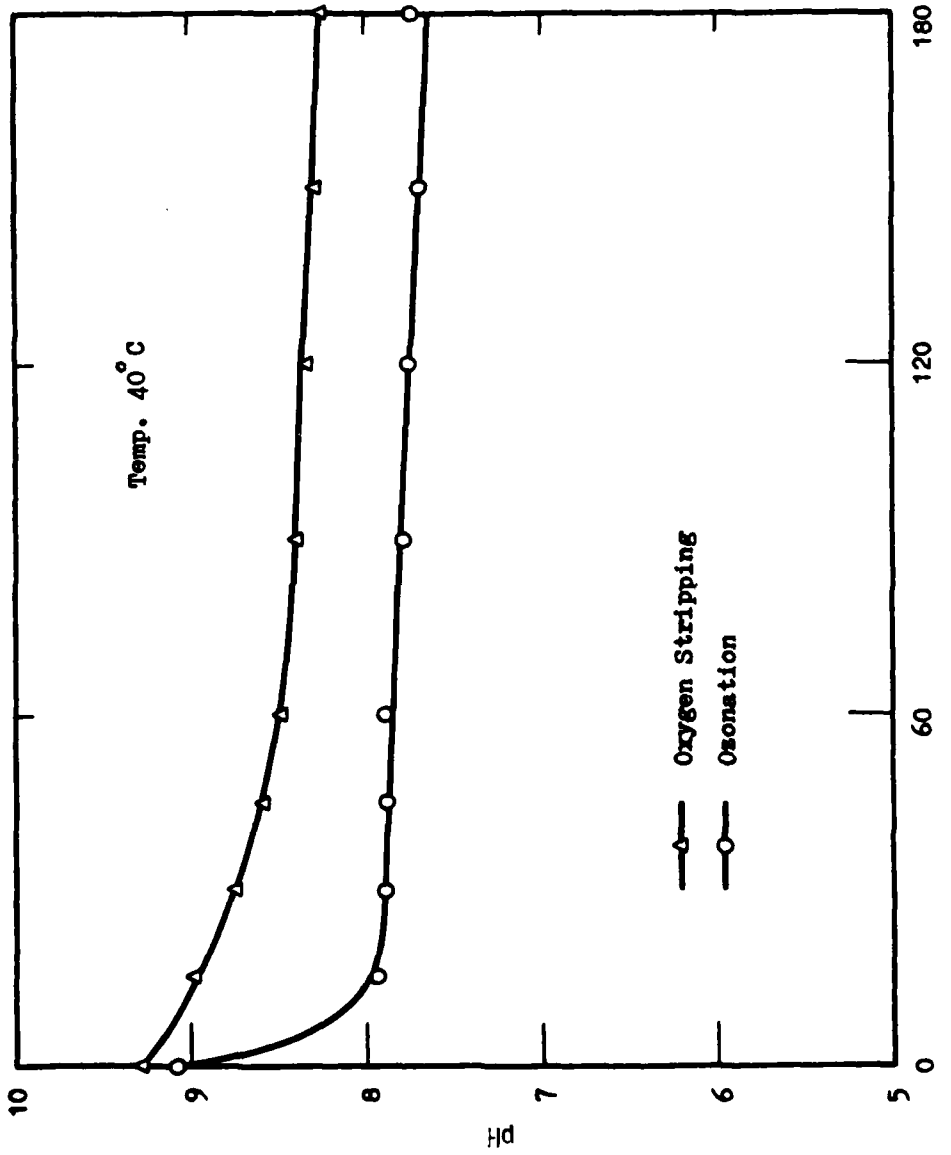

Figure 9. pH Variation of Hospital Composite RO Permeate During Course of Oxygen Stripping and Ozonation.

Task	April 1975															May 1975		
	2	4	6	8	10	12	14	16	18	20	22	24	26	28	30	2	4	6
Acclimation of Sludge[a] RO Permeates	1/4		1/2		3/4		1[c]											
Raw Feed							1/8		1/3		1/2		3/4		1[d]			
Biological Treatment[b]													———		———			
Receiving Preweighed Formulas from Walden					———													
Membrane Treatment Raw Feed (Control)										———								
Biologically Treated Feed															———			
Ozonation Study RO Permeates (Control)													———					
RO Permeates of Biologically Treated Feed																———		

a. Study on biological treatment will be conducted only when acclimated sludge is obtained. Nutrient addition will be practiced to ensure TOC:N:P = 40:5:1

b. Even when sludge acclimated in batch culture is obtainable, its growth in the continuous culture is yet to be determined.

c. The fractions indicate the permeate to sewage ratio by volume

d. The fractions indicate the raw feed to distilled water ratio by volume

Figure 10. Experimental Protocol on Biological Pretreatment of MUST Wastewaters Followed by UF-RO-O_3 Runs.

detention times, i.e., 4 and 6 hours, were selected. These resulted in a dilution rate, or growth rate, of 0.25 hr^{-1} and 0.167 hr^{-7}, respectively. If the microorganisms were unable to grow at such rates, they were washed out of the tank after a few volumes of turnover. The 6-hour retention was the longest one that could be incorporated into the design of the stabilization tank for an integrated MUST water processing element because of size and weight limitations. Results of these continuous runs at 35°C and pH 8 (the most optimum conditions for the biological growth) showed that little or no growth was observed with the raw composite waste in a fermentor containing 4 liters of sludge obtained from aerating a batch culture on raw composite waste for 24 hours. This was confirmed by TOC analysis of the effluent as well as the influent to the 4-liter fermentor.

Although 40% of TOC was removed when calculated on the basis of the TOC in the fermentor and that in the influent, that percentage was found to be attributed mainly to loss of TOC through foam separation during the aeration period of 4 and 6 hours rather than to removal by microbial growth. It was also shown that little or no removal of organics occurred by stripping under the operating conditions of the aeration process. An air flow rate of 1 liter per minute, or 0.25 v/vm, and an agitation speed of 695 rpm were employed in the aeration study.

Membrane ultrafiltration (UF) runs were performed using two Abcor's HFD-180 5-foot-long tubes pumping at a feed flow rate of 12 gpm (limited by the pumping capacity) at 30 psig. Although the operating conditions were not at their optimum compared to those of Walden's, they did permit comparison of performance between the biologically pretreated and the untreated raw wastes. Results of UF studies using composite wastes indicate a decrease of 50 to 67% of permeation flux when fed with the fermentor feed after 4 hours of aeration compared to a control run in parallel using the untreated composite waste. The operating temperature was 57°C for both runs to eliminate possible microbial growth during the 6 to 9 hours of run. However, rejection of TOC by UF increased from 44 to 63% at the same product water recovery, i.e., 75%, as can be seen in Table 8. This implies that a slimy layer might be formed on the UF membrane surface as a result of the presence of the biomass in the pretreated waste. This slimy layer serves as a secondary membrane gel layer responsible for the improved removal of TOC with a concomitant decrease in flux. The biomass was likely to come from the seed to the vessel and postgrowth of microorganisms in the container receiving effluent from the aeration vessel.

Reverse osmosis of UF permeates was conducted using a B-10 module (DuPont) operated at 750 psig and 21°C. RO rejection of TOC increased from 89% for the control to 93% for the UF permeate obtained from a biologically pretreated composite waste. The small increase in TOC rejection was attributable to the differences in product water recovery rate of 80%, whereas the biologically pretreated waste was operated at 66% product water recovery due to the lack of sufficient feed for the latter run. The residual TOC of the RO permeate obtained from the biologically pretreated wastes was about one-half that of the control, as shown in Table 8.

TABLE 8. EFFECT OF BIOLOGICAL PRETREATMENT (BP) OF COMPOSITE WASTE ON PERFORMANCE OF MEMBRANE PROCESSES

	TOC (mg/L)		Rejection (%)		Flux, Avg. (gal/day)		Product Water Recovery (%)	
	Control	BP	Control	BP	Control	BP	Control	BP
Ultrafiltration[a]								
Feed	187.1	214.3	--	--	--	--	--	--
Permeate	104.7	78.9	44	63	57	19	80	80
Reverse Osmosis[b]								
Feed	104.7	78.9	--	--	--	--	--	--
Permeate	11.3	5.6	89	93	4,280	4,109	80	66

a. Operating conditions: Two Abcor HFU-180 tubes, 2.2-ft^2 membrane area, 12 gpm, 30 psig, 57°C.
b. Operating conditions: B-10 Permeator, 4 gpm, 750 psig, 21°C with UF permeate as feed.

Ozonation studies on the RO permeates were conducted using the same fermentor for the biological pretreatment of wastes. An O_2 stream containing 2% ozone by weight, sparged at 0.25 v/vm, was supplied to the fermentor operated at 695 rpm. The temperature was controlled at 25°C. A 15-watt UV-germicidal lamp immersed in the fermentor was used for UV irradiation. Results of UV-ozonation runs are shown in Figure 11. The residual TOC after ozonation of the biologically pretreated sample was one-half that of the control, i.e., 2 mg/L vs. 4 mg/L. The time required for reaching such levels was also half of that for the biologically treated effluent as the initial TOC was one-half that of the control (see Fig. 11).

The results of the biological pretreatment of the MUST composite waste were promising in that the final ozonation requirement was cut by half and the residual organic content also was half the level of the control. This reduction was, however, at the expense of a severe flux decline for the UF step. As much as twice the UF membrane area might be required to accomplish this reduction. Of course, by increasing the feed flow rate for the UF run, the flux decline may be overcome somewhat. Since the UF step contributes to the insignificant improvement in removal of organic matter (see Table 8) after biological pretreatment of the composite waste, this advantage may be reduced greatly upon resumption of the permeation flux, as the slimy layer responsible for the improved organic removal will be removed.

One way to improve the biological efficiency of removing the bulk organic matter in wastes is to recycle the cell mass. A cell residence time of 1 day appears to be sufficient to simulate the batch run for 24 hours. A 30% reduction in organics was observed with the MUST composite waste after aeration in batch culture for 1 day. Although recycling the cell mass can be accomplished in the UF step, severe flux decline is anticipated when the cell concentrations start building up in the UF feed. In addition, the performance of the biological pretreatment step tends to vary as the waste composition varies. This is especially true when the laboratory waste is the only one discharged into the stabilization tank. Studies on the shock loading of the batch culture grown on composite waste showed that cells acclimated to the composite waste ceased to grow when the laboratory waste was added into it. Also, the excessive foam formation becomes a nuisance to the operation of the aerated stabilization tank. All of these problems are not in favor of the use of the biological pretreatment step. However, it is recommended that biological treatment with cell recycling be evaluated on a pilot-scale study using composite waste to fully assess the feasibility of the process.

In conclusion, the advantage of using the biological pretreatment of MUST hospital wastes for reducing the power requirement for the ozonation step may be offset by the additional cost for the preceding power requirements, such as agitation, sparging, and additional UF pumping. This should be investigated in a pilot-scale study, again, to fully assess the benefit of the pretreatment step.

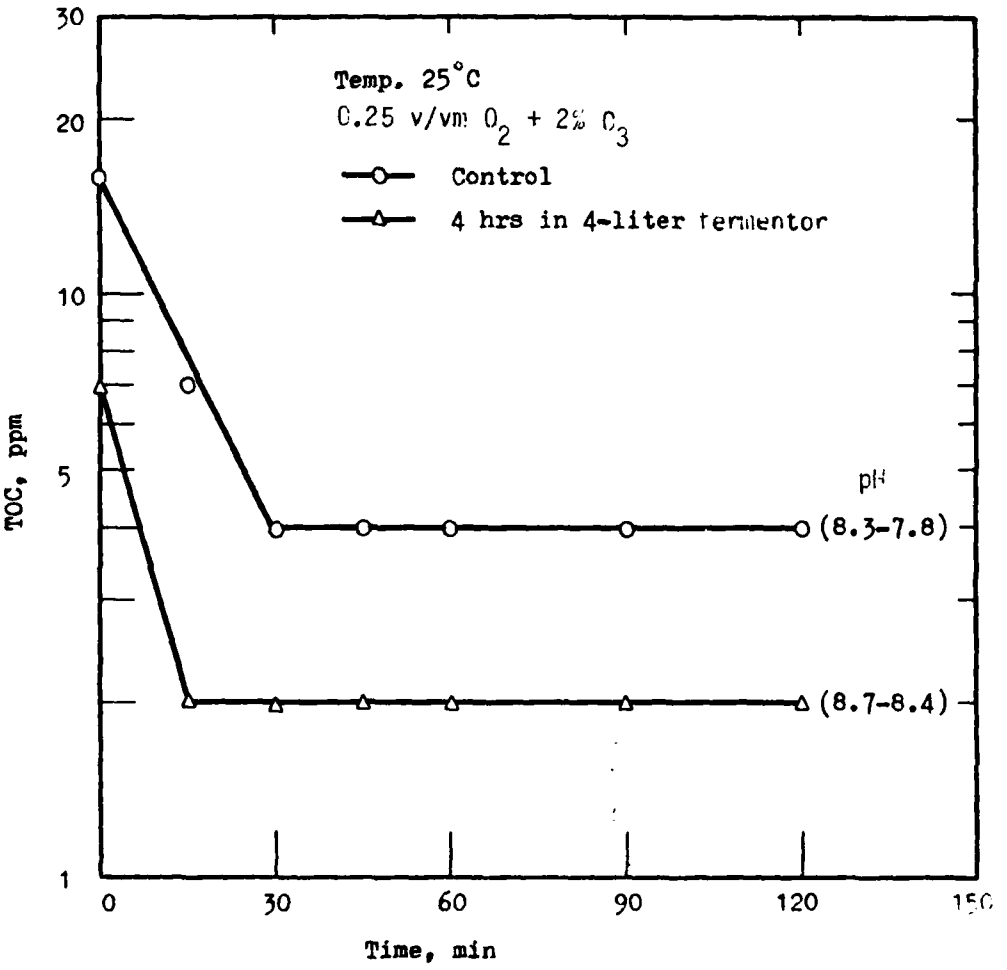

Figure 11. UV-Ozonation of Composite RO Permeates With or Without (Control) Biological Pretreatment.

ORGANIC ANALYSIS

The gas stripping and distillation techniques were thoroughly evaluated and then applied to the determination of volatile organics in treated hospital wastewaters. The distillation technique was also used in conjunction with headspace gas chromatography to determine volatile polar organics in treated wastewaters. The intermediately volatile (GC volatile) and nonvolatile (GC nonvolatile) organics were determined, respectively, by gas chromatography (GC) and high pressure liquid chromatography (HPLC) after sample solutions were subjected to liquid-liquid extraction and Kuderna-Danish (K-D) evaporation. A detailed review of the literature is given to describe the state-of-the-art analytical procedures for trace organics.

Literature Review

A thorough literature review on the concentration, identification, and determination of organics was conducted and is reported here. When considering concentration methods, two criteria must be kept in mind. First, a method is needed that does not alter chemical composition and recovers chemical substances in a nonselective manner. Second, an efficient analytical scheme must be employed because, after preconcentration, water will likely contain a large number of organics at still relatively low levels of concentration. Four excellent review articles covering identification of trace organics are available (Baker and Malo, 1967; Grob, 1973; Hrutfiord and Christman, 1972; Mieure and Dietrich, 1973). The entire range of preconcentration methods is detailed along with instrumental techniques of identification.

Recently, analytical methods for concentrating and determining organic compounds in water samples were thoroughly reviewed by Chian and DeWalle (1976). Guidelines for quantitative and qualitative screening of organic pollutants in water supplies were described by Suffet and Radziul (1976). A book entitled Identification and Analysis of Organic Pollutants in Water was written by Keith (1976).

Freeze Concentration

First to be considered is the method of freeze concentration. The early work of Shapiro (1961) demonstrated that the method was useful for concentration, but only limited use of this technique has been made in more recent studies. The principle involved is well known. When water is frozen slowly, the first ice crystals to form are relatively pure and clear. Dissolved solids and organic solutes remain in the unfrozen liquid and are gradually concentrated as the ice continues to form.

Baker (1965; 1967a, b; 1969; 1970) has investigated physical aspects (concentration of inorganics, ionic effects, ice washing, etc.) of freeze concentration. Kobayashi and Lee (1964) have studied concentration of chloride and Rhodamine B and showed that recovery efficiency appears to be more a function of the nature of the solute than of its concentration. By

far the most comprehensive study of freeze-drying is that of Kammerer and Lee (1969). They investigated concentration factors and recoveries of glucose, glycine, phenylalanine, and citric acid, and found that essentially complete recoveries at micrograms to milligrams per liter of these compounds levels were attainable. Agitation of the freezing samples presumably aided recoveries. It should be realized that the process consumes much time, and only moderate concentration factors (1 to 20) have been obtained. However, this technique has not been tried with volatile compounds.

Carbon Adsorption

Carbon adsorption of organics, which has seen widespread use as a research tool, is based on organic adsorption on granular activated carbon from a large volume of water, desorption with suitable solvents, and separation of the extract into strong and weak acids and basic and neutral fractions by differential solubility methods. This method is the accepted concentration technique in Standard Methods (1971). Unfortunately, it is subject to numerous criticisms that have been reviewed by Hoak (1962) and Baker and Malo (1967). Organics are adsorbed or desorbed selectively by carbon; some chlorinated hydrocarbons, for example, have shown almost quantitative recovery, while amino acids may be very poorly adsorbed. Also, this method subjects adsorbed organics to potential chemical and biological degradation prior to extraction. Finally, organic residues in fresh activated carbon have been a problem (Hoak, 1962).

Aside from use in determining amounts of organics in water (Lee et al., 1965), most carbon applications have been in recovering phenols and chlorinated phenols (Goren-Strul et al., 1966; Eichelberger et al., 1970). The role of surface acidity in the adsorption of organics has been examined (Coughlin and Ezra, 1968). Carbon was used for concentration in characterizing organic compounds in municipal water supplies by gas chromatography/mass spectrometry (GC/MS) (Kleopfer and Fairless, 1972). One interesting application used carbon for preconcentrating mercaptans, phenols, and organic acids followed by conversion to the pentafluorobenzyl derivatives and subsequent identification by electron capture gas chromatography (Kawahora, 1971).

Resin Adsorption

An adsorbent that overcomes some of the criticisms of carbon is a macroreticular styrene-divinyl benzene polymer (XAD series resins, Rohm and Haas). Both XAD-2 and XAD-7 were used for quantitative sorption of trace organics followed by selective desorption with appropriate eluents (Burnham et al., 1972). Trace amounts of contaminants in the well water of Ames, Iowa, were concentrated by XAD and identified by GC/MS.

In addition to treatment processes based on resin adsorption (Kennedy, 1973), analytical applications include analysis of organic materials in wastewater effluents after chlorination (Glaze et al., 1973) and use as a support for liquid-solid column chromatography (Grieser and Pietrzyk, 1973). Collection of trace organic contaminants in air has also been achieved by concentration on porous polymer beads (Williams and Unstead, 1968; Drarnuks et al.,

1971). Versino et al. (1976) determined organic micropollutants by passing air or water through a Tenax-GC trap followed by thermal desorption and injection into GC or GC/MS for analysis.

One serious deficiency of resin adsorption, however, is the lack of recovery of C_1-C_4 organics, e.g., short chain alcohols, aldehydes, ketones, and acids (Kunin, 1974). This effect has also been noticed by the University of Cincinnati group (Christian, 1973). Any analysis scheme using macroreticular resins would have to employ additional methods for concentrating the organics not recoverable by sorption onto the resins.

Solvent Extraction

Another popular method of concentration is solvent extraction. Much of the interest in liquid-liquid extraction lies in the analysis of pesticides (Environmental Protection Agency, 1971; American Chemical Society, 1972). Various types of continuous liquid solvent extractors have been proposed, both for solvents heavier and lighter than water (Werner and Waldichak, 1962; Goldberg et al., 1971; Campbell and Palmer, 1971). Extractor design and recovery data are also available (Kahn and Wayman, 1964; Goldberg et al., 1973).

Details of extraction procedures are included in an Environmental Protection Agency (EPA) report (1973). Chloroform is an excellent solvent because of its good solvency and the smaller and narrower solvent peak it gives compared to hydrocarbon solvents in GC with flame ionization detection. For concentrating the extraction solvent, the Kuderna-Danish concentrator is the most efficient method for large solvent volumes. It is unnecessary to dry the concentrated solvent before further analysis (Webb, 1964).

Numerous applications of liquid solvent extractions are in the literature. Organic compounds in river water were determined by Hites and Biemann (1972), as were petroleum hydrocarbons and fatty acids by Farrington and Quinn (1973) in wastewater effluents. Human urine has been extracted with ethyl ether to profile volatile metabolites (Zlatkis and Liebrich, 1971). The U.S. Public Health Service completed a comprehensive study on pesticides in drinking water from the Mississippi and Missouri Rivers (Schafer et al., 1969). A review of extraction and identification of organic material on airborne particulates has been prepared recently by Tomkins (1974).

Gas Stripping Technique

The last method to be considered was developed by Melpolder et al. (1953) for determining volatile hydrocarbons in water, more than two decades ago. Only in the last 2 years, however, has it received much attention as a promising technique for concentrating trace organics. The method is a type of "headspace and analysis," involving bubbling a gas through water and trapping the volatilized organics on a small amount of adsorbent (carbon, Tenax-GC, or in a cold trap) followed by introduction and subsequent analysis in a GC or GC/MS system. Although originally designed for hydrocarbons and

later used for that purpose (Lysyi et al., 1966; Swinnerton and Linnenbom, 1967), it recently has been extended for compounds with boiling points of up to 140°C (Novak et al., 1973). The water was stripped with helium and volatile components were caught in a liquid nitrogen trap. Rapid heating of the cold trap introduced the material into the GC. The concentration of organics was 2 to 3 orders of magnitude higher than with solvent extraction methods.

Grob (1973) has further extended the technique of Novak et al. (1973) to include substances up to C_{24} by making two modifications to Novak's system. First, a closed helium stripping system is used to reduce contamination from large volumes of helium gas. Second, a very small amount of charcoal is used instead of a liquid N_2 trap; this avoids unwanted moisture in the GC system. Zlatkis et al. (1973a,b) have used a similar system in profiling volatile organics in gases and biological fluids. Their method allows for heating of the water while it was being stripped, followed by collection on Tenax-GC, and then introduced to a GC. Tenax-GC is a porous polymer (2,6-diphenyl-p-phenylene oxide) that efficiently adsorbs and desorbs organics, and is capable of sustaining relatively high temperatures (375°C limit). Decomposition of Tenax-GC due to its reaction with nitrogen oxide or nitric acid to form 2,6-diphenyl-p-quinone was observed by Neher and Jones (1977) while sampling stack gases. However, it was observed that degradation of Tenax-GC does not affect the efficiency or capacity of a sampling system. Mieure and Dietrich (1973) have also used stripping analysis for determination of trace organics in air and water samples. Bellar and Lichtenberg (1974a) have recently shown that the ppt (µg/L) quantity of organics having a boiling point of less than 150°C and a solubility in water of less than 2% can be determined satisfactorily with the gas stripping method. Bellar et al. (1974a) have also identified and quantified some organohalides in chlorinated drinking waters using stripping followed by GC/MS analysis. Bellar et al. (1976) also determined vinyl chloride in water at the ppb level. The same setup as Bellar's has been employed by the EPA (1974) to determine qualitatively the organic contaminants in New Orleans area water supplies. Becka and Feltl (1977) used the stripping technique to concentrate hydrocarbons in the atmosphere of experimental biological containers on Porapak Q. A sample bottle purging method was used by Dressman and McFarren (1977) to determine sub-ppb levels of vinyl chloride in water.

High Pressure Liquid Chromatography

Although liquid chromatography (LC) is useful in separating the nonvolatile organic compounds and is comparable to GC separation for the volatile ones, identification of the nonvolatile organic compounds can be a problem. However, compared to GC, LC has certain advantages that GC cannot achieve (Kirkland, 1971). Nonvolatile compounds and thermally unstable compounds can be conveniently analyzed by LC but not by GC. Therefore, ionic compounds, labile, naturally occurring compounds, polymers, and high molecular weight polyfunctional compounds are included in the list of LC chromatographable compounds but not in the list for GC. Only about 20% of the known compounds lend themselves to analysis by GC. Although the

techniques of derivative GC, prolysis GC, and reaction GC can be employed to broaden the area of GC chromatographable species, interpretation of the chromatogram and control of the additional reaction process can become a problem. Another important advantage of LC is that the larger variety of moving and stationary phases available in LC permits a much wider range in selectivity. High pressure liquid chromatography (HPLC) greatly enhances the power of LC due to its speed and resolution.

The application of LC is very wide because it can analyze many varieties of compounds. It has been used by Burnham et al. (1972) successfully to identify and estimate the neutral organic contaminants in potable water. Trace organic contaminants at the ppm level were extracted by macroreticular resins (Fritz and Tateda, 1968). After the extraction, identification and quantitation were achieved by means of UV absorption or GC/MS technique. Carboxylic acids and phenols were extracted from water on a macroreticular weak anion exchange resin (Amberlyst) as well as on a XAD-2 column. The XAD-2 column has also been used to separate nitrophenols and chlorophenols from water by Grieser and Pietrzyk (1973). Bhatia (1973) has demonstrated that phenols in industrial wastewaters could be accurately determined by aqueous LC to levels as low as 10^{-6} M. Liquid chromatography was used instead of GC, even though phenols are low-boiling compounds, because of interference from tailing of the water peak, the appearance of memory or "ghost" peaks, and the upsetting of electrical stability of flame ionization detectors by water vapor that accompany GC.

Other applications of LC are briefly described below. With the HPLC technique, phthalic esters have been separated on a Corasil II column, TCA cycle organic acids on a Corasil II column, carbohydrate on a Vydac cation exchange column, and organic mercury compounds on a Corasil I column (Funasaka et al., 1974). Because organic mercury compounds are easily decomposed in the GC injection port, they cannot be quantified by GC; these compounds were quantified by atomic absorption (AA) techniques following LC separation. HPLC was used to separate 16 common street drugs by Chan et al. (1974) using Corasil II as the column packing; these drugs were further analyzed with UV or MS after LC separation. Oligonucleotides have been separated on an ion exchange HPLC by Gabriel and Michalewsky (1973). High speed gel-permeation chromatography has been used to characterize the polymeric materials and to obtain the molecular weight distribution (Cooper et al., 1973; Limpert et al., 1973). Different columns, properties, and applications have been discussed in detail (Kirkland, 1971; Takahagi and Setsuya, 1974; Pryde, 1974; Williams et al., 1973). Several methods have been used to identify an unknown compound after LC separation. Comparison of the retention time with known compounds using the refractive index (RI) or application of more sensitive UV detectors, micro IR spectroscopy of eluting peaks and even MS analysis of each eluting peak fraction are the commonly acceptable methods of identification, although they are tedious and time consuming.

Based upon this review of the literature, our efforts in analyzing the MUST hospital RO permeates are divided into two distinct areas: (1) analysis of volatile organics and (2) analysis of nonvolatile organics. It shoul

be realized that the volatile organics referred to here are limited only to those compounds that can be easily stripped off from sample solutions, whereas the nonvolatiles are those that cannot be easily stripped off. The latter can be further classified into GC volatiles and GC nonvolatiles. Of course, this depends on what GC column is used and how the column is operated in defining GC volatiles and nonvolatiles.

The term volatile organics used in this report is commonly referred to as purgeable organics, whereas GC volatiles are intermediately volatile organics. Since the bulk of the organics found in the RO permeates is volatile organics (i.e., purgeables), the term nonvolatiles will be used indiscriminately for both GC volatile and GC nonvolatile compounds throughout the text.

Determination of Volatile Organics

Headspace stripping of volatile organic compounds onto an adsorbing trap followed by thermal desorption into a gas chromatography or gas chromatography/mass spectrometry system for analysis has recently received widespread recognition in the area of pollution and medicine studies. Dowty et al. (1975b; Dowty and Laseter, 1975) have used this technique to analyze the halogenated hydrocarbons in New Orleans drinking water and blood plasma and to monitor the low molecular-weight volatile organics introduced in the municipal water treatment process. The same technique has recently been used by Politzer et al. (1975) to determine the volatile constituents of lung, brain, and liver tissues. In their studies, samples were first heated to 95°C and stripped for 1 hour with a stream of helium gas. Tenax-GC was used as the trapping material to adsorb the stripped organics. After stripping and adsorption, the trap was placed in the injection port of a gas chromatograph and desorbed at 200°C for about 7 minutes with the aid of GC carrier gas flow. The desorbed organics were further trapped by a gas chromatographic precolumn immersed in a -78°C dry ice-acetone bath. At the end of the desorption process, the volatile organics were transferred to and concentrated in the precolumn. The GC oven was then heated from room temperature to 170°C for GC analysis. The GC precolumn consisted of 1.5-m x 0.05-inch inner diameter, stainless steel tubing coated with Emulphor ON-870; the GC column employed was of the capillary type coated with 10% GE SF-96 and 1% Igepal CO880. For water sample analysis, the sample size was usually 700 mL, and glass condensers were employed to avoid collecting moisture in the trap. Organic compounds at ppb levels have been detected with this headspace stripping/GC technique. The same technique has been employed to test the New Orleans drinking water supply (Dowty et al., 1975a), using GC/MS techniques for identification purposes. Procedures for stripping and injecting volatile organics for gas chromatographic determinations have been automated (Dowty et al., 1976a), and a computer-based chromatograph has been developed for automated water pollution analyses (Dowty et al., 1976b). Also described was a device requiring no valving, which provides a simple means for transferring volatiles adsorbed on a substrate from that substrate to a gas chromatograph-mass spectrometer (Ligon and Johnson, 1976). Komers and Sir (1976) determined methanol and ethanol in aqueous solutions at the

ppm level by the gas stripping/GC method after converting alcohols to alkyl nitrites. Equipment and a procedure for stripping trace organic substances from water was described by Grob and Zurcher (1976). A closed stripping loop was employed. Organics were recovered from the adsorbent by organic solvent extraction instead of thermal desorption for GC determination. The headspace stripping technique was also used by Smith et al. (1977) to determine organic gases from poultry manure. Methanol, ethanol, n-propanol, 2-butanol, 2-butanone, acetone, and many other compounds were determined at ppm levels after they were concentrated on a Porapak Q5-Carbosieve B trap.

Wilkinson et al. (1975) have used the headspace gas chromatographic method to determine ethanol in blood samples. A sample of only 20 to 50 µL was warmed in a 60°C water bath for 3 minutes. Less than 1 mL of headspace gas was sampled and injected into the GC. Porapak Q was used as the GC packing. The sensitivity was 3 µg/mL. The headspace GC technique has also been used to analyze qualitatively lacquer and similar solvent mixtures (Levadie and MacAskill, 1975). Recently, a semi-automatic headspace sampling and GC gas-injection system has been developed by Cowen et al. (1975). The sampling system was integrated into the GC system using an 8-port gas sampling valve. With the advent of such a system, the sample throughput rate can be improved greatly. A new headspace gas-injection system incorporating a variable volume device was described by Vitenberg et al. (1975). It allows repeated injections without changing the concentration of substance distributed between the gas and liquid phases. An automated headspace gas sampling and injection system is also available from Perkin-Elmer, Model F-42 GC (Perkin-Elmer, 1977). Liquid as well as solid samples can be analyzed (Kolb, 1976).

A direct aqueous injection/GC/quadruple mass spectrometric procedure was considered as a supplement to conventional solvent extraction in analyzing water and wastewater samples for volatile compounds that cannot be found with solvent extraction (Harris et al. (1974). Many organic solvents can be determined at concentrations of 1 to 50 ppm using conventional data acquisition techniques. The detection limit can be lowered to about 50 ppb using real-time data acquisition from subsets of the ions used in conventional mass spectrometry. Also, chemical ionization mass spectrometry has been used to determine organic compounds in aqueous solutions at the ppm level (Price et al., 1975). The principal reagent ions are $H_3O^+ (H_2O)_n$ where n = 0-5.

Determination of Nonvolatile Organics

Organic compounds that cannot be stripped easily from the sample solution with the headspace method are referred to as nonvolatile organics. The techniques available for analyzing nonvolatile organics will be reviewed in this section. In general, solvent extraction or resin adsorption is the method commonly used for concentration, with GC or liquid chromatography being used for analysis.

Phenols in water have been determined by the technique of resin adsorption and GC by Chriswell et al. (1975), who used the A-26 anion-exchanger (Diamond Shamrock) to adsorb phenolate from water after the pH was adjusted to basic. The adsorbed phenolates were converted to phenols and then eluted from resins. After concentration by evaporation, the eluants were analyzed by GC. The GC columns used were 5% OV-17 on Chromosorb W AW DMCS and Tenax-GC. Gold (1975) has used carbon black to adsorb carcinogens and oxygenated polyaromatics. Rosen's fractionation procedures (Rosen and Middleton, 1955) were followed to separate the saturated hydrocarbons, polycyclic aromatic hydrocarbons, and polar compounds on silica gel from the neutral eluants. The fraction of polycyclic aromatic hydrocarbons was separated on a GC column using SE-52 on Chromosorb W. The polar compounds were separated by reverse-phase high-pressure liquid chromatography on a Perkin-Elmer Octadecyl Sil-X-1 column with a mixture of 30% water and 70% methanol as the mobile phase. The polycyclic aromatic hydrocarbons in white petroleum products were separated by gradient elution adsorption chromatography on alumina or by gel permeation chromatography and identified using fluorescence and phosphorescence spectrometry (Popl et al., 1975). The polycyclic aromatic hydrocarbons were concentrated by frontal elution on silica gel. They were separated from polar compounds by adsorption chromatography on basic alumina. Ford et al. (1975) have used methylene chloride to extract pesticides from water and have determined pesticides by GC with 10% DC-200 on a Gas Chrom Q column and 1.5% OV-17 and 1.95% QF-1 on Gas Chrom Q. The vinyl chloride monomer was extracted with m-xylene and then determined by GC with a 5% SE-30 on a Chromosorb G column (Ernst and Van Lierop, 1975). Renberg (1974) has employed ion-exchange techniques for determining chlorinated phenols and phenoxy acids in organic tissue, soil, and water. The water sample was eluted through a Sephadex QAE 25 anion exchanger. The chlorinated phenols and phenoxy acids were eluted with acidified methanol and then extracted with benzene. Methyl ether of phenols and methyl ester of phenoxy acetic acids were determined by GC after methylation with diazomethane. Carpenter et al. (1976) used N-vinyl-2-pyrrolidone polymer to separate and concentrate phenolic materials from dilute aqueous solutions. Phenolic compounds were then recovered with a 4 M urea solution. Tenax-GC has been used to extract pesticides and polynuclear aromatic hydrocarbons from surface and drinking water samples (Leoni et al., 1975). Diethyl ether was used to recover organic compounds from the Tenax-GC column. The recovery was better than 90%. An XAD resin sorption and ether elution procedure has been employed by Junk et al. (1976) to recover pesticides from water. Phenolic compounds were also determined by GC after formation of TMS derivatives (Fell and Lee, 1976; Drawert and Leupold, 1976; Casteele et al., 1976) and acetate derivatives (Fell and Lee, 1976). Determination of phenols by the 4-aminoantipyrine method (Standard Methods, 1971) was automated with a Technicon AutoAnalyzer (Gales and Booth, 1976).

Determination of Carboxylic Acids

Formate has been quantitatively determined by Carter and Moore (1975) in plating baths by simply using a TOC analyzer. Samples were analyzed in the 90°C vaporization zone instead of in the pyrolysis zone. The formate concentration was calculated from the difference in TOC between acidified and

unacidified samples. Phenacyl esters of fatty acids have been formed using crown ethers as catalysts and determined by liquid chromatography using UV detection at 254 nm (Durst et al., 1975). Aliphatic acids (C_2-C_8) were extracted from biological materials with a chloroform/ethanol (94:6) solution. 2,2,2-trichloroethyl esters of the acids were prepared from 2,2,2-trichloroethanol (Alley et al., 1976), and the halogenated esters were then determined by electron-capture GC. Volatile fatty acids (C_2-C_5) were vacuum distilled from biological material for later GC determination (Tyler and Dibdin, 1975). Formic and acetic acids were determined by GC after steam distillation of aqueous samples, evaporation of alkaline distillate, and acidification of concentration distillate (White and Leenheer, 1975). A 4-foot glass column packed with 100/120 mesh Porapak Q coated with 3% phosphoric acid was used. The detection limits for formic and acetic acids were 1 ppm and 30 ppb, respectively. Dicarboxylic acids such as citric, succinic, malic, and tartaric acids were determined in grape must and wine by high-pressure LC on an Aminex A-6 cation exchanger column (Rapp and Ziegler, 1976). Harris (1975) reviewed the determination of fatty acids by reaction GC. However, formic, acetic, and propionic acids were not included.

Carboxylic acids including formic, acetic, and pyruvic acids were determined at sub-ppm levels by a colorimetric method (Kasai et al., 1975; Nakajima et al., 1976). Hydroxamic acid was formed through a direct coupling of carboxylic acid and hydroxylamine by the aid of dicyclohexylcarbodiimide. Separation and determination of carboxylic acids have also been automated (Kasai et al., 1977). Formic and acetic acids as well as other fatty acids were determined by thin-layer chromatography (TLC) after reaction with a fluorescent reagent (Dunges, 1977). Acetate and acetic acid were measured at ppm levels by laser raman spectrometry (Cunningham et al., 1977). Deguchi et al. (1977) chromatographed formate, acetate, oxalate, citrate, and many inorganic anions on a Sephadex G-15 column with elution by sodium chloride solution. These ions were followed by examining the concentration distribution of the background electrolyte (sodium chloride) by argentimetry. Carboxylic acids (C_1-C_{24}) in aqueous solution were determined by capillary GC at ppb levels after esterification with ethyl iodide (Gloor and Leidner, 1976).

General

The apparatus for concentrating volatile organic pollutants from water for GC determinations is available commercially from Tekmar Company (Grote, 1975). It is essentially based on Bellar's system (Bellar and Lichtenberg, 1974b). Dilling et al. (1975) have studied the evaporation rates and reactivities of methylene chloride, chloroform, 1,1,1-trichloroethane, trichloroethylene, tetrachloroethylene, and other chlorinated compounds in dilute aqueous solutions. They found that 50% of these five compounds was evaporated in less than 30 minutes and 90% in less than 90 minutes when stirred at 200 rpm in water at about 25°C in an open container. Addition of various contaminants to the water had relatively little effect on the rates

of evaporation or disappearance of these chlorinated compounds. The study implies that the low molecular-weight chlorinated hydrocarbons would not persist in well-mixed natural water bodies because of evaporation. Evaporation rates of chloromethanes, ethanes, ethylenes, propanes, and propylenes from dilute aqueous solutions were later studied by Dilling et al. (1977). Pellizzari et al. (1975a) evaluated the collection efficiencies of various adsorbents while concentrating hazardous vapors from a flowing stream. Tenax-GC, Porapak Q, Chromosorb 101, and Chromosorb 104 were shown to give better than 90% efficiencies in trapping vapors of epoxides, β-lactones, sulfonates, sulfones, N-nitrosamines, chloroalkyl ethers, aldehydes, and nitro compounds from synthetic air-vapor mixtures at 0.25 L/minute. Carbowax 600 and 400, as well as oxypropionitrile coated on or chemically bonded to supports, was also found very efficient. The thermal desorption of organic vapor from adsorbents was also studied by the same research group (Pellizzari et al., 1975b). The percent recovery of several hazardous vapors adsorbed on Tenax-GC using thermal desorption was again better than 90% at 50- and 100-ng levels.

Trace amounts of vinyl chloride in air were determined by a concentrator GC system (Ahlstrom et al., 1975). Vinyl chloride was adsorbed from the air stream on an activated charcoal trap. The trap was then heated at 400°C for 2 minutes in the injection port of a gas chromatograph to desorb vinyl chloride for GC determination using a Porapak QS column at 90°C. Hydrogen cyanide and sulfur dioxide in air were also determined with the same technique (Liebman et al., 1975) using Carbosieve B as the adsorbent and Carbosieve B/Porapak QS in the GC column. A similar technique was used to determine organic vapors in air to obtain characterization profiles for pollution studies (Bertsch et al., 1974). Tenax-GC was the adsorbent. The desorbed volatiles were concentrated in liquid N_2-cooled precolumn before being analyzed by GC.

Austern et al. (1975) found that 58% of trichloroethylene was lost during Kuderna-Danish (K-D) concentration of Freon extracts because of the high volatility of this compound. With other model compounds studied by these authors, the recovery from water by Freon extraction and K-D concentration was 99% at the ppb level. These compounds consisted of styrene, p-xylene, ethylbenzene, nitrobenzene, acetophenone, o-anisidine, anethole, turpentine, nonyl phenol, and dimethyl phthalate. A simple condenser was installed on the top of the Synder column of the K-D evaporator to recover the solvent for reuse (Wauchope, 1975). One microgram of trifluralin, a herbicide with a relatively high vapor pressure, was added to 200 mL of n-hexane or methylene chloride for K-D evaporation. The recovered solvent was further evaporated to 5 mL using a K-D and analyzed by GC. The concentrated solvent contained no detectable amount of trifluralin (detection limit ~ 1 pg), showing that the n-hexane or methylene chloride recovered from the above setup can be reused for a savings of about $0.50 for every 200 mL of glass-distilled common solvents. Pollution and fire hazards are also reduced. A spray vaporization technique was used by Chriswell (1977) to remove trace amounts of organics from water.

Trace amounts of volatile halogenated hydrocarbons in water can be determined by GC after extraction by pentane (Richard and Junk, 1977) and by methylcyclohexane (Mieure, 1977). Kaiser and Oliver (1976) equilibrated water under a reduced pressure and sampled headspace gas for the determination of volatile halogenated hydrocarbons by ECD-GC. These methods are more rapid than the gas stripping technique. Morris and Johnson (1976) observed that turbidity is an indicator of elevated organics loading resulting from agricultural runoff, which is a source of halomethanes in drinking water. Suffet et al. (1976) identified 1,1,1-trichloroacetone in drinking water as the precursor in haloform reactions. Analytical methods for determining haloforms in drinking water were reviewed by Kissinger and Fritz (1976).

Development of a Distillation Technique for Determining Volatile Organics in RO Permeates

The concentrations of the low molecular-weight volatile compounds present in the permeates of MUST wastewaters are generally on the order of ppm as can be seen from Tables 6, 7, and 9 for methanol, ethanol, acetone, ether, and formaldehyde. It is therefore possible to employ direct GC injection to analyze these compounds with a suitable GC column under proper GC operating conditions. The RO permeates of several MUST wastewaters including that of the laboratory waste from Walden Research were analyzed on a Carbowax 1500/Carbopack A column (alcohol column). The concentrations of methanol and ethanol determined are listed in Table 9. The results of analysis show that, at least for the determinations of methanol and ethanol in RO permeates of composite and laboratory wastewater, the direct GC injection technique is applicable. However, concentration methods are needed if trace amounts of volatile polar water-soluble organics are to be determined.

TABLE 9. CONCENTRATIONS OF METHANOL AND ETHANOL IN RO PERMEATES OF WASTEWATERS

	Concentration (ppm)			
	TOx Composite	Tx Shower	Tx Laundry	Walden Lab. Waste
Methanol	262.0 (98.25)[a]	Not detected	Not detected	237.5 (89.06)
Ethanol	28.1 (14.66)	31.6 (16.49)	Not detected	8.0 (4.17)

a. Equivalent TOC in ppm.

Preliminary Evaluation of Distillation Technique

The distillation technique was evaluated as to its capability to concentrate the volatile organics. The volatile organics present in RO permeates are mainly low molecular-weight polar compounds and are thus highly soluble in water. As such, they are not expected to be extracted efficiently with organic solvent from aqueous solutions. Neither is the freeze-drying technique expected to perform as well because the vapor pressure of these low molecular-weight volatile compounds are higher than that of ice. On the other hand, the distillation technique takes advantage of high vapor pressure for the volatile compounds and is therefore expected to concentrate volatiles in distillate.

A simple distillation apparatus consisting of a 250-mL round bottom flask, one 1.85-inch Vigreux fractionation column with 11-indentation, a distilling head with a thermometer, a water cooling condenser, and a distillate collector was used. The sample solution was distilled and the vapor temperature was controlled at 100°C. The Vigreux column provides a relatively high throughput with a low holdup. The height equivalent to a theoretical plate (HETP) is about 7 to 12 cm. One hundred milliliters of 1 ppm mixture each of methanol, ethanol, acetone, isopropanol, diethyl ether, and methyl ethyl ketone were distilled and the first 10 mL of distillate were collected. Similarly, 1 liter of 1 ppm mixture was distilled in a 2-liter flask and the first ten 10-mL distillate fractions were collected separately. Distillate was analyzed by GC on the alcohol column.

Results of these tests are tabulated in Table 10, which lists the concentration of all the distillate fractions. From the listed concentration, the percentage of recovery can be calculated. For example, the percentage of recovery for each component is equal to the listed concentration multiplied by 10 for the first 10-mL distillate from distilling 100 mL distillate from distilling 1 liter solution. The percentage recovery is the same as the listed concentration for the first ten 100-mL distillate fractions from distilling 1 liter solution. As can be seen from the first row of data in Table 10, with the exception of methanol, the concentration is increased by a factor between 3 and 8 for the first 10-mL distillate from the 1-liter sample compared to that from the 100-mL sample. Later fractions from the 100-mL sample were also collected and tested. In the second 10-mL fraction, only 1.4 ppm of methanol and 0.8 ppm of ethanol were detected. For the first 100-mL distillate from distilling 1 liter of solution, the calculated concentration is enhanced by a factor of about 9 for ethanol, acetone, and methyl ethyl ketone; about 10 for isopropanol; about 6 for methanol; and only about 4 for ether. The concentration enhancement is quite significant for the first 10-mL distillate from distilling 1 liter of sample solution. Methyl ethyl ketone is concentrated from 1 to 61 ppm. Methanol is only enhanced by a factor of 11, which is the lowest among the six compounds tested. As can be seen from Table 10, later fractions eventually dilute the first 10-mL distillate.

TABLE 10. RECOVERY OF VOLATILES BY DISTILLATION TECHNIQUE[a]

Fraction	Concentration (μL/L) Methanol	Ethanol	Acetone	iso-propanol	Ether	Methyl Ethyl Ketone
A. Collection of First 10-mL Distillate from 100-mL Sample Solution of 1 μL/L						
1st 10 mL	6.7	7.9	8.3	8.3	4.0	7.8
B. Collection of First Ten 10-mL Distillate Fractions from 1-Liter Sample Solution of 1-ppm Mixture						
1st 10 mL	10.9	22.0	44.0	31.2	31.5	61.0
2nd 10 mL	7.9	13.3	19.1	22.8	6.2	17.4
3rd 10 mL	7.5	11.6	11.5	13.1	2.3	7.9
4th 10 mL	6.1	8.8	2.2	9.7	1.0	3.6
5th 10 mL	7.0	8.3	4.6	7.4	0.6	1.9
6th 10 mL	6.2	7.6	3.0	5.4	0.5	0.9
7th 10 mL	4.4	5.7	1.7	3.7	0.0	0.3
8th 10 mL	4.1	4.9	1.0	2.4	0.0	0.0
9th 10 mL	4.3	4.2	0.8	2.0	0.0	0.0
10th 10 mL	3.8	3.8	0.6	1.5	0.0	0.0
1st 100 mL[b]	6.2	9.0	9.4	9.9	4.2	9.3

a. Results are obtained from one experimental run.
b. Calculated concentrations if ten 10-mL fractions were mixed.

In practice, it is suggested that the first 10-mL distillate be collected for analysis whether distilling 100 mL or 1 liter of solution. Although it might be expected that higher concentrations could be found in the earlier few milliliters of the distillate than that of the first 10 mL, high variation in concentration from run to run can result, because it takes a few milliliters of distillate to wet the glass wall before the distillate is collected in sizable amount. The recovery is somewhat better when collecting 100-mL distillate from 1 liter of sample than 10 mL from 100 mL of sample. If the amount of sample was not a limiting factor, distillation of 1 liter of sample solution to collect the first 10-mL distillate is recommended to concentrate volatiles. However, if this is the case, distillation of 100 mL of sample with the collection of the first 10-mL distillate is the alternative.

Concentration of Trace Low Molecular-Weight Volatile Polar Organics in Water by Distillation Method

Introduction. While conducting research on the posttreatment of reverse osmosis permeates and activated carbon effluents originating from hospital wastewaters for potential reuse, it was necessary to determine sub-ppm levels of low molecular-weight water-soluble volatile polar organics (VPO's), such as methanol, ethanol, propanol, acetone, methyl ethyl ketone, and lower aldehydes, which normally pass through the RO membrane (Chian and Fang, 1974). Direct injection of an aqueous solution containing these VPO's into a gas chromatograph provides only limited success at ppm levels, as mentioned earlier. The use of preconcentration methods is thus necessary when working at sub-ppm levels.

Most of the well-developed concentration methods (Bellar and Lichtenberg, 1974b; Grob et al., 1975; Junk et al., 1974; Bertsch et al., 1975) were found to be unsuitable for low molecular-weight water-soluble VPO's, though they were successfully used for concentrating from water less water-soluble volatile organics such as higher alcohols, ketones, aldehydes, ethers, and esters as well as halogenated, aliphatic, and aromatic hydrocarbons. Liquid-liquid extraction is not applicable because the solubility of low molecular-weight VPO's in water is high and also because of the nonpolar nature of most extracting solvents when extracting organics from water. Sorption on macroreticular resins fails to retain low molecular-weight VPO's because of their high solubility in water and poor sorption efficiencies. Gas stripping onto polymer adsorbents for concentrating low molecular-weight VPO's is only partially successful due to low stripping efficiency and breakthrough of these compounds from the adsorbents (Bertsch et al., 1975; Kuo et al., 1977b). Freeze-drying, e.g., at -50°C, is not expected to be satisfactory because the vapor pressures of the VPO's are higher than that of ice at that temperature.

Membrane/mass spectrometry has been employed to determine some of the VPO's, such as acetone and 2-propanol, by direct injection of a few milliliters of aqueous sample (Mieure et al., 1976). The reported detection limit is approximately 50 ppb for both compounds. Because a mass spectrometer is not available in this laboratory, it was not evaluated for its potential application.

Distillation technique has been used by Loy (1973) as an EPA procedure to preconcentrate volatile organics in distillate before gas chromatographic runs. The basic principle of this technique is to take advantage of the high volatility of VPO's to enrich them in a small volume of distillate from distilling a large volume of aqueous sample. Two-stage distillation was employed by Low (1973) to distill 500 mL of sample solution and to collect 1 mL of final distillate. The recovery was generally lower than 70% for many compounds studied including low molecular-weight VPO's. These compounds could be determined by gas chromatography at 1 to 10-ppb level after preconcentration by distillation. The lower limit was achieved when a larger sample was distilled and distillates were combined for a final distillation to collect 1 mL of distillate for gas chromatographic analysis. The purpose of this study was to investigate further whether distillation could be used as a simple, unique, and highly efficient method for concentration low molecular-weight VPO's for subsequent analysis by gas chromatography. In addition to single-stage and two-stage distillation, fractionation column, sample volume, effect of salting out, and the physical-chemical criteria governing the efficiencies of the distillation method were also thoroughly examined.

Apparatus. Test solutions were distilled in a conventional glass apparatus equipped with a 30 cm by 25.4 mm outside diameter Vigreux fractionation column (K-503500 size 222; Kontes Glass Co., Vineland, NJ) having 11 indentations or a column of the same length packed with glass beads. One and 2-liter round bottom flasks were used for distilling 500-mL and 1-liter aqueous solutions, respectively. Various amounts of the distillate were collected as required. In addition, a micro apparatus was used to distill 100 mL of aqueous solution and collect 10 mL or less of distillate. It consisted of a 250-mL flask and a 13 cm by 19.1 mm outside diameter Vigreux fractionation column (K-28670 Bantam-ware; Kontes Glass Co., Vineland, NJ) having 10 indentations.

The distillates were analyzed with a Hewlett-Packard 5750B gas chromatograph equipped with a flame ionization detector (FID) and a 183 cm by 2 mm inside diameter glass column packed with 0.2% Carbowax 1500 on 60/80 mesh Carbopack C (Supelco, Inc., Bellefonte, PA). The gas chromatograph oven temperature was programmed from 60° to 150°C at a rate of 8°C/minute with a 2-minute initial and a 5-minute final holding time.

Reagents. A standard stock solution of each compound was prepared from ACS reagent grade chemicals using distilled, deionized water. The solutions were mixed and diluted prior to conducting the experiments. The aldehyde mixture was, however, prepared separately because these compounds could not be resolved from some of the alcohols and ketones using the gas chromatographic column described previously. During the distillation process, the vapor temperature between the fractionation column and the condenser was held at 100°C. In the study of the two-stage distillation process, the first 100 mL of distillate obtained from distilling a 1-liter solution was redistilled and the first 10 mL of distillate was collected for analysis. To study the effects of salting out, 213 grams of dried sodium sulfate was added to a flask containing 1 liter of solution. In all cases, averaged concentrations were reported from either duplicate or triplicate runs.

Fractionation Column and Sample Volume. To compare the efficiency of the Vigreux and the glass bead packed fractionation columns in concentrating the low molecular-weight VPO's, the first 100 mL of distillate, collected from distilling 100, 500, and 1,000 mL of solution, were analyzed on the gas chromatograph. The results are shown in Table 11. Except for diethyl ether, the glass bead column yielded a higher concentration of the test compounds in the distillate for all three sample volumes, as can be seen from the concentration factors in Table 11. The higher vapor pressure of diethyl ether, which tends to evaporate from the distillate during the distillation process, might account for the inconsistent results. The loss of organics from distillate, however, can be eliminated by chilling the distillate collector.

The improvement in concentrating efficiency using a glass bead column as compared to a Vigreux column is greater for compounds having higher polarity and for larger sample volumes. The improvement, however, is insignificant for compounds that are less polar or have higher molecular weights, particularly if the sample volume is smaller.

Data from Part A of Table 11 are plotted in Figure 12 to better demonstrate the relationship between sample volume and the concentration of low molecular-weight VPO's in the distillate. The fact that the amount of each compound collected in a given volume (e.g., the first 10 mL) of distillate does not increase linearly with the increase in sample volume according to the broken line in Figure 12 indicates that the relative volatility (α_{12}) of these model compounds--the ratio of their vapor pressure to that of water--is not infinite. Also, it is worthwhile to note that the increase in concentration of these compounds in the first 10 mL of distillate starts leveling off as the sample size increases. For each compound, the relative concentration at which the concentration in the distillate starts to level off can be related to the α_{12} of the compound.

Values of α_{12} for representative model compounds are given in Table 12. They were calculated according to the equation shown in the footnote to the table. In general, a higher value of α_{12} is characteristic of the relatively nonpolar compounds. For example, methanol, which is relatively polar, has a much smaller value of α_{12} than the less polar methyl ethyl ketone. As a result, the concentration of methanol in the distillate is lower, especially under conditions where leveling off occurs. Therefore, the sample volume at which leveling off will occur can be determined by the α_{12} of each compound. A smaller value of α_{12} will cause the distillate concentration to level off at a smaller sample volume, as can be seen from Figure 12 and the values of α_{12} from Table 12. Therefore, the increased concentration in the distillate that results from distilling a larger volume of sample solution is more distinct for less polar compounds or compounds having larger values of α_{12}.

TABLE 11. CONCENTRATION OF VOLATILE POLAR ORGANIC COMPOUNDS IN FIRST 10 mL OF DISTILLATE

	Methanol	Ethanol	Acetone	2-Propanol	Diethyl Ether	Methyl Ethyl Ketone	Acetal-dehyde	Propional-dehyde
A. Glass-bead-packed column								
1. 100 mL of 10 µL/L mixture								
Conc., µL/L	77.9	87.9	94.5	90.8	55.9	86.3		
& Recovery	77.9	87.9	94.5	90.8	55.9	86.3		
Conc. factor relative to Vigreux column	1.26	1.16	1.05	1.04	1.05	0.98		
2. 500 mL of 10 µL/L mixture								
Conc., µL/L	146.5	198.5	352.5	298.5	245.0	392.5		
% Recovery	29.3	39.7	70.5	59.7	49.0	78.5		
Conc. factor relative to Vigreux column	1.11	1.09	1.01	1.06	0.59	1.01		
3. 1,000 mL of 10 µL/L mixture								
Conc., µL/L	147.5	220.0	516.5	368.5	480.5	623.0		
% Recovery	14.75	22.0	51.65	36.85	48.05	62.3		
Conc. factor relative to Vigreux column	1.17	1.19	1.15	1.15	0.79	1.13		
B. Vigreux column								
1. 100 mL of 10 µL/L mixture								
Conc., µL/L	62.0	75.8	90.2	87.4	53.1	88.5	94.1	93.0
% Recovery	62.0	75.8	90.2	87.4	53.1	88.5	94.1	93.0
2. 500 mL of 10 µL/L mixture								
Conc., µL/L	132.5	182.9	348.0	280.5	412.0	390.5		
% Recovery	26.5	36.6	69.6	56.1	82.4	78.1		
3. 1,000 mL of 10 µL/L mixture								
Conc., µL/L	216.3	184.4	447.8	320.3	609.5	549.5		
% Recovery	12.63	18.44	44.78	32.03	60.95	54.95		

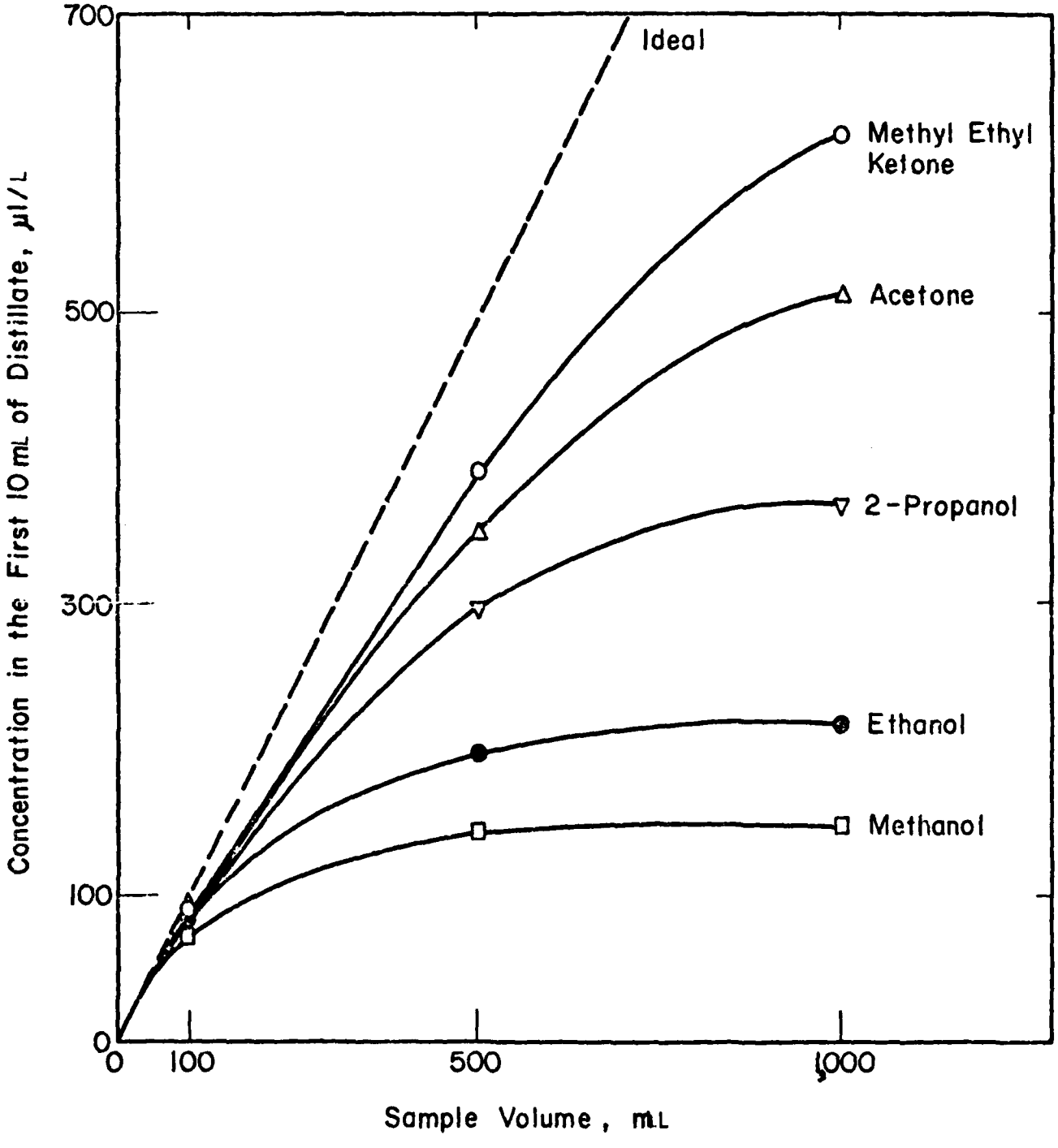

Figure 12. Relation of Concentration of Low Molecular-Weight Volatile Polar Organic Compounds in Distillate and Sample Volume.

TABLE 12. RELATIVE VOLATILITY (α_{12}) OF VOLATILE POLAR ORGANIC COMPOUNDS IN DILUTE AQUEOUS SOLUTION

Compound	Boiling Point (°C)	P_2[a] (mm-Hg)	P_1/P_2[b]	γ_1[c]	α_{12}[d]
Methanol	64.7	185.1	4.1	2.3	9.4
Ethanol	78.4	332.8	2.3	> 4.7[e]	> 10.7[e]
2-Propanol	82.5	292.8	1.9	11.0	21.3
Acetone	56.2	125.0	6.1	7.8	47.2
Methyl Ethyl Ketone	79.6	349.5	2.2	31.6	68.6
Acetaldehyde	20.2	17.8	42.8	4.9	205.8

a. P_2, vapor pressure of water at the boiling point of the model compound.

b. P_1, vapor pressure of the model compound at boiling point, i.e., 760 mm Hg.

c. γ_1, activity coefficient of solute at infinite dilution and 100°C (see Perry's Chemical Engineers' Handbook, 1963).

d. Relative volatility, α_{12}, between the model compound and water; $\alpha_{12} = (P_1/P_2)(\gamma_1/\gamma_2)$. Activity coefficient, γ_2, for water is equal to unity in dilute aqueous solution.

e. γ_1, and thus α_{12} for ethanol, was calculated based on data obtained at 25°C; hence, γ_1 and α_{12} should be higher at 100°C.

Two-Stage Distillation. It may be seen from Part D of Table 13 that, on the average, approximately 90% of the model compounds can be recovered in the first 100 mL of distillate from a 1-liter sample. Approximately 80% can be recovered in the first 10 mL of distillate from a 100-mL sample. Therefore, if the 100 mL of distillate is redistilled to obtain 10 mL of distillate (two-stage distillation), the overall recovery will be approximately 72% while reducing the volume by a factor of 100. The final concentration in the distillate obtained from this two-stage process is consequently about 720 µL/L if a feed solution containing 10 µL/L of the compounds is used. The two-stage distillation process can thus be employed to increase the concentration of the VPO's by almost two orders of magnitude.

The experimentally determined concentration shown in Part A of Table 13 agrees very well with that shown in Part C, which was obtained by calculations based on the data in Part D for two individual distillation stages. These results illustrate that the recovery in the multistage distillation process is the product of the recovery in each individual stage. Comparison of the results given in Tables 11 and 13 shows that the final concentration using the two-stage process is greater than that obtainable with any single-stage distillation process.

The enhancement factor given in Table 13 is the ratio of the concentration obtained by two-stage distillation (Part A) to that for single-stage distillation (Part B). It is greater for the highly polar compounds or for compounds having smaller values of α_{12}, such as methanol and ethanol, than for the less polar ones. This difference results from the fact that, for a 1-liter sample, the recovery of highly polar compounds in the 100 mL of distillate from the first stage of a two-stage process is greater than the recovery in the first 10 mL of distillate from a single-stage distillation. The enhancement factor for diethyl ether is less than unity, possibly the result of evaporation loss (as discussed previously) or of experimental errors.

This study therefore shows that two-stage distillation is a useful means of concentrating VPO's and is particularly useful for enriching highly polar compounds such as methanol and ethanol. It should be mentioned, however, that experimental time is doubled and that a larger volume of sample solution (e.g., 1 liter should be available.

Distillation with Micro Apparatus. In the distillation process, the first few milliliters of distillate contain higher concentrations of VPO's than the subsequent ones. Later portions of distillate will therefore eventually dilute the early ones. Hence, the smaller the amount of distillate collected, the higher the final concentration will be. With the use of a micro apparatus, as little as 1.5 mL of distillate can be collected from 100 mL of sample solution. Figure 13 shows the concentration profiles of various low molecular-weight VPO's in distillates collected in sequence. As can be seen, the concentration in each successive 1.5-mL fraction of distillate decreases logarithmically, which agrees with the theory describing a simple distillation process (Treybal, 1968). This decrease is greater for the less polar compounds due to their greater relative volatility.

TABLE 13. TWO-STAGE DISTILLATION[a]

	Methanol	Ethanol	Acetone	2-Propanol	Diethyl Ether	Methyl Ethyl Ketone
A. Two-stage distillation[b]						
Conc. in distillate, µL/L or % Recovery	39.7	58.8	81.4	82.2	21.0	72.3
Conc. enhancement[c]	3.64	2.67	1.85	2.63	0.67	1.19
B. Single-stage distillation[d]						
Conc. in distillate, µL/L or % Recovery	10.9	22.0	44.0	31.2	31.5	61.0
C. Two-stage distillation						
Calculated Conc., µL/L	41.5	71.1	78.0	82.2	16.8	72.5
D. First-stage distillation[e]						
% Recovery	62	90	94	99	42	93
Second-stage distillation[f]						
% Recovery	67	79	83	83	40	78

a. Vigreux column used throughout.
b. One liter of feed solution at 1 µL/L → 100 mL of distillate → 10 mL of distillate.
c. Concentration enhancement relative to using single-stage distillation as shown in part B.
d. Distillation of 1 L of sample solution to collect 10 mL of distillate.
e. Distillation of 1 L of sample solution to collect 100 mL of distillate.
f. Distillation of 100 mL of sample solution to collect 10 mL of distillate.

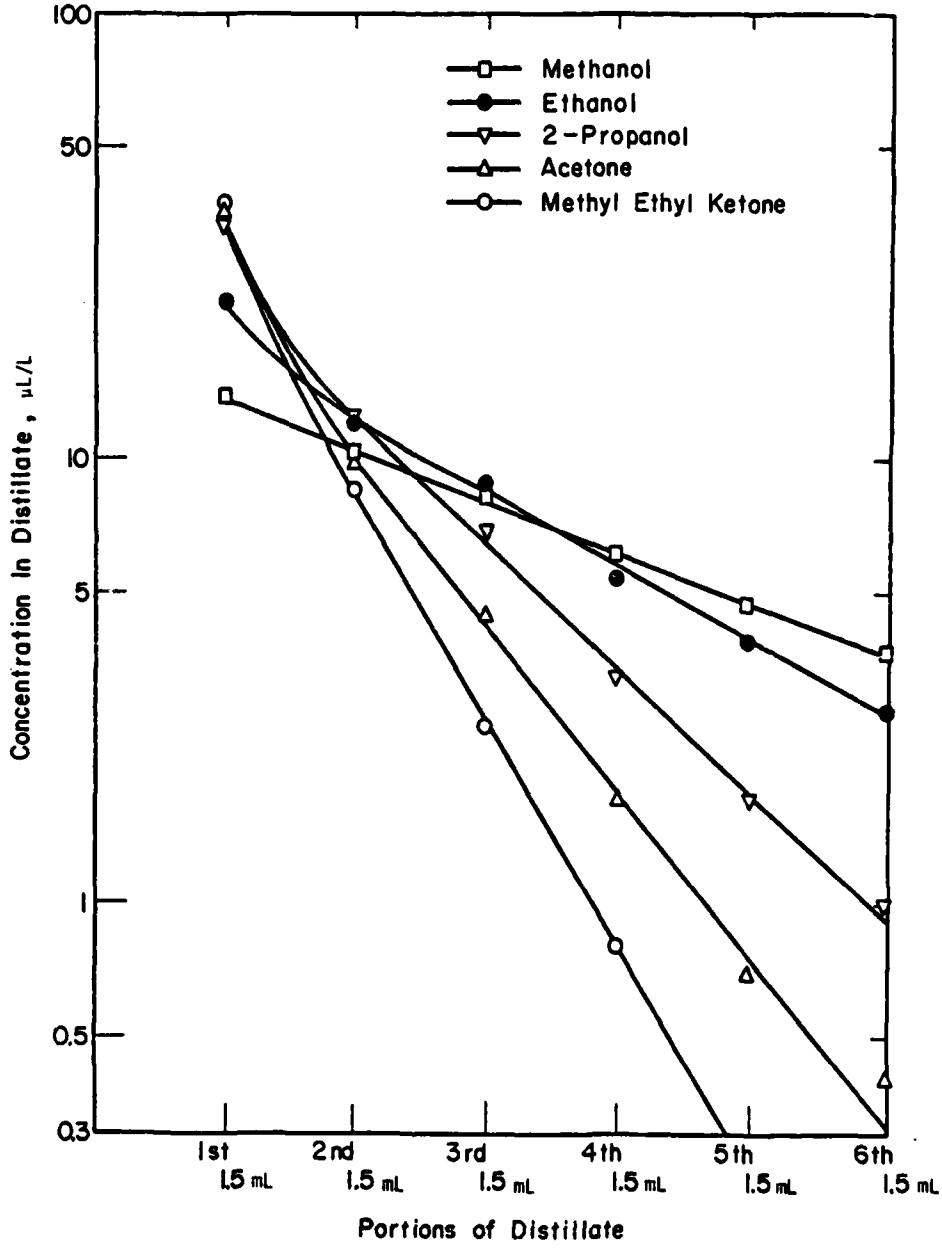

Figure 13. Concentration Profile of Low Molecular-Weight Volatile Polar Organic Compounds in Successively Collected Distillates.

The decrease in concentration from the first to the second fraction, however, is somewhat greater than the exponential drop seen in the later portions, particularly with the less polar compounds. A slight variation in the volume of distillate collected during the early stages of distillation (e.g., the first 1.5 mL of distillate) would consequently cause a greater percentage of error in concentration than it would in the later ones (e.g., the second 1.5 mL of distillate). Therefore, the error would be less in collecting a larger volume of distillate. Obviously, an improvement in the precision of the analysis will have to be compensated by collecting a larger volume of distillate of lower concentration. By using an internal standard in distillation, perhaps less than 1.5 mL of distillate could be collected for analysis while maintaining acceptable precision.

The concentration of low molecular-weight VPO's in the first 1.5 mL of distillate is higher than or comparable to that shown in Table 11 if the sample solutions have a feed concentration of 1.0 μL/L and also comparable to that shown in Table 14, which shows the concentration in 10 mL of distillate derived from 1-liter of sample solution. These results demonstrate that distillation with micro apparatus is the method of choice for concentrating low molecular-weight VPO's if the sample volume is limited to 100 mL and if 1.5 mL of distillate is enough for subsequent chemical analysis. The fact that the total recovery in the 9.0 mL of distillate obtained with the micro apparatus is either slightly better than or comparable to the recovery in the 10 mL of distillate from 100 mL of solution with a large apparatus (as shown in the last row of Table 13) indicates that fractionation efficiency is not at all sacrificed with the use of micro apparatus.

Effect of Salting Out. To determine whether "salting out" the volatile organics in the distillate would improve the recovery of these compounds, sodium sulfate was added to a sample solution containing 12 model compounds, mainly lower alcohols and ketones. The results are shown in Table 14. The enhancement factor due to the effect of salting out is greater for the highly polar compounds or compounds having lower relative volatilities. The enhancement is a result of the increased activity coefficient and thus of the volatility of the organic compounds in the presence of salt in the solution. The activity coefficient of a nonelectrolyte is related to the ionic strength of the solution according to the equation derived by Debye and McAulay (Laitinen, 1960),

$$\log \gamma_o = k\mu$$

where γ_o is the activity coefficient of the nonelectrolyte, μ is the ionic strength of the solution, and k is the salting coefficient, an empirical constant that is positive in the case of salting out. The enhancement thus indicates that the salting-out coefficient is greater for the highly polar organic compounds. Also, the equation shows that if the ionic strength of the solution is doubled, the activity coefficient γ_o will increase to the square of its previous value. The concentration of organics in the distillate is thus appreciably enhanced as a result of increasing the ionic strengths of the solution.

TABLE 14. EFFECT OF SALTING OUT

	Conc. in the first 10 mL of distillate from distilling 1,000 mL of 1 µL/L mixture[a]											
	Methanol	Ethanol	Acetone	2-Propanol	Diethyl Ether	1-Propanol	Methyl Ethyl Ketone	Ethyl Acetate	2-Butanol	1-Butanol	3-Pentanone	n-Amyl Alcohol
A. Without sodium sulfate addition												
Run 1, µL/L	13.7	22.0	50.5	37.9	64.8	31.9	63.9	76.7	49.1	43.5	70.4	51.0
Run 2, µL/L	11.9	19.7	49.3	34.8	42.3	29.0	62.6	72.3	47.6	40.6	69.5	47.9
Run 3, µL/L	12.4	21.5	50.3	38.2	34.2	31.7	67.3	76.2	51.0	43.0	75.7	53.8
Avg. Conc., µL/L	12.7	21.1	50.0	37.0	47.1	30.9	64.6	75.1	49.2	42.4	71.9	50.9
% RSD[b]	7.3	5.7	1.3	5.1	33.7	5.2	3.8	3.2	3.5	3.7	4.7	5.9
% RSD[c] of relative conc.	7.7	4.7	2.9	2.7	34.4	3.2	0.8	2.6	--	3.5	2.1	1.9
B. With sodium sulfate addition												
Run 1, µL/L	24.7	49.9	80.6	71.5	30.3	68.4	83.6	77.9	84.4	83.5	80.0	88.5
Run 2, µL/L	26.2	52.4	89.5	81.0	45.1	76.1	96.9	92.6	89.2	89.6	89.2	93.5
Run 3, µL/L	27.9	56.6	89.0	82.3	59.9	76.5	97.7	97.6	91.0	92.5	95.1	96.8
Avg. Conc., µL/L	26.3	53.0	86.3	78.3	45.1	73.7	92.7	89.4	88.2	88.5	88.1	92.9
% RSD[b]	6.1	6.4	5.8	7.5	32.8	6.2	8.5	11.5	3.9	5.2	8.6	4.5
% RSD[c] of relative conc.	3.3	3.3	3.1	3.4	29.4	2.4	4.8	8.0	--	2.0	5.0	1.0

a. Glass-bead-packed column was used.
b. RSD = relative standard deviation.
c. Calculated on the relative concentration with 2-butanol as the internal standard.

As can be seen in Part B of Table 14, the concentration of the less polar compounds, such as methyl ethyl ketone, in the distillate can be enhanced by almost two orders of magnitude compared to that in the feed solution. Assuming that the detection limit of the gas chromatograph is approximately 0.5 ppm for the less polar compounds, then they can be determined at the 5-ppb level by direct injection of the distillate into a gas chromatograph under the experimental conditions used. For the highly polar compounds, such as methanol, the detection limit is approximately 40 ppb. These detection limits are comparable to that reported by Low (1973) using different distillation procedures. Improvement in concentration factor by distilling a large sample volume sometimes is limited, as discussed previously. However, combining the distillates obtained from several portions of the sample followed by distilling the resulting composite will greatly improve the concentration factor as has been observed by Low (1973).

Statistical data are also included in Table 14 to show the percent relative standard deviation (%RSD) based on triplicate runs. Precision is improved by a factor of approximately 2 if 2-butanol is employed as the internal standard. 2-Butanol was selected as the internal standard because it is well resolved from the other model compounds studied and because it has a medium value of recovery and a medium gas chromatographic retention time.

Summary. From these studies, it can be seen that the physicochemical criteria governing the efficiency with which volatile organic compounds can be concentrated by the distillation technique are as follows: (1) for compounds of the same carbon number, the concentration of aldehydes in the distillate is higher than that of corresponding ketones, which in turn is higher than that of corresponding alcohols; (2) within each chemical class, compounds with longer chains are more highly concentrated than those with short chains; and (3) branched isomers are more highly concentrated than the normal ones (e.g., 2-propanol > 1-propanol, and 2-butanol >1-butanol). These can be explained by their differences in polarity or solubility in water as well as by their relative volatilities.

The use of a simple distillation method was not successful in concentrating acetic acid even when the solution was made strongly acidic. This result is attributed to the very highly polar nature of acetic acid, which forms a strong hydrogen bond with water. However, the use of steam distillation followed by evaporation of the alkaline distillate (White and Leenheer, 1975) and simple evaporation of alkaline sample solution (Chian and Kuo, 1976) was found to be effective in concentrating both acetic acid and formic acid. Loy (1973) found that di-n-propylamine and di-n-butylamine can be concentrated by distillation after aqueous solutions are made strongly basic.

The distillation technique can be employed to concentrate other low molecular-weight organics having a favorable volatility relative to water. It should be noted, however, that in certain cases undesirable chemical reactions or the decomposition of organics might occur during distillation at elevated temperatures. For example, esters could be hydrolyzed at an appreciable rate in a base solution at elevated temperatures. Better recovery is expected for the less polar organics than for the more polar water-soluble VPO's because the values of relative volatility are higher for the former

compounds. Other concentration methods should also be considered if the compounds of interest are beyond the range of the low molecular-weight (>85) water-soluble VPO's studied here. For example, the use of a gas-stripping method to concentrate organics onto a polymer adsorption trap at room temperature was found to be more effective for the less polar volatile organics having a solubility of less than 2% (Bellar and Lichtenberg, 1974b; Grob et al., 1975; Kuo et al., 1977). Liquid-liquid extraction and sorption on a solid adsorbent are more favorable methods for concentrating the higher molecular-weight (>150) and less polar organic compounds that are less volatile and less water-soluble (Webb, 1975; Junk et al., 1974).

RO permeates can be routinely analyzed for low molecular-weight VPO's using the distillation technique followed by direct injection of distillates into a gas chromatograph. Combining the distillation technique with the evacuated gas sampling/gas chromatographic method (Cowen et al., 1975) permits one to determine low molecular-weight VPO's at the ppb level. The results of using this combined technique are presented elsewhere (Chian et al., 1977, as well as in this report. Low molecular-weight VPO's can also be determined at sub-ppb levels by subjecting the distillate to analysis by the sparging sampling/gas chromatographic method (Kopfler et al., 1976) or the membrane/mass spectrometric method (Mieure et al., 1976). These combined techniques further demonstrate the usefulness of the distillation technique in the determination of low molecular-weight VPO's.

From this study on concentrating low molecular-weight (e.g., >85) VPO's by distillation, it is concluded that salting out along with the use of an internal standard can improve the recovery and precision of distillation processes using a glass bead packed column. If experimental time is not a limitation and if a large volume of sample (e.g., 1-liter) is available, the two-stage distillation technique is recommended, using a micro apparatus for the second stage distillation so as to collect less than 10 mL (e.g., 1.5 mL or less) of distillate for analysis.

If time is a limiting factor, collecting the first 10 mL of distillate from a 1-liter sample with a large apparatus would be the method of choice. If, however, time and sample volume are both limited, 100 mL of sample solution can be distilled with a micro apparatus. In that case, either 10 mL or a smaller amount of distillate (e.g., 1.5 mL or less) can be collected for analysis. The latter approach is recommended, provided that the volume is sufficient for subsequent chemical analysis.

Determination of Volatile Polar Organics in RO Composite Permeates

The RO composite permeates listed in Table 15 were concentrated with the distillation technique; their distillates were then analyzed for volatile organics. Sample D is an ozonated and chlorinated permeate.

TABLE 15. IDENTIFICATION OF RO PERMEATES ANALYZED FOR VOLATILE COMPOUNDS BY DISTILLATION/GC TECHNIQUE

Sample Coded at U.I.	A	B	C	D
Sample Coded by Walden	Test #1	Test #2	Test #3 or IT-3-2	Chlorinated IT-7-3
	RO Permeate Hospital Composite	RO Permeate Lab Waste	RO Permeate Time Varying Hospital Composite	MUST Composite UF, RO, O_3, and Cl_2
Supplier	Walden	Walden	Walden	USAMBRDL
Date Received	Aug. 20, 1975	Aug. 20, 1975	Aug. 26, 1975	Nov. 24, 1975
Date Distilled	Dec. 4, 1975	Dec. 15, 1975	Dec. 15, 1975	Dec. 5, 1975

One hundred milliliters of sample were saturated with dried sodium sulfate and distilled with a micro distillation apparatus to collect the first 10 mL of distillate. From this distillate, four 2-mL portions were pipetted and injected into 15-mL serum bottles. Another 1 mL of distillate was spiked with 1 µL/L of 2-butanol. The remaining 1 mL of distillate was used for TOC determination. The spiked distillate was analyzed by GC for volatile organic compounds on a Carbowax 1500 column using the direct injection technique. The serum bottles were shipped to USAMBRDL to be analyzed by the headspace vacuum sampling/GC technique (Cowen et al., 1975).

A standard solution containing 1 µL/L of each compound was first tested to determine the concentration factor for each compound. The results are shown in Table 16. The concentration factor is greater than 9 (the recovery is greater than 90%) for most of the compounds.

The GC working conditions are as follows: N_2 flow 25 mL/minute, oven temperature programmed for 60° to 150°C at 8°C/minute with 2-minute initial hold. Peaks were tentatively identified by the relative GC retention time.

Table 17 summarizes the results. Methanol, acetone, 2-propanol, 1-propanol, methyl ethyl ketone, and diethyl ether were found in RO permeates. However, only acetone was present in all four samples. As can be seen in Table 17, methanol is the major component determined in Sample B, while acetone was the principal constituent in Sample D. Sample C was found to have the least amount of volatile organics.

TABLE 16. CONCENTRATION FACTORS OF MODEL COMPOUNDS

Conc. in Distillate[a]	Methanol	Ethanol	Acetone	2-Propanol	Diethyl Ether	1-Propanol	Methyl Ethyl Ketone	Ethyl Acetate	2-Butanol	1-Butanol	3-Pentanone	n-Amyl Alcohol
Trial 1, µL/L	9.22	9.77	9.81	9.46	2.15	9.64	7.70	4.15	9.04	8.98	6.71	8.70
Trial 2, µL/L	9.38	9.80	9.74	9.81	2.37	9.57	8.26	4.20	9.08	9.47	7.48	8.65
Avg. Conc. or Conc. Factor[b]	9.30	9.79	9.78	9.64	2.26	9.61	7.98	4.18	9.06	9.23	7.10	8.68
% Recovery	93.0	97.9	97.8	96.4	22.6	96.1	79.8	41.8	90.6	92.3	71.0	86.8

a. The first 10 mL of distillate from distilling 100 mL of combined standard solution at 1 µL/L.
b. Concentration factor is identical to the averaged concentration in the distillate since the starting concentration was 1 µL/L.

TABLE 17. CONCENTRATION OF VOLATILE ORGANIC COMPOUNDS IN MUST HOSPITAL RO PERMEATES

Sample[b]	Conc.[a] in first 10 mL of distillate from distilling 100 mL of sample solution saturated with sodium sulfate						
	Methanol	Acetone	2-Propanol	1-Propanol	Methyl Ethyl Ketone	Diethyl Ether	TOC_{cal}[c]
A, µL, L_d	0.456	0.088					
mg/L	0.135	0.043					0.178
B, µL/L	1135.604	83.208	1.436	0.471	0.726		
mg/L	337.274	40.439	0.672	0.227	0.388		379.000
C, µL/L		0.059		0.067			
mg/L		0.029		0.032			0.061
D, µL/L	3.990	7.237	0.116	0.471	1.157	0.088	
mg/L	1.185	3.517	0.054	0.227	0.618	0.040	5.641
	Concentration in RO Permeate[e]						
A, µL/L_d	0.049	0.009					
mg/L	0.015	0.004					0.019
B, µL/L	122.108	8.508	0.149	0.049	0.091		
mg/L	36.266	4.135	0.070	0.024	0.049		40.544
C, µL/L		0.006		0.007			
mg/L		0.003		0.003			0.006
D, µL/L	0.429	0.740	0.012	0.049	0.145	0.039	
mg/L	0.127	0.360	0.006	0.024	0.077	0.018	0.612

a. Averaged from triplicate runs.
b. See Table 15 for sample identification.
c. Calculated from volatile compounds determined.
d. As organic carbon.
e. Calculated by dividing the concentration in the distillate by the corresponding concentration factor listed in Table 16.

TABLE 18. PERCENT TOC OF IDENTIFIED COMPOUNDS IN RO PERMEATES AND IN THEIR DISTILLATES USING VOLATILE ORGANIC ANALYSIS

Sample	TOC cal. by Volatile Organic Analysis (mg/L)	TOC Determined by TOC Analyzer (mg/L)	% TOC of Identified Volatile Organics
1. RO Permeate			
A	0.02	8.54	0.23
B	40.54	72.80	55.69
C, IT-3-2	0.01	9.15	0.11
D, Chlorinated IT-7-3	0.61	7.51	8.12
IT-3-2[a]	7.3	10	73
IT-7-3[a]	2.1	7	30
2. Distillate of RO Permeate			
A	0.2	8.8	2.27
B	379.0	360.4	105.16
C, IT-3-2	0.1	6.2	1.61
D, Chlorinated IT-7-3	5.6	17.9	31.28

a. Obtained from USAMBRDL Memorandum Report 2-76, Subject: Analysis of Volatile Organic Compounds in Walden Research MUST Integrated Test Samples and in a Laboratory Waste Reverse Osmosis Permeate, dated December 4, 1975.

Table 18 shows the percentage of TOC determined in RO permeates and their distillates by the volatile organic analyses described in this section. As can be seen from Samples A and C, hospital composite RO permeates, TOC is contributed mainly by the nonvolatile organic compounds, because the percentage of TOC identified in these RC permeates is very low. Also, TOC in the distillate was not enhanced by the distillation technique. The low percentage of TOC determined in the distillate might indicate that most of the volatile compounds could not be eluted on a Carbowax 1500 column. Other columns that can elute low molecular-weight organic polar compounds should be investigated.

For Sample B, more than half of the TOC is contributed by the volatile compounds, which can be recovered completely in the distillate and subsequently determined on a Carbowax 1500 column. The major components in Sample B are methanol and acetone, which were shown in the previous work to be easily concentrated in the distillate and determined on the Carbowax 1500 column. Hence, the distillation/direct GC injection technique appears to be an effective means of analyzing the laboratory waste RO permeate for volatile organic compounds.

TABLE 19. CONCENTRATIONS OF VOLATILE COMPOUNDS DETERMINED IN RO PERMEATES

	ppm of Organic Carbon					
	Methanol	Acetone	2-Propanol	Diethyl Ether	1-Propanol	Methyl Ethyl Ketone
IT-3-2						
U.I.	--	0.003	--	--	0.003	--
USAMBRDL	5	2	0.2	0.1	--	0.1
Chlorinated IT-7-3						
U.I.	0.127	0.360	0.006	0.018	0.024	0.077
IT-7-3						
USAMBRDL	1	1	<0.1	<0.1	1	0.1

Sample D is a chlorinated, ozonated RO permeate (chlorinated IT-7-3) in which the volatile compounds consist of approximately 8% of TOC. The TOC in the distillate is enhanced by a factor of 2.4 to a concentration of 17.9 ppm. However, only 31% of the TOC in the distillate was identified. Other GC columns along with appropriate detectors, such as ^{63}Ni electron capture detector, could be used to determine the chlorinated compounds.

Results of analysis of RO permeates reported by USAMBRDL are also given in Part 1 of Tables 18 and 19 for comparison. As much as 73% of the volatile compounds were identified by USAMBRDL, whereas little or no enhancement of TOC in the distillate of Sample C was found in this study. The latter implies that the amount of volatile compounds in Sample C is relatively low. In general, the concentrations of volatile compounds reported by USAMBRDL are consistently higher than those obtained in this study (see Table 19). The identity of Sample C is therefore questionable.

It is seen from Table 18 that chlorination of Sample IT-7-3 does not reduce the amount of TOC in the sample. However, the concentration of volatile components decreases (see Table 19). It appears that those volatile compounds that can be eluted on the Carbowax 1500 column are not eluted after chlorination. Hence, only 31% of the TOC in the distillate of the chlorinated IT-7-3 (Sample D) was determined on the Carbowax 1500 column.

Distillation-Headspace-Gas Chromatographic Analysis for Volatile Polar Organics at ppb Levels

The distillation technique was combined with the headspace gas chromatographic method (Cowen et al., 1975) to determine volatile polar at ppb levels. The combined procedure (DHGC) and its applications were also discussed.

Experimental

Samples. Synthetic MUST hospital wastewaters were treated by ultrafiltration, followed by reverse osmosis and final ozonation (O_3) by Walden Research Division of Abcor, Inc., Cambridge, MA (Gollan et al., 1976). The integrated test protocol called for reusing the product water effluent from each test for the subsequent run's wastewater makeup. Samples of RO permeate and ozonated RO permeate from integrated tests 3 to 7 were sent via the U.S. Army Medical Bioengineering Research and Development Laboratory (USAMBRDL) to the University of Illinois where they were distilled and the distillates collected. A given amount of distillate from the samples and the standard solutions was stored in headspace serum bottles (Cowen et al., 1975), and mailed to USAMBRDL where headspace gas injection/GC analyses were performed.

Reagents. Standard stock solutions were prepared from ACS reagent-grade chemicals using distilled water. These stock solutions were then mixed and diluted with distilled water, which was freshly stripped at elevated temperature with purified nitrogen gas, to prepare standard solutions with concentrations ranging from 0.008 to 16 mg/L; n-butanol, internal standard, was added to give a 0.8-mg/L concentration.

Procedures for Distillation. One hundred milliliters of each sample solution were spiked with n-butanol to give a 0.8 mg/L level and saturated with 21.3 g of dried sodium sulfate in a 250-mL round-bottomed flask. A 7.75-inch Vigreux column was connected to the flask. A small distilling head with a thermometer and a small condenser attached was connected to the upper end of the Vigreux column. During the distillation process, the vapor temperature at the distilling head was controlled at 100°C by regulating the voltage supply to the heating mantle. Distillation continued until the first 1.5 mL of distillate was collected. From that amount, 1 mL was injected with a 2-mL syringe into a 15-mL headspace serum bottle containing 1.2 g dried sodium sulfate. Distillations were done in duplicate for each sample. The standard solutions and distilled water were distilled in the same way.

Apparatus and Procedures for Headspace Gas Analysis. Only a brief description of the valving system is given here, since it has been described in detail elsewhere (Cowen et al., 1975). Headspace bottles were heated in a 70°C water bath for at least 70 minutes. The headspace gas was injected via an eight-port gas sampling valve into a gas chromatograph equipped with flame ionization detectors. The gas chromatograph was fitted with a 183-cm, 2-mm inside diameter glass column packed with GP 0.4% Carbowax 1500 on 60/80 mesh Carbopack A (Supelco, Inc., Bellefonte, PA). After injection, the

column temperature was held at 60°C for 2 minutes, then increased at 8°C/minute to 150°C and held for 5 minutes. The carrier helium flow rate was 10 mL/minute. An electronic integrator was interfaced to the flame ionization detector for acquisition of retention time and peak area data. The ratios of the peak areas of the resulting chromatographs to internal standard peak area were used for standard curves.

Excluding the time required for heating and equilibrating the solution in serum bottles, which could actually be left unattended, the sample preparation and analysis time is less than 50 minutes. It takes approximately 25, 3, and 18 minutes, respectively, for distillation, headspace gas sampling and injection, and GC run.

Results and Discussion

The gas-liquid equilibrium headspace system has been used to determine the activity coefficient of solutes and the molar energy of mixing (Kolb, 1975) as well as the partition coefficient of solutes (Vitenberg, 1975). It has also been used to determine VPO's in water (Bassette et al., 1962; Ozeris and Bassette, 1963; Kepner et al., 1964). The principle of this technique for quantitative analysis is that, by injecting the equilibrated gas into the GC over a liquid phase, the solute concentration in the gas (C_G) can be determined. By knowing C_G, K_T, the partition coefficient between the liquid and gas phases, and the volumes of the liquid and headspace (V_L and V_G), the initial solute concentration (C_L°) before equilibrium can then be determined according to the following equation,

$$C_L^\circ = C_G(K_T V_L + V_G)/V_L$$

However, by fixing V_L and V_G, a calibration curve can be made to relate C_L° and C_G permitting quantitation without knowledge of the values of K_T. The values of C_G were determined experimentally by measurement of peak area relative to an internal standard peak area, and C_L° values were obtained by reference to the standard curve.

The basic principle of distillation for sample preconcentration has been described elsewhere (Chian and Kuo, 1976; Loy, 1973), as well as in this report. The technique takes advantage of the difference in volatility between the more volatile organics and less volatile water so that the VPO's can be concentrated in a small volume of distillate. The concentration factor is higher for compounds having a higher relative volatility. For example, a higher concentration factor can be expected for methyl ethyl ketone than for methanol.

In this study, a calibration curve was made for each solute to correlate its original concentrations in the standard solution to the GC peak area ratios obtained from the distillates of the standard solution using headspace gas analysis. A linear regression analysis of the calibration curve using five concentration points (0.008, 0.08, 0.8, 8, and 16 mg/L) was performed to obtain a least-squares fit. Linear standard calibration curves for methanol, ethanol, acetone, 2-propanol, n-propanol, methyl ethyl ketone, ethyl acetate, 2-butanol, 3-pentanone, and n-pentanol were obtained. The proportion of explained variation due to the linear relationship, r^2, was better than 0.97 for all model compounds. This fact indicates that the areas of the GC peaks, relative to the n-butanol internal standard area, were directly proportional to the original sample concentration with the DHGC procedure.

VPO's were tentatively identified according to the relative GC retention time with n-butanol as the internal standard. A representative chromatogram of a standard solution is given in Figure 14.

The results of wastewater analyses are shown in Table 20 in which solute concentrations of the original wastewater samples were determined using the calibration curves described previously. As can be seen, 2-propanol and methyl ethyl ketone were determined at concentrations as low as 8 µg/L. The detection limit was estimated to be about 4 µg/L for most of the compounds. This limit was determined by the background signal in distilled water blanks rather than by the sensitivity of the DHGC technique. The detection limit for methanol and ethanol was approximately 8 µg/L. The relative standard deviation, determined for independent triplicate runs of stock solutions containing 16 µg/L of methyl ethyl ketone, was 9.2%. With the exception of methanol, the concentrations determined for other compounds in this study agreed fairly well with those obtained by direct headspace GC analysis of the original samples without distillation preconcentration. There are discrepancies between the results of methanol determination using DHGC and headspace GC techniques because the concentration of methanol in most wastewater samples is beyond the sensitivity limit and, thus, accuracy of the headspace GC analysis, i.e., 5 mg/L. Ethanol, however, was not detectable without the preconcentration step (Table 20).

By use of the distillation preconcentration technique, the sensitivity of VPO determinations was greatly improved. The fact that the results of this study were obtained from distillates obtained in one laboratory and mailed to another for headspace analysis points to another potential advantage of the distillation technique: volatile organics can be distilled from a large sample at the sampling site and can be preserved in a small bottle for ease of storage, shipping, and subsequent analysis at a second laboratory, thus eliminating the problems associated with shipping large samples required for analysis. Degradation of the volatile compounds as a result of the presence of microorganisms can also be avoided by preserving the distillate instead of the original sample.

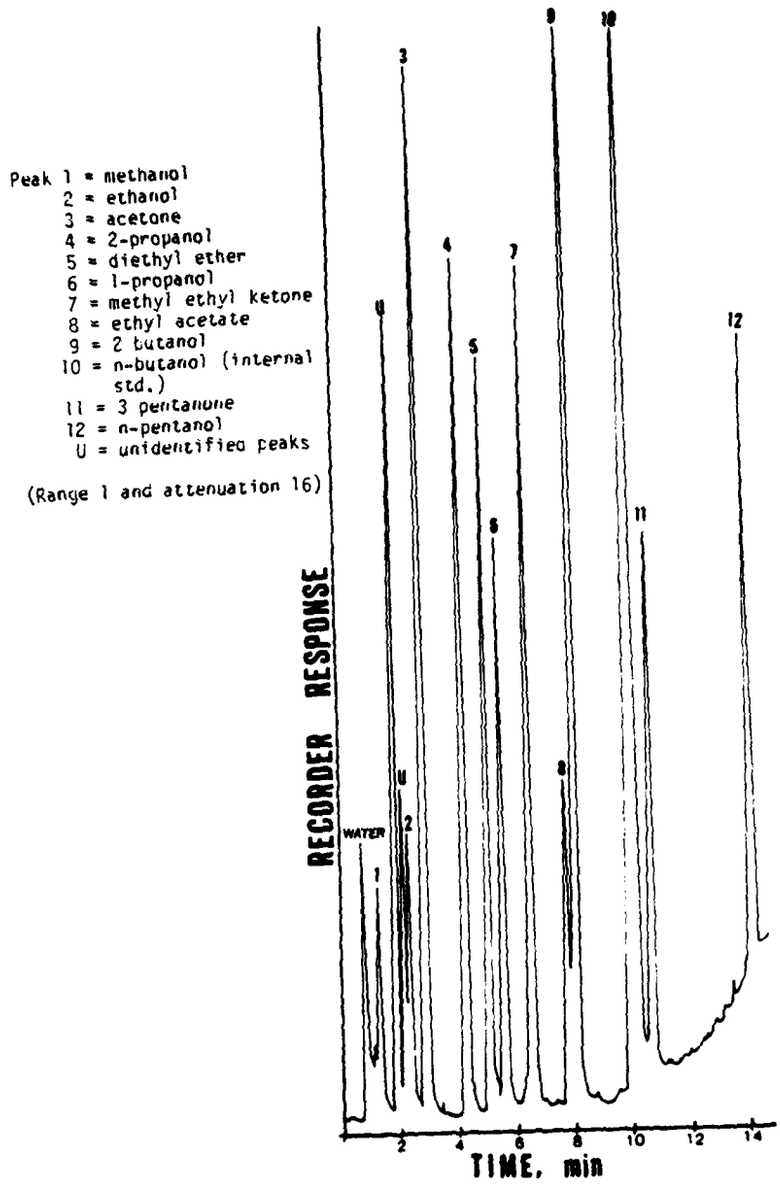

Figure 14. Headspace Gas Chromatogram of Distillate from 0.08 mg/L Standard Mixture of Volatile Compounds.

TABLE 20. QUANTITATIVE ANALYSES OF MUST HOSPITAL SYNTHETIC WASTEWATER SAMPLES BY DHGC TECHNIQUE

Sample	Concentration (μL/L)				
	Methanol	Ethanol	Acetone	2-Propanol	Methyl Ethyl Ketone
IT-3-RO	17.0	0.05	2.0	0.5	0.2
3-RO + O_3	0.7	0.06	2.0	0.05	0.1
IT-4-RO	15.0	0.03	1.0	0.4	0.1
4-RO + O_3	0.2	0.02	1.0	0.03	0.09
IT-5-RO	0.4	0.02	0.8	0.06	0.1
5-RO + O_3	0.3	0.02	0.6	0.03	0.03
IT-6-RO	16.0	0.04	0.9	0.2	0.2
6-RO + O_3	0.7	0.04	2.0	0.03	0.04
IT-7-RO	5.0	0.02	2.0	0.6	0.2
7-RO + O_3	1.0	0.03	1.0	0.03	0.1
7-RO + O_3[a]	0.1	>0.01	0.05	0.01	0.01

a. *Additional ozonation period of 3 hours.*

The sensitivity of the DHGC method can be further improved by analyzing a highly enriched distillate. As has been mentioned, one liter of sample solution or more can be distilled to recover almost completely the VPO's in 100 mL of distillate. A second distillation can then be performed to further concentrate the VPO's into a few milliliters of final distillate (Chian and Kuo, 1976). Headspace GC analysis of VPO's from distillates thus obtained is then possible at the ppb (μg/L) level or lower. Besides VPO's, other volatile, nonpolar, water-insoluble organics can also be determined by the DHGC method. The detection limit should theoretically be much lower because the concentration factor during the distillation step and the sensitivity during headspace GC analysis are much higher, a result of the higher relative volatility and smaller K_T of the volatile nonpolar compounds. Research is underway to investigate the application of the DHGC method in determining volatile, nonpolar compounds in water at the sub-ppb level.

Summary

VPO's at concentrations as low as 8 μg/L can be determined in treated hospital wastewaters by the distillation/headspace/GC method (DHGC). Determinations at the ppt level or lower are attainable by applying headspace analysis to highly enriched distillate samples using two or multistage

distillation. It is expected that this technique can be applied to determining volatile nonpolar waste insoluble organics at even lower concentrations. Besides the sensitivity of the DHGC technique, the possibility of processing samples onsite and the ease of preserving and shipping the distillate in serum bottles will lead to even broader applications.

Determination of Acetic Acid

Distillation of Acetic Acid

The distillation technique was also tested to concentrate acetic acid in the distillate. One hundred milliliters of a solution containing 200 µL/L of acetic acid were first adjusted to a pH ≤ 2 and distilled with a large apparatus equipped with a Vigreux column. The first and the second 10-mL fractions of the distillates were collected and, after adjusting for a pH ≤ 2, analyzed by GC on a 6-ft x 1/4-inch outside diameter glass column packed with 3% Carbowax 20 M/0.5% phosphoric acid on 60/80 Carbopack G, a GC oven was set at 160°C isothermally, and the nitrogen carrier flow was 25 mL/minute. The concentration of acetic acid in the distillates was determined with the aid of a calibration curve.

Table 21 shows the results of duplicated runs. The recovery was rather poor compared with the model compounds studied previously and the concentration factor is less than unity. The fact that the first 10-mL fraction contained less acetic acid than the second one and that the concentration factor was less than unity in both cases results from acetic acid having a higher boiling point (118.1°C). A totally different design of the distillation apparatus is needed to concentrate acetic acid. An efficient fractionation column with a reflux capability is needed to distill water so that a concentrated residue containing a higher concentration of acetic acid will result.

TABLE 21. DISTILLATION OF 100 mL OF 200 µL/L ACETIC ACID

	1st 10 mL of Distillate		2nd 10 mL of Distillate	
	Conc. (µL/L)	% Recovery	Conc. (µL/L)	% Recovery
Trial 1	34	1.7	74	3.7
Trial 2	41	2.1	91	4.6
Avg.	38	1.9	83	4.2

Concentration of Acetic Acid with Evaporation Technique

The direct evaporation technique was next evaluated for concentrating acetic acid. One hundred milliliters of a dilute acetic acid were adjusted to a pH > 11 with 50% sodium hydroxide solution and evaporated in a 250-mL Erlenmeyer flask on a hotplate to approximately 7 mL. After readjusting the pH to < 2, the concentrate was then transferred to a 10-mL volumetric flask and the volume was restored to 10 mL by adding distilled water. The concentrated acetic acid solution was analyzed by GC on an acid column.

The results of this study are shown in Table 22. The recovery is close to 100%. The concentration factor is therefore also 10, which is the maximum factor attainable under such experimental conditions. Higher concentration factors can be expected if a larger sample size is used to evaporate the solution to a final volume of less than 10 mL. The last three rows of Table 22 further show that no acetic acid was lost during the direct evaporation process.

Determination of Acetic Acid in RO Permeate

The evaporation technique was employed to determine acetic acid in Sample Test #7 (IT-3-3) received from Walden Research Lab. This sample is actually the ozonated IT-3-2. Five hundred milliliters of this sample were first concentrated to approximately 100 mL in a 1-liter Erlenmeyer flask. The solution was then transferred to a 250-mL Erlenmeyer flask for final evaporation to 10 mL. The concentration of acetic acid was determined to be 0.2 µL/L in Sample Test #7 without considering any interferences. The interference from the hydrolysis of acetic ester, e.g., ethyl acetate, should be very low, since it might not be present in the ozonated RO permeate as a result of removal by ozone gas stripping. Because of the limited amount of sample available, other samples were not analyzed for acetic acid. A total of 0.2 µL/L of acetic acid is equivalent to 0.11 ppm for TOC, which comprises approximately 1.4% of the TOC in Sample Test #7. The TOC of Sample Test #7 is 8.08 ppm.

Steam distillation can be utilized prior to the evaporation process to isolate acetic acid or formic acid from extraneous organic compounds and other nondistillable components to eliminate their interferences (White and Leenheer, 1975).

Development of Gas Stripping Technique for Determining Volatile Organics in RO Permeates

The headspace gas stripping technique and Bellar's stripping technique (Bellar and Lichtenberg, 1974b) were evaluated, and RO permeates were analyzed for volatile organics.

TABLE 22. CONCENTRATION OF ACETIC ACID BY EVAPORATION TECHNIQUE[a]

Sample Solution	Conc. of Acetic Acid (µL/L)	% Recovery
0.5 µL/L	5.5	100
0.5 µL/L	5.0	100
Avg.	5.3	105
1.0 µL/L	9.8	98
1.0 µL/L	10.2	102
Avg.	10.0	100
10.0 µL/L	103.0	103
10.0 µL/L	97.0	97
Avg.	100.0	100
100.0 µL/L	1,003	100.3
100.0 µL/L	1,011	101.1
Avg.	1,007	100.7
100.0 µL/L[b]	110.9	110.9
100.0 µL/L[b]	100.3	100.3
Avg.	105.6	105.6

a. 100 mL of solution were evaporated to 10 mL.
b. 100 mL of solution were evaporated to 10 mL and then diluted back to 100 mL.

Evaluation of Headspace Gas Stripping Technique

Stripping Efficiency for Model Compounds. The technique of dynamic headspace sampling using helium stripping has inherent advantages over all other methods for volatile organics. While other methods, such as distillation of volatiles for subsequent GC analysis, may well work for appropriate concentrations of easily separable substances, none approach the effectiveness of concentration and freedom from interferences that stripping offers.

The apparatus for stripping volatiles can be constructed from readily available laboratory equipment. The adsorbent precolumn contains 0.003 g of Tenax-GC, held in place by glass wool plugs, in a 1/4-inch outside diameter and 1-mm inside diameter glass tube. The method consists of heating an aqueous sample in oil bath at 100°C for 30 minutes and sweeping the volatiles into the precolumn with dried purified helium. The helium flow rate is 120 mL/minute. A condenser is added to avoid a large amount of H_2O reaching the precolumn. The stripping flask and the stripping apparatus used in this study are described later.

The dynamic headspace stripping technique was evaluated to study the efficiencies of stripping various groups of organic compounds from aqueous solutions. The stripping efficiency was determined based on the percentage of TOC removal. This was carried out comparing TOC of the sample solution before and after stripping. Results of stripping experiments are shown in Table 23. Each model compound was stripped and analyzed for TOC individually. As can be seen from Table 23, except for the two acids that are very polar and highly soluble in water, the stripping efficiencies of other compounds are between 90 and 96%.

Stripping of mixtures at two concentration levels was also conducted to study the stripping efficiency of the mixtures as a function of time. Figure 15 shows the percentage of organic compounds remaining in aqueous solution versus time as plotted on the semi-log paper while stripping at 80°C at a helium gas flow rate of 120 mL/minute over a sample of 100 mL. Whereas the alcohols under this study are stripped quite efficiently, as shown by the rapid logarithmic decrease in concentrations versus time, the mixture of phenol and o-toluidine, as shown by the top two lines, are poorly removed. The rate of stripping appears to be somewhat higher with the solutions containing a lower concentration of organics as shown clearly by both sets of curves in Figure 15. The fact that the rate of stripping does not decrease with a decrease in the concentration of the organics to be stripped is rather important while establishing conditions of stripping using higher concentration of organics for ease of measurements. Therefore, the conditions established for stripping will be good for any solutions having concentrations lower than that studied.

Stripping of RO Permeates of MUST Wastewaters. The RO permeates of MUST hospital wastewaters were analyzed for volatile organics. After adjusting the pH to 2.0, samples were stripped at 85°C by helium at a flow rate of 80 mL/minute. During stripping, volatile organics were transferred from sample solution to the adsorption trap, which consisted of a piece of glass tube containing Tenax-GC as adsorbent. The stripping lasted 30 minutes. The GC column used was a 6-ft glass column that had a small U-bend at one end of the column close to the injection port. The trap and the GC column were fabricated so that, after connecting the trap to the column by means of an 1/4-inch to 1/4-inch Swagelok union, the column would just fit into the GC oven and the trap would fit into the injection port. A beaker of dry ice mixed with acetone was used to chill the U-bend portion. Thus, volatile organics were desorbed from the trap under the heat of the injection port and concentrated at the U-bend portion of the GC column by means of carrying gas. This transferring of volatile organics from the trap located in the GC injection port to the GC column corresponds to the normal sample introduction or injection into the GC column with a syringe. After sample introduction to the U-bend, the GC oven was heated up without temperature programming to a final temperature of 135° and the GC chromatogram was obtained.

TABLE 23. STRIPPING EFFICIENCY FOR MODEL COMPOUNDS

Chemical Group	Compound	Boiling Point (°C)	TOC Removal (%)[a]
Ketone	3-pentanone	102.7	95
	Acetone	56.2	94
Alcohol	n-butanol	117.5	96
	Methanol	64.96	95
Aldehyde	Butanal	75.7	90
	Propanal	48.8	96
Acid	Butanoic acid	163.5	~1
	Acetic acid	118.5	~2

a. Average of three stripping tests.
Condition: 200 mL of 20 ppm of individual organic stripped for 30 min, at 100°C of oil bath, helium flow rate of 120 mL/min.

The GC instrument used was a HP 5750 B with a dual-flame ionization detector. The GC column was a 6-ft x 2-mm inside diameter x 1/4-inch outside diameter glass column packed with 0.3% Sp-1000, 0.3% H_3PO_4 on 60/80 Carbopack A. This column works very well for separation of C_2-C_6 fatty acids and will be referred to as acid column. This column is based on the work of Corcia (1973a). In addition, this column can separate C_1-C_5 alcohols and phenolic compounds. Corcia has demonstrated the separation of o, m, and p cresols; he has also studied the separation of dichlorophenols and nitrophenols with this column (1973b). The operating conditions of the GC are as follows: The oven, injection port, and detector temperatures were 135°C, 180°C, and 200°C, respectively. The nitrogen carrier gas, hydrogen gas, and air flow rate were 20, 40, and 460 mL/minute, respectively.

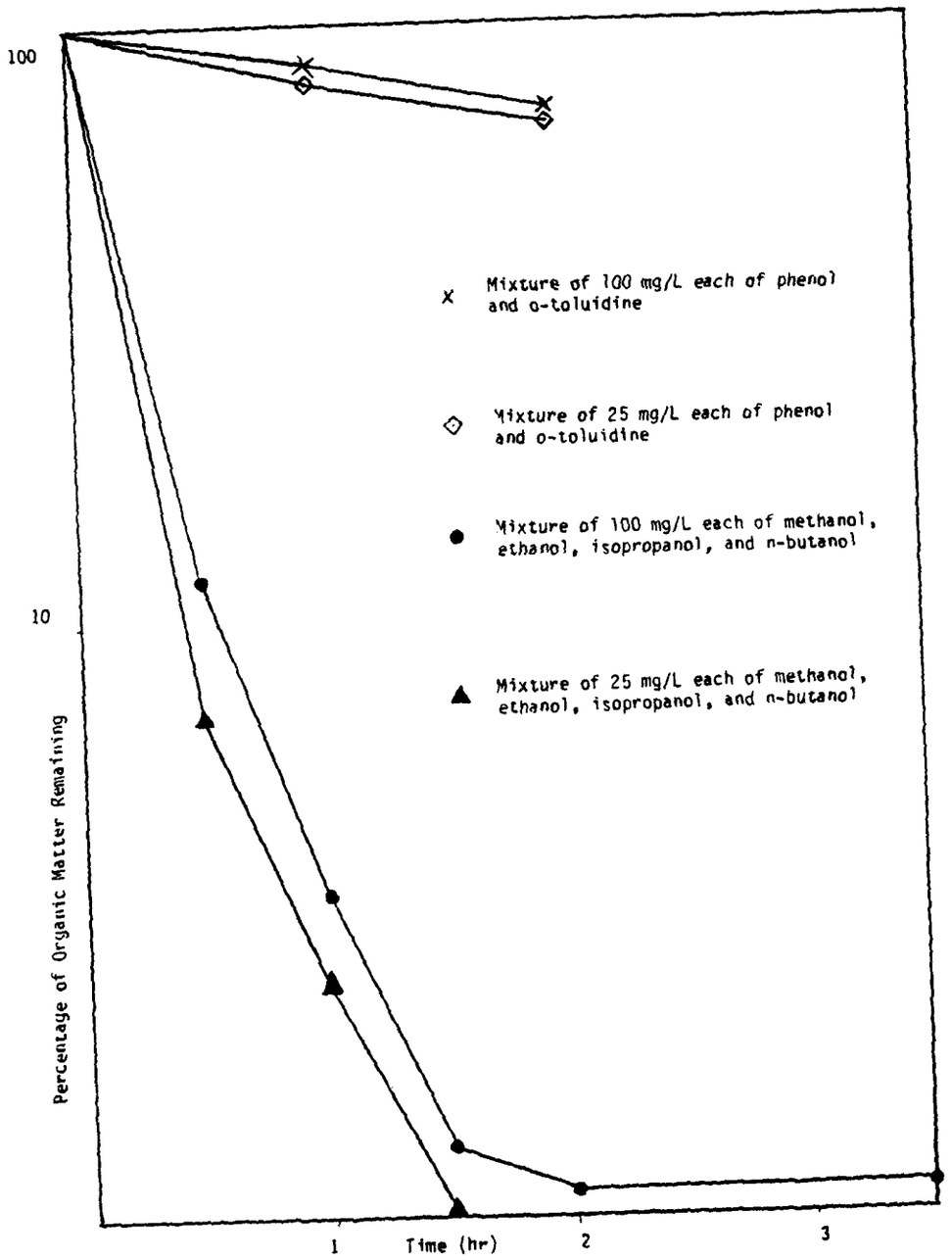

Figure 15. Removal of Organic Matter by Stripping.

Table 24 shows the major constituents found in various RO permeates identified based on retention times after helium gas stripping. The number of unknown peaks is also given. The percentage of volatiles present in the RO permeates is high, averaging 45% in laundry and shower RO permeates as can be seen from the third column of Table 24. However, only 28% of TOC in the composite RO permeate can be stripped off under the prevailing stripping conditions. Whereas the volatile organics in the RO permeates of kitchen, laundry, shower, and operating room wastes can be characterized rather satisfactorily when compared with the retention times on the gas chromatograms, the large number of unknowns found in the RO permeates of laboratory and composite wastes, however, require further identification with the GC/MS system. Appendix B gives the gas chromatograms of the RO permeates after stripping.

TABLE 24. STRIPPING OF MUST WASTEWATERS

Sample	TOC	% TOC Stripped	Identified Compounds	Number of Unidentified GC Peaks	
				Strong	Weak
Laundry (A-RO Permeate)	6.3	43	Acetone	1	2
after stripping	3.6				
Shower (B-RO Permeate)	25	48	Ethanol	2	2
after stripping	13		acetone		
			isopropanol		
			propanol		
Laboratory (C-RO Permeate)	10.8	--	Methanol	4	4
after stripping	11.3		ethanol		
			acetone		
			butyraldehyde		
Composite (D-RO Permeate)	430	28	Methanol	6	2
10x after stripping	310		ethanol		
			acetic acid		
			formaldehyde		
Operating (RO Permeate)					
Walden	10.0	--	Ethanol	--	2
after stripping	10.5				
Kitchen (RO Permeate)					
Walden	4.8	--	--	--	1
after stripping	3.4				

Samples adjusted to a pH of 2, stripped at 85°C, 80 mL/min He flow rate for 30 min.

Recovery of Volatile Organics by Gas Stripping Technique. The effect of stripping temperature on the removal of butanal and 3-pentanone from aqueous solutions and the efficiencies of the Tenax-GC columns in trapping these compounds were studied. The adsorption efficiencies were evaluated by connecting two traps or precolumns in series. Figure 16 shows that the adsorption of 3-pentanone by the Tenax-GC precolumn is quite complete even at the highest temperature of stripping studied when 100 mL of solution containing 10 µg/L were used. Figure 17, however, shows that appreciable amounts of butanal escaped through the first Tenax-GC precolumn and was subsequently trapped by the second Tenax-GC precolumn in series. The fact that butanal is detected in the second precolumn while being stripped at low temperature indicates that poor adsorption by the first Tenax-GC is not attributed to the exhaustion of the capacity of the resin. Instead, the unfavorable distribution adsorption coefficient of butanal between the adsorbent resin and the carrying gas helium has accounted for the inefficiency of Tenax-GC in adsorbing butanal. The same was observed with ethanol as shown in Figure 18. The fact that the peak responses of ethanol from the two precolumns are almost parallel to the abscissa of stripping temperature indicates that distribution of ethanol between the resin and helium reached equilibrium. Because of the poor adsorption efficiency of Tenax-GC towards these polar organic compounds, quantitative analysis of these compounds is impractical.

A major effort is therefore necessary to develop more efficient precolumns for the adsorption and subsequent desorption of these volatile polar organic compounds for the purpose of quantitative analysis. The addition of a second precolumn in series containing more polar solid adsorbents or the polar stationary phases as used in GC columns may be beneficial. The use of a second cryogenic capillary precolumn, or packed precolumn, appears to be promising in adsorbing whatever polar organic compounds pass through the first precolumn containing Tenax-GC. The use of two precolumns in series has been investigated by Swinnerton and Linnenbom (1967). However, the major disadvantage of this approach is that it not only doubles the number of GC runs, but also complicates the quantitative analysis due to partial adsorption of the polar and the intermediate polar organic compounds on the first Tenax-GC precolumn. On this basis, it appears to be necessary to emphasize developing only one precolumn that can retain all of the volatile organics while stripping with helium gas. The only nonselective precolumn that will adsorb efficiently both the polar and the nonpolar compounds would be the cryogenic capillary precolumn. However, this method is rather sensitive to the moisture content of the stripping gas after it leaves the stripper as it may develop ice and subsequently clog the capillary coil. It may also give an undesirable large water peak to overshadow the more volatile organics that appear in the early stage of the GC run.

As a result of the above study, it was felt that a more thorough evaluation of the stripping technique should be conducted. Therefore, the efficiency of stripping, adsorption, and desorption was studied. This was done by characterizing different types of stripping vessels under various stripping conditions, and using different trapping adsorbents. The results are reported in the following two sections.

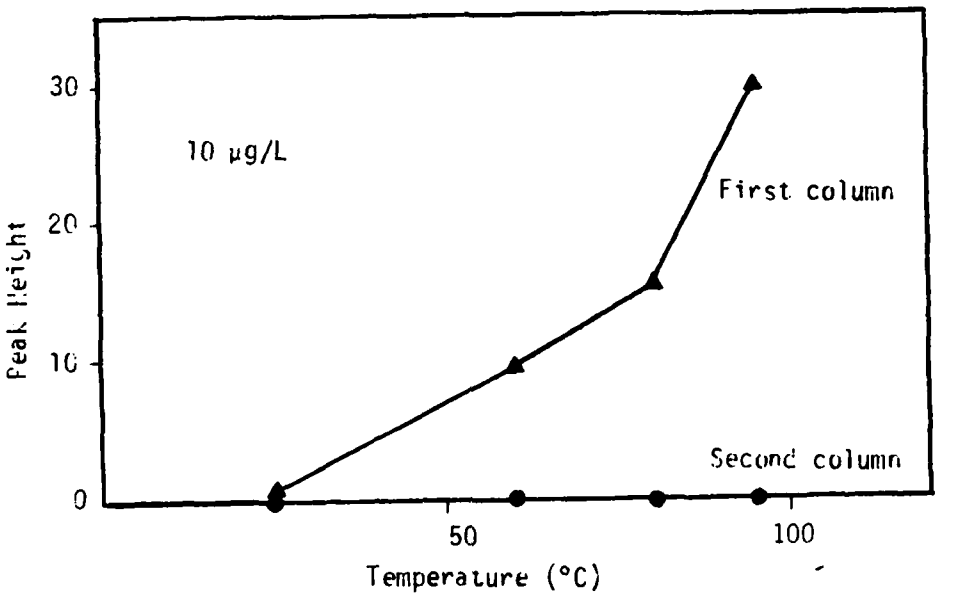

Figure 16. Effect of Stripping Temperature on Removal of 3-Pentanone and Adsorption Efficiency of Tenax-GC Precolumns.

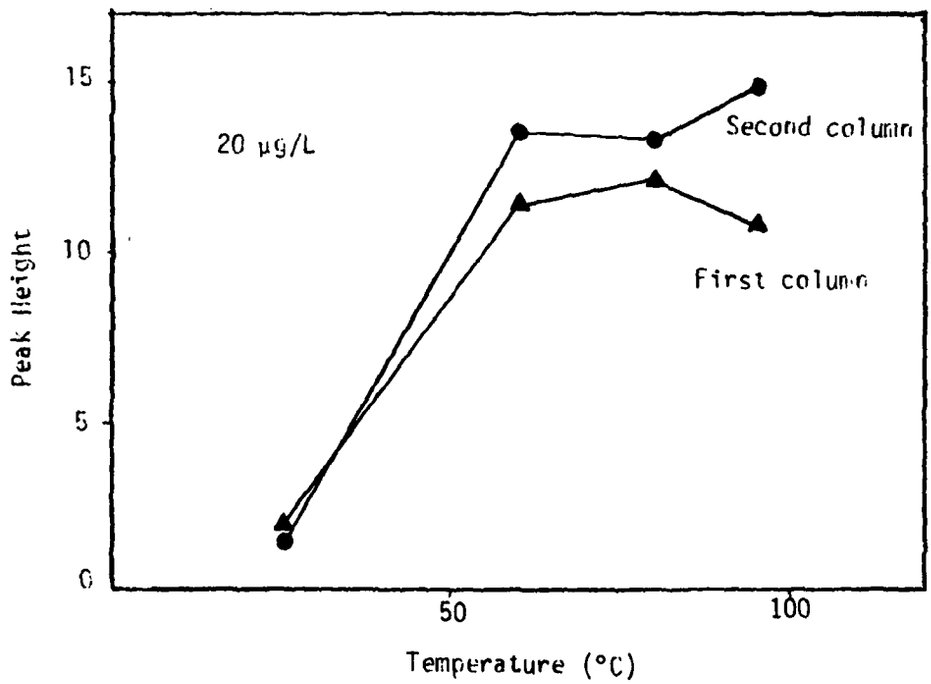

Figure 17. Effect of Stripping Temperature on Removal of Butanal and Adsorption Efficiency of Tenax-GC Precolumns.

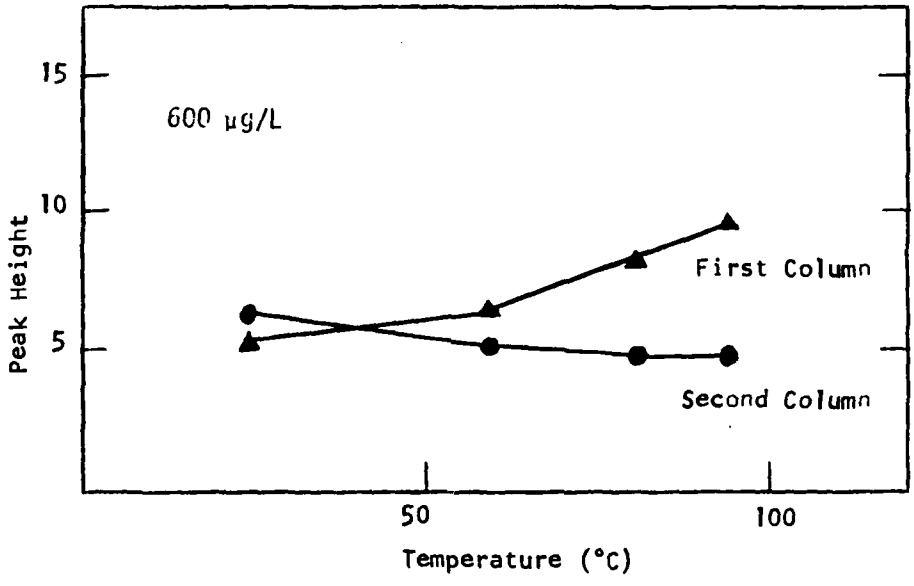

Figure 18. Effect of Stripping Temperature on Removal of Ethanol and Adsorption Efficiency of Tenax-GC Precolumns.

Stripping Efficiencies and Stripping Vessels. Three different types of stripping vessels have been studied to evaluate their stripping efficiency by means of TOC determination. Their dimensions are depicted in Figures 19, 20, and 21. The volume mark for 100 mL of sample solution is also shown in these figures. The stripping bubbler Model 1 shown in Figure 19 is a 125-mL bubbler equipped with a frit. The stripping bubbler Model 2, which also has a frit to the narrow cylinder bottom, is shown in Figure 20. Figure 21 shows the 1-liter stripping flask that has been used previously for stripping volatile organic compounds. This stripping flask is not equipped with a frit. Instead, the headspace stripping is functioning. Solution in the flask is stirred by a magnetic stirring bar during the stripping. The setup for the stripping apparatus is depicted in Figure 22.

The stripping efficiency was first studied at different helium flow rates with the stripping bubbler Model 1. The bubbler, which contained 100 mL of 50-ppm n-butanol solution, was heated in an 80°C oil bath. The TOC of the solution was measured at a given interval, e.g., 20 minutes, over a period of time while stripping with helium. A fresh solution was used for each stripping experiment. The longest stripping time studied was 140 minutes. The log of percentage of TOC remaining vs. time is shown in Figure 23. As can be seen in this figure, the higher the helium flow rate, the higher the first-order rate constants for stripping result. Figure 24 shows the stripping for 60 minutes at 80°C. Within the range of helium flow rates studied, it appears that the stripping efficiency is proportional to the helium flow rate. Although a higher flow rate will achieve a better stripping efficiency for a fixed stripping time, one should realize that there is a limit since the higher the flow rate, the higher the pressure has to be applied to the stripping apparatus. It may cause the glass joint to leak or even explode, especially when a tightly packed trap is connected to the top of the condenser as shown in Figure 22. Also, at a higher stripping gas flow rate, the solute molecules may not have enough time to equilibrate with the adsorbent, which will result in just passing through the trap without being adsorbed completely. It was found that 120 mL/minute was a practical flow rate to use.

A study on the stripping time profile for the three different stripping vessels was then carried out. The helium flow rate and the oil bath temperature were set at 120 m/Lminute and 80°C, respectively. It is obvious that the stripping flask (Figure 21) gives the best stripping result. This indicates that the large gas-liquid interface obtainable with the stripping flask enhances the mass transfer of volatile compounds from the liquid to the gaseous phase, particularly with the help of stirring to increase the interfacial surface renewal rate. The stripping bubbler Model 2 (Figure 20) performs the poorest of the three evaluated because the stirring of solution by helium bubbles is less extensive and the helium bubbles are guided upward by the narrow cylinder located at the bottom, which prevents the bubbles from spreading outward in the large round flask. Actually, this model is designed for stripping a small sample volume. In bubbler Model 1, better stirring by bubbles overcomes the smaller gas-liquid interface.

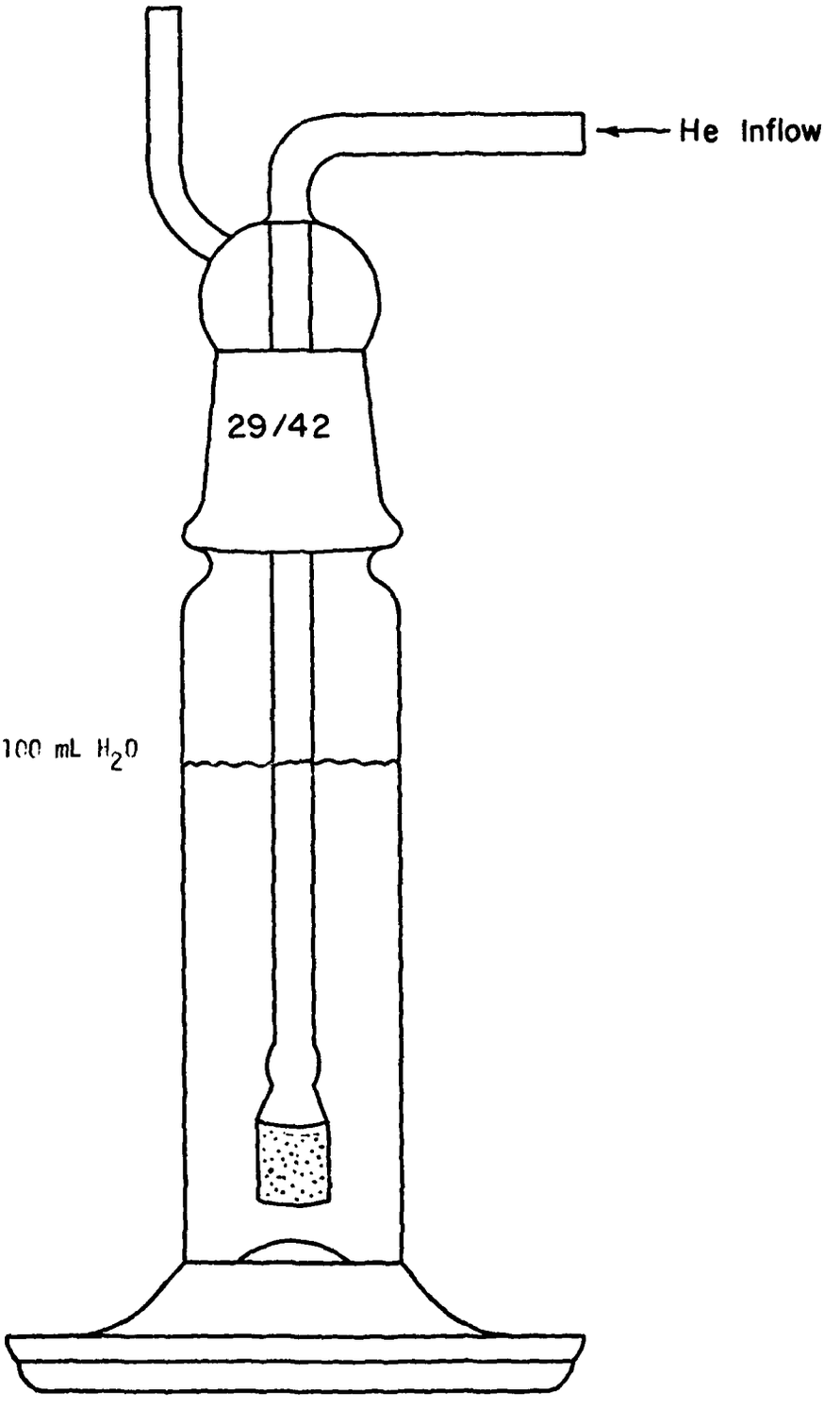

Figure 19. Conventional Gas Scrubber (Bubbler 1).

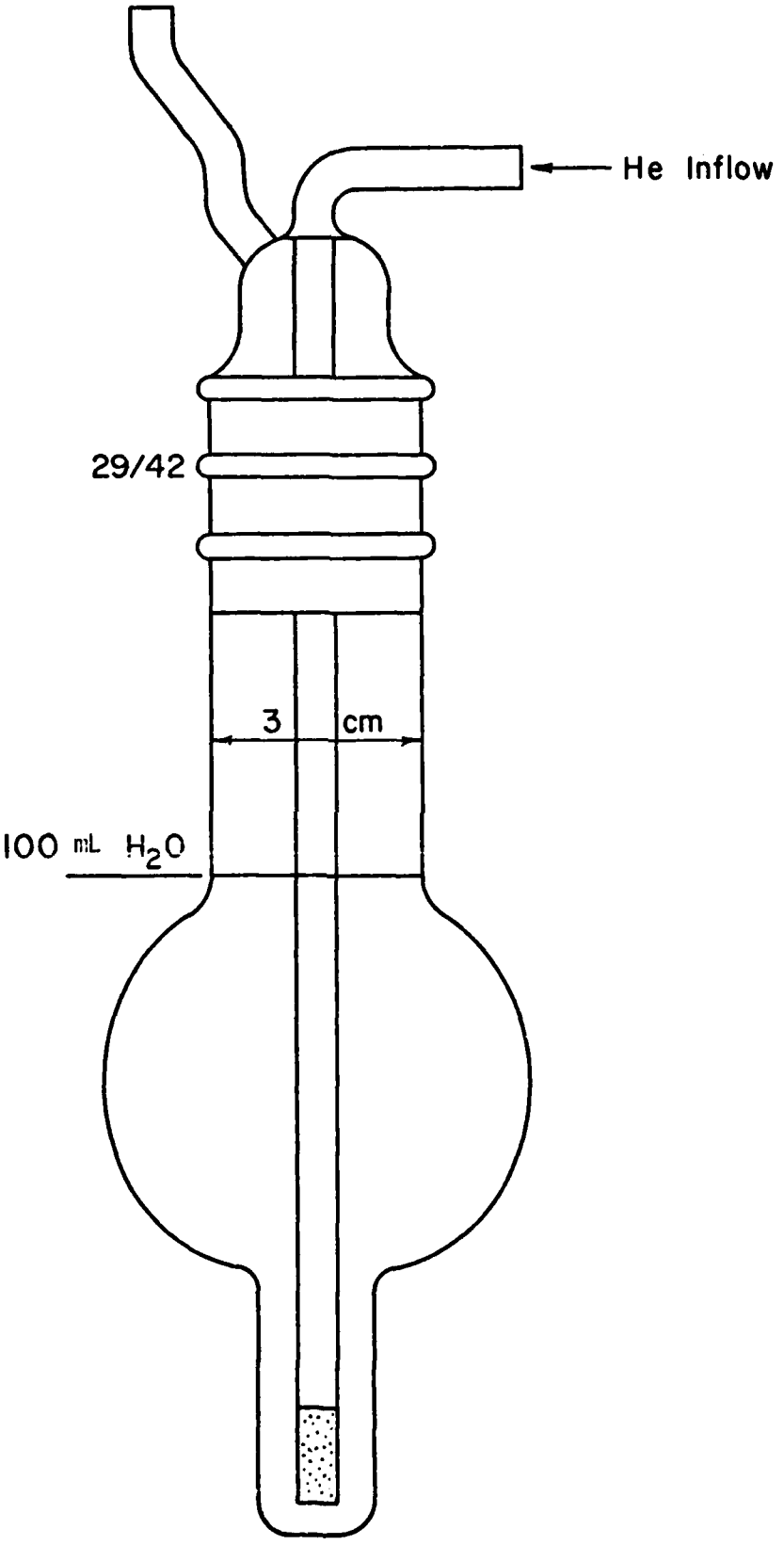

Figure 20. Stripping Bubbler (Bubbler 2).

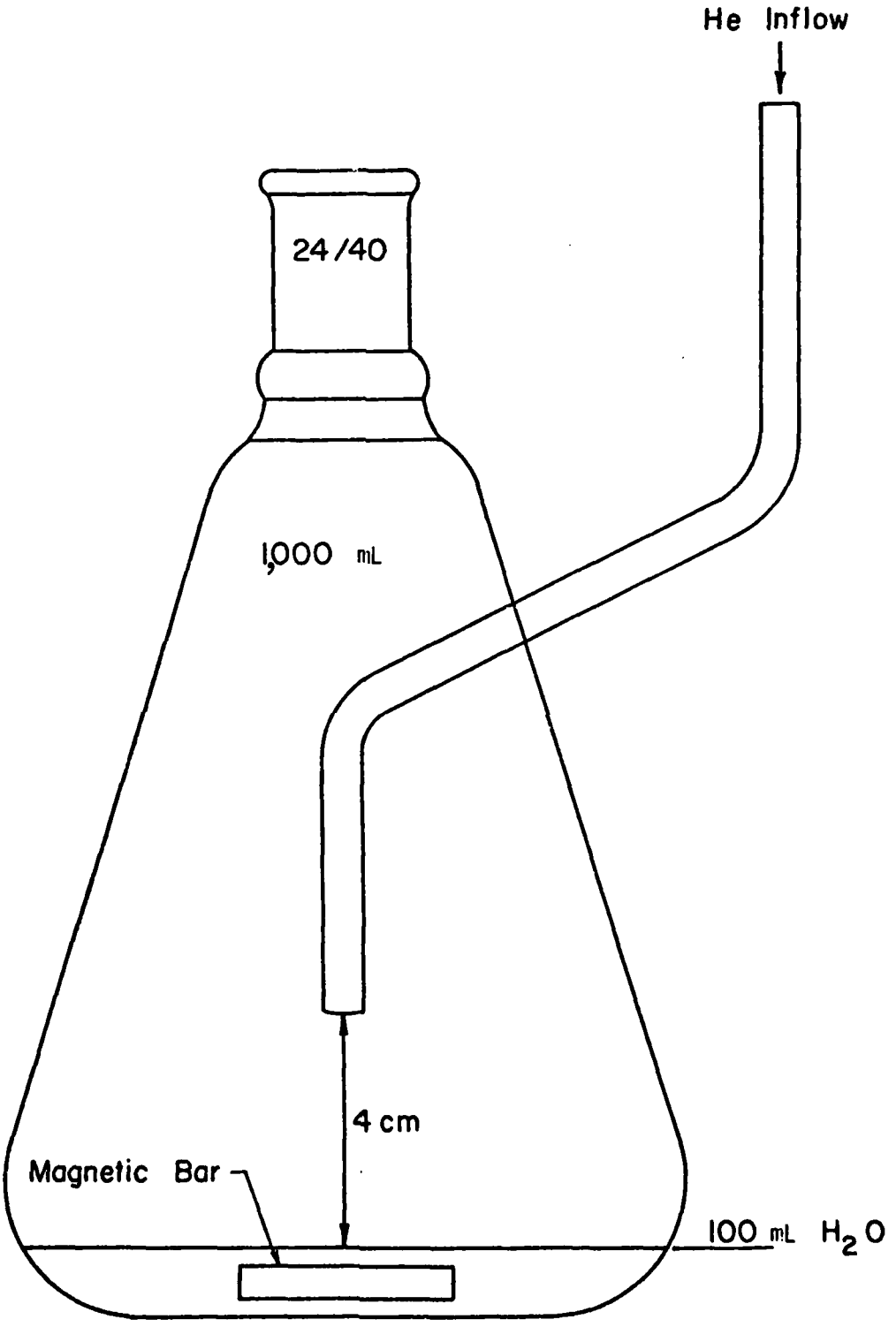

Figure 21. Stripping Flask.

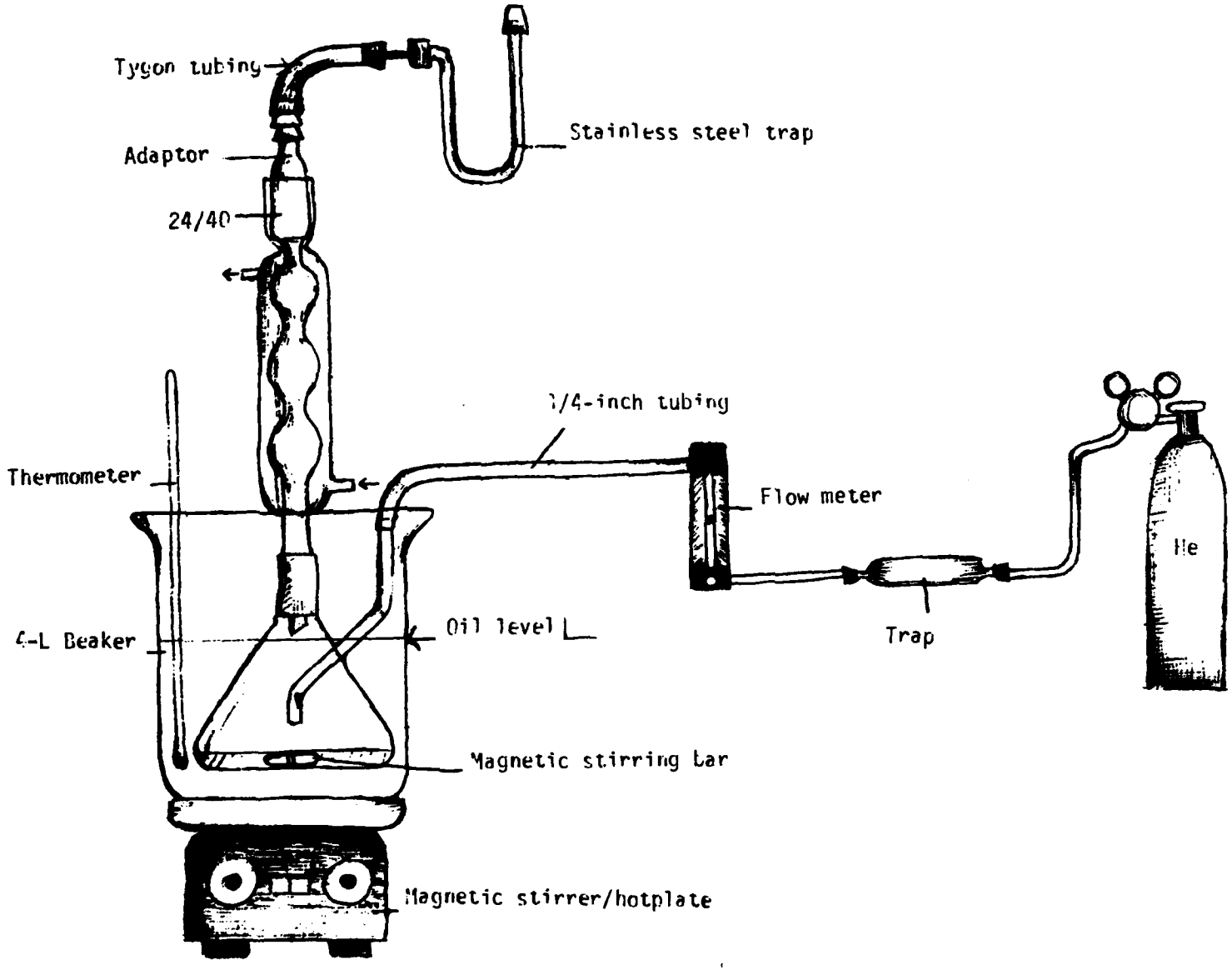

Figure 22. Stripping Apparatus.

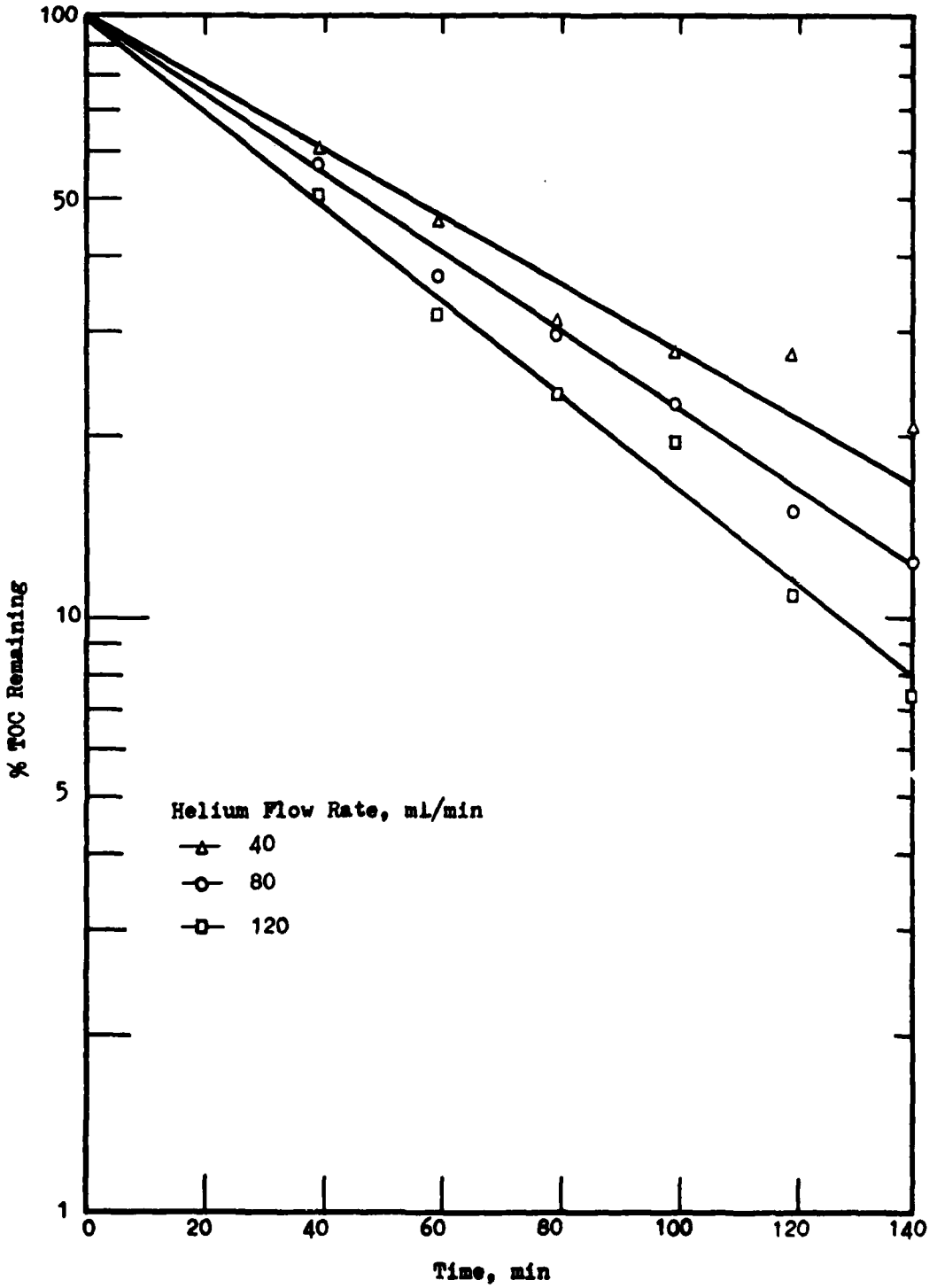

Figure 23. Stripping Time Profile at Different Helium Flow Rates for n-Butanol.

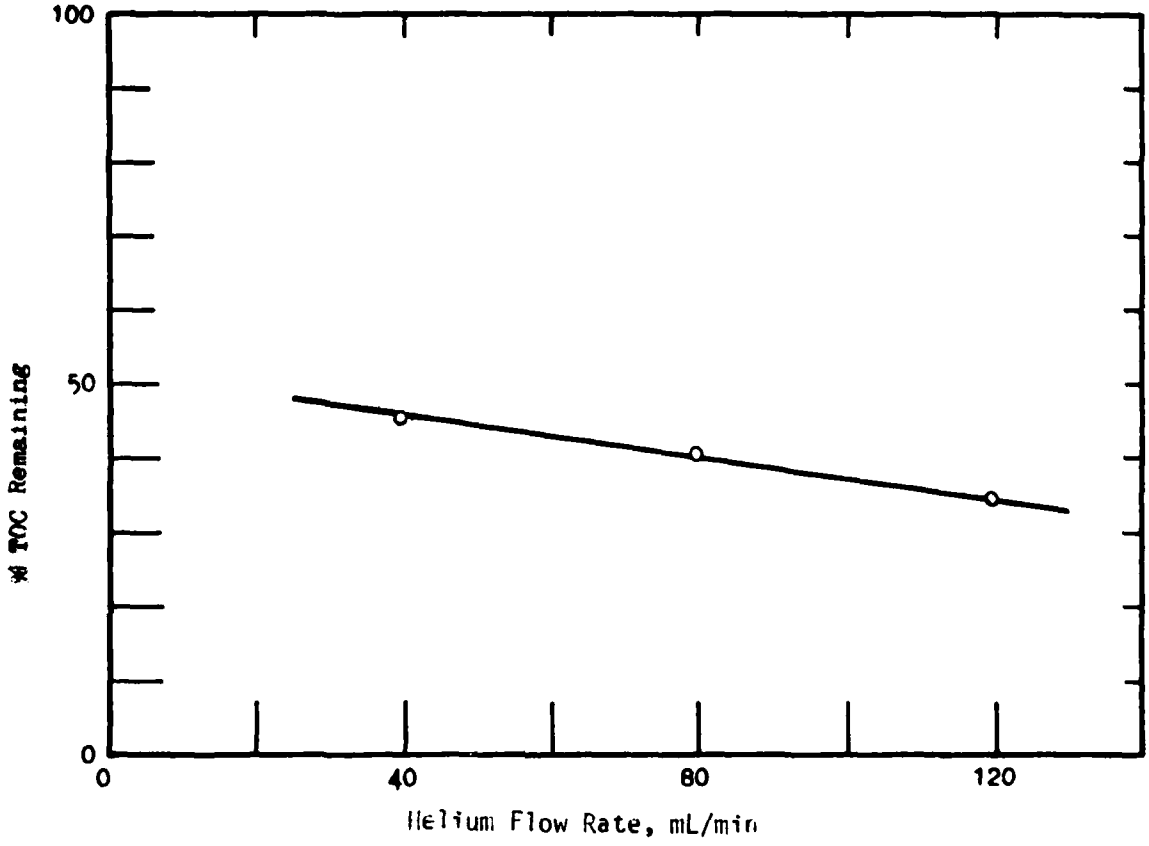

Figure 24. Stripping Efficiency at Different Helium Flow Rates for n-Butanol.

In summary, a good stirring of solution and a large gas-liquid interface are the two essential factors that provide the stripping flask with the best features for stripping. In Figure 25, the stripping efficiency of the flask in 80°C and 100°C oil batch temperatures with a helium flow rate of 120 mL/minute is also shown. A higher rate of stripping is observed at an oil bath temperature of 100°C. Though the oil bath was controlled at 100°C, the water in the flask was not boiling because of heat loss through evaporation and poor heat transfer through the glass container. It may be desirable to strip volatile compounds at a higher temperature if they are heat stable. However, if stripped at a temperature where the vapor pressure of water is too high, the water vapor may condense and subsequently clog the trap. Also, the water vapor may compete for the active sites on the adsorbent.

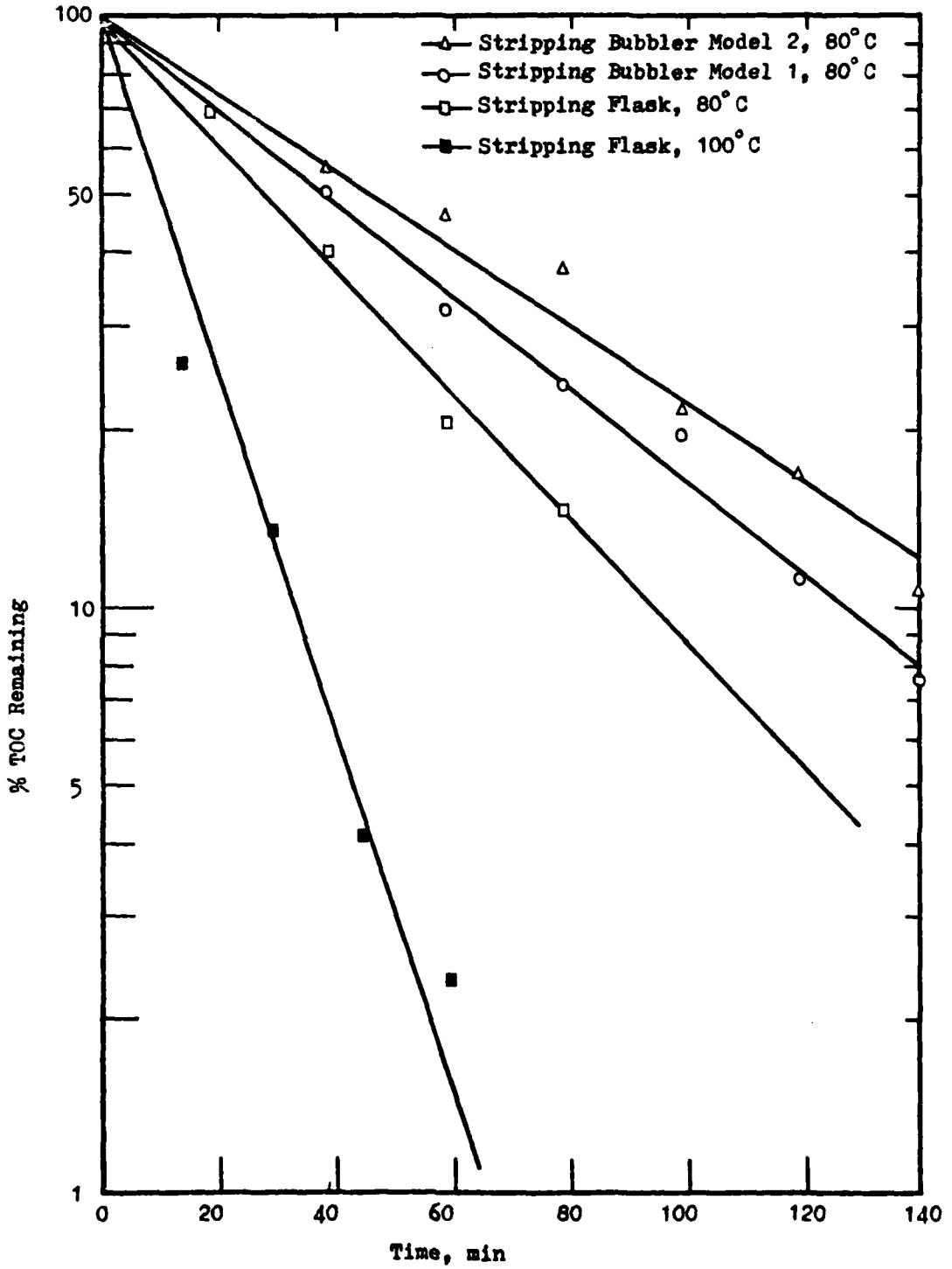

Figure 25. Stripping Time Profile for Three Different Stripping Vessels.

Adsorption and Desorption of Volatile Compounds for Different Adsorbents. The success of using the stripping methods for analyzing volatile compounds lies in their efficiency of stripping from the solution, adsorption on and desorption from the adsorbent, as well as in the sensitivity of the analytical method used to determine these compounds following the desorption process. However, a complete stripping-off of volatile compounds from the samples does not imply a complete adsorption on the adsorbent. Similarly, a complete adsorption does not ensure a complete desorption from the adsorbent. The stripping efficiency has been studied and reported in the previous section. Studies on the adsorption and desorption efficiency of different adsorbents are presented in this section.

The apparatus of stripping and adsorption is shown in Figure 22. The adsorption trap is a 1/8-inch outside diameter, stainless steel thin-wall tubing in which 0.5 g adsorbent is packed for a length of about 10 cm. The dimension of the trap is given in the upper right corner in Figure 26 in which the diagram of the injection system is shown. The 4-way valve used is a stainless steel ball valve, Model SS 43YF2 from Whitey Co., Oakland, CA. The nitrogen flow is introduced into the GC injection port through the injection needle (gauge 26, 02-0778, Supelco, Inc.) and combined the carrier nitrogen in the GC injection port to make up a total carrier flow. It is usually best to control the carrier flow through the injection needle at 10 mL/minute and the total flow at 25 mL/minute. After the adsorption trap is heated in a 160°C oil bath or in an oven for 5 minutes, the valve handle is turned 90 degrees to allow the nitrogen to flow through the heated trap to the GC injection port. The volatile compounds are then desorbed and swept into the GC column by the nitrogen carrier gas. The total carrier flow decreases during the injection because the fine packing in the trap restricts the flow. The half width of sample peak is broadened about twice as much as compared to that by direct GC injection. The peak broadening is caused by the existence of a large dead volume in the connecting tubing as shown in Figure 26 and the slower nitrogen flow due to the resistance of the adsorbent to gas flow. The broadening is also probably due to slow desorption from the trap resulting in a diffuse plug injection. A faster flow through the trap seems desirable to reduce the spreading, but the resulting higher pressure may cause leaking at the joint where the injection needle is epoxied to the stainless steel tubing that is connected to the 4-way valve. Also, the dead volume in the trap can be reduced by using a shorter tubing, which is just long enough to accommodate an adequate amount of adsorbent, and by employing an electric heater around the trap instead of an oil bath that needs a longer tubing to ensure a complete immersion of the adsorbent section into the oil bath. Figure 27 shows the GC chromatogram obtained with this 4-way valve injection system. A modified injection system that does not have these problems is described later.

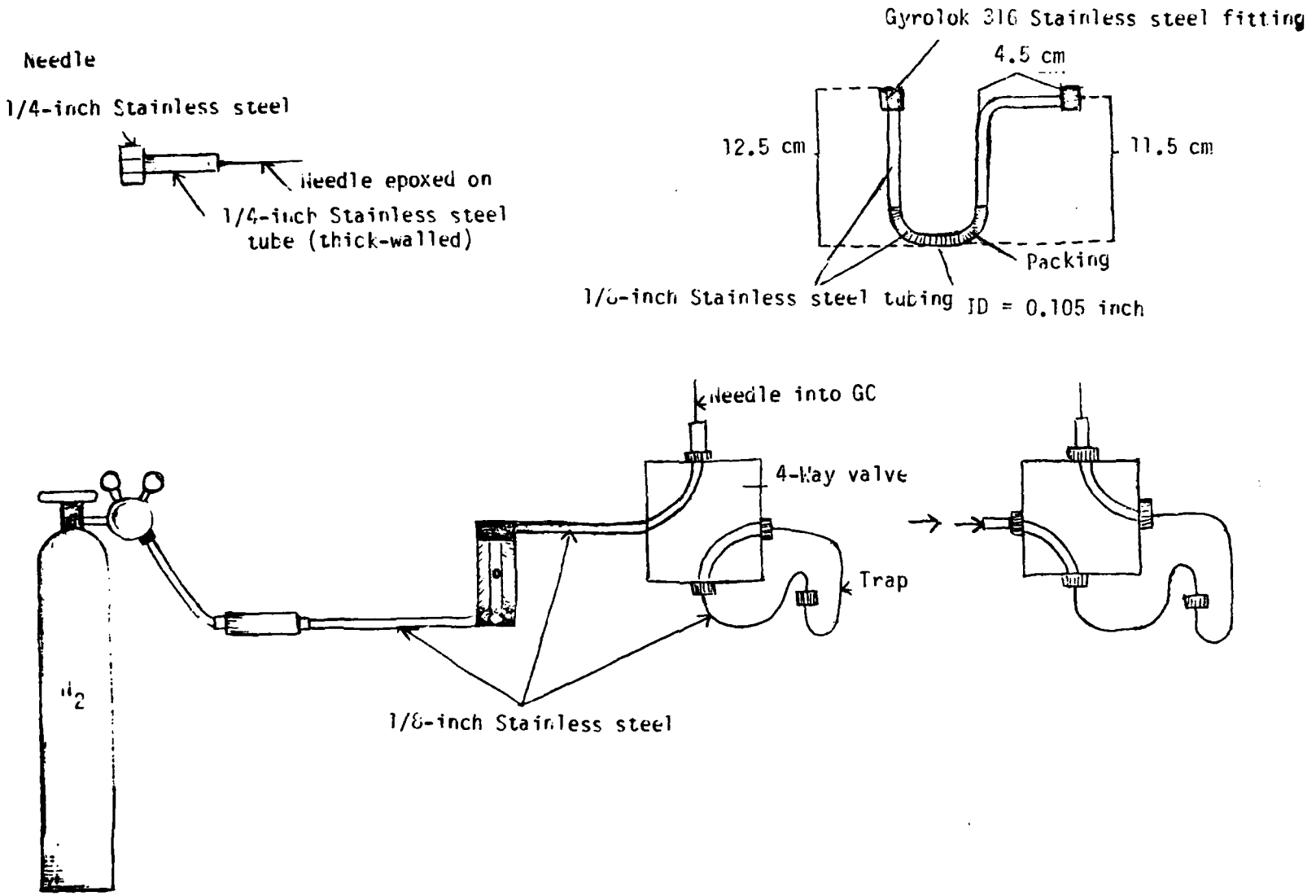

Figure 26. Diagram of 4-Way Valve Gas Injection System for GC Injection.

AD-A111 391 ILLINOIS UNIV AT URBANA F/G 13/2
FUNDAMENTAL STUDY ON THE OZONE POSTTREATMENT OF REVERSE OSMOSIS--ETC(U)
MAR 81 E S CHIAN, P P KUO, B J CHANG DAMD17-75-C-5006
UNCLASSIFIED NL

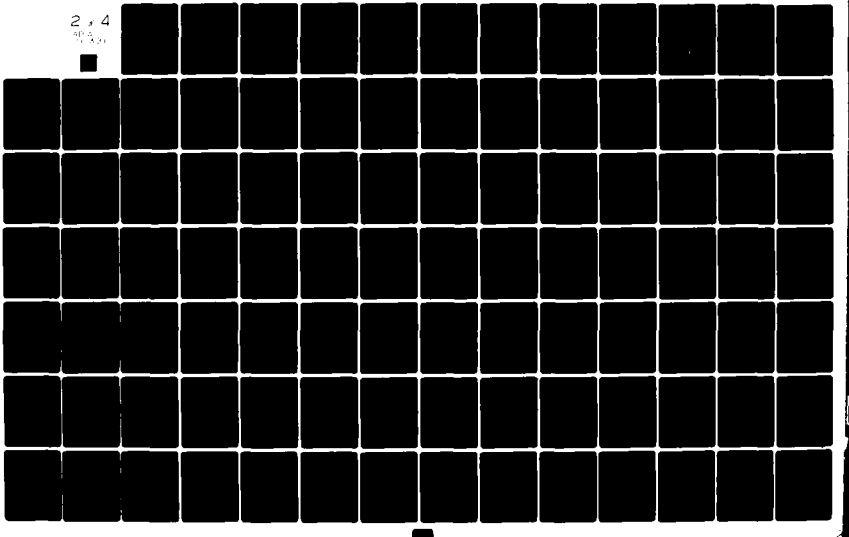

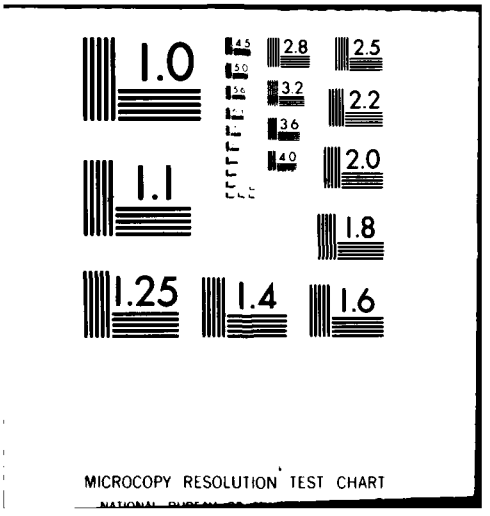
1.0
1.1
1.25
1.4
1.6
1.8
2.0
2.2
2.5
2.8
3.2
3.6
4.0
4.5
5.0
MICROCOPY RESOLUTION TEST CHART

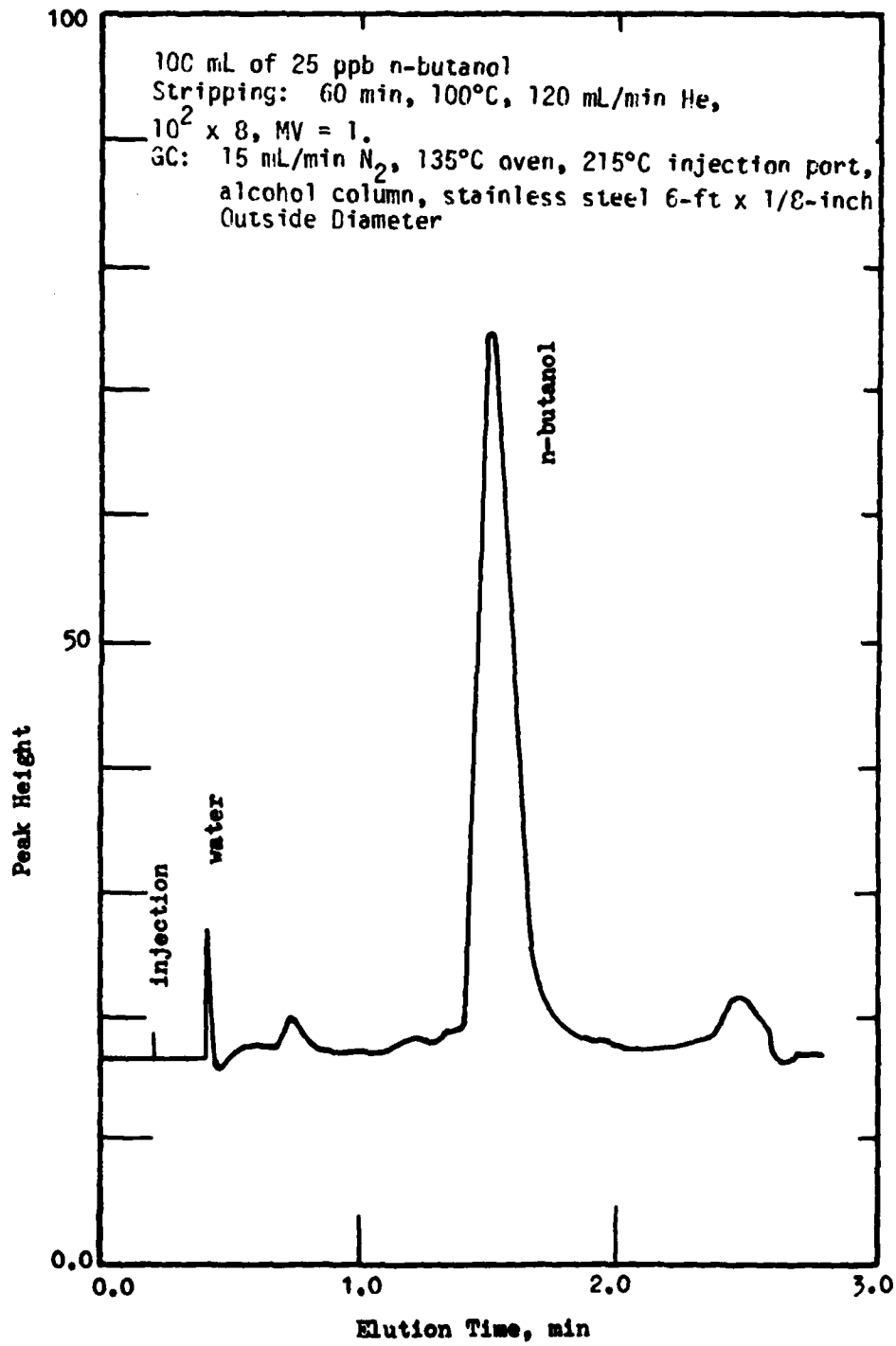

Figure 27. GC Chromatogram of n-Butanol Obtained by Use of 4-Way Valve Injection System.

Three different adsorbents were evaluated for their adsorption and desorption efficiency. The characteristics of these adsorbents are tabulated in Table 25. The GC column used is a 6-ft 1/8-inch outside diameter, stainless steel tubing packed with GP 0.4% Carbowax 1500 on Carbopack A. This column packing and column will be referred to as the alcohol packing and alcohol column in the following text. The alcohol packing was developed from the work of Corcia et al. (1973). The packing is even lower in polarity than the nonpolar squalene. Besides separating alcohols, it is also useful for the separation of short-chain aldehydes and ketones.

TABLE 25. CHARACTERISTICS OF GC PACKINGS USED AS ADSORPTION MATERIAL IN STRIPPING METHOD

Adsorbent	Mesh Size	Maximum Temperature	Separation Property	Supplier
GP 0.4% Carbowax 1500 on Carbopack A	80/100	170°C	Alcohols, aldehydes, and ketones	Supelco, Inc., Bellefonte, PA
Chromosorb 101	60/100	300°C	Glycols, alcohols, and free acids	Supelco, Inc., Bellefonte, PA
Tenax-GC	35/60	375°C	High boiling polar compounds, alcohols, polyethylene glycol compounds, diols, phenols, mono and diamines, ethanolamines, amides, aldehydes, and ketones	Applied Science Laboratories, Inc., State College, PA

Results of adsorption and desorption experiments are tabulated in Table 26. The third column also lists the stripping helium flow rates. Lower helium flow rates have to be used for those traps with alcohol packing and Chromosorb 101 because their mesh sizes are larger, i.e., the size of the packing material is smaller than that of Tenax-GC. The flow rate used was 30 mL/minute when two alcohol traps were connected in series. For low stripping gas flow rates, the stripping efficiency will be poorer as shown in Figure 24. The stripping efficiency at 120 mL/minute is 1.16- and 1.26-fold better than that at 60 and 30 mL/minute, respectively. The fourth column of Table 26 lists the GC retention time. Longer retention times have resulted when a 4-way valve injection system is used. This is expected because the sample has to travel from the trap to the GC injection port rather than being injected directly into the column. This results in a longer retention time.

TABLE 26. ADSORPTION AND DESORPTION EFFICIENCY OF n-BUTANOL WITH THREE DIFFERENT ADSORBENTS

Adsorbent	Sample	Stripping Helium Flow Rate (mL/min)	t_R (min)	Relative Peak Area of n-butanol: Stripping & Trap (4-way valve)	Relative Peak Area of n-butanol: Direct Application on Adsorbent (4-way valve)	Direct GC Injection
	1 µL of 500 ppm		1.11			12,720
	1 µL of 2,500 ppm		1.10			65,680
Alcohol	1 µL of 500 ppm		1.33		12,117 (95.3%)	
Alcohol	100 mL of 5 ppb	30	1.33	7,366, 1st trap (57.9%)		
			1.33	4,756, 2nd trap (37.4%) 12,122, total (95.3%)		
Alcohol	100 mL of ppb	30	1.46	6,752, 1st trap (10.3%)		
			1.56	5,068, 2nd trap (7.7%) 11,820, total (18.0%)		
Chromosorb 101	1 µL of 2,500 ppm		1.27		30,855 (47.0%)	
Chromosorb 101	100 mL of 25 ppb	60	1.18	14,822 (22.3%)		
Tenax-GC	1 µL of 2,500 ppm		1.24		45,845 (69.8%)	
Tenax-GC	100 mL of 25 ppb	120	1.35	45,600 (69.4%)		

The last column lists the relative peak area using the direct GC injection technique. These numbers will be referred to as the maximum peak areas that can be obtained assuming 100% efficiency for all the stripping, adsorption, and desorption steps. The amount of n-butanol in 1 μL of 500 ppm solution is equal to that in 100 mL of 5 ppb solution. Similarly, 1 μL of 2,500 ppm is equal to 100 mL of 25 ppb. The sixth column of Table 26 lists the relative peak area when 1 μL of sample solution is directly applied to the trap and then heated up for injection. This will therefore show the desorption efficiency. The fifth column lists the relative peak area using the stripping technique. By comparing columns 5, 6, and 7 of Table 26, the efficiency of adsorption and desorption is thus calculated. Since the stripping efficiency has been evaluated in the previous section and the desorption efficiency can be obtained from the results in the sixth column, the adsorption efficiency can thus be evaluated from the results in the fifth column.

The stripping efficiency is about 99.5% under the conditions studied as shown in Figure 25. The percentage shown in the parentheses of Table 26 indicates the percent recovery of n-butanol as compared to results from the direct GC injection, which are listed in the last column of Table 26. In other words, they illustrate the efficiency of adsorption and desorption in the fifth column and the efficiency of desorption in the sixth column assuming the stripping efficiency, i.e., 99.5%, can be considered as 100%. As shown in the sixth column, desorption efficiency is 95.3% for the alcohol trap. From column 5, it is seen that the first alcohol trap adsorbs and later desorbs 57.9% of n-butanol and the second trap 37.4%. The sum of these two traps accounts for 95.3%, which is equal to desorption efficiency. This value indicates that the alcohol trap efficiency is limited by the desorption process under the conditions studied for stripping 100 mL of 5 ppb n-butanol solution when the alcohol trap is used. In the case of stripping 100 mL of 25 ppb n-butanol solution, the first and the second alcohol traps account for 10.3% and 7.7%, respectively. The sum is 18%. The low efficiency can be explained by saturation of alcohol traps. This is based on the fact that the relative peak area for the first trap when 100 mL of 5 ppb solution is stripped is approximately equal to that for the first trap while stripping 100 mL of 25 ppb solution. The same is observed for the second trap (Table 26). Saturation could be the case when the active sites on the adsorbent are either occupied by water vapor, which leaves fewer sites for trapping n-butanol molecules, or actually saturated with adsorbed n-butanol molecules.

Of course, one can use a larger amount of adsorbent to solve the problem of saturation, but the GC peak may be broadened due to the spreading of the eluted sample. It is apparent that in order to give a wider dynamic range, a large amount of adsorbent should be used to avoid saturation. This amount should be determined experimentally as it may differ from solute to solute. For example, if the amount of alcohol adsorbent were 5 times that used, it would then adsorb most of the n-butanol molecules from 100 mL to 25 ppb solution, as 18% times 5 is 90% (Table 26). In the case of Chromosorb 101, the desorption efficiency is 47.0% and the adsorption efficiency is 47.4%, which is the ratio of 22.3% and 47.0% as given respectively in columns 5 and 6 of

Table 26. For the Tenax-GC trap, the desorption efficiency is 69.8%, which limits the efficiency of adsorption and desorption, since 69.4% is recovered from the trap (column 5 of Table 26). For the Chromosorb 101 trap and the Tenax-GC trap, which are composed of porous polymer, the desorption temperature could be increased to improve the desorption efficiency.

Evaluation of Bellar's Stripping Technique

The Bellar and Lichtenberg Stripping Apparatus. The efficiency of the Bellar and Lichtenberg stripping apparatus (Figure 28) was compared with that of the stripping flask (Figure 21). The results in Table 27 show that this apparatus offers higher efficiency under the same stripping conditions. Thus, dynamic headspace stripping, even with stirring of the liquid phase as in the stripping flask, is not as efficient as stripping by thoroughly mixed gas bubbles, as in the Bellar and Lichtenberg apparatus. Mieure et al. (1976) also found that the Bellar and Lichtenberg apparatus was the highest in stripping efficiency of the four apparatus studied, which included a conventional scrubber, a continuous headspace sampler, and a modified Bellar and Lichtenberg apparatus. The continuous headspace sampler was similar to the stripping flask (Figure 21), and the conventional scrubber is essentially the same as shown in Figure 19.

It should be mentioned that although the Bellar and Lichtenberg apparatus can provide a very high stripping efficiency, the amount of organics stripped is limited by the sample volume of 5 mL. The amount of organics stripped will eventually determine the sensitivity of the gas stripping/gas chromatographic analysis, which, in turn, is determined by the level of background contamination of the system. A direct, 100-fold scale-up of the stripping apparatus was not satisfactory because the same stripping efficiency could not be maintained (Kopfler et al., 1976). With the stripping flask, a few hundred milliliters of sample solution can be stripped and a higher stripping gas flow rate can be employed to compensate for the lower stripping efficiency obtained under a lower stripping flow. The stripping of many model compounds using the larger stripping flask at a higher stripping flow is very effective as discussed previously (Table 23).

Stripping Efficiency. Part A of Table 28 shows the stripping efficiency for various low molecular-weight alcohols, ketones, and aldehydes using the Bellar and Lichtenberg apparatus at room temperature (23°C) and at 95°C with a helium flow rate of 20 mL/minute. As can be seen from the table, the stripping efficiency at 23°C is very poor for all of the model compounds tested, whereas the removal after 60 minutes of stripping at 95°C was almost complete for ketones and aldehydes. However, the removal of alcohols at 95°C varied from 50% for methanol to 90% for 2-butanol and 1-pentanol, as a result of the high solubility and polarity of the lower alcohols. As shown in Part B of Table 28, the removal efficiency for ethyl acetate is only 70% when the sample is stripped at 23°C for 60 minutes, whereas its removal is 98% after 20 minutes of stripping at 95°C. As for diethyl ether, 99% removal can be achieved within 10 minutes of stripping at 95°C, while it takes 40 minutes at 23°C. The data in Part C of Table 28 show that the removal

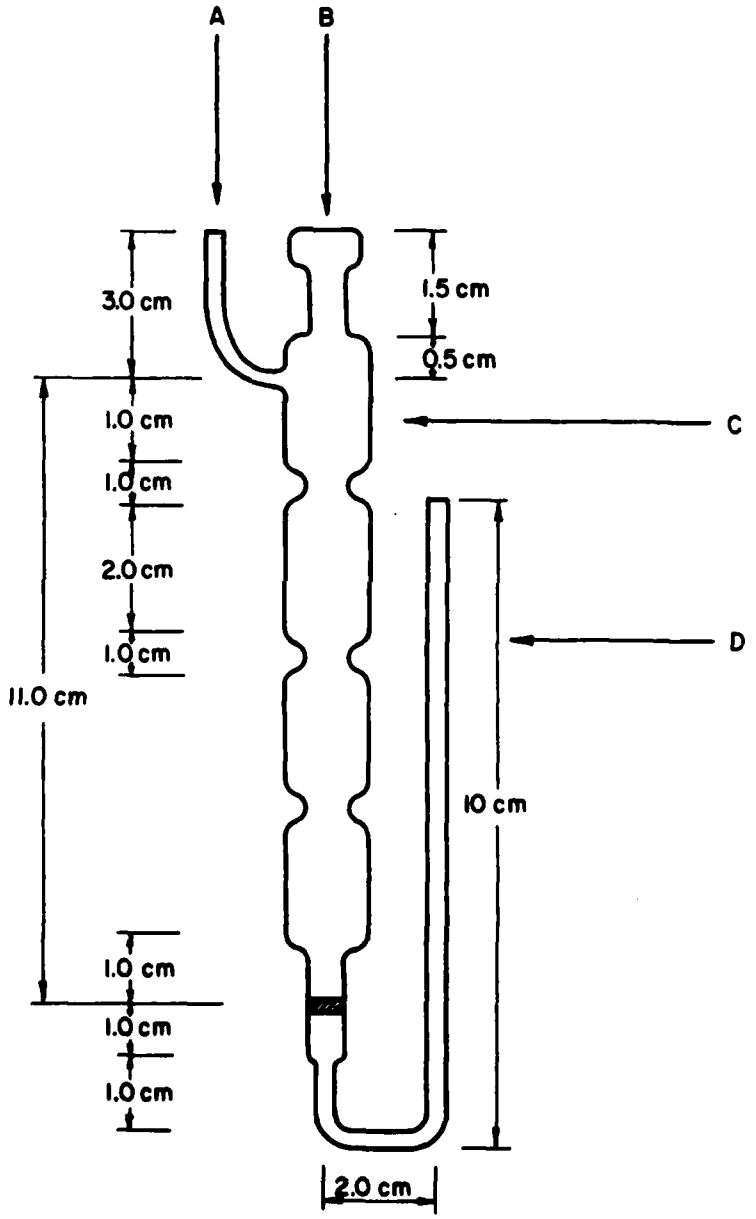

Figure 28. Dimension of Bellar's Purging Device.

TABLE 27. COMPARISON OF STRIPPING EFFICIENCIES OF SEVERAL MODEL COMPOUNDS WITH LARGE STRIPPING FLASK AND BELLAR AND LICHTENBERG APPARATUS AT ROOM TEMPERATURE

Stripping Time (min)	% Remaining[a]			
	Stripping Flask		Bellar and Lichtenberg Stripping Apparatus	
	Acetone	1-Butanol	Acetone	1-Butanol
20	98.6	99.9	84.4	97.4
40	95.9	99.5	79.5	94.8
60	92.5	99.3	70.6	89.6
	Methylene Chloride	Chloroform	Methylene Chloride	Chloroform
5	55.3	44.8	20.6	11.4
10	52.6	42.9	4.8	1.9
15	44.1	37.1	1.1	
20	40.3	30.9		
30	27.4	17.2		

a. Stripping of 80 ppm of test solution by a helium flow of 20 mL/min and at room temperature.

TABLE 28. STRIPPING OF VOLATILE POLAR WATER-SOLUBLE ORGANICS WITH BELLAR AND LICHTENBERG APPARATUS AT ROOM AND ELEVATED TEMPERATURES

Compound	Mol. Wt.	Boiling Point (°C)	Solubility[a,b] (wt %)	Stripping Temp. (°C)	% Remaining Stripping Time (min) 10	20	30	40	50	60
Part A Alcohols, Ketones, and Aldehydes[d]										
Methanol	32.04	64.7	∞	23	99.8	98.5	97.2	96.1	94.6	93.6
				95	91.2	81.1	71.6	64.8	57.1	50.8
Ethanol	46.07	78.4	∞	23	99.1	96.5	96.0	95.1	93.7	92.3
				95	89.9	79.8	67.0	59.8	54.7	44.9
1-Propanol	60.09	97.8	∞	23	99.4	97.5	97.0	95.0	91.8	91.5
				95	87.9	73.4	57.7	46.7	33.4	24.7
2-Propanol	60.09	82.5	∞	23	99.0	97.5	96.0	95.1	93.0	89.1
				95	83.1	68.6	51.2	35.4	26.4	18.3
1-Butanol	74.12	117.3	7.9	23	99.3	97.4	96.9	94.8	91.2	89.6
				95	83.4	77.7	55.3	37.4	26.7	17.3
2-Butanol	74.12	99.5	12.5	23	99.6	97.2	93.2	90.4	88.7	87.1
				95	82.0	56.1	34.8	22.7	14.4	9.1
1-Pentanol	88.15	137.3	2.6	23	98.7	96.8	91.3	89.2	88.9	88.5
				95	82.7	64.2	39.4	22.5	13.6	8.2
Acetone	58.08	56.6	∞	23	89.9	84.4	82.6	79.5	73.9	70.6
				95	82.0	55.4	30.4	19.1	9.3	6.2
2-Butanone	72.10	79.6	26.7	23	94.5	89.7	85.4	76.6	73.1	65.4
				95	74.7	38.9	14.3	5.4	1.7	0
3-Pentanone	86.13	101.7	∞	23	81.1	74.0	65.5	59.2	51.6	47.4
				95	51.7	15.1	2.9	0		
Acetaldehyde	44.05	20.2	∞	23	90.5	84.5	75.3	66.2	62.3	55.6
				95	60.9	15.4	2.7	0.4	0	
Propional-dehyde	58.08	49.5	13.8	23	89.9	83.6	71.5	70.8	65.6	60.6
				95	67.3	24.4	16.1	10.5	7.0	4.4
Butyraldehyde	72.10	75.7	3.5	23	76.3	61.9	50.9	43.1	34.6	25.1
				95	67.9	18.1	7.7	2.8	0	
Part B Ethyl Acetate and Diethyl Ether[e]										
Ethyl Acetate	88.12	77.1	8.5(15)	23	80.4	67.3	49.9	46.9	39.0	31.3
				95	22.8	1.5	0			
Diethyl Ether	74.12	34.6	6.5	23	31.9	10.6	3.3	1.1	0	

					Stripping Time (min) 1.2	2.5	5	7.5	10	15
Diethyl Ether				95			11.0		0.7	0
Part C Methylene Chloride and Chloroform[e]										
Methylene Chloride	84.94	40.5	2.0	23		40.5	20.6	10.2	4.8	1.1
				95		15.7	2.0	0.5	0	
Chloroform	119.39	61.2	0.8	23		31.1	11.4	4.1	1.9	0
				95		9.1	0.6	0.1	0	
Part D Benzene and Toluene[f]										
Benzene	78.11	80.1	0.07(22)	23		15.5	3.7		0.3	
				95	15.0	2.0	0			
Toluene	92.15	110.6	0.05(25)	23		15.9	3.8		0.3	
				95	19.3	1.8	0			

a. Solubility at 20°C, otherwise temperature was indicated in parentheses.
b. Solubility data were obtained from Perry's Chemical Engineering Handbook, McGraw Hill, New York (1963).
c. 8 mL of test solution were stripped in the Bellar and Lichtenberg stripping apparatus by helium gas at 20 mL/min.
d. Initial concentration was 80 ppm except for butyraldehyde, which was 40 ppm.
e. Initial concentration was 70 ppm.
f. Initial concentration was 45 ppm.

of methylene chloride and chloroform at 23°C is almost complete within 15 and 10 minutes of stripping, respectively, while the removal at 95°C is quite complete within 7.5 minutes of stripping for both compounds. The removal of benzene and toluene is very efficient at either 23°C or 95°C, as shown in Part D of Table 28; the stripping efficiencies obtained at 23°C for acetone, 2-butanone, methylene chloride, chloroform, and benzene agree very well with the literature values (Bellar and Lichtenberg, 1974b; Mieure et al., 1976).

Although stripping of VPO's at an elevated temperature (95°C) is more effective than that at room temperature, it should be cautioned that in certain cases, undesirable chemical reactions might have occurred upon heating of samples. For example, halomethanes were found to form resulting from the reaction of free chlorine present in drinking water (Kopfler et al., 1976; Bellar et al., 1974b). Acetone and other methyl ketones (VPO's) have been shown to be some of the precursors of halomethanes (Rook, 1976).

Fractional purging or fractional stripping has been employed by Kopfler et al. (1976) to selectively determine volatile organics in water. Three consecutive 30-minute strippings were performed for each sample, the first at 6°C to remove the most volatile nonwater-soluble organics, the second at at 95°C to remove most of the remaining volatile nonwater-soluble organics, and the final one at 95°C to detect volatile water-soluble organics. Fractional purging is one approach to detect organics selectively according to their volatility and solubility. Consequently, it simplifies the identification process during subsequent GC or GC/MS analyses and may also eliminate the breakthrough of organics on the adsorbent. From the data shown in Table 28, it appears at least possible to first detect compounds having solubilities of less than 2% by stripping at 23°C for 15 minutes and then to detect those having solubilities greater than 2% by stripping at 95°C for 60 minutes.

Relative volatility is the major factor in determining the stripping efficiency if the mass transfer of solute molecules from the bulk of the liquid to the gas-liquid interface is not the rate-limiting factor during the entire stripping process. Unfortunately, published values of the relative volatility of most of the compounds studied were not available, and thus it was not possible to correlate the stripping efficiency with the relative volatility of the compound of interest. Nevertheless, it should be mentioned that (1) because volatility is a product of the activity coefficient and the vapor pressure of the pure compounds and (2) because the activity coefficient is a function of the concentrations of the dissolved solutes, the stripping efficiency is dependent on total solute concentration, which is predominantly governed by salt concentration. Therefore, to achieve reliable organic preconcentration or sampling onto the adsorbent by stripping, steps should be taken to minimize any variation of total solute concentration from one sample to another. This precaution is particularly important if the samples to be studied have a wide variation of total solute concentration, as is the case, for example, with sea water as compared to drinking water. The stripping efficiency for an organic compound present in an unknown matrix can be determined by employing a standard addition

technique. This process is too difficult, however, if many unknown matrices are encountered and many compounds are to be determined. Saturating sample solutions with a certain salt may be a suitable means to control the total solute concentration and therefore the relative volatility of the compounds of interest. Since adding salt to the sample solution enhances the relative volatility, it also increases the stripping efficiency. The effect of salting out has been studied for lower ketones by Mieure et al. (1976) and has been employed in determining organic constituents present in drinking water (Novak et al., 1973).

Adsorption and Desorption Efficiencies. Desorber 2 of Bellar's system (Bellar and Lichtenberg, 1974b) was constructed, although modified to suit our needs. Figure 29 shows the desorber with modifications indicated. First, a syringe needle of 02-0778 of Supelco, Inc. (needle for 701 RN syringe) was fitted onto the 1/16-inch end of the Swagelok reducing union with a regular 1/16-inch Swagelok nut. No ferrules were needed because there was a Teflon seal on the base of the syringe needle to ensure a gas-tight connection after the nut was screwed on to hold the needle. Second, a copper constantan thermocouple wire was used to control the temperature inside the desorber. Third, a 1-ft heating tape was wrapped around the desorber of the 1/4-inch stainless steel tubing as a heating element. The tape was made from a 2-ft length of 1/2-inch wide heating tape by cutting it in half. Heating was controlled by a temperature controller (Model 32-06-09 DIN-Size, Waynco, Inc., Winona, MN). The latter two modifications allow the desorbing temperature to be controlled well within ± 2°C.

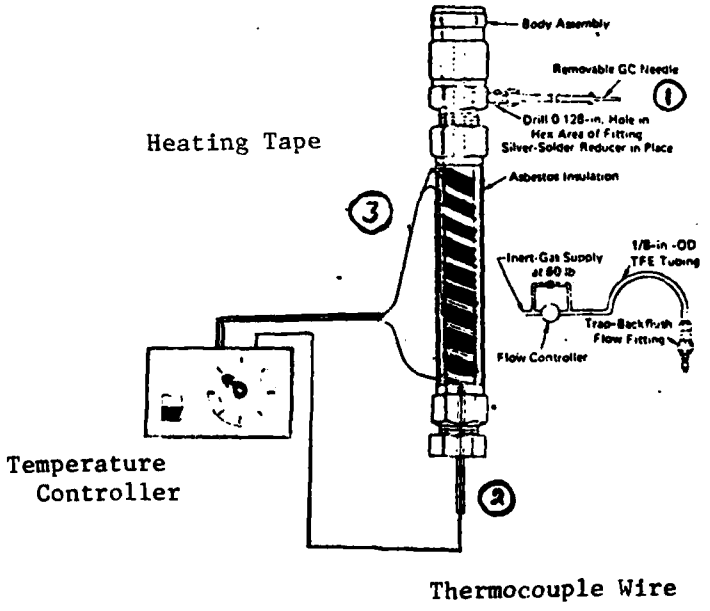

Figure 29. Desorber.

As shown in Figure 29, the thermocouple wires were inserted into a 1.5-inch length of 1/8-inch outside diameter thin-walled stainless steel tubing, and the junction of the thermocouple wires was silver-soldered to the sealed end of the tubing. The tubing was put through the hole drilled on the face of the end cap. The tubing was then silver-soldered on the end cap so that the thermocouple junction reached almost to the end of the trap after the end cap was screwed to the desorber. The end cap with thermocouple wires can be removed from the desorber and used independently as a temperature monitor or sensor. The desorber temperature was sensed by thermocouple wires connected to the temperature controller, which regulated the power supplied to the heating tape to maintain a constant temperature inside the desorber. The controller is rated for operation from room temperature up to 1,000°F, but the upper range for the copper-constantan thermocouple wires is only 750°F (~400°C).

Several difficulties were experienced in testing the desorber in our laboratory. The desorber can only sustain temperatures up to 450°F (232°C), limited by the maximum temperature of Viton O-ring in the quick connect. Thus, the temperature inside the adsorbent can be no higher than approximately 180°C. Although Bellar and Lichtenberg (1974b) used a desorption of 130°C, the desorption temperature for quantitatively releasing adsorbed organics from Tenax-GC should be at least 200°C to cover a wide variety of compounds of interest, as was observed in our laboratory. In addition, conditioning of Tenax-GD adsorbent should take place at about 325°C. The outer surface of the adsorbing trap is enclosed and heated inside the desorber and therefore contributes blank contamination on gas chromatograms, a higher undesirable situation when determining trace amounts (ppb or less) of organics. Besides, a large investment would be required if several traps are in demand because each trap requires one quick connect. The desorber as well as the injection system was therefore redesigned, and they are described in the following.

A block diagram of the gas chromatographic injection system is shown in Figure 30, and its components are listed in Table 29. The carrier gas line to the gas chromatographic injector on the HP 5750B gas chromatograph was disconnected at the flowmeter outlet line (1/8-inch copper tubing) and connected to the 4-way valve, as shown in the figure. The carrier gas line and the valve were both maintained at 70°C by two 4-foot-long heating tapes. The heating jacket was maintained at 250°C (measured inside the jacket) by a heating cord. The temperature inside the adsorbent was 200°C. The helium carrier gas flow rate was 20 mL/minute. The operation of the gas chromatographic injection system is described below. The adsorption trap is connected to the injection unit as shown in Figure 30. The heating jacket is slid over the trap, and after 1 minute the valve is turned to the dotted position. The helium gas thus carries the thermally desorbed organics from the trap to the gas chromatographic column, which is maintained at room temperature. After 3 minutes of injection, the valve is turned, and the heating jacket is removed and returned to its original position. The gas chromatographic oven temperature is then programmed to increase as desired.

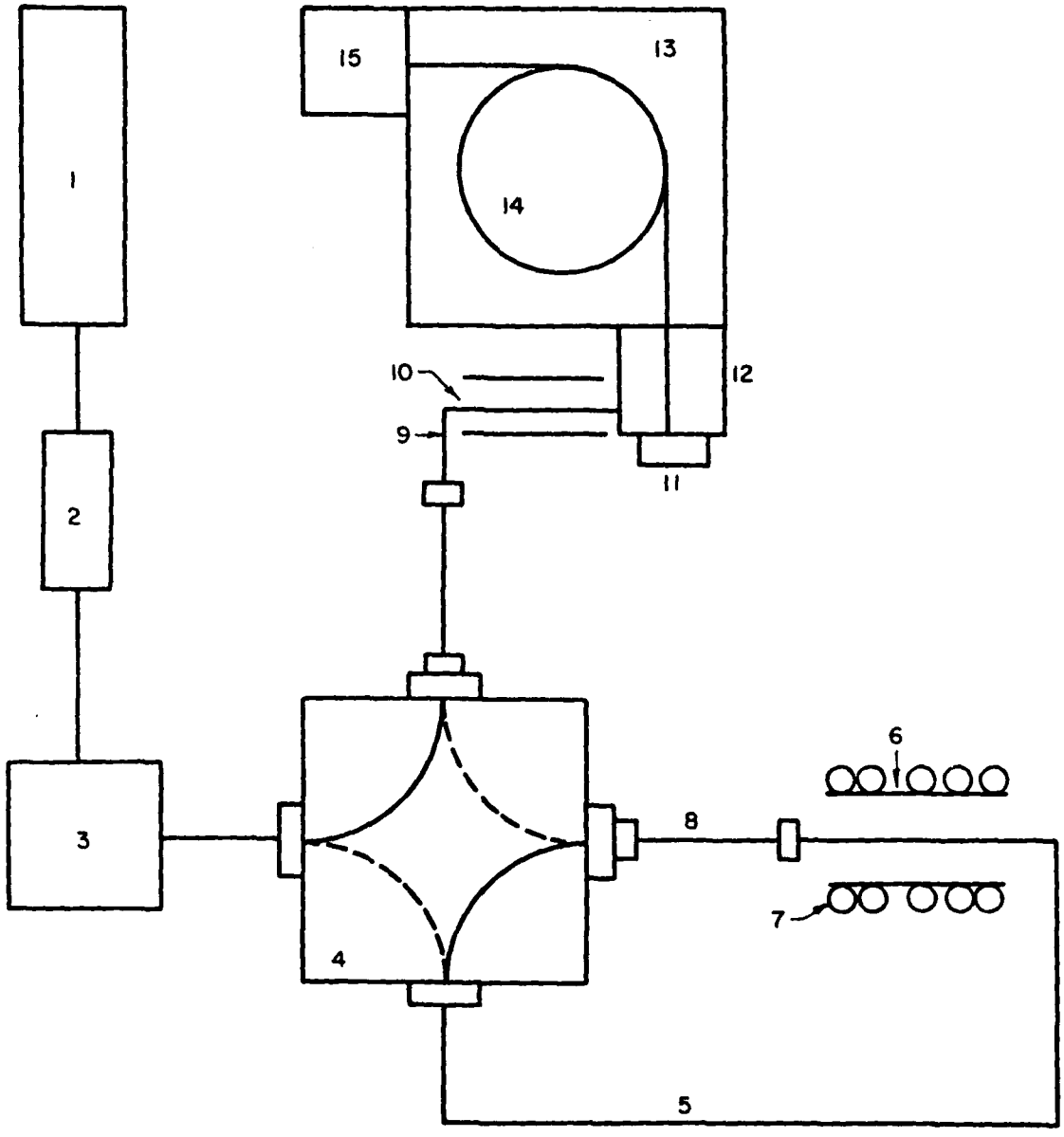

Figure 30. Block Diagram of Gas Chromatographic Injection System.

TABLE 29. COMPONENTS OF GAS CHROMATOGRAPHIC INJECTION SYSTEM

1.	Helium gas tank.
2.	5 A molecular-sieve trap (Supelco, Inc., Bellefonte, PA).
3.	Flow controller, model 8744 (Brooks Instrument, Bloomington, IL).
4.	4-way valve, model SS 43YF2 (Whitey Co., Oakland, CA).
5.	1/4-inch outside diameter, stainless steel.
6.	Heating jacket, 7/8-inch outside diameter, 3/4-inch inside diameter brass tubing.
7.	Heating cord, 6-ft-long (Cole-Parmer, Chicago, IL).
8.	Adsorption trap, 7-inch-long, 1/4-inch outside diameter, stainless steel tubing packed with adsorbent.
9.	Carrier gas line.
10.	Heating oven, heated by a 4-ft-long, 1/2-inch-wide heating tape (Cole-Parmer, Chicago, IL).
11.	Gas chromatographic injector head.
12.	Gas chromatographic injector oven.
13.	Gas chromatographic column oven.
14.	Gas chromatographic column.
15.	Flame ionization detector.

Numbers are keyed to Figure 30.

A 325°C oven was used to condition Tenax-GC traps with helium or nitrogen gas flowing through them overnight. The traps were removed from the oven and cooled to room temperature before being used to adsorb organics. Gas flow was maintained during cooling.

The GC column used for separating alcohols, ketones, aldehydes, diethyl ether, and ethyl acetate was 0.2% Carbowax 1500 on 80/100 mesh Carbopack C (Supelco, Inc., Bellefonte, PA) on a 6-ft x 1/4-inch outside diameter glass column. For determining methylene chloride, chloroform, benzene, and toluene, a 6-ft x 1/8-inch outside diameter stainless steel column packed with 0.4% Carbowax 1500 on 80/100 mesh Carbopack A (Supelco, Inc., Bellefonte, PA) was used. This column was conditioned at 200°C.

The adsorption and desorption efficiencies of three adsorbents were evaluated using 1-butanol as the model compound. The results were discussed previously. Chromosorb 101 exhibits the poorest adsorption efficiency and Tenax-GC the best. When desorbing at 150°C, the maximum temperature for the Carbowax 1500/Carbopack A, Chromosorb 101 provides the poorest desorption efficiency and Carbowax 1500/Carbopack A the best. When desorbing at 200°C, however, the desorption efficiency for Tenax-GC is comparable to that of Carbowax 1500/Carbopack A. The Tenax-GC was thus chosen as the sole adsorbent for extensive study because of its high adsorption and desorption efficiencies as well as its thermal stability.

Tenax-GC, 0.4 g, was packed into each adsorption trap. The temperature inside the adsorbent was 200°C during the desorption process. Table 30 shows the adsorption and desorption efficiencies as well as the stripping efficiency and overall recovery. The adsorption efficiency shown in Table 30 was obtained from stripping sample solutions at concentrations ranging from 0.08 to 8 ppm and desorption efficiency was obtained accordingly within this concentration range. Experimental work on stripping the sample solutions within the above concentration range could not be done because of the limitation of the sensitivity of the GC to analyze directly the stripped aqueous solutions. Therefore, a study on stripping efficiency was made with solutions at a higher concentration (see footnotes to Table 28). The desorption efficiency was calculated using the stripping efficiency obtained above. The radioactive tracing technique could very well be implemented for elucidating the stripping efficiency for solutions at the ppb level as well as for monitoring adsorption and thermal desorption from Tenax-GC trap. The desorption efficiency is generally better than 80% except for methanol and toluene. A higher desorbing temperature would perhaps improve the desorption of toluene. The small retention volume for methanol on the GC column results in a diffused injection and thus a broad peak. The low recovery might be a result of that effect rather than low desorption efficiency. Diffused injection can be avoided by cooling the front section of the GC column with dry ice or liquid-nitrogen bath during the thermal desorption process and rapidly heating the cooled section to permit fast injection.

TABLE 30. ADSORPTION AND DESORPTION EFFICIENCIES FOR MODEL COMPOUNDS

Compound	Stripping[a]	Adsorption[b]	Desorption[b]	Overall
Methanol[c]	49.2	--	43.3	--
Ethanol	55.1	21.3	80.7	9.5
1-Propanol	75.3	74.7	79.1	44.5
2-Propanol	81.7	79.7	85.9	55.9
1-Butanol	82.7	82.3	88.0	59.9
2-Butanol	90.9	75.9	87.3	60.1
1-Pentanol	91.8	91.1	83.8	70.1
Acetone	93.8	100.1	94.6	88.8
2-Butanone	100.0	99.4	86.6	86.1
3-Pentanone	100.0	92.4	92.7	85.7
Acetaldehyde	99.6	79.5	81.3	64.4
Propionaldehyde	89.5	78.5	81.8	57.5
Butanal	97.2	84.3	100.6	82.4
Ethyl Acetate	98.5	91.0	91.7	82.2
Diethyl Ether	100.0	89.6	90.5	81.1
Methylene Chloride	90.9	84.5	91.8	76.7
Chloroform	100.0	79.3	95.1	75.4
Benzene	99.7	98.5	90.0	88.4
Toluene	99.7	99.2	73.5	72.7

a. Alcohols and ketones were stripped at 95°C for 1 hour; aldehydes at 95°C for 40 min; and ethyl acetate and diethyl ether at 95°C for 20 min. For methylene chloride and chloroform, stripping was conducted at room temperature for 15 min. For benzene and toluene, stripping was carried out at room temperature for 10 min. For all cases, the helium flow rate was 20 mL/min. The data of stripping efficiency were obtained from Table 28.

b. Adsorption was studied for 8 mL of solutions at 0.08, 0.8, 4.0, and 8.0 ppm and desorption was studied accordingly within this range.

c. See text for explanation.

Desorption was also carried out at 150°C for 3-pentanone and 1-butanol. The results indicate that the desorbing temperature should be high enough to ensure a quantitative release of the organics from the adsorbent. It seems that the desorbing temperature should be at least 200°C.

As shown in Table 30, the adsorption efficiency is generally better than 75% except for methanol and ethanol. Poor adsorption of methanol and ethanol is attributable to the polar nature of these compounds relative to that of Tenax-GC. Also, it can be noticed that the adsorption of alcohols and aldehydes on the Tenax-GC is not as effective as the adsorption of ketones and aromatic compounds, another example of the effect of polarity between the adsorbent and the adsorbate on the efficiency of adsorption. The adsorption and desorption efficiencies for acetone agree very well with those reported by Versino et al. (1974).

Breakthrough was observed for methanol, ethanol, 2-propanol, and 1-propanol as they were detected in the second adsorption trap, which was connected in series with the first one. In fact, methanol was hardly detected in the first trap and only 14% of the total methanol stripped from the solution was retained in the second one. Such breakthrough of methanol was also observed by Bertsch et al. (1975). Furthermore, the methanol must have been displaced away from the first trap; otherwise, the methanol content would have been equal in both traps, assuming that sorption equilibrium had been established. The presence of moisture on the stripping gas that carries stripped organics from the solution to the adsorption Tenax-GC trap will decrease the specific retention volume on the Tenax-GC by 15% for methanol, 11% for ethanol, and 1.3% for propanol (Janak et al., 1974). Consequently, displacement and breakthrough will occur sooner in the presence of water moisture. That situation evidently was encountered in this study, as the stripping of alcohols was conducted at an elevated temperature, i.e., 95°C for 60 minutes.

Two approaches can be followed to eliminate the amount of moisture in the stripping gas. The first approach is to strip the sample solution at a lower temperature and the second one is to install a fractionation column between the stripping vessel and the adsorption trap. The former will, however, need a longer stripping time to achieve a quantitative recovery of the VPO's. This may cause breakthrough to occur because a larger volume of stripping gas would have to pass through the adsorption trap. As to the second approach, an appreciable amount of moisture can only be eliminated when a highly efficient fractionation column is used. Condensing water vapor during the stripping is, however, not necessary, according to the authors' experience. Perhaps the best approach to avoid breakthrough is to use an adsorption trap containing a larger quantity of Tenax-GC (>0.4 g). However, it should also be noted that injection into the GC/MS of an excessive amount of water retained in the trap, resulting from stripping of aqueous solution at an elevated temperature, is detrimental to the magnetic deflection mass spectrometer. It was found that approximately 1 mg of water can be tolerated by the Varian-MAT 311A GC/MS. An appreciable amount of water can be removed from the Tenax-GC trap by passing a stream of helium through

the trap at room temperature at a rate of 40 mL/minute for 5 minutes prior to heat desorption. This may result in loss of some organic compounds having small values of specific retention volume. However, the possibility of losing a small amount of such organic compounds does not affect the GC/MS identification as quantitation of organics is normally carried out separately on another GC operated in parallel.

The breakthrough of highly polar volatile organics was also noticed by other investigators in sampling volatile organics onto the Tenax-GC traps in the analysis of polluted air (Bertsch et al., 1974) and sage-leaf (Novotny et al., 1974).

In addition, the Tenax-GC trap was saturated, after sorption equilibrium was established and before breakthrough occurred, after adsorbing approximately 20 µg of such alcohols as 1-butanol, 2-butanol, and 1-pentanol. This conclusion was reached because the percentage recovery of these alcohols on the Tenax-GC trap from stripping an 8-ppm solution is only half of that from stripping a 4-ppm solution. Another possible cause of the decrease in recovery is the development of a nonlinear adsorption isotherm at higher concentrations. Difficulties in determining alcohols with a Tenax-GC precolumn are thus apparent when breakthrough, saturation, and displacement occur.

With the use of 120 mL of aqueous sample, most of the VPO's tested can be determined at the ppb level or lower by gas chromatography while incorporating procedures of gas stripping, sorption, and thermal desorption. The percent relative standard deviation obtained from four separate analyses is generally better than 10% at ppb levels.

The gas stripping/gas chromatographic method has found its application in determining trace amounts of VPO's present in effluents from various physical-chemical processes treating water and wastewaters. One such example is the use of this method to determine VPO's in the effluent of the reverse osmosis process treating MUST (Medical Unit Self-Transportable) hospital wastewaters (Chian and Kuo, 1976). Similar to reverse osmosis, activated carbon is also ineffective in removing water-soluble VPO's, and the gas stripping/gas chromatographic method can be used to determine VPO's in the treated effluent. The significance of determining such compounds is in the reuse of treated effluents, especially for potable purposes. Also, the technique has been used to determine VPO's in surface water (Chian et al., 1976). Acetone and ether at ppb levels were easily determined.

Summary. It should be realized that volatile organics quantitatively or even qualitatively determined by the gas stripping/gas chromatographic procedure can be reliable only when the adsorption and desorption efficiencies as well as the stripping efficiency for organics have been experimentally determined. These factors are particularly critical in determining lower alcohols and other highly volatile organics having a small specific retention volume on the adsorbent, because they are highly subject to breakthrough

and displacement. If breakthrough and displacement occur, the organic composition on the adsorbent will not represent the composition in the water sample. Instead, a distorted analytical result will be obtained. Though the gas stripping/gas chromatography is a highly sensitive method for determining VPO's, a quantitation, or even determining the presence or absence of a particular compound, must be carried out with caution.

Determination of Volatile Organics in RO Permeates

Volatile organic compounds were determined in RO permeates obtained from Malden Laboratory by the gas stripping/gas chromatographic analysis using Bellar's procedure. Samples were stripped at 95°C for 1 hour for determining volatile polar water-soluble organics and also stripped at room temperature for 20 minutes for determining volatile nonpolar water-insoluble organics. The latter analyses were performed in order to detect nonpolar compounds that might be present in the RO permeates in trace amounts or formed during the process of ozonation or ozonation-chlorination of the RO permeates. The results are shown in Tables 31 and 32. The concentrations of acetone, 2-propanol, and methyl ethyl ketone agree very well with those obtained by the headspace gas chromatographic technique (Cowen and Cooper, 1975) and by the distillation headspace gas chromatographic technique (Chian et al., 1977b). Methanol and ethanol were not determined because of their serious breakthrough on the Tenax-GC adsorption trap as described previously. As can be noticed in Table 32, nonpolar compounds are present in samples at the nL/L (~ppb) level except for chloroform, the concentration of which ranges from 0.015 to 0.124 μL/L (~ppm). Thus, nonpolar compounds are present in the samples only in trace amounts and account for a negligible amount of the total organic carbon (see the last two columns of Table 32). This agrees with the prediction based on the characteristics of the RO separation of organic compounds for those RO permeates without further ozonation and ozonation-chlorination (Fang and Chian, 1976). Chlorination of Sample IT-7-3 does not increase the concentrations of volatile chlorinated organics.

Identification of Volatile Organics by GC/MS

Identification of volatile organic compounds present in the treated wastewaters is done by GC/MS and GC. The instrument available for this study consists of a Varian Aerograph Series 1200 and a Hitachi-Perkin-Elmer RMU-6E Mass Spectrometer. The interface between GC and MS is a Watson-Biemann separator. An Apectrosystem 100 Varian Data Machine is used to accept the output of the MS, to store the processed results, and to output the mass chromatograms and the mass spectra of the peaks. The machine is controlled by the input through a teletype. However, Varian Aerograph Series 1200 is an older gas chromatograph that can accept only a 1/8-inch stainless steel column. This undesirable feature may limit the range of application because certain analyses are preferably done on glass columns due to their chemical inertness (Ottenstein and Bartley, 1971; Ackman, 1972). The detection limit of the GC/MS instrument used is generally on the order of micrograms, which is rather insensitive compared to the more sensitive unit with nanogram detection limit. As such, a sample preconcentration prior to GC/MS run is essential.

TABLE 31. CONCENTRATIONS OF VOLATILE POLAR WATER-SOLUBLE ORGANICS DETERMINED IN RO PERMEATES

Sample	Concentrations in μL/L (~ppm)			
	Acetone	2-Propanol	Diethyl Ether	Methyl Ethyl Ketone
IT-3-2	3.8	0.5	--	0.02
3-3	3.6	0.03	--	0.2
IT-4-2	1.4	0.7	--	0.2
4-3	0.7	0.04	--	0.1
IT-5-3	0.5	0.1	--	0.1
5-4	0.2	0.06	--	0.05
IT-6-2	0.3	0.2	--	0.1
6-3	0.5	0.08	--	0.07
IT-7-2	2.3	0.4	--	0.3
7-3	0.6	0.05	--	0.04
7-3A	0.02	< 0.01	--	0.02
Test #3 or IT-3-2[a]	0.01	< 0.01	0.01	--
Chlorinated IT-7-3	0.4	< 0.01	< 0.01	

a. See Table 15.

TABLE 32. CONCENTRATIONS OF VOLATILE NONPOLAR WATER-INSOLUBLE ORGANICS DETERMINED IN RO PERMEATES

Sample	Concentrations in µL/L (~ppb)						Sum of TOC of VNO (ppb)[b]	TOC of Sample (ppm)
	Methylene Chloride	Chloroform	1,1,1-Trichloro-Ethane	Benzene	Bromoform	Toluene		
IT-3-2	3	--	--	1	2	1	2.4	10
3-3	3	32	--	3	2	1	7.4	5
IT-4-2	4	--	--	1	--	--	1.5	10
4-3	3	124	--	2	--	--	14.7	7
IT-5-3	6	36	11	2	3	3	18.7	8
5-4	5	19	9	2	--	1	7.0	3
IT-6-2	6	15	--	2	--	1	5.1	10
6-3	6	17	--	2	--	--	4.4	3
IT-7-2	8	23	--	2	--	1	6.2	11
7-3	9	39	--	1	--	3	8.8	7
7-3A	3	20	--	2	--	1	5.2	4
Test #3 or IT-3-2[a]	40	60	--	--	--	1	12.5	9
Chlorinated IT-7-3	0	35	--	2	--	3	8.9	8

a. See Table 15.
b. Sum of TOC of determined volatile nonpolar water-insoluble organics.

The working conditions of the GC/MS are listed briefly below,

Column: 6-ft, 1/8-inch stainless steel column packed with 0.4% Carbowax 1500 on Carbopack A, 80/100 mesh

He flow rate: 25 mL/minute

Injection port temperature: 180°C

Oven temperature: 110°C

M/E range: R900 (Calibrated from 18 to 900)

Source or ionizing voltage: 22 electron volts

Electron magnetic voltage: 2.0 kilovolts

Mass spectra of ethanol and acetone are obtained by direct GC injection of 1 µL of aqueous solutions. The mass chromatogram of acetone is shown in Figure 31 where water is the first peak and acetone is the second. The mass spectrum of acetone peak is shown in Figure 32. Figure 33 shows the mass chromatogram of ethanol spiked with acetone, where acetone appears as the last peak and ethanol is the middle one. The mass spectra of ethanol and acetone from the spiked sample are shown in Figures 34 and 35, respectively. The mass spectra of ethanol and acetone are taken as the references for identification of ethanol and acetone. One µL of 10^4 ppm ethanol and one µL of 10^4 ppm acetone are directly applied to the adsorption trap filled with Tenax-GC. The amount of ethanol and acetone present in the trap is equivalent to strip 100 mL of 100 ppb ethanol and 100 ppb acetone solution with 100% stripping efficiency and 100% adsorption efficiency. The sample is injected with the injection system shown in Figure 26 as described previously. The mass chromatogram obtained is shown in Figure 36. The mass spectra of the second and third peaks are shown in Figures 37 and 38, respectively. The first peak is a water peak. These two peaks are then identified by comparing their mass spectra with the references as shown on Table 33. The consistency of the mass ion intensity ratio between two major peaks is observed in the last two columns. This demonstrates that the intensity ratio of major M/E species is a reliable parameter to identify the unknown peak.

RO permeates of 10x hospital (HC) and 1x laboratory wastewaters were stripped out and analyzed by GC/MS. The Bellar and Lichtenberg stripping apparatus (Bellar and Lichtenberg, 1974b) was used. The sample size was 5 mL. The injection procedure is the same as described in Adsorption and Desorption of Volatile Compounds for Different Adsorbents. Volatile organics that are able to be identified by GC/MS analysis are listed in Table 34. Only methanol and acetone in RO permeate of 10x HC and methanol in RO permeate of 1x laboratory wastewaters can be identified positively. Although many peaks have been observed on the gas chromatograms as shown in Appendix II, only a few peaks appeared on the mass chromatograms obtained on this study. The sensitivity of the GC/MS apparently limits the identification of other peaks present in smaller quantities.

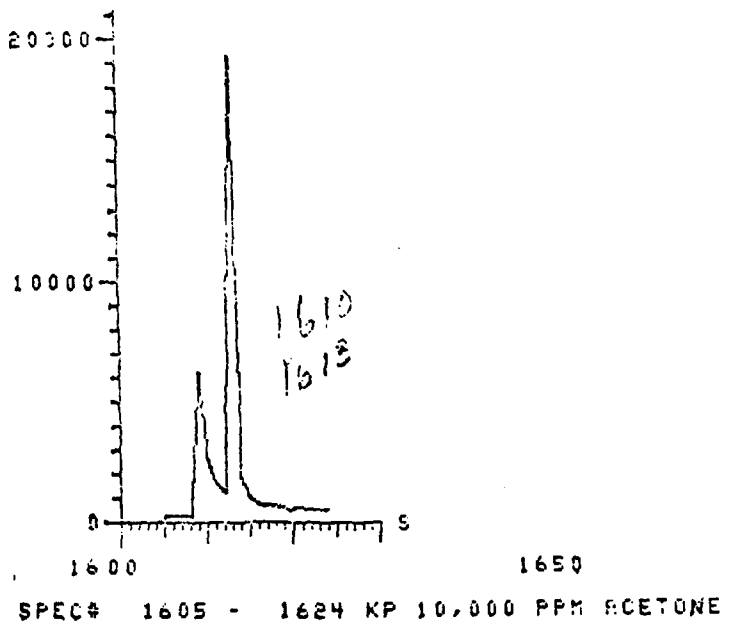

Figure 31. Mass Chromatogram of Acetone Solution.

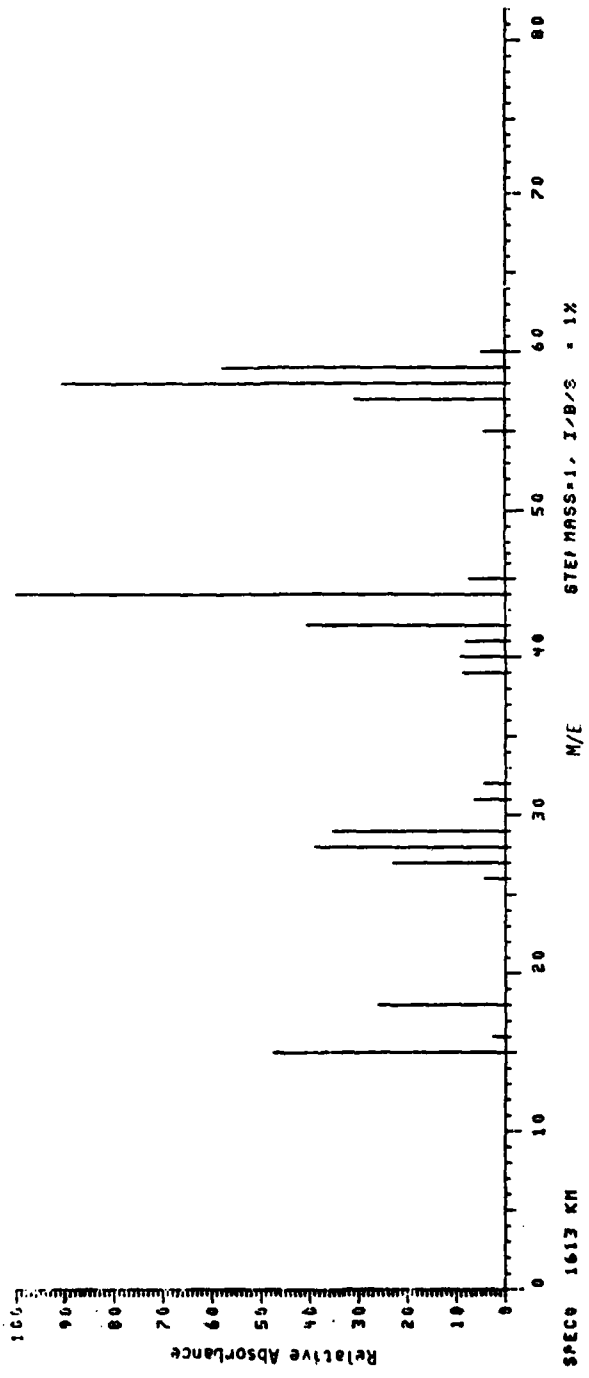

Figure 32. Mass Spectrum of Acetone Peak.

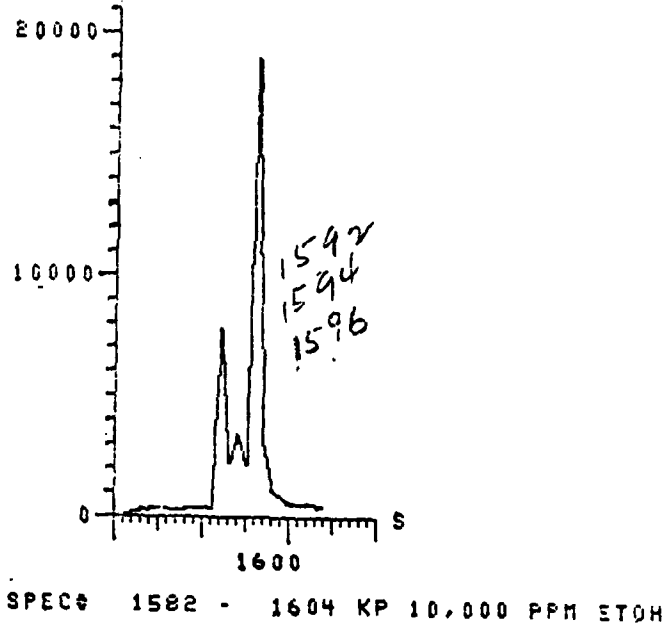

Figure 33. Mass Chromatogram of Ethanol Solution Spiked with Acetone.

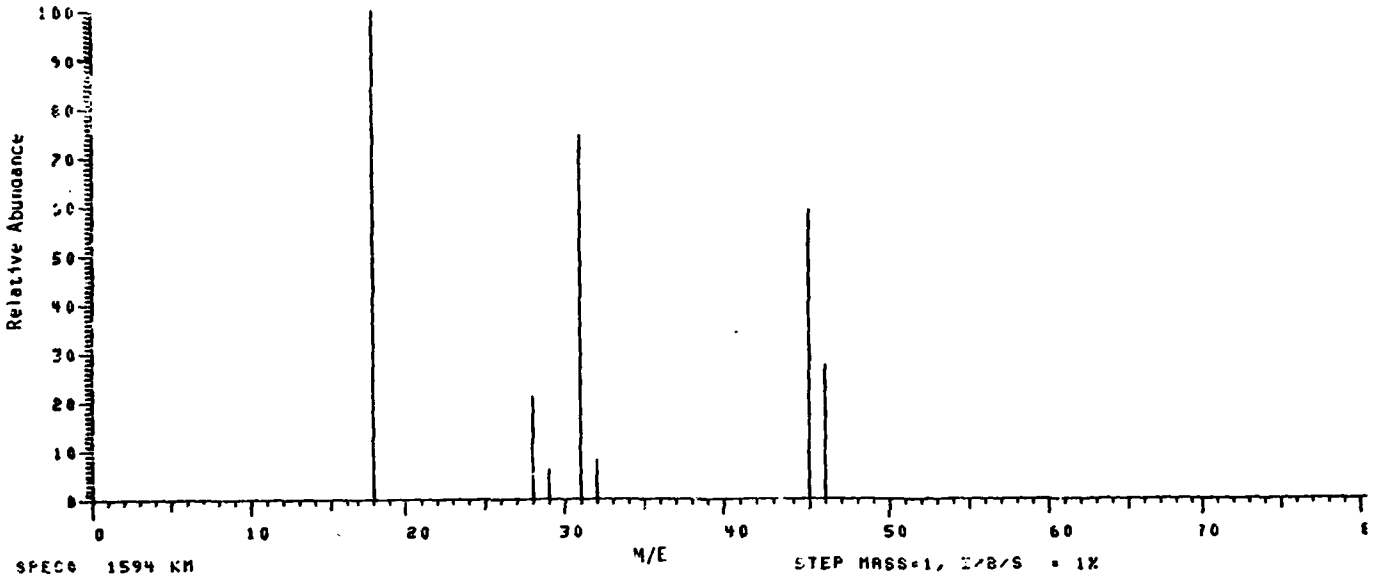

Figure 34. Mass Spectrum of Methanol Peak.

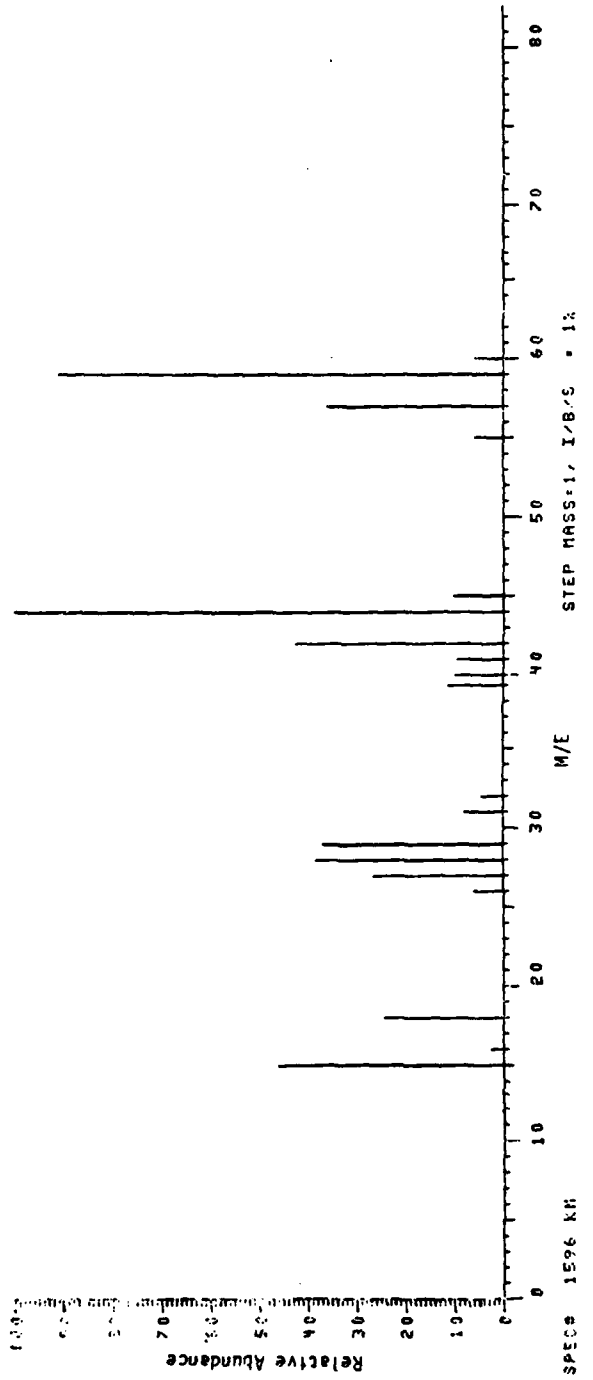

Figure 35. Mass Spectrum of Acetone Peak.

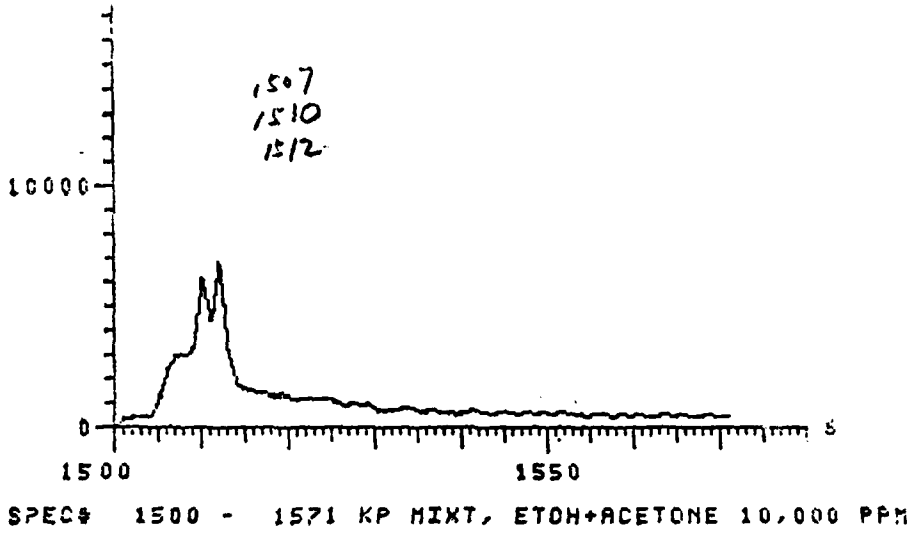

Figure 3f. Mass Chromatogram of Simulated Unknown.

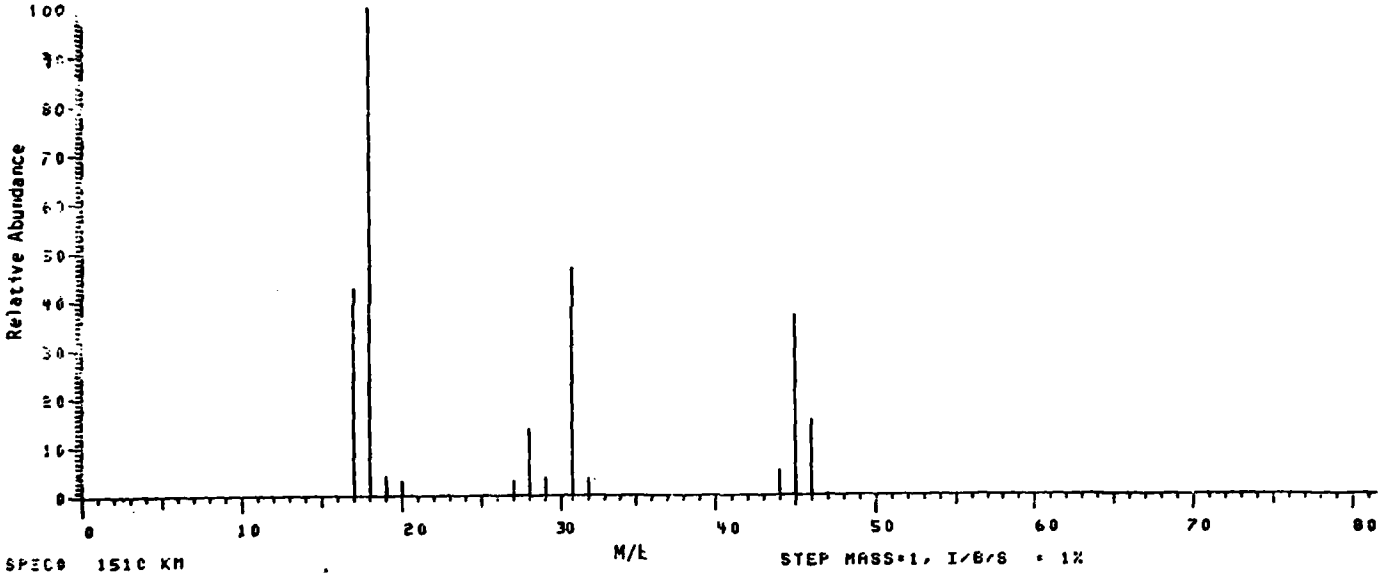

Figure 37. Mass Spectrum of Second Peak Appearing in Figure 35.

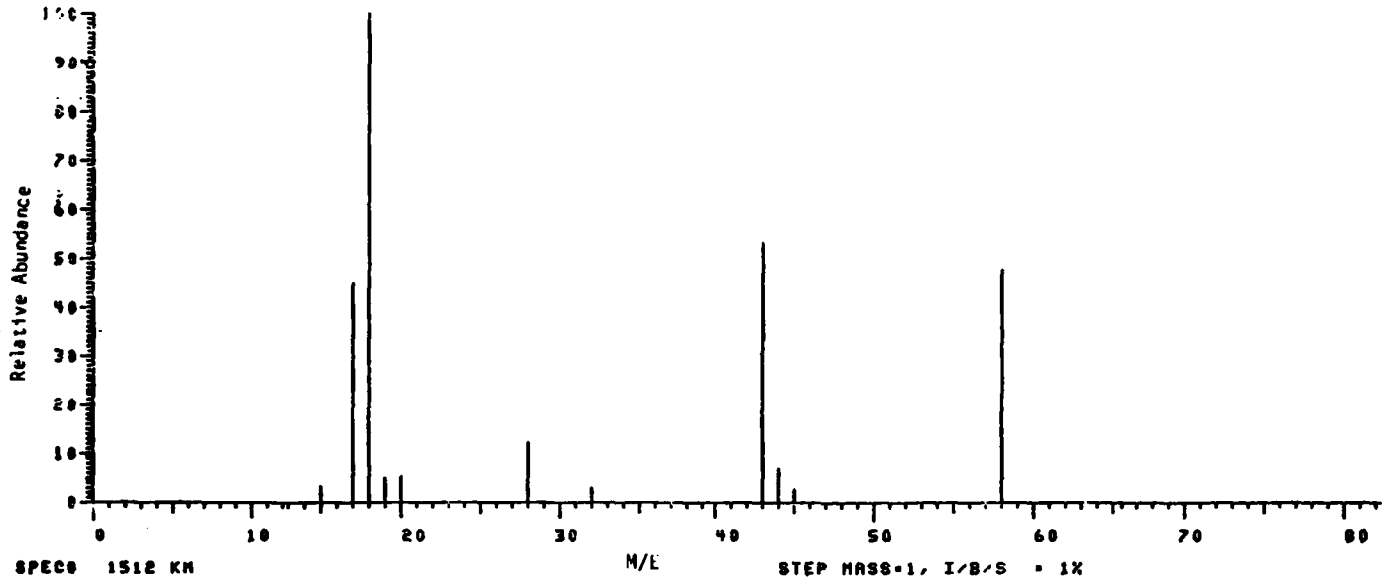

Figure 38. Mass Spectrum of Third Peak Appearing in Figure 35.

TABLE 33. IDENTIFICATION OF ETHANOL AND ACETONE BY COMPARING MASS ION INTENSITY RATIO OF MAJOR M/E SPECIES

Sample	Mass Chromatography Peak	Mass Ion Intensity of Major M/E's				Intensity Ratio	
		M/E = 31	M/E = 45	M/E = 44	M/E = 58	45/31	58/44
Reference acetone	Acetone			30,624	27,614		90.17
Reference ethanol	Acetone			31,866	29,088		91.28
Spiked with acetone	Ethanol	8,694	6,919			79.58	
Simulated unknown	Ethanol	10,429	8,199			78.62	
	Acetone			12,709	11,505		90.53

TABLE 34. VOLATILE ORGANICS IDENTIFIED BY GC/MS

RO Permeate of 10x EC	RO Permeate of 1x Laboratory
Methanol	Methanol
Acetone	Ether (?)
Ether (?)	n-Butanol (?)

The injection technique described in Stripping of RO Permeates of MUST Wastewaters was used in obtaining the chromatograms shown in Appendix II. Unfortunately, it is not applicable to the GC/MS unit because when the trap is connected to the GC column, the carrier flow is disturbed as is the pressure and background in the MS system. Thus, a 4-way valve gas injection system is incorporated (Figure 26). However, the peak is broadened somehow as discussed previously. Therefore, peak overlapping may occur and sometimes will cause difficulty in MS identification. The injection technique described in Adsorption and Desorption Efficiencies and in Figure 30 when combined with Varian-MAT 311A GC/MS provides a simple means of injection and results in well resolved and sharp peaks (Chian et al., 1976).

Determination of Nonvolatile Organics by HPLC

The technique of high pressure liquid chromatography (HPLC) is employed for the analysis of nonvolatile organic compounds present in the RO permeates of MUST wastewaters. Organic compounds are concentrated by solvent extraction followed by evaporation of solvent. o-Toluidine (Aldrich Chemical Company, Inc., Milwaukee, WI) and N,N-diethyl-m-toluamide (Eastern Kodak Co., Rochester, NY) were selected as representative nonvolatile organic compounds since they are present in the wastewaters and can be extracted by chloroform. They are used mainly for evaluating the liquid chromatography (LC) technique. Determination of these compounds in the 1x RO composite waste was also conducted.

The HPLC is an ISCO Model 1440 (Instrumentation Specialties Company, Lincoln, NE) equipped with a UV detector at 254 nm. Three columns, i.e., Corasil I, Corasil II, and Porasil T (Waters Association, Inc., Milford, MA) were tested. The choice of this mode of liquid-solid adsorption chromatography was used because it can resolve compounds with different functional groups and isomers. p-Toluidine (Aldrich Chemical Company, Inc., Milwaukee, WI) is also included in the study. The UV absorption spectra of these three compounds were scanned on a Beckman Spectrophotometer, Acta III (Fullerton, CA). They all show a broad adsorption band extending from 210 to 300 nm. Therefore, the UV detection at 254 nm on the HPLC is a good choice. Results in selecting the best column are described in the next paragraph.

Corasil I and Corasil II columns are packed with pellicular silica beads. They are both polar columns, but the former contains beads having a surface area of 7 m^2/g and the latter 14 m^2/g. The Porasil T column is packed with porous silica beads. From the basic column properties of these columns, one can predict that Porasil T will retain the polar compounds the most and the Corasil I column the least. The results of LC separation based on retention time, t_R, are shown in Table 35. The solvent strength of n-hexane is not strong enough to elute the N,N-diethyl-m-toluamide; consequently, ghost peaks appear in the next liquid chromatogram and thus interfere with the o-toluidine and p-toluidine peaks. The capability of Corasil I and Corasil II columns to resolve the ortho and para isomers of toluidine is demonstrated (Table 35) when n-hexane is used as the mobile phase.

Since chloroform has a medium solvent strength in the eluotropic series, it is expected to be able to elute the toluamide and also to resolve toluamide and toluidine. However, resolution of these compounds on the Corasil I column is poor (Table 35) because Corasil I either is not polar enough or does not have a large enough surface area to retain the species long enough to achieve the separation. Of course, other solvents with solvent strength falling between that of n-hexane and chloroform might be used for elution and resolution of these compounds. In fact, when 7T methanol in n-hexane was used as the mobile phase, resolution of o-toluidine and N,N-diethyl-m-toluamide was not attained on Corasil II (Table 35). The separation is satisfactory when chloroform is used as the mobile phase on Porasil T columns. Therefore, Porasil T and chloroform is the system of choice for the column and the mobile phase. The flow rate is set at 80 mL/hour. A higher or lower flow rate does not seem to improve the resolution.

Methyl benzoate is chose as the internal standard for both qualitative and quantitative analyses. An internal standard is particularly necessary for liquid-solid adsorption chromatography because the water content on the adsorbent varies from time to time due to the desorption or adsorption of water via mobile phase. A series of standard solutions of o-toluidine and N,N-diethyl-m-toluamide mixture is prepared in chloroform, and calibration curves of both are obtained. The operating conditions for Porasil T/chloroform system are 80 mL/hour at 24 kg/cm^2. Duplicate runs were made. The result is tabulated in Table 36, and calibration curves are shown in Figures 39 and 40. As can be noted from Table 36, either retention time or ratio of retention time is quite reproducible, although they are not as reproducible as that shown in Table 35 because of varying water content in chloroform from batch to batch. It is therefore suggested that the same batch of mobile phase solvent be used to complete the entire analysis or that the internal standard technique should be employed. Figures 39 and 40 show the peak area ratio calibration curves and peak height ratio calibration curves, respectively.

TABLE 35. SEPARATION OF o-TOLUIDINE, p-TOLUIDINE, AND N,N-DIETHYL-m-TOLUAMIDE BY LIQUID CHROMATOGRAPHY

Column	Mobile Phase	Separation - t_R (sec)		
		o-Toluidine	p-Toluidine	N,N-Diethyl-m-toluamide
Corasil I	n-Hexane	77	105	-
	Chloroform	37	40	42
Corasil II	n-Hexane	100	140	--
	7% Methanol in n-hexane	65	Not tested	69
Porasil F	Chloroform	77	94	106

TABLE 36. RESULTS OF QUALITATIVE AND QUANTITATIVE STUDY ON o-TOLUIDINE AND N,N-DIETHYL-m-TOLUAMIDE WITH METHYL BENZOATE AS THE INTERNAL STANDARD

Conc. of Methyl Benzoate (ppm)	t_R (sec)	Conc. of o-Toluidine	t_R (sec)	Ratio of t_R	Ratio of Peak Area	Ratio of Peak Height
50	54	3.88	73	1.35	0.135	0.118
	53		72	1.36	0.106	0.082
50	54	7.75	73	1.35	0.232	0.203
	54		72	1.33	0.265	0.232
50	55	15.50	73	1.33	0.471	0.412
	54		73	1.35	0.550	0.427
50	53	31.01	75	1.42	0.835	0.742
	52		72	1.39	1.139	0.760
Conc. of Benzoate (ppm)	t_R (sec)	Conc. of N,N-Diethyl-m-Toluamide (ppm)	t_R (sec)	Ratio of t_R	Ratio of Peak Area	Ratio of Peak Height
50	54	21.61	102	1.89	0.250	0.140
	53		102	1.92	0.233	0.138
50	54	43.21	103	1.91	0.519	0.303
	54		103	1.91	0.506	0.295
50	55	86.41	104	1.89	1.015	0.592
	54		104	1.93	1.078	0.581
50	53	172.83	105	1.98	2.465	1.315
	52		103	1.98	2.309	1.066

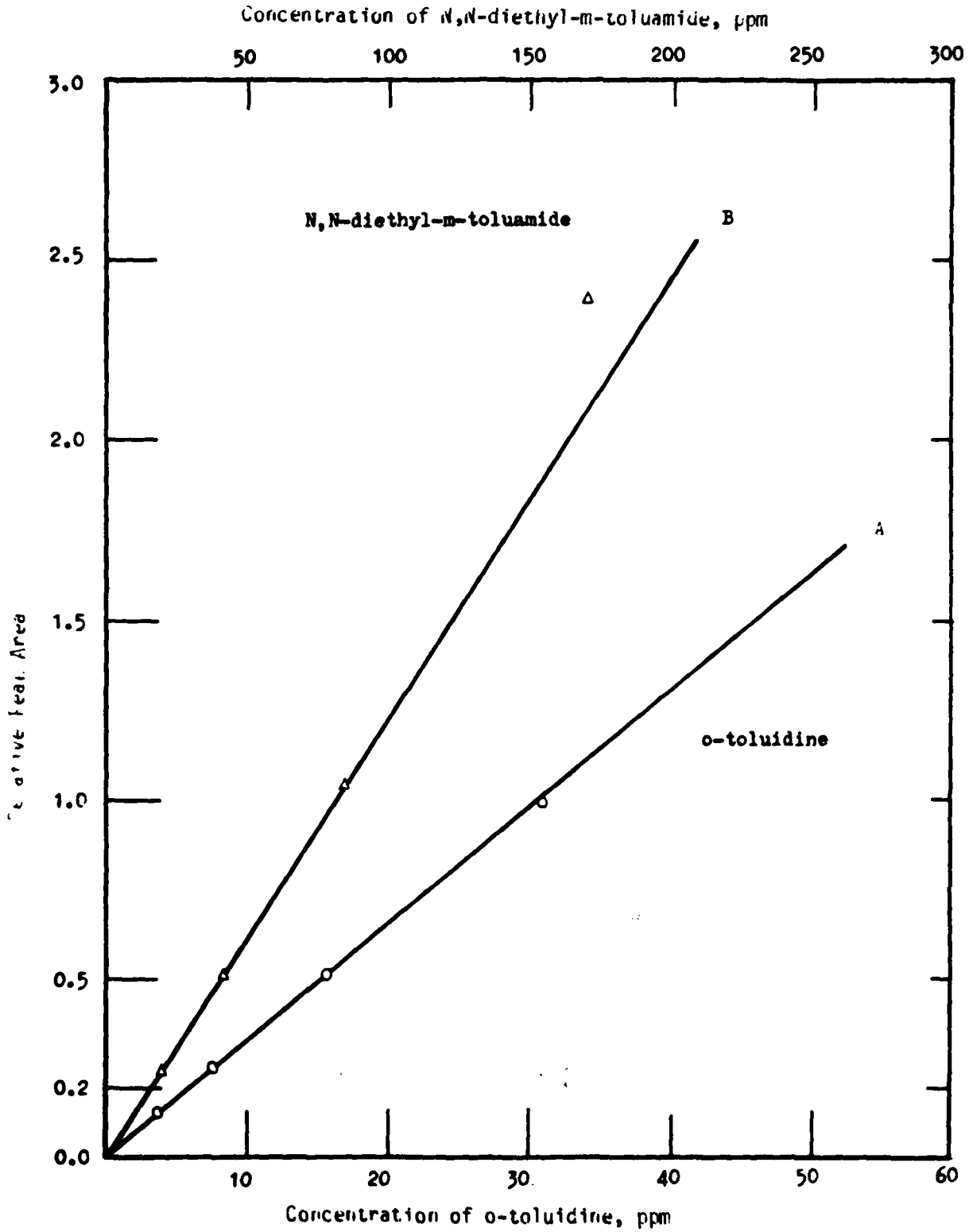

Figure 39. Peak Area Ratio Calibration Curves for o-Toluidine and N,N-Diethyl-m-Toluamide.

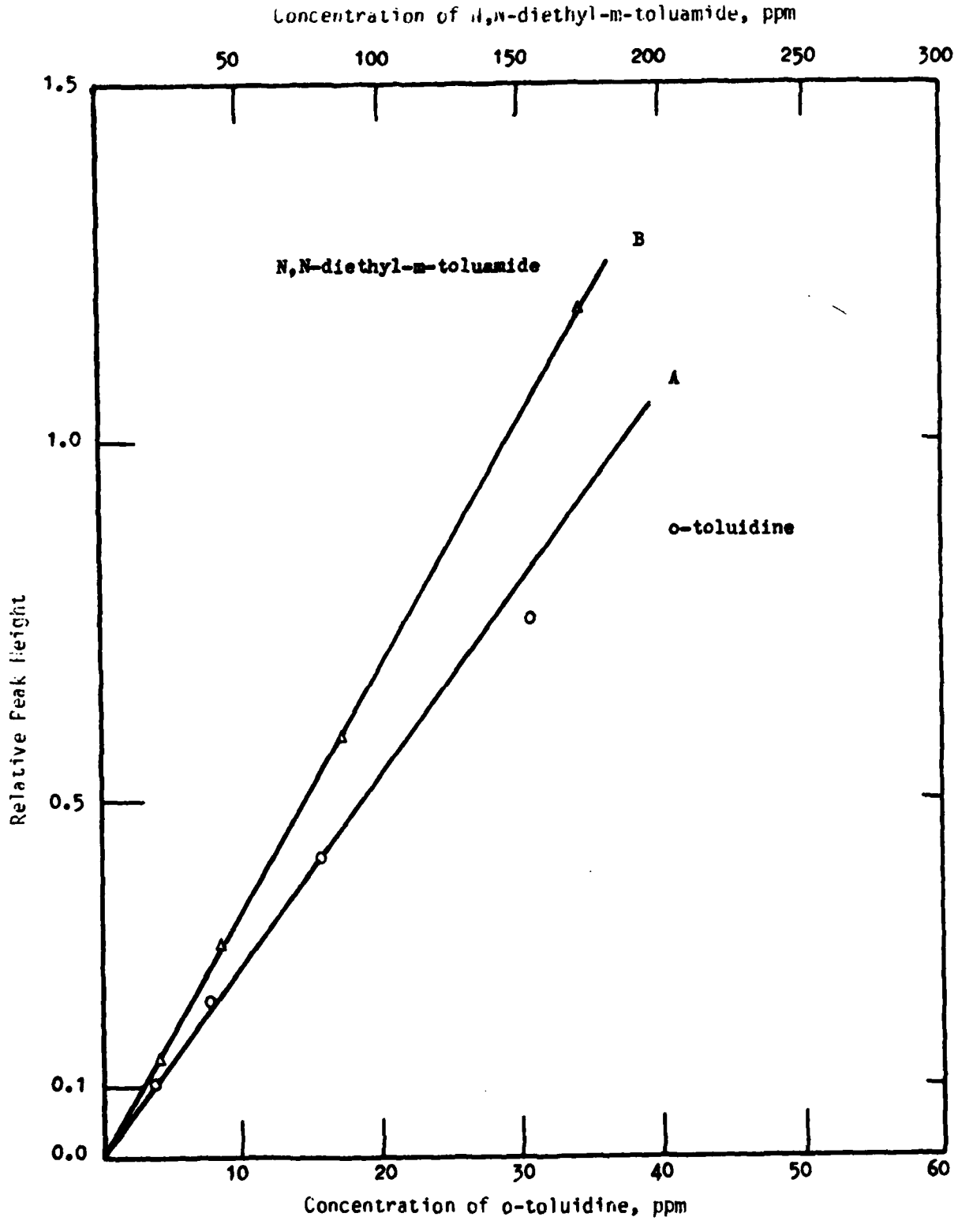

Figure 40. Peak Height Ratio Calibration Curves for o-Toluidine and N,N-Diethyl-m-Toluamide.

Because there is difficulty in measuring the half band width of the LC peaks, the ratio of peak area is somewhat more scattered than the ratio of peak height. However, straight calibration curves are obtained with both techniques and for both components.

The noise on the HPLC system is about 0.1 milliabsorbance unit. If the detection limit is defined as the concentration of the sample that produces a signal equal to twice the noise fluctuation, the detection limit is about 0.1 and 0.5 ppm for o-toluidine and N,N-diethyl-m-toluamide, respectively. The concentrations of these two components in the untreated MUST wastewaters are approximately on the order of 10^{-2} and 10^{-1} ppm, respectively. Assuming the rejection by membrane during the RO treatment is 50% for the aromatic polyamide membrane, the concentration level will then be on the order of 5×10^{-3} and 5×10^{-2} ppm, respectively. This indicates that a concentration process with a 100-fold concentration factor should be sought in order to be able to determine o-toluidine and N,N-diethyl-m-toluamide by the HPLC technique under the same condition studied.

Solvent extraction followed by evaporation concentration can be employed easily to implement this requirement. The technique of chloroform extraction and concentration by Kuderna-Danish (K-D) concentrator has been suggested by Webb (1964). If 20-fold concentration is good enough, then freeze drying is an alternative. However, direct injection of aqueous samples into the HPLC may cause some disturbance because of the change of water content on the adsorbent or the solubility problem. This can be resolved if an entirely different HPLC column and mobile phase solvent are used, which are suitable for aqueous samples and have satisfactory sensitivity.

The procedure of extraction and concentration that is briefly described here is similar to that described by Webb (1964). A total of 250 mL of aqueous sample is extracted with 50 mL of chloroform. The mixture is well shaken in a 500-mL separatory funnel and then left to come to equilibrium for 30 minutes. The bottom organic layer is drained off and collected. Another 50 mL of chloroform is added to the aqueous layer and the second extraction is carried out. Two chloroform extracts are combined and transferred to the K-D concentrator (Kontes Glass Co., Vineland, NJ), which consists of a 3-ball condenser, a 250-mL flask, and a 10-mL graduated receiver. The latter two components are joined and fastened with two springs. The extract is filled up in the receiver and occupies about one-third of the flask volume. One glass bead is added into the receiver to aid in boiling. The K-D evaporator is then placed in a 100°C water bath so that the bath covers the receiver up to the spring position and the hot steam reaches the bottom of the flask. The extract is boiled down to about 5 to 6 mL and then the whole concentrator is removed from the hot bath to allow it to cool and drain off. The receiver is taken off and the extract is further blown down to 3 mL with a stream of helium or nitrogen gas. The concentrated extract is then spiked with internal standard and is ready for LC injection.

The calibration curves are shown in Figure 41. Curves A and B are for o-toluidine and N,N-diethyl-m-toluamide, respectively. Standard solutions are prepared in water and then go through the extraction and concentration processes. The treatment of 1x RO permeate of composite waste is similar. The LC chromatograms of the 1x RO permeate and its o-toluidine and N,N-diethyl-m-toluamide spiked solution are shown in Figure 42. The two components are identified according to the relative retention time as shown in Table 37. With the help of the calibration curves, the concentrations of o-toluidine and N,N-diethyl-m-toluamide in the 1x composite RO permeates were found to be 6.50 ppb and 1.38 ppm, respectively. The value of 1.38 ppm for N,N-diethyl-m-toluamide is higher than that expected, i.e., 0.483 ppm. Perhaps there are other components that appear at, or close to, where the N,N-diethyl-m-toluamide peak is on the chromatogram. In fact, the relative retention time of the unknown peak appears at 1.85 to 1.86, which is somewhat lower than the standards as can be noted from Table 37. Other LC columns or independent analytical methods should be sought for further identifying the unknown peak more closely. The value of 6.50 ppb for o-toluidine is about what would be expected.

Evaluation of Solvent Extraction Technique for Determining Nonvolatile Organics

Solvent Extraction of Phenolic Compounds

Selection of Organic Solvent and pH Adjustment of Aqueous Sample. The efficiency of solvent extraction followed by K-D concentration was evaluated to determine a suitable organic solvent and the optimum pH for extraction of phenolic compounds. Aqueous solutions containing model compounds were adjusted to pH's of 2 and 7 and extracted by either chloroform or methylene chloride. After pH adjustment, 1 liter of a mixture containing 0.5 ppm of each of the model compounds was extracted twice with 50 mL of organic solvent. The combined extract was concentrated to 1.0 mL in a micro K-D evaporator. The finally concentrated extract was then analyzed by GC.

Also, 100 mL of each solvent was spiked with 1 mL of a 500-ppm mixture of model compounds and then K-D concentrated to 1 mL to study the efficiency of K-D concentration. Extraction and K-D concentration were both done in duplicate. The GC column used was a 6-ft x 2-mm inside diameter glass column packed with 0.2% SP-1000 on Carbopack A, 60/80 mesh. The GC oven was programmed from 240°C to 280°C at 60°C with a 9-minute initial hold and a 10-minute final hold. Although the oven temperature is too high for this light GLC liquid phase, it gives a better separation of the model compounds than when operated at a lower temperature. However, it was found that after 2 months of extensive use, the column started deteriorating. o-Benzyl-p-chlorophenol was determined on the Tenax-GC column. The GC oven was programmed from 270°C to 300°C at 30°C/minute with both initial and final holds for 6 minutes.

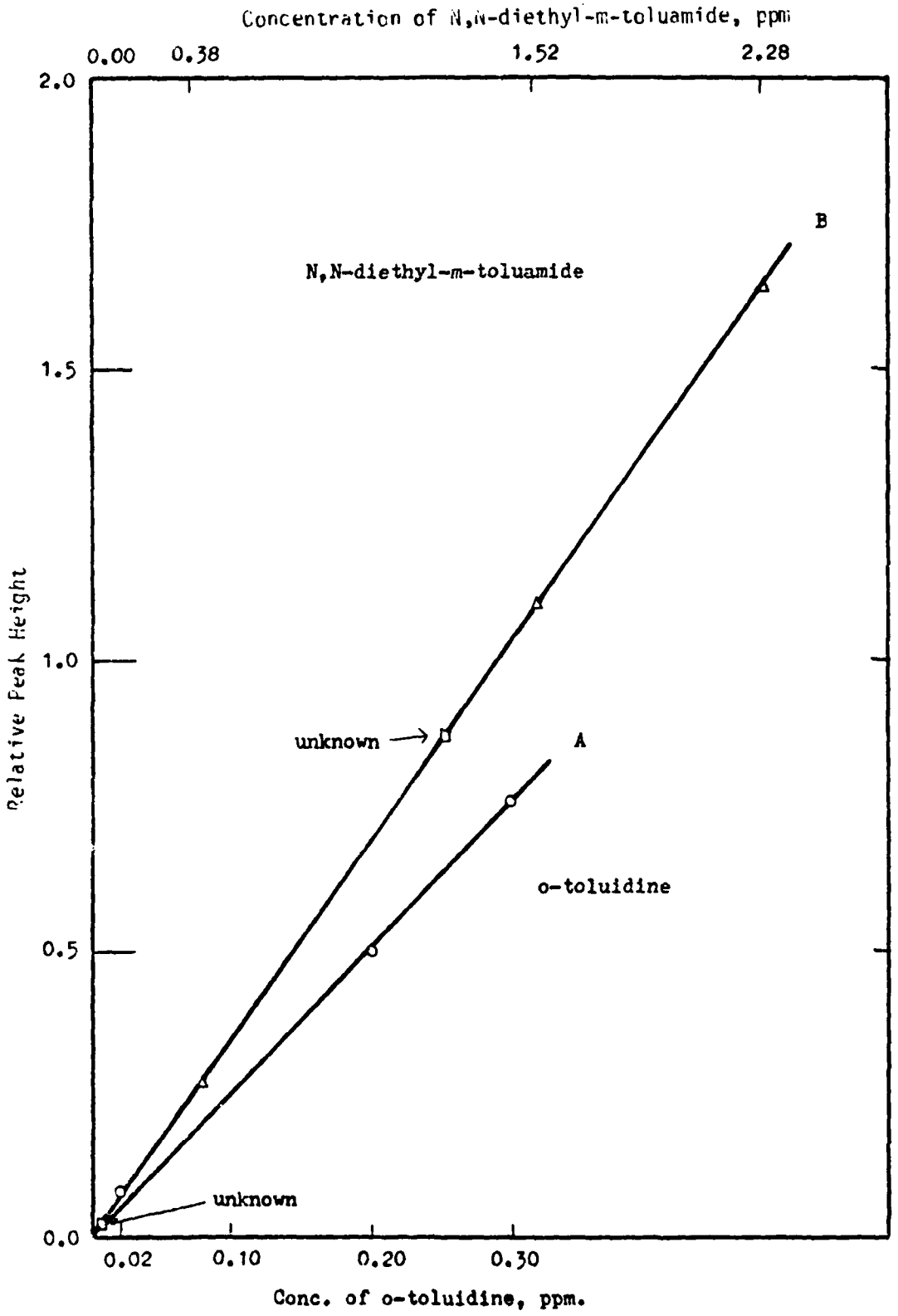

Figure 41. Calibration Curves for o-Toluidine and N,N-Diethyl-m-toluamide.

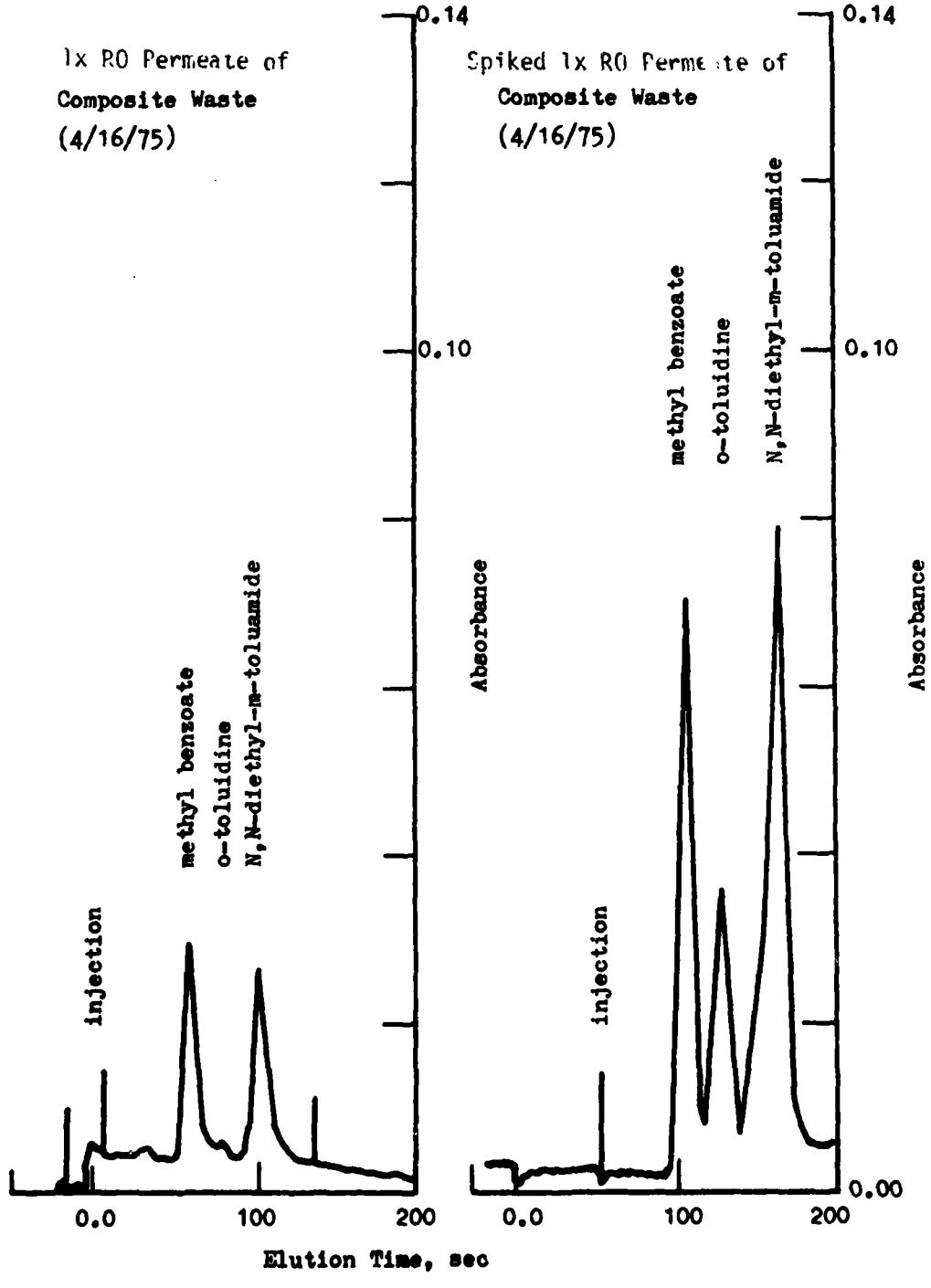

Figure 42. LC Chromatograms of 1x Composite RO Permeate After Treatment Extraction and Concentration, and Its Spiked Solution.

TABLE 37. RETENTION TIME AND RELATIVE RETENTION TIME OF o-TOLUIDINE AND N,N-DIETHYL-m-TOLUAMIDE

Sample	Methyl Benzoate t_R (sec)	o-Toluidine t_R (sec)	o-Toluidine Rel. t_R	N,N-Diethyl-m-toluamide t_R (sec)	N,N-Diethyl-m-toluamide Rel. t_R
Std. 1	54	73	1.35	102	1.89
	51	70	1.37	98	1.92
Std. 2	54	75	1.39	105	1.94
	51	72	1.41	102	2.00
Std. 3	53	73	1.38	105	1.98
	49	70	1.43	100	2.04
Unknown	53	73	1.38	98	1.85
1x RC	51	69	1.35	95	1.86
Spiked Unknown	54	72	1.33	108	2.00

Table 38 shows the extraction and K-D concentrating efficiencies for phenolic compounds. For both solvents, the recovery is better when the solution is extracted at a pH of 2. Neutral species of all these phenolic compounds are favorably formed at a pH of 2, resulting in more efficient extraction by the organic solvent. The table also shows that methylene chloride gives better overall efficiency (combination of extraction and K-D concentration) than chloroform. Thus, methylene chloride rather than chloroform should be chosen as the organic solvent for extracting phenolic compounds from aqueous solutions. Furthermore, the solutions should be adjusted to a pH of 2 before extraction.

As indicated in Table 38, the extraction efficiency with methylene chloride at pH 2 ranges from 90 to 110% except for phenol, o-cresol, and p-cresol. K-D efficiencies are better than 92% except for o-benzyl-p-chlorophenol. The low efficiency for that substance may be the result of experimental errors. The overall solvent extraction/K-D concentration efficiency is better than 91% except for phenol, cresols, and 3,4-dimethylphenol. However, better than 60% efficiency can be achieved for cresols and 3,4-dimethylphenol.

TABLE 38. EXTRACTION AND K-D CONCENTRATION EFFICIENCIES FOR PHENOLIC COMPOUNDS[a]

Compounds	Phenol	o-Cresol	p-Cresol	2-Ethyl Phenol	2,6-Dimethyl Phenol	2,4-Dimethyl Phenol	2,3-Dimethyl Phenol	3,4-Dimethyl Phenol	o-Phenyl Phenol	α-Benzyl-p-Chloro-Phenol
Methylene Chloride										
pH 2										
Extraction Eff.	28.1	75.8	66.3	100.1	100.0	98.1	98.9	89.8	104.0	109.9
K-D Conc.	94.4	93.1	92.7	83.9	93.0	93.3	93.0	93.8	96.1	83.1
Ext./K-D Conc.	26.5	70.6	61.6	94.0	100.4	91.5	92.0	84.2	100.0	91.3
pH 7										
Extraction Eff.	17.1	65.8	54.3	99.6	94.3	89.2	91.3	89.9	105.0	122.9
Ext./K-D Conc.	16.1	61.3	50.3	83.6	87.7	83.2	84.9	84.3	100.9	102.1
Chloroform										
pH 2										
Extraction Eff.	8.7	57.2	43.8	85.0	85.3	80.8	75.0	85.7	90.3	92.2
K-D Conc.	90.1	88.4	85.4	87.1	94.1	92.4	93.3	93.4	96.0	94.7
Ext./K-D Conc.	7.8	50.6	37.4	74.0	80.3	74.7	70.0	80.0	86.7	87.3
pH 7										
Extraction Eff.	7.1	53.1	41.2	84.3	83.6	79.5	84.7	79.3	91.1	93.1
Ext./K-D Conc.	6.4	46.9	35.2	73.4	78.7	73.5	79.0	74.1	87.5	88.2

a. Percent recovery; average of duplicate runs.

Recovery of Phenolic Compounds with Different Extraction/Concentration Methods. Table 39 shows the percentage of recovery of phenolic compounds with different extraction/concentration methods. The ion-exchange method is the best in recovering phenol and cresols. Extraction at a pH of 7 is the poorest. Extraction with a 1:1 mixture of methylene chloride and diethyl ether provides a higher recovery than does methylene chloride alone. The technique of XAD-4 extraction/ether solution for recovering phenolic compounds offers little improvement over extraction at a pH of 2. For the rest of the compounds studied, extraction with methylene chloride is better than with the 1:1 methylene chloride/ether mixture. Results from USAMBRDL research into ion-exchange methods for extracting phenolic compounds should be included in a comparison of techniques leading to the selection of a proper analytical method for concentrating these phenolic compounds from RO permeates.

Solvent Extraction of o-Toluidine and N,N-Diethyl-m-Toluamide

In a previous study (Section on Determination of Nonvolatile Organics by HPLC), o-toluidine and N,N-diethyl-m-toluamide were extracted by chloroform from the RO permeate of composite waste and were tentatively determined by HPLC after the extract was concentrated by K-D evaporation. This study has demonstrated that HPLC is a powerful analytical tool and that the technique of extraction and K-D concentration is applicable to concentrating these compounds. It has been felt since then that further study should be carried out on the use of these methods for quantitative analysis. Therefore, the recovery of these two compounds by solvent extraction and K-D concentration must be studied and other analytical quantification techniques should be explored. The work reported in this section was directed toward that goal.

The same experimental procedures used for phenolic compounds were followed. However, methyl benzoate was incorporated into the standard solutions as an internal standard. The methyl benzoate can be added to the sample before extraction or to the concentrated extract. Adding it before extraction provides an internal standard for the entire analytical procedure, including sample pipetting, extraction, K-D evaporation concentration, GC injection, and GC elution. Spiking the concentrated extract, on the other hand, provides a standard only for GC injection and GC elution. The sample was spiked before extraction in this study in order to obtain the recovery of methyl benzoate. In the future, methyl benzoate will be used as an internal standard for both HPLC and GC.

GC, instead of HPLC, was employed as an analytical technique in this study. The column used was a 6-ft x 1/8-inch outside diameter stainless steel column packed with 60/80 mesh Tenax-GC (Applied Science Laboratories, Inc., State College, PA). The GC oven was programmed from 250°C to 300°C at a rate of 20°C/minute with a 4-minute initial hold and a 3-minute final hold. The nitrogen carrier flow rate was 15 mL/minute. The temperature of the injection port and the flame ionization detector was 320°C. Hydrogen flow and air flow were 30 and 300 mL/minute, respectively.

TABLE 39. PERCENT RECOVERIES OF PHENOLIC COMPOUNDS BY DIFFERENT EXTRACTION/CONCENTRATION METHODS

Compound	pH 2 CH_2Cl_2 Ext./ K-D Conc.[a]	pH 2 CH_2Cl_2-Ether Ext./K-D Conc.[a]	pH 7 $CHCl_3$ Ext./ K-D Conc.[b]	pH 2 CH_2Cl_2-Ether Ext./K-D Conc.[c]	pH 2 XAD-4 Ext./Ether Elu./Evap. in Specially Designed Flask[d]	12< pH< 12.5 A-26 1X/4M HCl Elu. CH_2Cl_2 Ext./ Evap. in Specially Designed Flask[e]
Phenol	26	72	19	72	40	94
o-Cresol	71	112			73	92
p-Cresol	62	85	50			88
2-Ethylphenol	94	94		73		
2,6-Dimethylphenol	100	76				
2,4-Dimethylphenol	92	80				
2,3-Dimethylphenol	92	86				
3,5-Dimethylphenol					79	
3,4-Dimethylphenol	84	84				
o-Phenylphenol	100	95				
o-Benzyl-p-chlorophenol	91	38				

a. Results were obtained from our research group. Average of duplicate runs.
b. Webb (1974).
c. EPA (1975).
d. Junk et al. (1974).
e. Chriswell et al. (1975).

TABLE 40. EXTRACTION AND K-D CONCENTRATION EFFICIENCIES FOR METHYL BENZOATE, o-TOLUIDINE, AND N,N-DIETHYL-m-TOLUAMIDE[a]

Compounds	Methyl Benzoate	o-Toluidine	N,N-Diethyl-m-Toluamide
Methylene Chloride			
pH 7			
Extraction Efficiencies	97.8	94.1	85.4
K-D Concentration	98.1	97.0	102.4
Ext./K-D Concentration	95.9	91.3	87.5
Chloroform			
pH 7			
Extraction Efficiencies	90.3	93.9	92.9
K-D Concentration	100.9	98.2	96.4
Ext./K-D Concentration	91.1	92.2	89.6

a. Percent recovery; average of duplicate runs.

Table 40 shows the percent recovery of the compounds by extraction and K-D concentration with either methylene chloride or chloroform as the organic solvent. Both solvents resulted in approximately the same overall efficiency when extraction was carried out at a pH of 7. The overall recovery was about 90% or better. Recovery could perhaps be improved when extracting basified samples.

Determination of Nonvolatile Organics in RO Composite Permeates

Nonvolatile organics were determined by GC after methylene chloride extraction and K-D concentration. Experimental conditions for GC analysis and procedures for extraction and K-D concentrations were the same as described previously. The volume of the final extract, however, was 0.5 mL. Three extracts, i.e., neutral, acidic, and basic, were obtained from each sample. Table 41 shows the extraction scheme. After K-D concentration to 0.5 mL, extracts were sealed in 1-mL Teflon-lined septum glass vials (Hewlett Packard, Skokie, IL) and crimped for storage. Two extraction procedures were performed for sample C as shown in Table 41. One method was to extract neutral species first and then to extract the acidic and basic fractions. The other method was to acquire the acidic fraction before the basic and neutral extractions were carried out.

TABLE 41. EXTRACTION AND CONCENTRATION PROCEDURES

Sample Code[a]	A Test #1	B Test #2	C Test #3 or 1T-3-2	
Sample Volume	500 mL	1 L	1 L	1 L
2-Ethylphenol spiking	2.074 ppb	2.074 ppb	2.074 ppb	2.074 ppb
First pH adjustment	7	7	7	2
K-D Concentration extraction	A-N	B-N	C-N-1	C-A-2
Second pH adjustment	2	2	2	12
K-D Concentration extraction	A-A	B-A	C-A-1	C-B-2
Third pH adjustment	12	12	12	7
K-D Concentration extraction	A-B	B-B	C-B-1	C-N-2

a. See Table 15.

Nonvolatile organics identified in different extracts of the RO permeates are listed in Table 42. No organics could be observed on the gas chromatograms for basic extracts and extract C-N-2. Identifications were based on relative retention times using 2-ethylphenol as the internal standard except for o-toluidine and N,N-diethyl-m-toluamide, to which the retention time was adopted. Phenol could not be positively identified because it was absent during the preliminary study using chloroform as the organic solvent. The methylene chloride blank concentrated by K-D evaporation shows a peak at 1.15 minute, but this peak is ahead of the phenol peak at 1.35 minute. The appearance of the phenol peak on the tailing shoulder of the solvent peak might cause a deviation in its retention time and therefore affect its identification. The absence of phenol in extracts A-N, B-N, C-N-1, and C-A-1 further indicates that the identification of phenol is questionable. Two other unidentified peaks appeared between 2,4-dimethylphenol and 2,3-dimethylphenol and between 2,3-dimethylphenol and 3,4-dimethylphenol. They were denoted as unknowns X and Y, respectively, and quantified as 2,4-dimethylphenol and 3,4-dimethylphenol.

TABLE 42. CONCENTRATIONS OF NONVOLATILE ORGANICS IDENTIFIED IN RO PERMEATES

	Concentrations (ppb)									
	A-N	A-A	B-N	B-A	C-N-1	C-A-1	C-A-2	A	B	C
Phenol	-	18	-	4	-	-	16	9	2	5
o-Cresol	-	t[a]	-	-	-	t	t	t	-	t
p-Cresol	-	t	-	-	-	-	t	t	-	t
2,6-Dimethylphenol	-	-	-	-	-	-	t	-	-	t
2,4-Dimethylphenol	-	t	-	-	-	-	-	t	-	-
Unknown X (as 2,4-Dimethylphenol)	-	-	1	27	1	4	2	-	14	2
2,3-Dimethylphenol	-	-	-	-	-	2	1	-	-	1
Unknown Y (as 3,4-Dimethylphenol)	-	-	-	30	5	6	2	-	15	4
3,4-Dimethylphenol	-	2	-	-	-	-	3	1	-	1
o-Phenylphenol	2	-	-	-	t	-	-	2	-	t
o-Toluidine	171	-	t	-	-	-	-	171	t	-
N,N-Dimethyl-m-toluamide	-	-	-	-	61	-	56[b]	-	-	61

a. t represents < 0.5 ppb.
b. Correction for extraction/concentration efficiency was not done.

Concentrations of the nonvolatile organics identified in RO permeates are shown in Table 42. The extraction and K-D concentration efficiencies shown in Table 38 were taken into account in calculating the concentrations. Concentrations less than 0.5 ppb are denoted as t (trace). The compounds identified in acidic extracts should also be present in neutral extracts in the case where the neutral extraction was carried out first and extraction efficiencies at pH 7 and pH 2 were comparable to those shown in Table 38. The concentrations determined from both extracts of RO permeates should then be equal if no experimental errors were introduced. The presence of compounds in neutral extracts, however, does not guarantee their detection in acidic extracts because the neutral extracts should contain the major portion of these compounds, leaving only a minor portion to be extracted into the acidic extracts. Small amounts of these compounds might not be detected by GC because of the limitations of the GC sensitivity. Extract C-A-2 was obtained before C-B-2 and C-N-2. It therefore contained a major fraction of the nonvolatile organics, leaving no compounds in extracts C-B-2 and C-N-2. The last three columns show the concentrations determined in RO permeates after considering the above factors. The average concentration was taken if the compound appeared in both acidic and neutral extracts or only in the acidic extracts. The average concentration was taken if the compound appeared in both acidic and neutral extracts or only in the acidic extracts. The only two nonvolatile organics present in RO permeates in noticeable amounts were o-toluidine and N,N-dimethyl-m-toluamide, but they account for only a small fraction of the total organics in the RO permeates.

Summary of Organic Analyses

Table 43 summarizes the TOC and percent TOC of accounted volatile and nonvolatile organics. The accounted TOC was very low for hospital composite RO permeates (samples A and C) and 55.7% for laboratory RO permeate (sample B). Urea may contribute a great portion of the TOC, as has been found to be true at USAMBRDL for other samples. Low molecular-weight carboxylic acids may account for some at the sub-ppm level, as shown in section on Determination of Acetic Acid in RO Permeate.

It can be concluded that distillation/GC or distillation/headspace/GC and extraction/GC are the optimum methods for determining volatile polar organics and nonvolatile organics in RO permeates. Attention should also be given to the selection of gas chromatographic columns. For example, basic columns should be tested in analyzing basic extracts as well as distillates. Since volatile nonpolar organics are present at ppb levels, analysis for these substances can be neglected unless their toxicity is of interest. Analyses for urea and lower carboxylic acids, however, should be performed.

TABLE 43. TOC AND PERCENT TOC OF ACCOUNTED ORGANICS

Samples[a]	A	B	C
TOC, ppm (determined by TOC analyzer)	8.54	72.80	9.15
TOC, ppm (determined polar organics from VOA by distillation/GC method)[b]	0.02	40.54	0.01
TOC, ppm (determined non-polar organics from VOA by stripping/GC method)[c]	NA[d]	NA	0.01
TOC, ppm (determined non-volatiles from NVOA by extraction/GC method)[e]	0.18	0.03	0.07
ΣTOC, ppm (from VOA and NVOA)	0.20	40.57	0.09
% of Accounted Organics	2.3	55.7	1.0

a. See Table 15 for sample coding.
b. Obtained from Table 18.
c. Obtained from Table 32.
d. NA denotes not available.
e. Obtained from Table 42.

DETERMINATION OF GLYOXAL, METHYLGLYOXAL, AND DIMETHYLGLYOXAL BY GAS CHROMATOGRAPHY

The analytical method for determining glyoxal, methylglyoxal, and dimethylglyoxal in an aqueous mixture by flame ionization detection/gas chromatography (FID-GC) was developed. After their reaction with o-phenylenediamine, glyoxal, methylglyoxal, and dimethylglyoxal were respectively converted to quinoxaline (Q), 2-methylquinoxaline (MQ), and 2,3-dimethylquinoxaline (DMQ) according to the condensation reaction described by Fieser and Fieser (1967). The reaction was modified by Nojima et al. (1974) for the determination by ECD-GC. To improve the sensitivity, the reaction mixture was subjected to benzene extraction followed by K-D evaporation. The K-D concentrate was then analyzed by FID-GC.

The GC column used was a 183-cm x 6.35-mm outside diameter (6-ft x 1/4-inch outside diameter), 2-mm inside diameter glass column packed with 3% OV-17 on 100/120 Gas Chrom Q. The GC oven temperature was held initially at 130°C for 2 minutes and then programmed to increase at a rate of 40°C/minute to 200°C and held for 1 minute. The nitrogen flow rate was 25 mL/minute. Figure 43 shows the GC separation of the reaction products and o-phenylenediamine. The reaction products derived individually from glyoxal (Alderich Chemical Company, Inc., Milwaukee, WI), methylglyoxal (Pfaltz & Bauer, Inc., Stamford, CT), and dimethylglyoxal (Chem Service, West Chester, PA) were identified by comparing the retention times for the products and the standard methanolic solutions of Q, MQ, and DMQ (Alderich Chemical Company, Inc.). The reaction yields of Q, MQ, and DMQ were calculated by comparing the GC peak heights for the reaction products and their standard solutions.

For the reaction, 10 mL of standard aqueous glyoxals (mixture of glyoxal, methylglyoxal, and dimethylglyoxal) were mixed with 10 mL of 0.185 M methanolic o-phenylenediamine solution in a 50-mL round bottom flask. One milliliter of 10% aqueous sodium bisulfite solution was added to the mixture just before heating. The mixture (1:1 methanol/water) was then refluxed at a rate of one drop per second for 30 minutes. A heating mantle was stirred by a 1/4-inch-long Teflon-coated magnetic bar. A 7-inch-long water-cooling condenser was used for refluxing. The yields of Q, MQ, and DMQ, determined for a 1,000-ppm mixture of glyoxals, were 83.1%, 36.5%, and 54.6% and the standard deviations determined for three independent runs were 0.4%, 1.2%, and 1.0%, respectively.

The reaction conditions such as the amount of o-phenylenediamine, the amount of sodium bisulfite, the reaction time, and the presence of other glyoxals were studied. The reaction yield did not change in the presence of other glyoxals, indicating the reaction was not interfered by other glyoxals. The yield of Q dropped from 83% to 64% and the yields of MQ and DMQ did not change as the concentration of o-phenylenediamine decreased from 0.185 M to 0.0185 M. It was found, however, that the yields were 81%, 32%, and 33%, respectively, for Q, MQ, and DMQ when 1 mL of 0.185 M methanolic o-phenylenediamine was used to react with 10 mL of glyoxals. These results indicate that the reaction yield of Q is determined by the concentrations

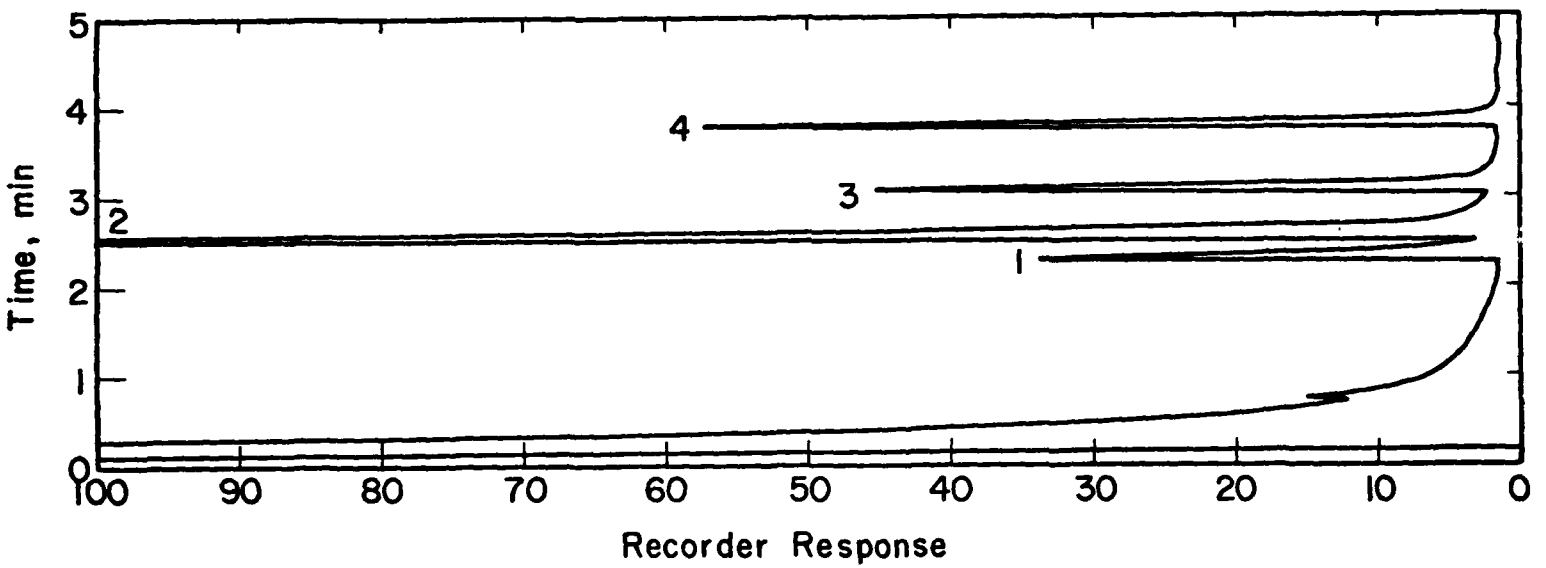

Figure 43. Gas Chromatogram of K-D Concentrate Obtained from a 100 mg/L Standard Aqueous Mixture of Glyoxal, Methylglyoxal, and Dimethylglyoxal After Their Reaction with o-Phenylenediamine Followed by Benzene Extraction and K-D Evaporation. Peak (1) = Quinoxaline, (2) = o-Phenylenediamine, (3) = 2-Methylquinoxaline, and (4) = 2,3-Dimethylquinoxaline.

of o-phenylenediamine and methanol in the reaction mixture and the yields of MQ and DMQ are determined by the amount of methanol. The complication observed for the change of the yield of Q probably arises because of the limited solubility of o-phenylenediamine (one reactant) in water. While methylglyoxal and dimethylglyoxal are more soluble in methanol than in water, higher yields of MQ and DMQ can be expected for a reaction mixture containing larger amounts of methanol. The amount of sodium bisulfite, studied in the range of 0.1 to 2 mL, did not appear to affect the yield. In fact, the same yields of Q, MQ, and DMQ were obtained without the addition of sodium bisulfite solution to the reaction mixture. It was also observed that the length of the reaction time (refluxing time) did not affect the yields and refluxing was not at all necessary.

The detection limits were 0.5, 3.0, and 0.8 ppm, respectively, for glyoxal, methylglyoxal, and dimethylglyoxal. In order to improve the sensitivity, solvent extract and K-D concentration were performed following the reaction. The entire analytical procedures are described below. Ten milliliters of standard aqueous glyoxals or sample solution are pipetted to a 22-mL test tube to which 1 mL each of 0.185 M methanolic o-phenylenediamine solution and 10% aqueous sodium bisulfite solution are then introduced. The test tube is stoppered and shaken. Thirty minutes later, 5 mL of benzene are added and the tube is stoppered and shaken. After the benzene and water layers become clearly separated, 4 mL of the top benzene layer are pipetted to the 4-mL tube of a micro K-D evaporator. The K-D evaporation is then carried out over a 100°C water bath until the benzene extract is concentrated to 0.5 mL. Then 2 μL of the concentrate is analyzed by GC.

The yields of Q, MQ, and DMQ were 81%, 32%, and 33%, respectively. The corresponding extraction efficiencies were 27%, 85%, and 83%; and the efficiencies of K-D concentration were 95%, 98%, and 94%. The relative standard deviation, determined for triplicate runs of 10 ppm mixtures, was 2.0%, 4.3%, and 2.5%, respectively, for glyoxal, methylglyoxal, and dimethylgloxal with corresponding detection limits of 0.08, 0.05, and 0.2 ppm. The correlation coefficients of the linear regression curves for the analytical calibration curves for glyoxals were 1.0 using three concentration points, i.e., 2, 10, and 100 ppm.

DETERMINATION OF PYRUVIC AND GLYOXYLIC ACIDS

A literature review on the analytical methods for determining pyruvic and glyoxylic acids is given. Glyoxylic acid was determined colorimetrically by Kramer et al. (1959) after the acid was converted to formazan. Many aldehydes and other organics will cause interferences (Kramer et al., 1959). Sokol (1977) determined glyoxylic and pyruvic acids as hydrazones in the presence of acetaldehyde. Although separate quantitation of hydrazones derived from pyruvic and glyoxylic acids were not possible by the colorimetric method, Sokol (1977) identified these acids by paper chromatography. Later, Terada et al. (1977) separated hydrazones by HPLC with a Zipax Permaphase AAX column. Kallio and Linko (1973) determined glyoxylic, pyruvic, and other keto acids at ppb levels by GC following methylation of hydrazones.

Pyruvic acid and Krebs cycle keto acids have been methylated by diazomethane (DAM) and determined by GC (Simmonds et al., 1967). Rosenquist et al. (1972) determined lactic, pyruvic, and glyoxylic acids by GC after formation of TMS derivatives. These acids were concentrated in Dowex and eluted with formic acid solution. Glyoxylic acid was also determined by GC after reaction with dimedone or N,N'-diphenylethylene-diamine followed by TMS derivatization of reaction products (Chalmers and Watts, 1972). Formation of oximes followed by TMS derivatization allowed the determination by GC of glyoxylic acid (Lancaster et al., 1973; Sternowsky et al., 1973) and pyruvic acid (Lancaster et al., 1973). Pyruvic acid was determined by GC after formation of methoxime followed by TMS derivatization (Horning et al., 1968) or by DAM methylation (Ishitoya et al., 1970). Pyruvic acid was also determined by GC as a TMS derivative of ethoxime or benzoxime (Chalmers and Watts, 1972) or quinoxalinol (Langenbeck et al., 1977). Pyruvic acid has also been determined at sub-ppm level by a colorimetric method following ion-exchange separation (Nakajima et al., 1976; Kasai et al., 1975). The analytical procedures were automated by Kasai et al. (1977).

OZONATION OF MODEL COMPOUNDS

Literature Review

A review of the literature on ozonation was conducted and is summarized here prior to the presentation of experimental results. Although the review was not intended to be exhaustive, it included many excellent articles covering a wide spectrum of ozonation studies.

The oxidation of organics by ozone in solvents other than water has been extensively studied. The use of water as a solvent in ozonation experiments has received very little attention until recently. Ahmed and Kinney (1950) investigated ozonation of humic acids in an alkaline solution. They found that both carbonic and oxalic acids appeared to be primary products and accounted for about 65% of the carbon. Practically all of the remaining carbon was converted to almost colorless, water-soluble, ozone resistant acids. Of these acids, only acetic acid was identified.

The use of ozone to oxidize aqueous solutions of malonic acid was conducted by Dobinson (1959). It was shown that the pathway of the reaction appeared to lead through tartronic acid to mesoxalic acid, which was, in turn, oxidized to oxalic acid and carbon dioxide.

Eisenhauer investigated the reaction between ozone and dilute solutions of pure phenol (1971). He proposed a mechanism that involved the formation of catechol and o-quinone. No additional evidence was obtained to elucidate the details of the subsequent ozonation of o-quinone to carbon dioxide and water. He pointed out that the pH dependence of the initial phase of phenol oxidation reflected that the reaction was ionic and should not involve the formation of intermediate hydrogen peroxide.

Ozonation of phenol in aqueous solutions has recently been studied in further detail and reaction products were determined by Gould and Weber (1976). It was concluded that ring cleavage was much preferred to hydroxylation of phenol. Glyoxal and glyoxylic acid were identified as the reaction products resulting from ring cleavage, while catechol and hydroquinone were formed by hydroxylation of phenol. The latter two substances were detected only during the early stage of ozonation and accounted for only about 10% of the initial phenol concentration. It was suggested that glyoxal was further oxidized to glyoxylic acid, which, in turn, was oxidized to carbon dioxide and water. Oxalic acid was also detected in the reaction mixture. However, the formation and fate of oxalic acid was not discussed. It was proposed that glyoxylic acid could be oxidized by some mechanism to carbon dioxide without passing through the oxalic acid stage. The removal rates for chemical oxygen demand (COD) and total organic carbon (TOC) were also studied. Two distinct rates were observed. The fact that the final rate was much smaller than the initial rate might indicate that aliphatic compounds were less reactive toward ozone than were aromatic compounds.

Recently, studies on ozonolysis of chlorophenols and maleic acid in aqueous solution were reported by Gilbert (1975). It was found that ozone oxidation of mono-, di-, and trichlorophenols converted the organic chlorine to chloride. The oxidation products were determined to be of carbonyl compounds and/or carbonyl carboxylic acids and some leftover chlorinated aliphatic compounds. Dechlorination is therefore not 100% complete. The ozone oxidation of maleic acid gave glyoxylic acid, oxalic acid, formic acid, and carbon dioxide. Hoigne and Bader (1975) have provided experimental evidence that the main oxidizing intermediates formed in alkaline water upon decomposition of ozone are the hydroxyl radicals. This thesis is, however, contrary to Eisenhauer's argument. Hoigne and Bader (1975) proposed that substantial information on the reactions of these radicals is applicable to evaluating the actions initiated by ozone in water whenever predecomposition is involved.

Ozone/UV oxidation of chlorinated compounds in water has been investigated by Prengle et al. (1976). It was observed that for compounds such as pentachlorophenol with a strong UV absorption characteristic the chlorine atoms were released very rapidly to form chloride ions. For compounds that absorb UV weakly, dechlorination occurred by oxidation, releasing the atoms as chlorine and then forming hypochlorous acid. Chloroform absorbs UV very weakly and therefore dechlorination involves both mechanisms, i.e., oxidation and UV absorption.

An excellent review by Peleg (1976) discusses the chemistry of ozone in water and the disinfection potentials of ozone and its dissociation species. A mechanism for ozone decomposition in water was proposed; at high pH values, it followed the mechanism demonstrated by Gorbenko-Germanov and Kazieva (1973).

Hoigne and Bader (1976) proposed and later supported the reaction scheme for the ozonation of organic substrates from studies of relative reaction rates. For compounds with highly selective groups such as unsaturated organic, chromophoric organic, or amino compounds, direct reaction with ozone molecules will proceed very rapidly. The direct reaction is the primary pathway in acidic solutions. On the other hand, if reaction conditions are chosen that

lead to prior ozone decomposition in an alkaline medium, hydroxyl radicals are the main oxidative species. Acetic and oxalic acids react with hydroxyl radicals two to three orders of magnitude slower than do aromatic hydrocarbons, unsaturated compounds, aliphatic alcohols, or formic acid. Therefore, acetic and oxalic acids were postulated or observed as the intermediates that were difficult to oxidize further to carbon dioxide. Carbonate or bicarbonate ions were found by the authors to have a protective effect on ozone decomposition. That is, they consume hydroxyl radicals and thus terminate the hydroxyl-radical-initiated chain reactions that would otherwise cause ozone decomposition. The authors also pointed out that because hydroxyl radicals react very fast with many types of dissolved organics, they might well be scavenged before they could encounter a suspended particle, resulting in a low yield in the oxidation of particulate matter. The same situation might occur in disinfection processes if hydroxyl radicals were the main oxidative species. In many systems, however, secondary intermediates of lower reactivity, such as organic peroxy radicals, can be formed from the reaction between hydroxyl radicals and dissolved organics, and they may survive until they encounter dispersed particles or microorganisms.

Hewes et al. (1974) studied the oxidation of five refractory organic compounds (acetic acid, ethanol, glycine, glycerol, and palmitic acid) by ozone and ultraviolet light. The results of this study, along with those of another study on TNT by Fochtman and Huff (1975), have demonstrated the potential of using ozone-UV in combination for the oxidation in aqueous solution of chemical species that would otherwise be difficult to oxidize by ozone alone. TOC analysis of the solutions and GC analysis of some of the organics were conducted in both studies. The specific degradation products were not, however, determined during the course of ozonation and UV-ozonation.

Electrophilic attack of ozone on hydrogen atom α to ether bond was postulated from the ozonation study of ether and polypropylene oxide by Price and Tumolo (1964, 1967). The same mechanism was adopted to interpret the experimental results produced by the ozonation of 1% polyethylene glycol (molecular weight 8,000) in aqueous solution at a pH of 12 (Suzuki, 1976). High molecular-weight polyethylene glycol can be degraded by ozone so that it can be used by microorganisms. The effectiveness of using ozone in the treatment of photographic processing wastes (Bober and Dagon, 1975) and dye wastes (Snider and Porter, 1974) was also studied.

Introduction

Nine model compounds were subjected to ozonation and UV-ozonation individually. The objectives were to investigate TOC removal, to study ozonation intermediates and products. The model compounds studied were 1-propanol, propionic acid, 2-propanol, methyl ethyl ketone (MEK), acetic acid, diethyl ether, o-toluidine, methanol, and N,N-diethyl-m-toluamide. They were selected as model compounds because they have been identified in the RO permeates of hospital composites.

The ozonation study was conducted with a 4-liter fermentor equipped with a 15-watt low-pressure mercury germicidal lamp. The major ultraviolet energy was emitted at a wavelength of 253.7 nm. The fermentor was operated with a stirrer speed of 695 rpm. Constant temperature was maintained by a controller located in a separate water bath. The pH was held constant by a pH controller, which activated a solenoid valve to add NaOH to the fermentor when the pH dropped below the preset value. Hydrochloric acid was introduced manually if the pH increased. Ozone was produced by a W.R. Grace Model LG-2-L2 ozone generator from a cylinder of dried oxygen. The ozone concentration in the feed gas to the fermentor was 33 mg/L at a flow rate of 1 L/minute. Later, a 5-liter New Brunswick fermentor (New Brunswick Scientific, New Brunswick, NJ) was used and ozone was generated by a Welsbach Model T-408 ozone generator (Philadelphia, PA) with a feed gas to the fermentor at a concentration of 25 mg/L and a flow rate of 4 L/minute.

Every 15 or 30 minutes during the ozonation or UV-ozonation, 20 mL of solution was drawn and stored in a refrigerator at 4°C for later chemical analysis. In addition, another 5 mL of solution was drawn and immediately analyzed iodometrically for dissolved ozone using Shechter's method (1973).

A Beckman Model 915 TOC analyzer was used for TOC determinations. Gas chromatographic analyses were performed on an HP 5750 B gas chromatograph equipped with dual flame ionization detectors (FID's). A 6-ft x 1/8-inch outside diameter, stainless steel column packed with 0.4% Carbowax 1500 on 80/100 Carbopack A (alcohol column) was used for determining alcohols, ketones, aldehydes, diethyl ether, ethyl acetate, and ethyl formate. Later, this column was replaced by a 6-ft x 1/4-inch outside diameter glass column packed with 0.2% Carbowax 1500 on 80/100 Carbopack C. Monocarboxylic acids, C2 to C6, were determined by directly injecting the aqueous solution onto a 6-ft x 1/4-inch outside diameter glass column packed with 0.3% SP-1000/0.3% H_3PO_4 on 60/80 Carbopack A (acid column). A 60/80 Carbopack B/3% Carbowax 20 M/0.5% H_3PO_4 was later used as the packing material. Bethge and Lindstrom's method (1974) was adopted to determine formic and acetic acids. The benzyl esters of acids were separated and determined on a 6-ft x 1/4-inch outside diameter glass column packed with 3% butane-1,4-diol succinate polyester on 100/120 AW Chromosorb W. One ppm of formic acid and 0.5 ppm of acetic acid can be easily identified with this method. Oxalic acid was determined on the above GC column after it was converted to dimethyl oxalate using diazomethane. Glyoxylate was determined by a colorimetric method described by Kramer et al. (1959). Determination of formaldehyde was accomplished by injecting 1 mL of headspace gas onto the alcohol column using the headspace injection technique (Cowen et al., 1975). Later, the chromotropic acid method (Houle et al., 1970) was used to determine formaldehyde. By directly injecting the aqueous solution onto a 6-ft x 1/8-inch outside diameter, stainless steel column packed with 35/60 Tenax-GC, o-toluidine and N,N-diethyl-m-toluamide were determined.

Ozonation and UV-Ozonation of 1-Propanol

The aqueous solution of 1-propanol having an initial concentration of 408 mg/L was ozonated at a pH of 9 and a temperature of 25°C for 1 hour. The dissolved ozone concentration was found to be zero, which indicated that the reaction was carried out under mass transfer limitation. The high decomposition rate of ozone at a pH of 9 also accounted for the low dissolved ozone concentration. The decrease of TOC and 1-propanol as well as the formation of propionaldehyde are shown in Figure 44. A carbon balance showed that 1-propanol and propionaldehyde accounted for all of the carbon present in solution (see Figure 45).

UV-ozonation of 1-propanol at an initial concentration of 410 mg/L was conducted under the same conditions as in the previous experiment. The results are shown in Figure 46. Again, the dissolved ozone was not detected, indicating that the reaction was mass-transfer limited. A carbon balance, shown in Figure 47, also demonstrated that 1-propanol and propionaldehyde accounted for all of the carbon.

In both experiments, a higher TOC removal rate was reached after the peak of propionaldehyde formation, suggesting that the TOC was probably removed through the stripping of propionaldehyde. In other words, ozonation and UV-ozonation of 1-propanol first converted 1-propanol to propionaldehyde, which was then stripped under the experimental conditions. Our experience indicates that propionaldehyde will be stripped under the given conditions (Chian and Kuo, 1975).

Ozonation and UV-Ozonation of Propionic Acid

Ozonation of propionic acid was conducted with and without UV irradiation at a pH of 9 and a temperature of 25°C for 2 hours. The results are shown in Figures 48 and 49. Dissolved ozone was again absent from the solutions. Since propionic acid did not contribute to all of the carbon present (see Figure 50), there must have been intermediate products produced that were not detected with the use of the acid GC column.

The reduction of 1-propanol and propionic acid follows a first-order kinetic equation, as illustrated in Figures 51 and 52, respectively. UV irradiation appeared to enhance the removal rates of both compounds by ozonation. Since all of the experiments were performed under an apparent mass-transfer limitation--i.e., the dissolved ozone was zero--results of studies with and without UV irradiation appear to support the assumption that autooxidation or radical formation may be involved in ozone oxidation.

Ozonation and UV-Ozonation of 2-Propanol

For the rest of the model compounds, the reactor was operated in a reaction-rate limiting condition by using lower substrate concentrations. Dissolved ozone concentrations were determined at 4 ppm or higher, showing that all ozonation runs were not conducted under mass-transfer-limited conditions.

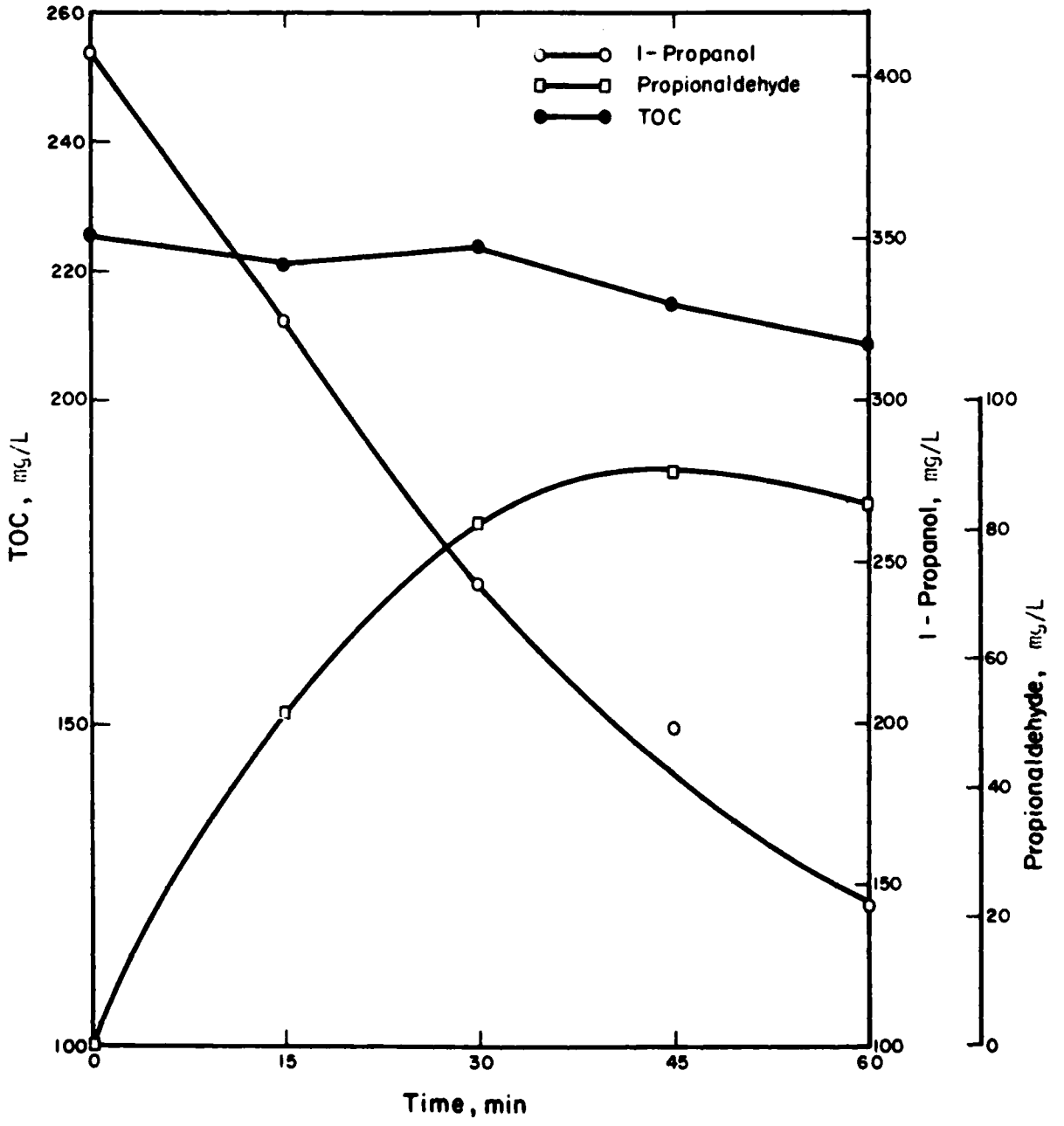

Figure 44. Ozonation of 1-Propanol.

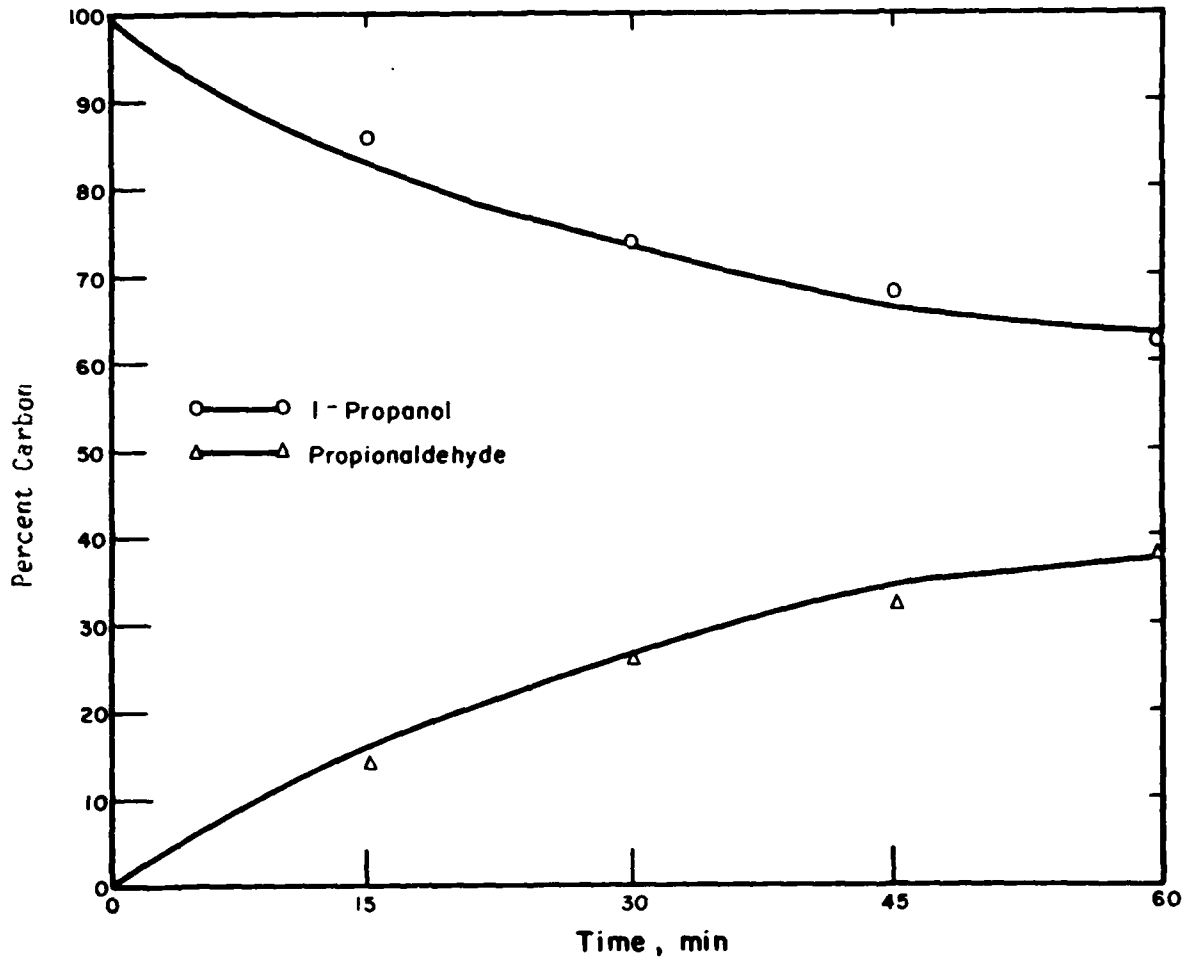

Figure 45. Yields of Ozonation Products from 1-Propanol.

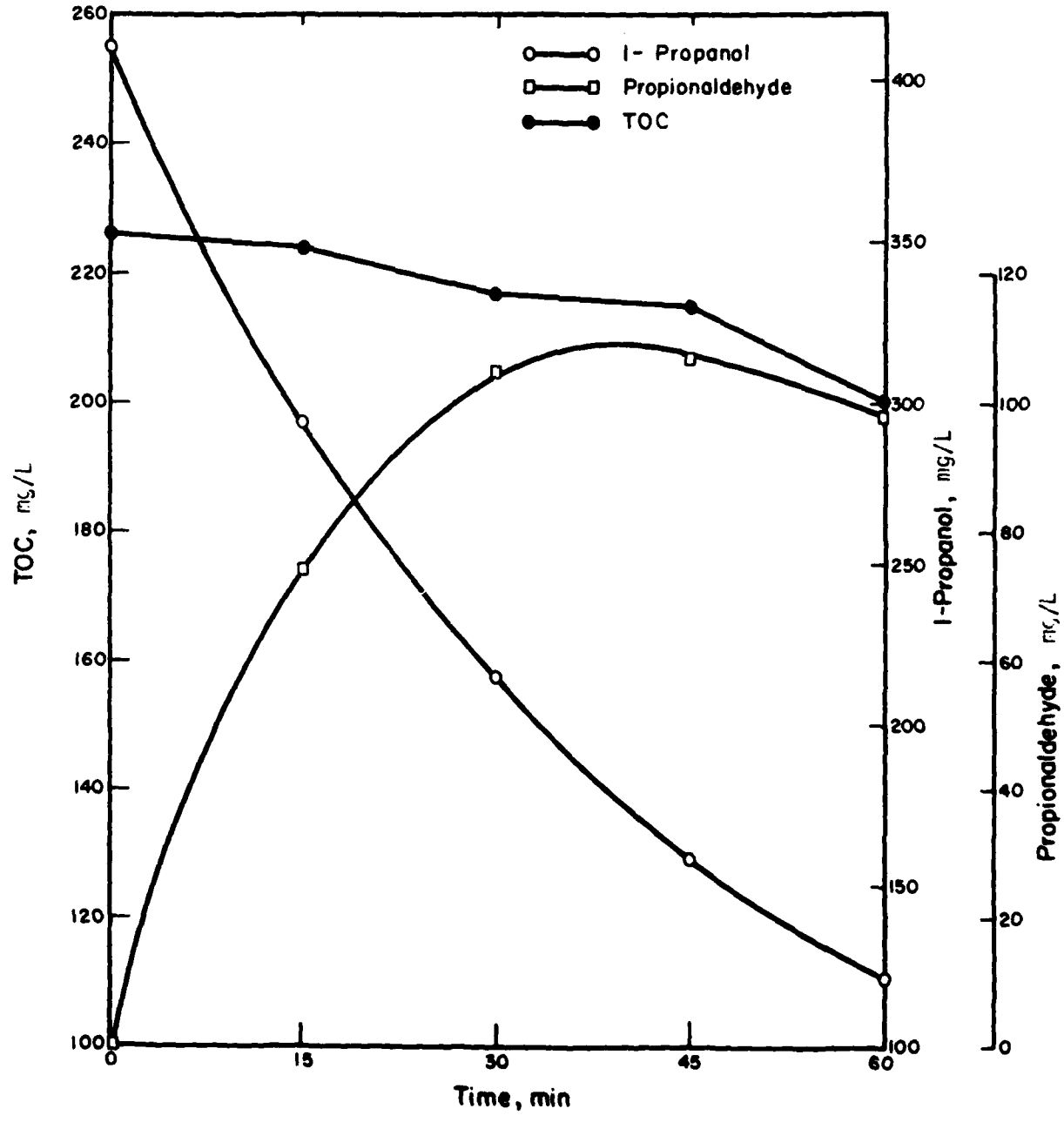

Figure 46. UV-Ozonation of 1-Propanol.

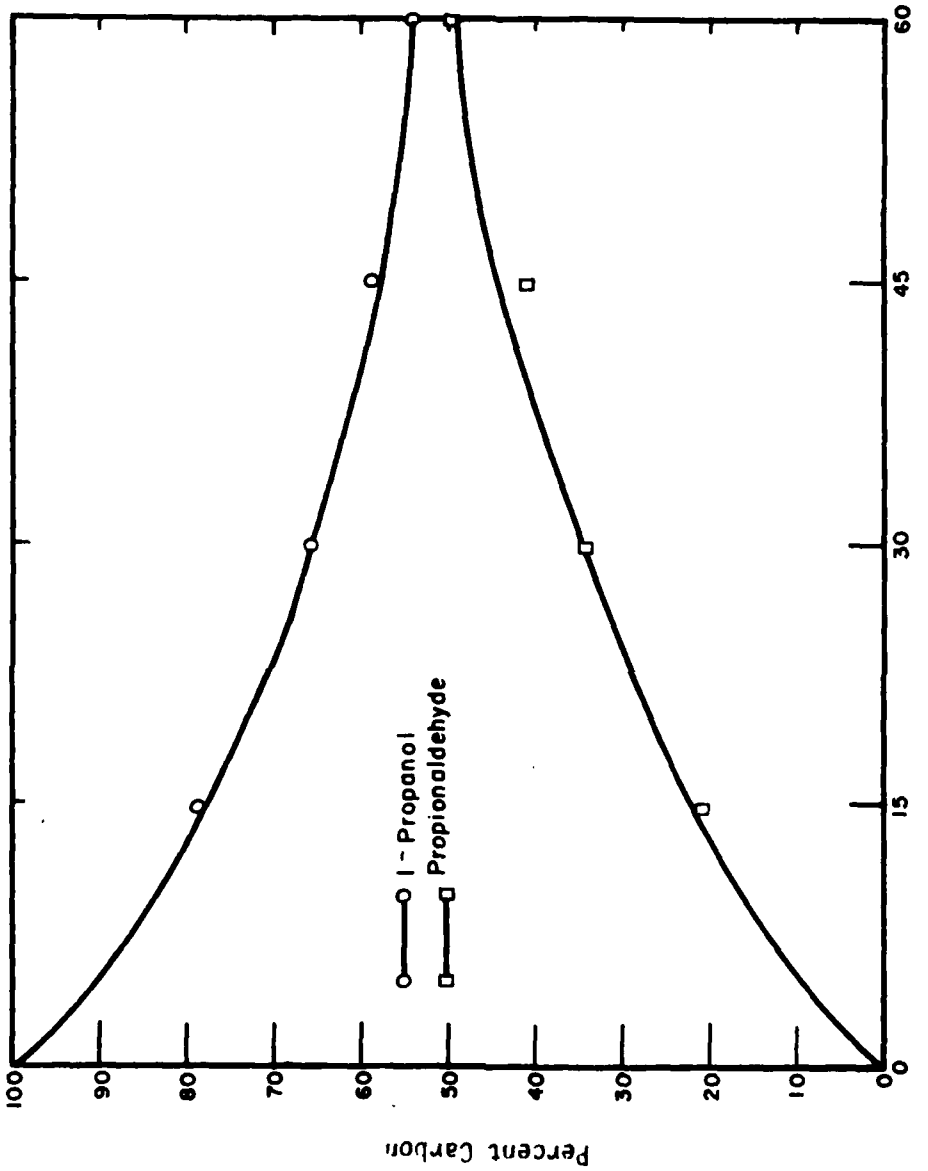

Figure 47. Yields of UV-Ozonation Products from 1-Propanol.

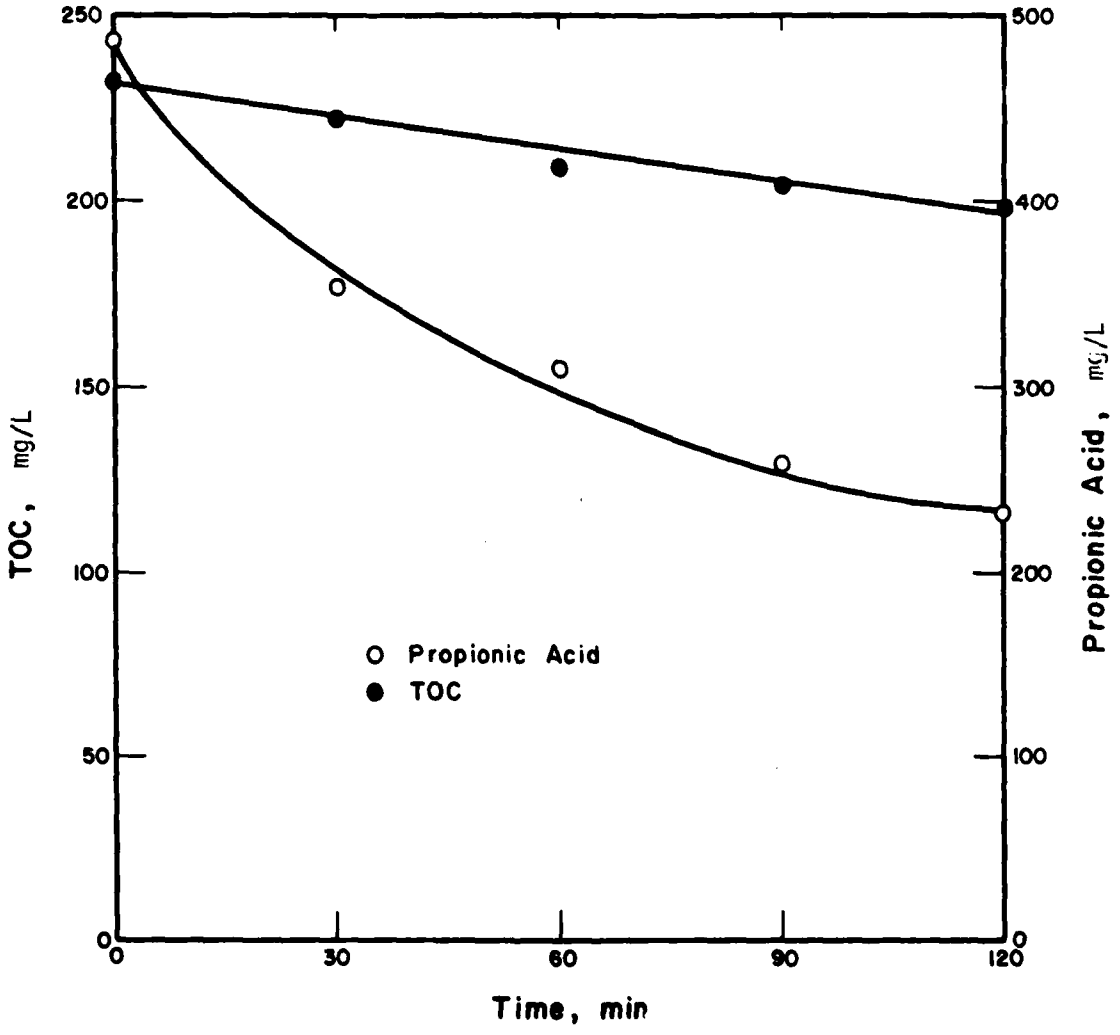

Figure 48. Ozonation of Propionic Acid.

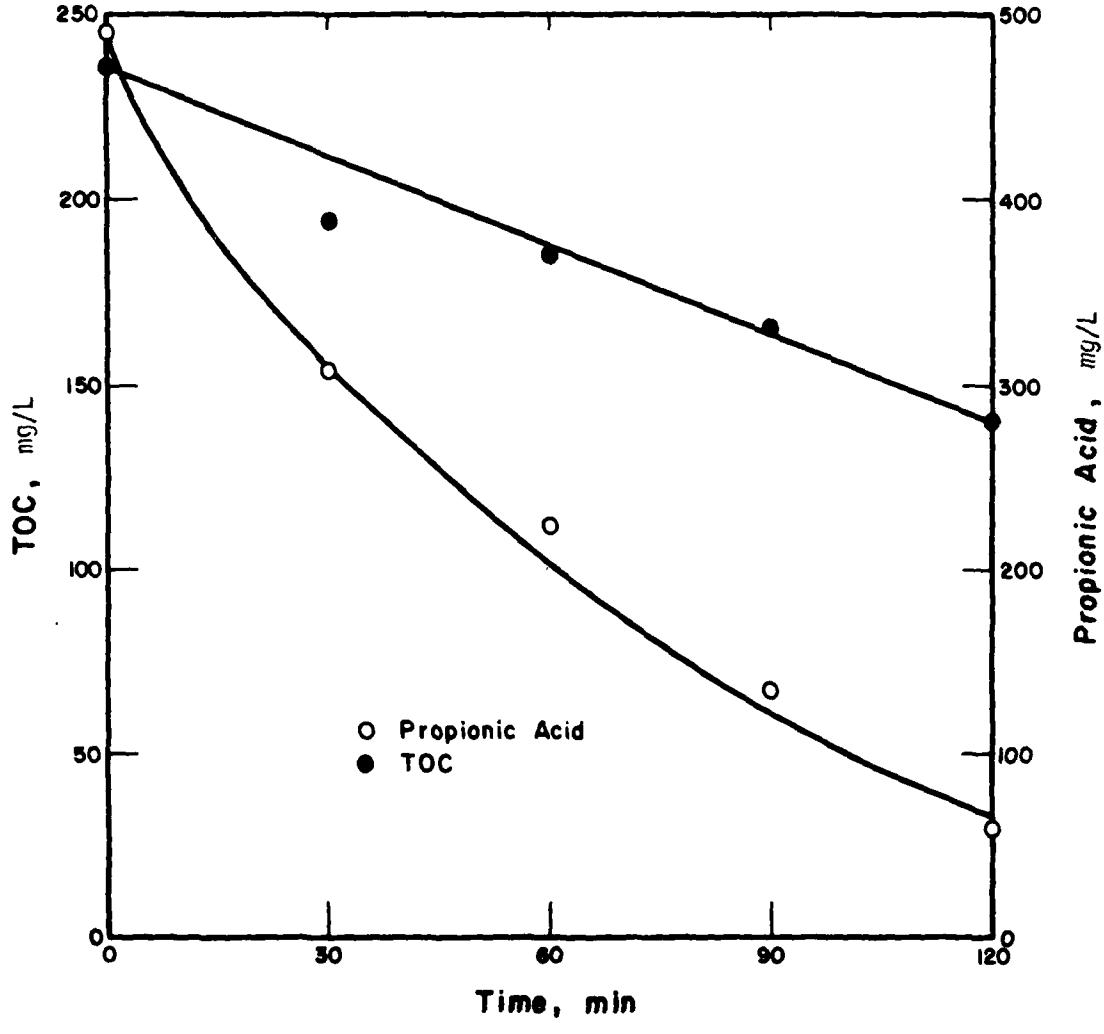

Figure 49. UV-Ozonation of Propionic Acid.

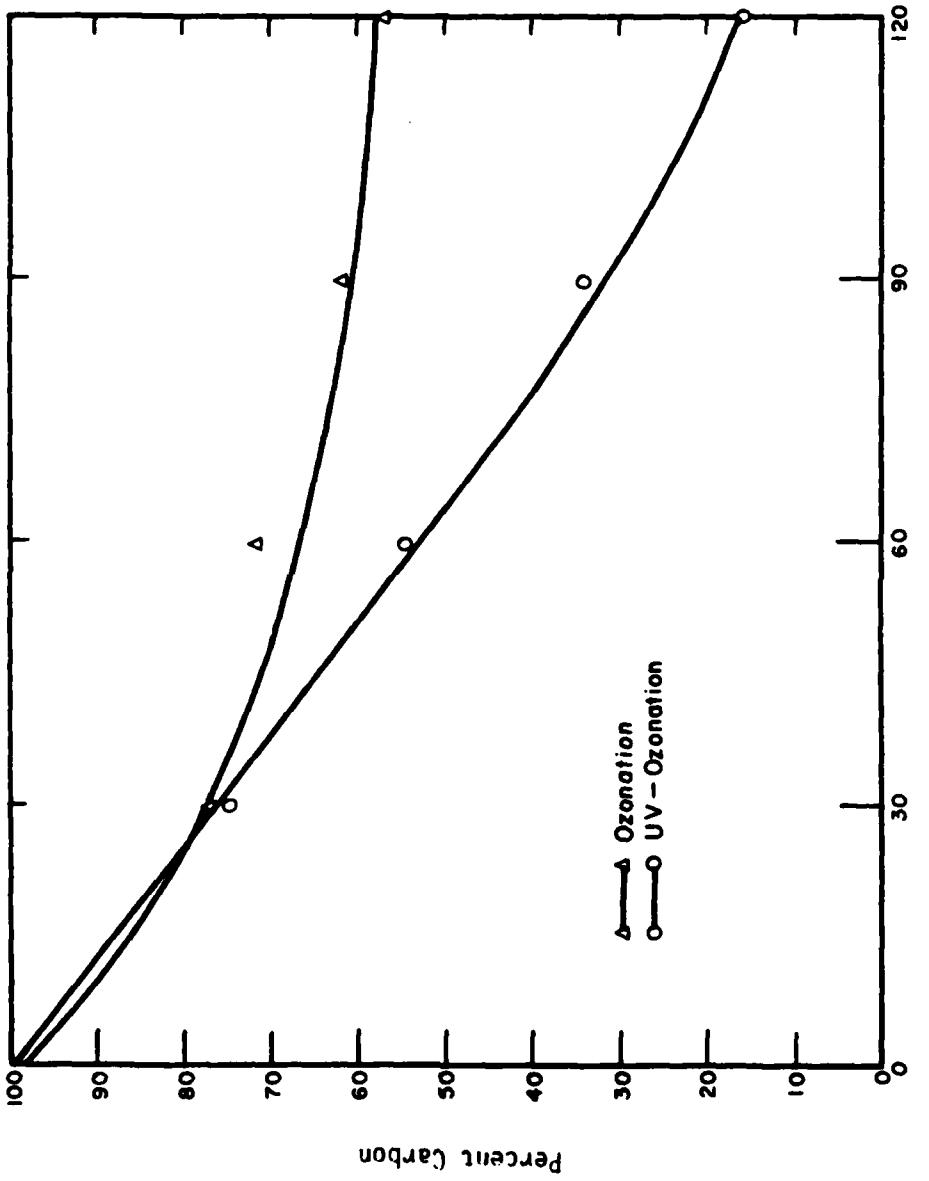

Figure 50. Percent Carbon Contributed by Propionic Acid in Ozonated Propionic Acid Solution.

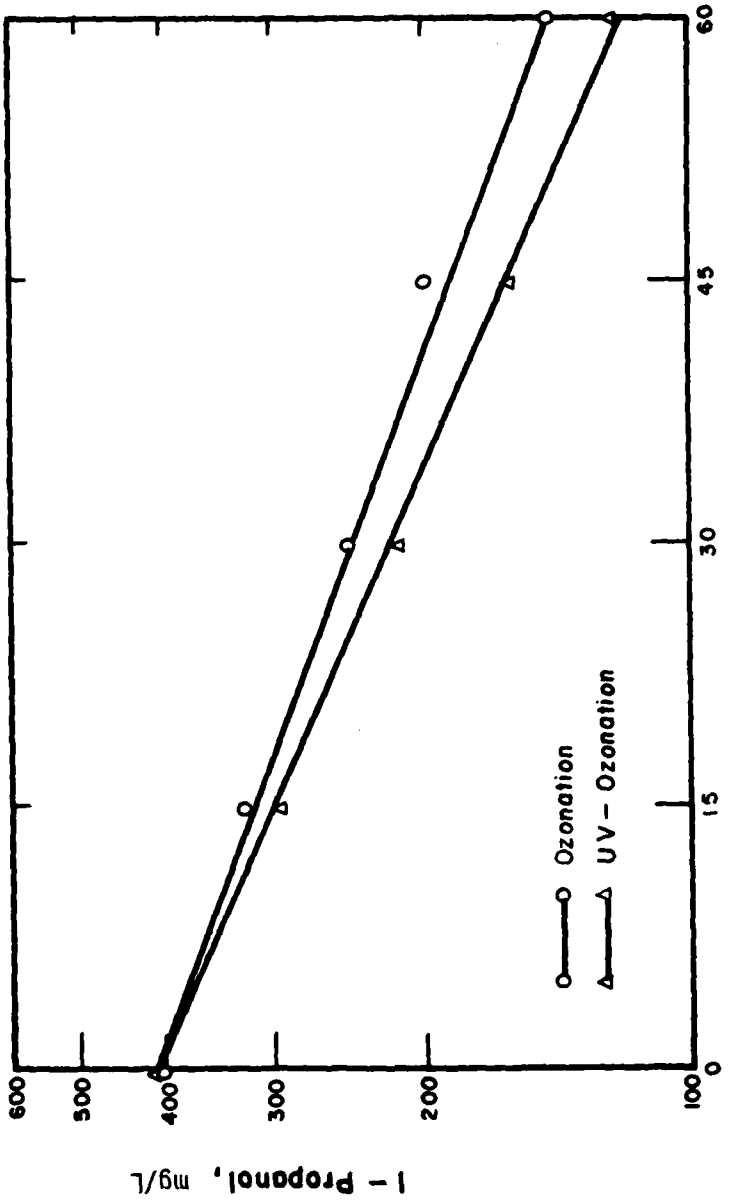

Figure 51. Removal of 1-Propanol by Ozonation.

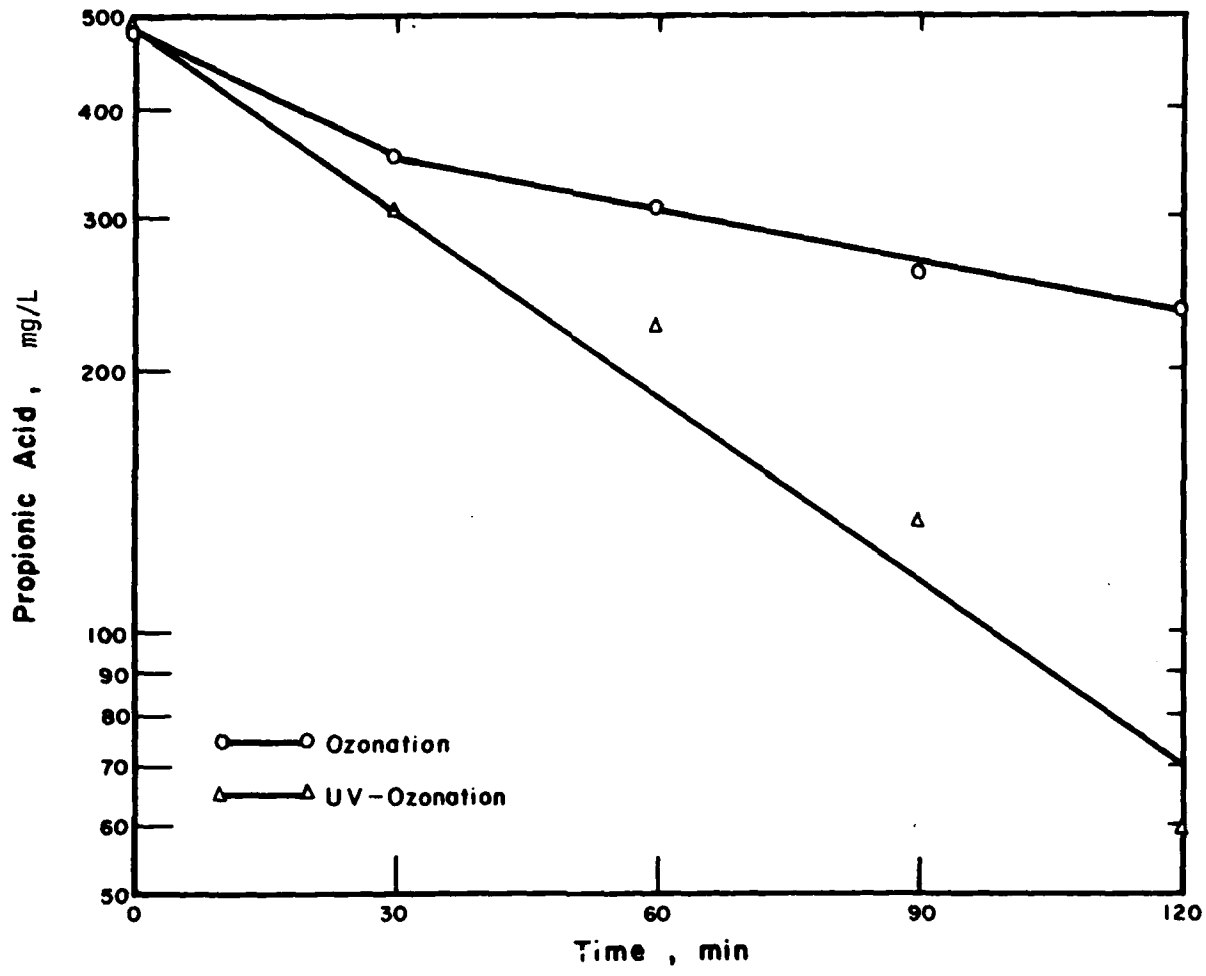

Figure 52. Removal of Propionic Acid by Ozonation.

Ozonation of 2-propanol at a pH of 7 and a temperature of 25°C resulted in removal of 17% of the TOC. It was found that 2-propanol was completely oxidized to acetone at the end of a 2-hour ozonation period (Figure 53). Using the acid column, no monocarboxylic acids were detected in the samples. The TOC calculated from the concentrations of 2-propanol and acetone accounted for over 85% of the TOC of the reaction mixture. The remaining 15% of the TOC may be accounted for by the oxidation of acetone to form intermediate products, which could not be detected by the two GC columns employed. The observed 17% removal of TOC may be contributed mainly by the stripping of 2-propanol and acetone. The TOC removal through the production of CO_2 is probably unimportant under these experimental conditions.

UV-ozonation of 2-propanol substantially improved the rate of TOC removal. An initial TOC of 110 mg/L was reduced to 20 mg/L after 135 minutes of UV-ozonation, corresponding to a TOC removal of 82%. Acetone formation was again found as 2-propanol was oxidized. Determinations of 2-propanol and acetone showed that 2-propanol disappeared completely after approximately 30 minutes, at which time acetone reached its maximum level. The latter, in turn, decreased to zero after approximately 75 minutes. It is suspected that oxidation of acetone to CO_2 through some intermediate steps is the major mechanism for the TOC removal observed. The apparent discrepancy between the TOC determined experimentally and that calculated from the amount of 2-propanol and acetone (see Figure 54) may have been caused by the presence of intermediate products resulting from the further oxidation of acetone. In view of the fact that addition of NaOH was required to maintain a constant pH during the reaction, these intermediate products may be of an acid nature, probably carboxylic acids. Later, it was found that further ozonation of acetone will form acetic and oxalic acids as well as trace amounts of formic acid and formaldehyde (Table 44). Other suspected intermediates are pyruvic and keto malonic acids.

Oxygen stripping of 2-propanol was conducted at 25°C and the results are shown in Figure 55. It is seen that only 9% of the TOC was removed by oxygen stripping. This experiment was originally intended to be used as a control. It did not serve the purpose, however, because acetone resulting from the oxidation of 2-propanol in the ozonation as well as UV-ozonation runs could also be stripped off.

Ozonation and UV-Ozonation of Methyl Ethyl Ketone

Methyl ethyl ketone (MEK) was subjected to ozonation at a pH of 7 and a temperature of 25°C. The aqueous solution of MEK was found to be rather unaffected by ozonation under the experimental conditions. The TOC calculated from the amount of MEK in solution accounted for over 85% of the TOC. Only a small amount of acetate was produced in the sample (Figure 56). The decrease in MEK concentrations was attributed mostly to stripping. This factor probably accounts for the major fraction of the 40% of the TOC removed after ozonation for 2 hours (Figure 56). As can be seen in Figure 57, after 105 minutes of UV-ozonation, the MEK was depleted completely. Acetate was identified as one of the degradation products. Acetate reached its maximum and then decreased to zero as shown in Figure 57. Trace amounts of acetone

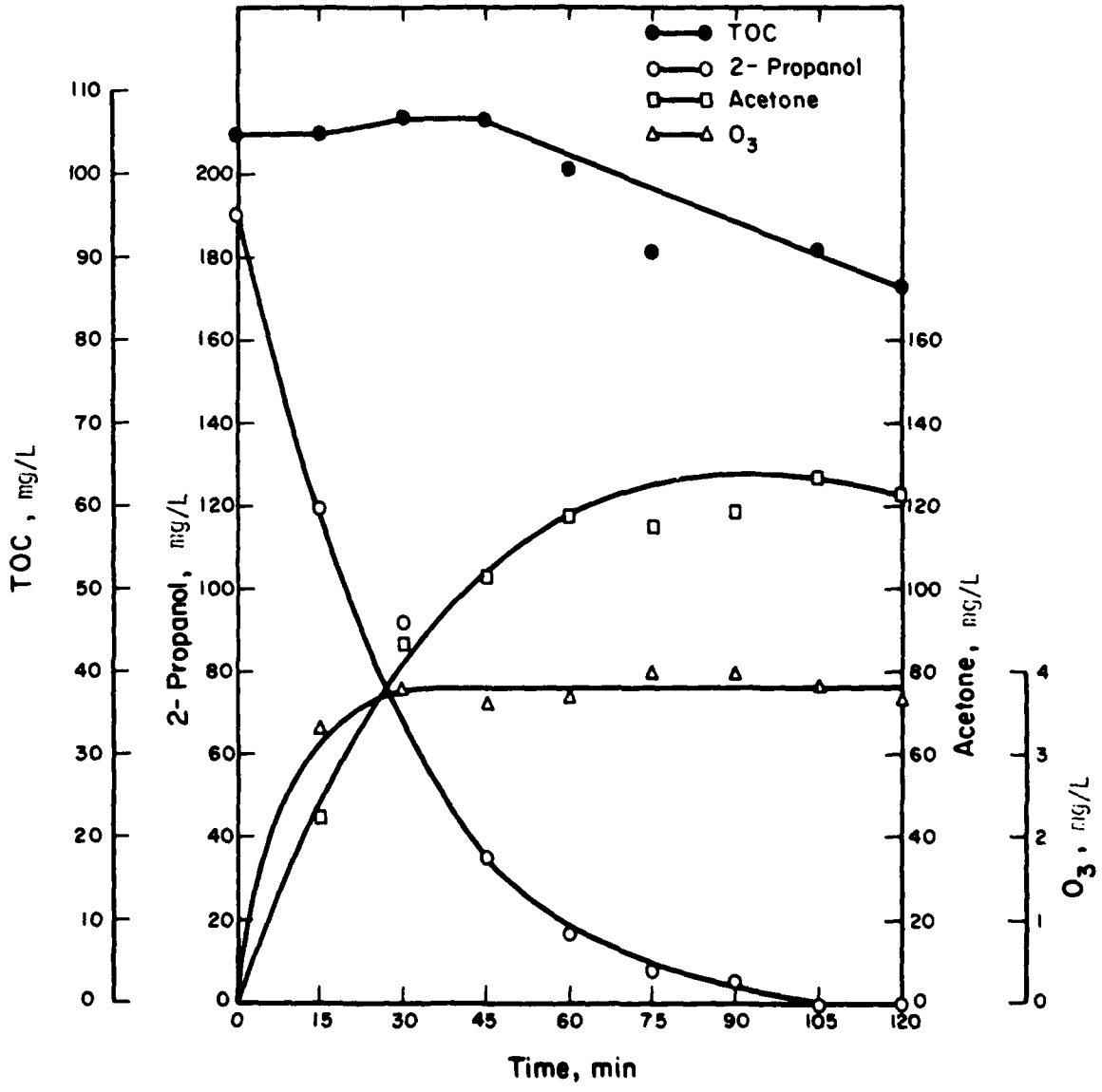

Figure 53. Ozonation of 2-Propanol.

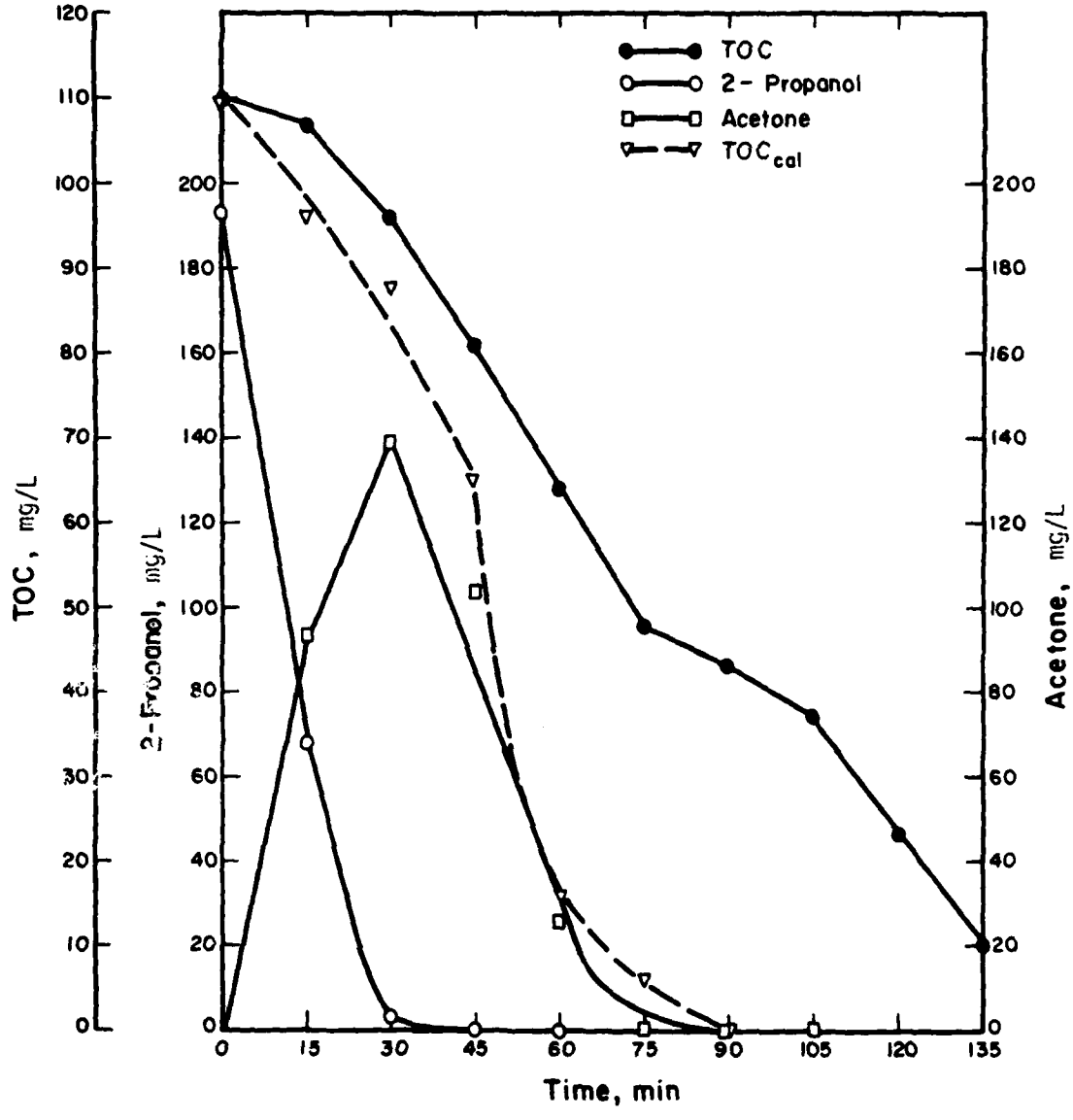

Figure 54. UV-Ozonation of 2-Propanol.

TABLE 44. CONCENTRATION OF DETERMINED ORGANIC COMPOUNDS IN UV-OZONATED ACETONE MIXTURES

Ozonation Time (min)	Concentration of Organic Carbon (mg/L)						
	Acetone	Formaldehyde	Formic	Acetic	Oxalic	ΣO.C.[a]	TOC[b]
0	65.7	-	-	-	-	65.7	66
30	18.8	1.6	0.7	8.5	1.5	31.1	49
60	2.5	0.5	0.2	5.9	7.1	16.2	29

a. Sum of concentration of organic carbon (ΣO.C.) of determined organic compounds.
b. Total organic carbon (TOC) of ozonation mixtures determined on TOC analyzer.

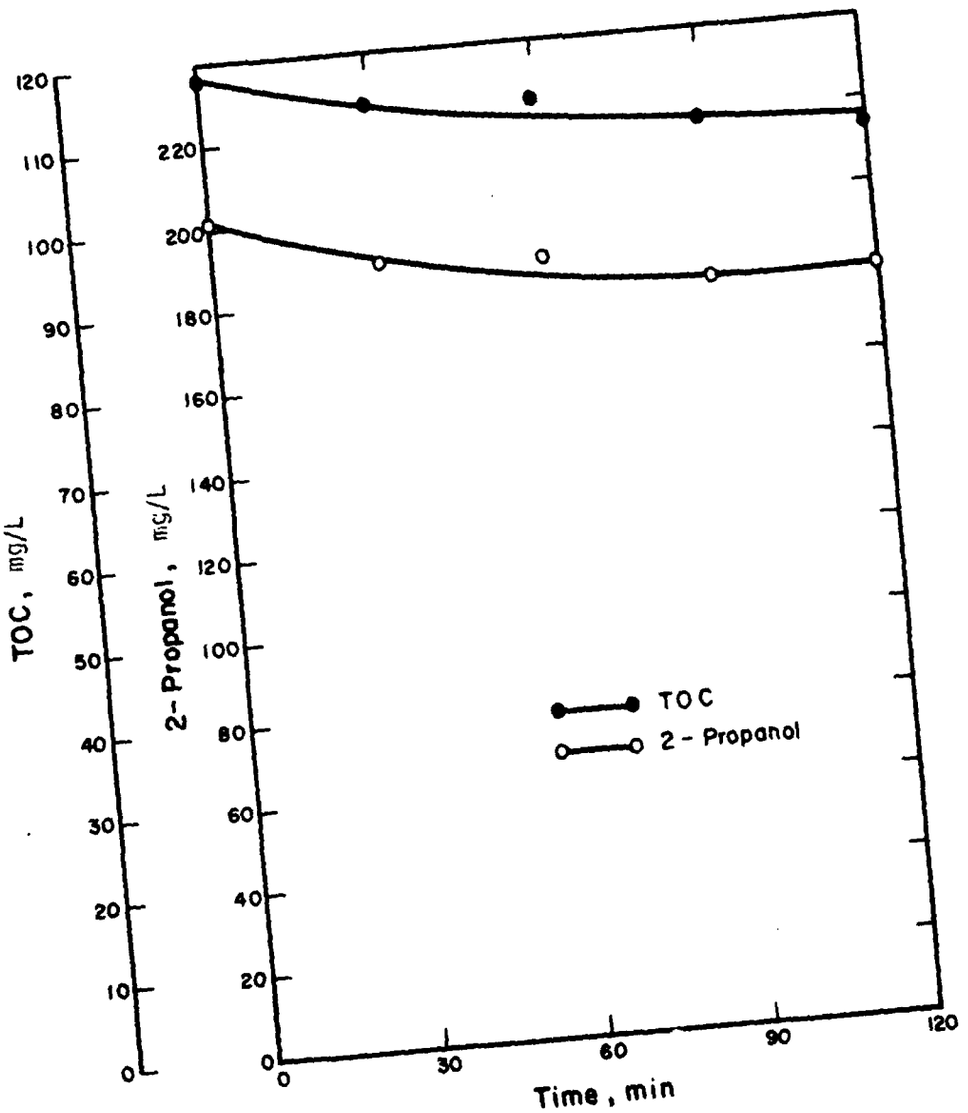

Figure 55. Oxygen Stripping of 2-Propanol.

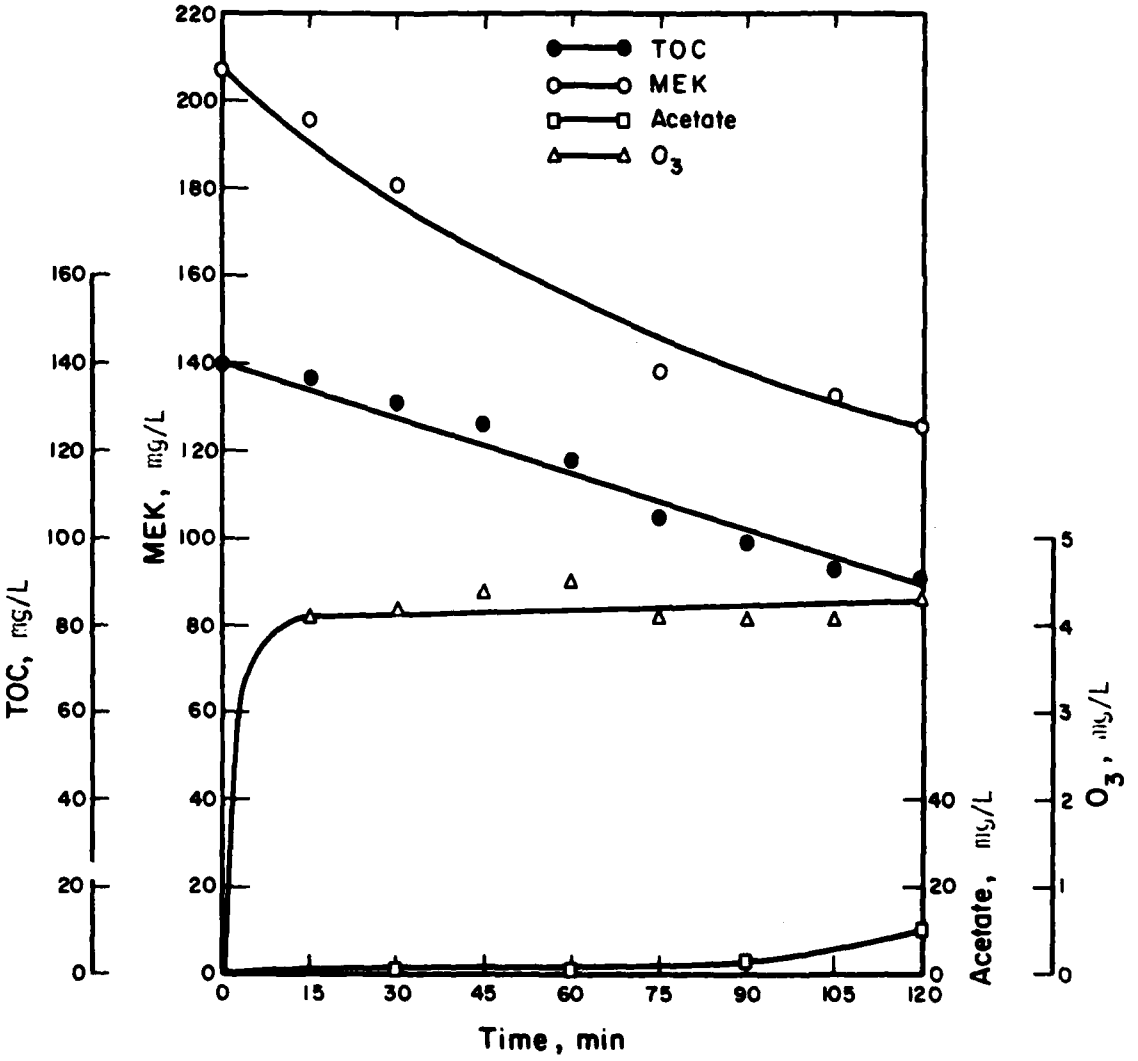

Figure 56. Ozonation of Methyl Ethyl Ketone.

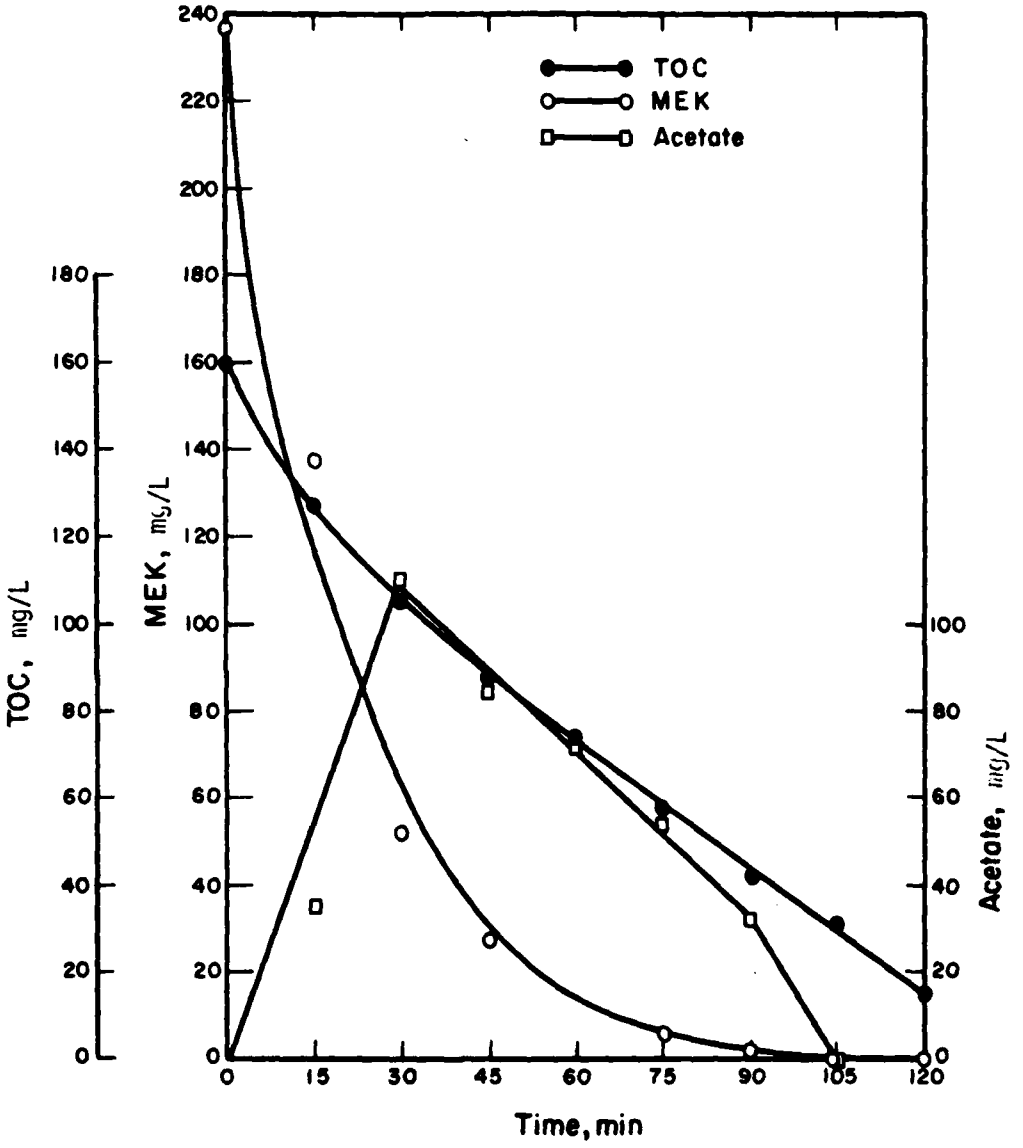

Figure 57. UV-Ozonation of Methyl Ethyl Ketone.

and ethanol were also detected by using the alcohol column. The amount of TOC not identified may have been in the degradation products resulting from further oxidation of acetate, including compounds such as glyoxylate and oxalate.

Ozonation and UV-Ozonation of Acetic Acid

Ozonation of acetic acid was conducted at 25°C. An initial pH of 7 was obtained by adding NaOH solution, but no further pH adjustment was made during the experiment. The pH of the ozonated solution was therefore always higher than 7, implying that ozonation was actually carried on acetate instead of acetic acid.

Ozonation of sodium acetate resulted in a 14% removal of TOC (Figure 58). Glyoxylate as determined by a colorimetric method (Kramer et al., 1959) was found to increase as time increased; nevertheless, it was at a very low concentration. Except for the last sample, the TOC calculated from acetate accounted for over 90% of the TOC present. The observed 14% removal of TOC probably resulted from the oxidation of the intermediate products produced by the ozonation of acetate.

UV-ozonation of acetate substantially improved the TOC removal. No acetate was found after 75 minutes of reaction (Figure 59). Glyoxylate at lower concentrations than those found in the previous ozonation run remained at a fairly constant level during the first hour of UV-ozonation reaction. After that, it disappeared. No alcohols or monocarboxylic acids other than acetate were detected by the use of the alcohol column and the acid column. Therefore, the discrepancy between the observed and the calculated TOC could only be attributed to the presence of formate and/or oxylate. It was first thought that formate was the degradation product of acetate. However, after converting organic acids to benzyl esters followed by GC determination (Bethge and Lindstrom, 1974), no benzyl formate was found. It was therefore suspected that oxalate was the degradation product. Titration of the degradation products by permanganate, a standardization procedure for permanganate solution involving the use of sodium oxalate, as described in Standard Methods (1971), showed that the results thus obtained gave good agreement between the experimentally determined and calculated TOC (Figure 60). A spot test confirmed the presence of oxalate (Feigl and Anger, 1966). Later, oxalate was determined by GC after it was converted to dimethyl oxalate (Webb et al., 1973). The results agreed fairly well with data obtained by the permanganate titration procedure.

Ozonation and UV-Ozonation of Diethyl Ether

Ozonation of diethyl ether was conducted at 25°C and a pH of 9. Ethyl acetate and acetate were the major degradation products, as shown in Figure 61. It was also found that diethyl ether was not completely degraded by ozone. It was quite resistant to degradation at low concentrations, i.e., toward the end of the ozonation process, and a varying small quantity of it was present in solution most of the time. This phenomenon was also observed in UV-ozonation of diethyl ether. Further studies are needed to confirm this

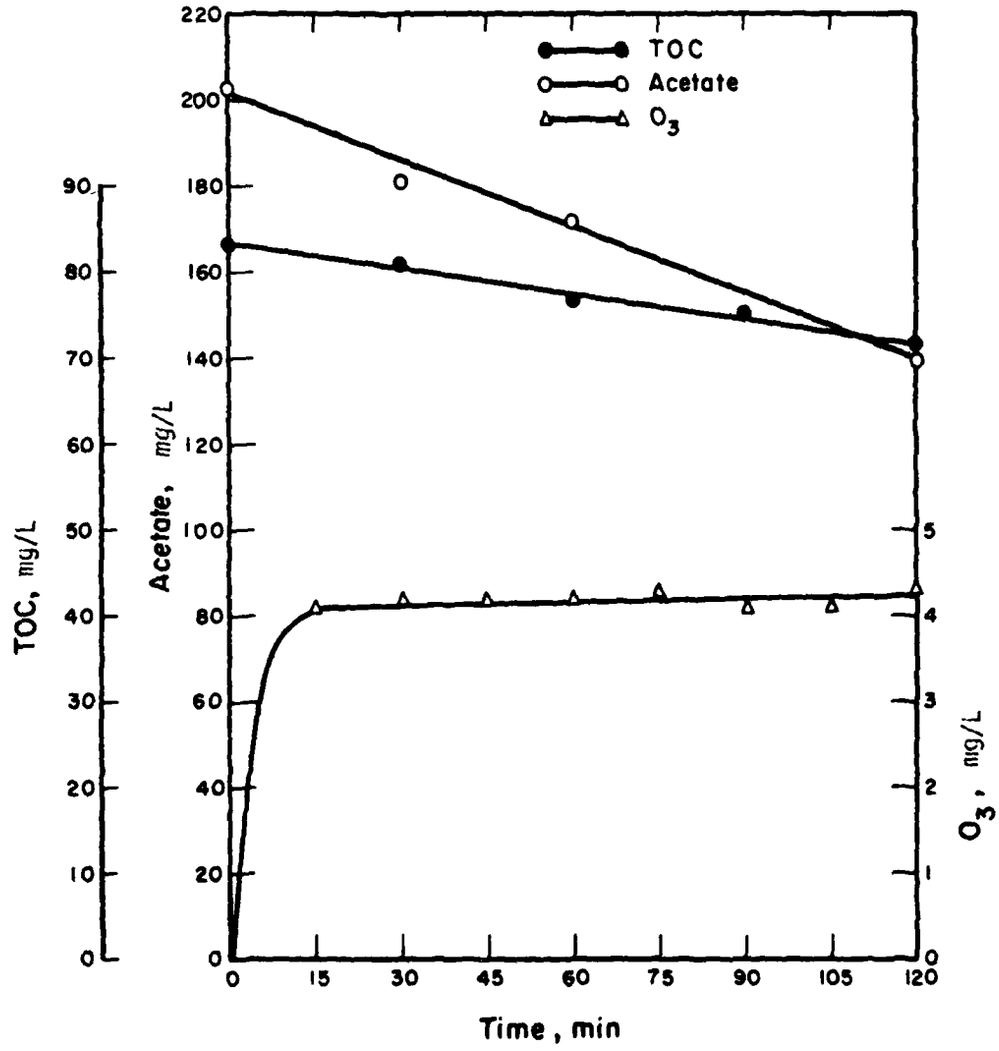

Figure 58. Ozonation of Sodium Acetate.

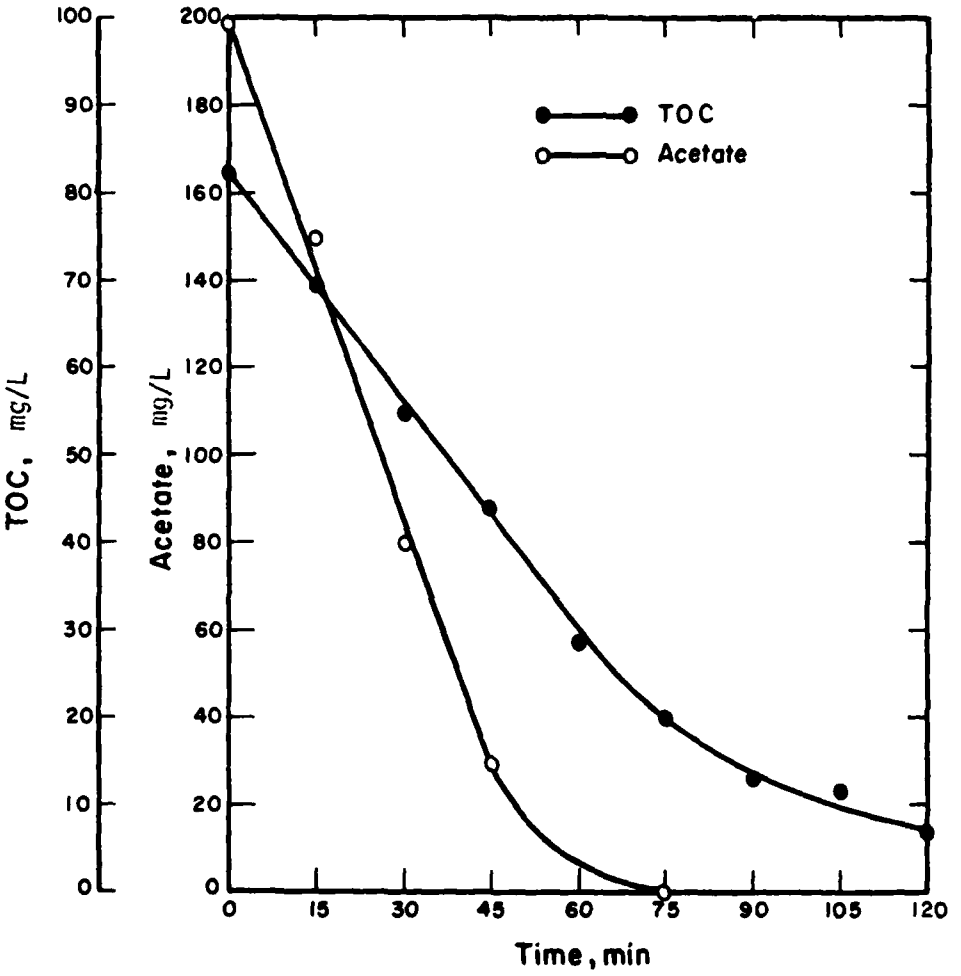

Figure 59. UV-Ozonation of Sodium Acetate.

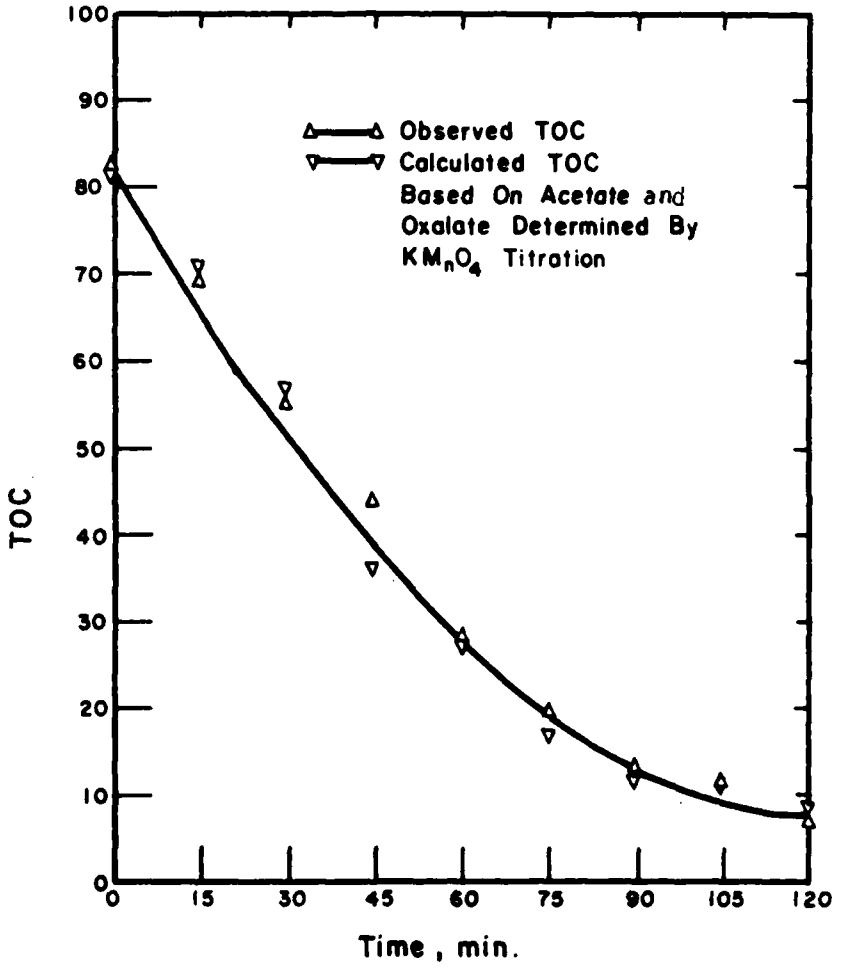

Figure 60. Observed TOC and Calculated TOC in UV-Ozonation of Sodium Acetate.

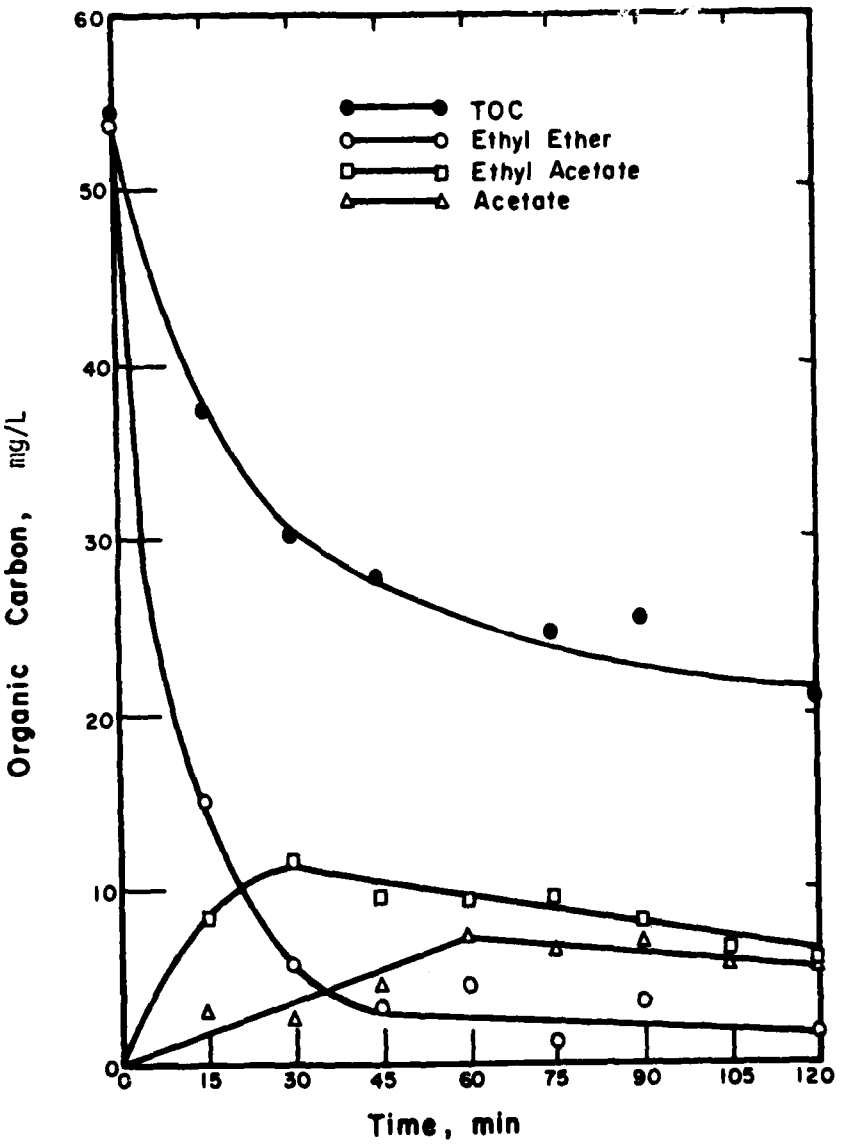

Figure 61. Ozonation of Diethyl Ether.

observation before an explanation can be given. Other degradation products present in small concentrations include acetaldehyde, methyl formate, ethanol, acetone, and ethyl formate. These results are reported in Table 45. An overall TOC removal of 61% was obtained in the run. Two different TOC removal rates were observed. The lower rate occurred during the later stages when ethyl acetate and acetate were the major components of the organic carbon. The initial higher rate may be due to the stripping of diethyl ether and the degradation products such as acetaldehyde, ethanol, and acetone. Good agreement between the experimentally determined TOC and the calculated TOC indicates that all the major degradation products have been accounted for (Figure 62).

UV-ozonation of diethyl ether resulted in a much greater TOC removal (94%) than ozonation alone (Figure 63), because of the further oxidation of ethyl acetate and acetate to CO_2 in the presence of UV irradiation. It appears that the formation of acetate followed two pathways, one from ethyl ether directly and the other from ethyl acetate. The latter is of interest and deserved further study. Other degradation products in the UV-ozonation of diethyl ether are reported in Table 46. None of these products were present in significant amounts. Good agreement between the observed and calculated TOC's is also demonstrated in Figure 64.

It was suspected that the UV-ozone degradation pathway of acetate was through glyoxylate and oxalate to CO_2. This mechanism was observed in this study by quantitative determination of oxalate and glyoxylate for the acetate runs. A similar result was obtained in the diethyl ether run, in that the acetate concentration decreased to zero while the oxalate concentration reached its maximum. That glyoxylate was found at a low concentration suggests that its degradation is not the rate-determining step in TOC removal. Since the amount of oxalate formed was not equal to the amount of acetate present, it is possible that glyoxylate, the precursor of oxalate, can be oxidized to CO_2 directly.

Ozonation and UV-Ozonation of o-Toluidine

Ozonation of o-toluidine performed at 25°C and a pH of 9 resulted in a 42% removal of TOC, as shown in Figure 65. No o-toluidine was detected after 15 minutes of reaction. Acetate was found presented at about 10 ppm as carbon and only gradually decreased as the reaction went on. Oxalate was found to be present in concentrations somewhat higher than that of acetate, indicating that its formation was probably via more than one route. Glyoxylate was present in low concentrations, as reported in Table 47. Oxalate appears to be rather ozone resistant. This aspect of oxalate deserves to be studied in the future.

Two distinctly different zero-order TOC removal rates were demonstrated in UV-ozonation of o-toluidine (Figure 66). The cause of this phenomenon is not understood at present. In the first 15 minutes of reaction, o-toluidine disappeared completely. The formation of acetate and oxalate during the initial stages was observed, but neither substance was present after 75 minutes of reaction. Glyoxylate was found in trace amounts as shown in Table 47.

TABLE 45. DEGRADATION PRODUCTS OTHER THAN ETHYL ACETATE AND ACETATE IN OZONATION OF DIETHYL ETHER

Ozonation Time (min)	Acetaldehyde mg/L as C	Methyl Formate mg/L as C	Ethanol mg/L as C	Acetone mg/L as C	Ethyl Formate mg/L as C
15	2.2	1.1	2.1	1.1	1.9
30	2.0	0.1	1.7	0.4	0.5
45	1.7	0.4	1.6	0.6	1.0
60	1.6	1.7	1.8	2.2	0.7
75	0.9	0.1	0.8	0.2	2.5
90	0.8	0.6	0.9	0.8	1.1
105	0.5	0.2	0.6	0.6	0.9
120	1.5	1.4	1.1	1.6	1.6

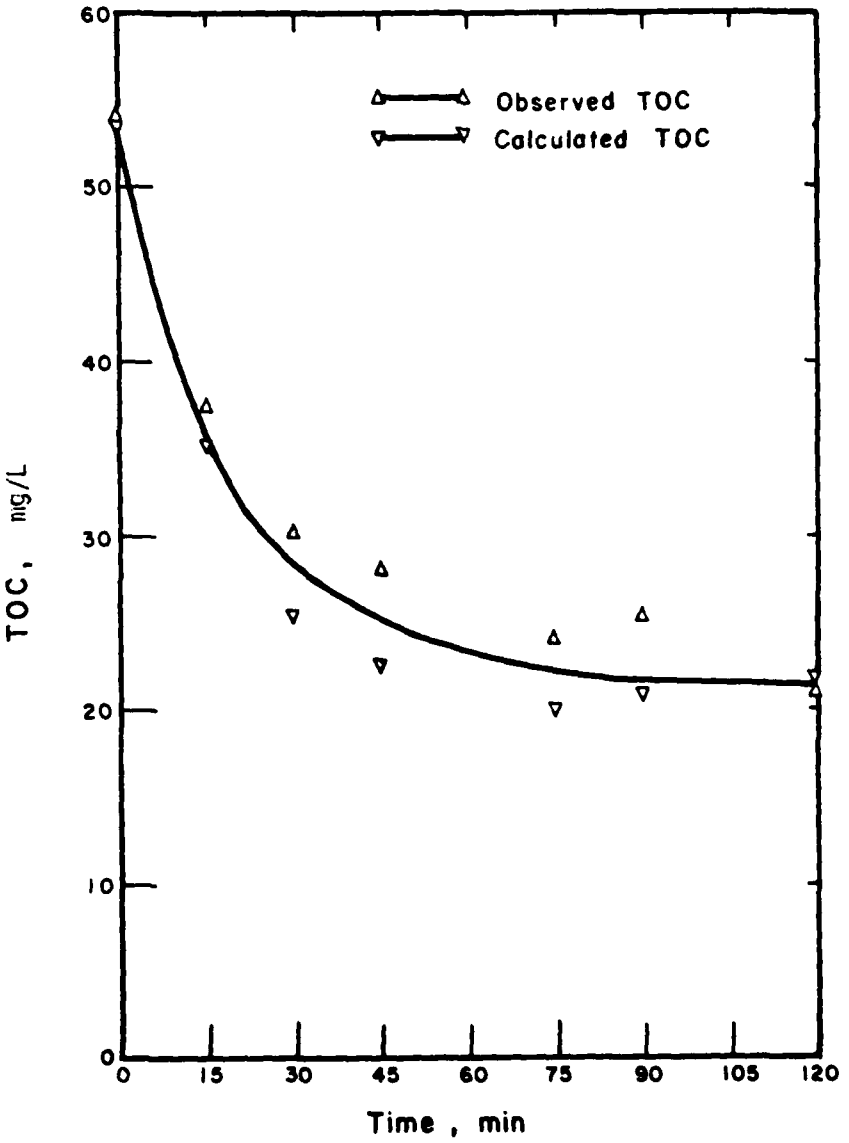

Figure 62. Observed TOC and Calculated TOC in Ozonation of Diethyl Ether.

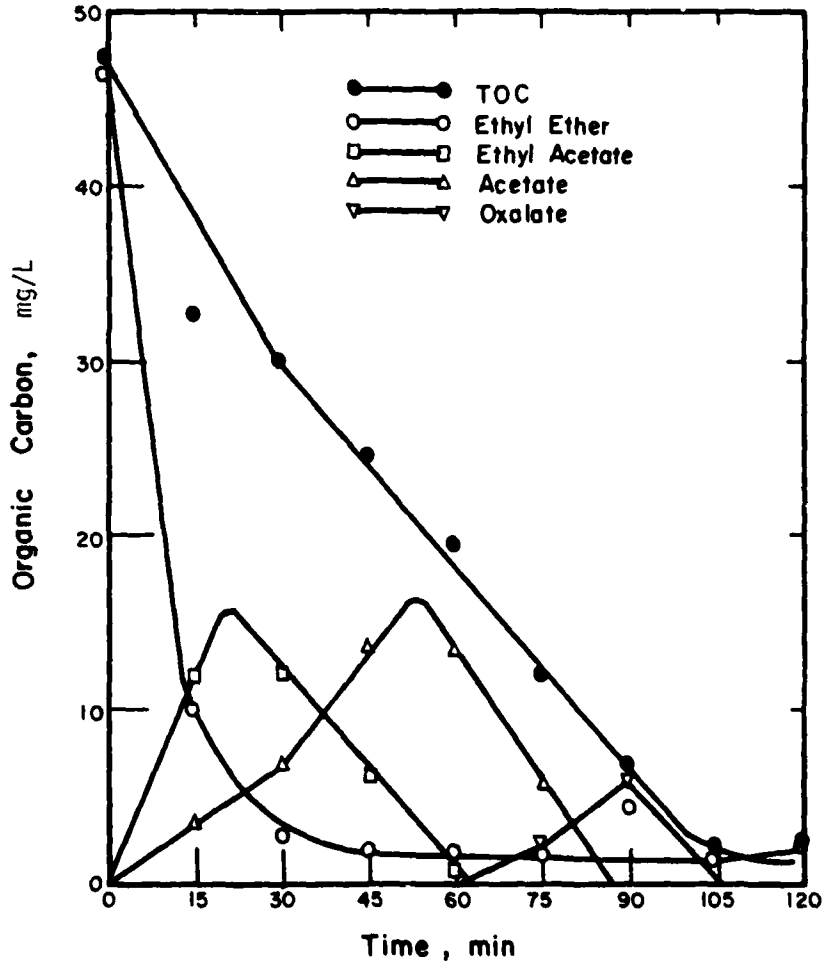

Figure 63. UV-Ozonation of Diethyl Ether.

TABLE 46. DEGRADATION PRODUCTS OTHER THAN ETHYL ACETATE, ACETATE, AND OXALATE IN UV-OZONATION OF DIETHYL ETHER

UV-Ozonation Time (min)	Acetaldehyde mg/L as C	Methyl Formate mg/L as C	Ethanol mg/L as C	Acetone mg/L as C	Ethyl Formate mg/L as C
15	2.2	0.2	1.4	0.4	1.5
30	0.7	0.2	0.7	0.7	1.5
45	0.3	0	0.2	0.3	0.9
60	0.2	0.4	0.3	0.7	0.6
75	0.1	0.1	0.1	0.3	0
90	0	0	0.3	0.4	0
105	0	0.2	0.2	0.4	0.2
120	0	0.2	0.2	0.6	0.3

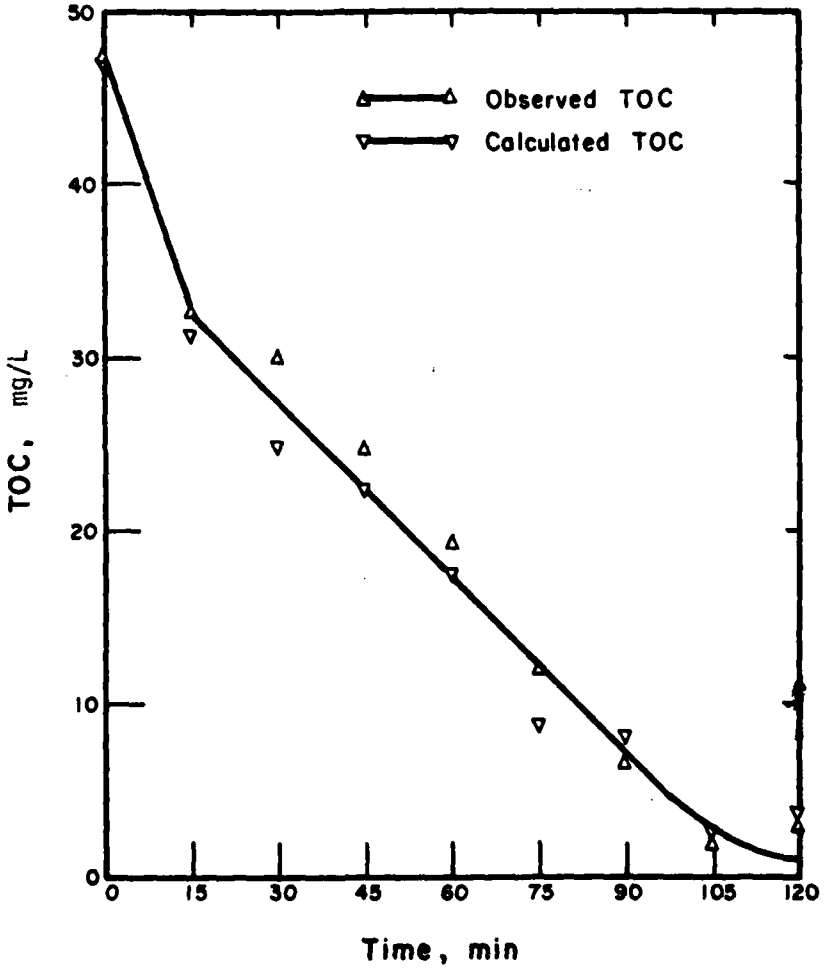

Figure 64. Observed TOC and Calculated TOC in UV-Ozonation of Diethyl Ether.

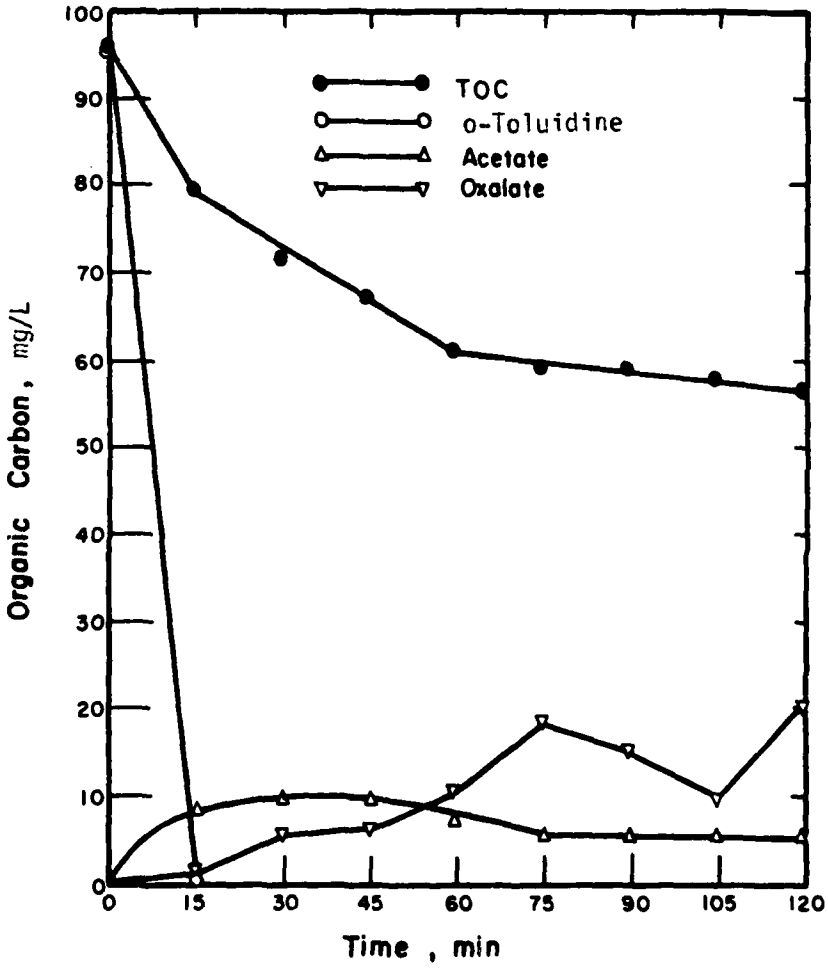

Figure 65. Ozonation of o-Toluidire.

TABLE 47. GLYOXYLATE IN OZONATION AND UV-OZONATION OF o-TOLUIDINE

Time (min)	Glyoxylate (mg/L)	
	Ozonation	UV-Ozonation
30	5.0	3.5
45	2.9	0.8
60	2.5	0.5
75	2.0	-
90	2.0	0.6
105	2.6	0.5
120	1.9	0

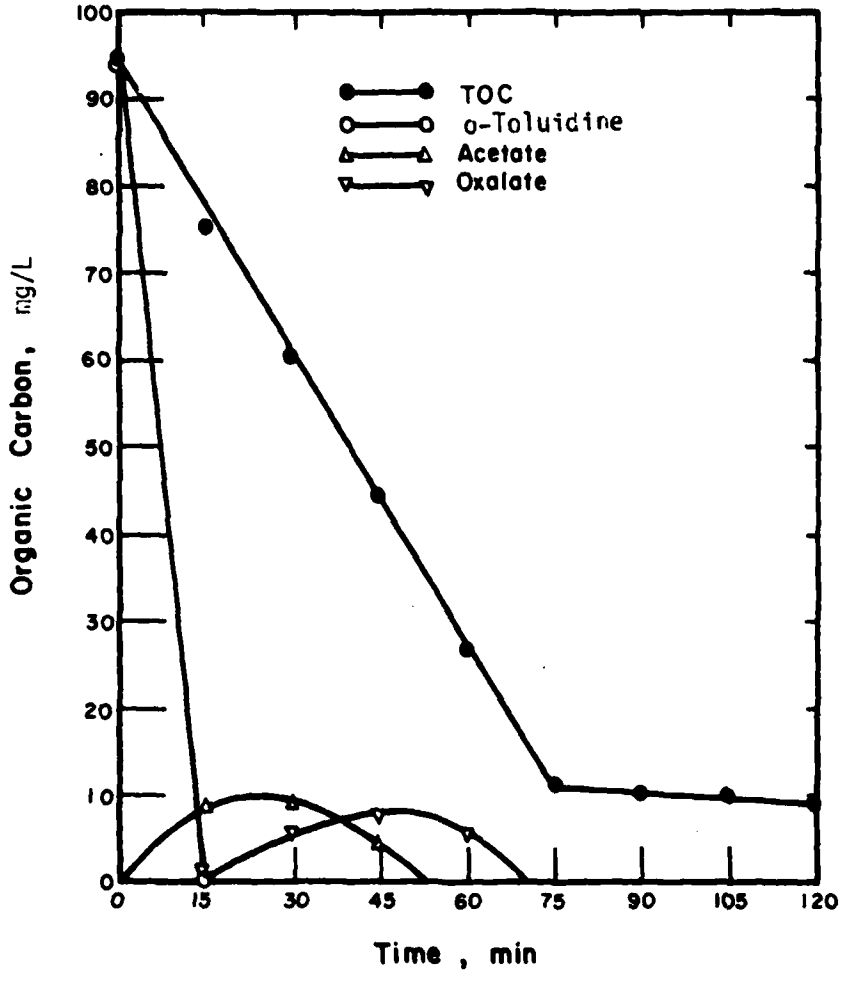

Figure 66. UV-Ozonation of o-Toluidine.

An appreciable amount of organic carbon was not accounted for in both ozonation and UV-ozonation of o-toluidine. Glyoxal is excluded from being an important component because it would be present in significant amounts only in the first 15 minutes or so under the reaction conditions (Gould and Weber, 1976). Cleavage of the benzene ring appears to be the major mechanism by which o-toluidine disappears, as no aromatic compounds were detected by GC using a Tenax-GC column or by UV-adsorption from 210 to 270 nm. The use of the alcohol column and acid column failed to show the presence of volatile aldehydes, ketones, esters, and carboxylic acids. Therefore, the unaccounted organics are likely of aliphatic amino compounds.

A nitrogen balance was attempted. However, determination of total Kjeldahl nitrogen suffered from the small sample volume, and the nitrogen balance was therefore not carried out. Determination of nitrate-nitrogen was conducted according to Standard Methods (1971) with the assumption that nitrate concentration was negligible for a system in such a high oxidation state. It is understood that the method of correction for dissolved organics may not be applicable; nevertheless, the results thus obtained indicate a general trend of nitrate concentration in the samples (Table 48). The final nitrate-nitrogen accounted for approximately 34 and 40% of the initial nitrogen present in ozonation and UV-ozonation runs, respectively. The nitrogen not accounted for is probably present as organic nitrogen and/or stripped off as NH_3.

TABLE 48. NITRATE-NITROGEN IN OZONATION AND UV-OZONATION OF o-TOLUIDINE

Time (min)	NO_3-N (mg/L)	
	Ozonation	UV-Ozonation
15	3.6	2.4
30	3.8	4.0
45	4.7	5.0
60	5.0	4.6
75	5.2	4.6
90	5.3	5.4
105	5.2	5.8
120	5.4	6.2

Ozonation and UV-Ozonation of Methanol

Ozonation of methanol was conducted at 25°C and a pH of 9. Formaldehyde and formic acid were the only two ozonation products identified. They and the residual methanol do not account fully for the total organic carbon through the ozonation course (Figure 67). This result is entirely unexpected if one assumes that the oxidation course simply followed the path from methanol to formaldehyde to formic to carbon dioxide. The percent organic removal after 2 hours of ozonation was about 72%. Organic removal seemed to be retarded after 75 minutes of ozonation. Organic carbon not accounted for might result from the presence of certain refractory compounds formed during the early stage of ozonation and accumulated toward the latter stage. Leaching of organic compounds from the Plexiglas reactor might be another source of such organics. The same situation was encountered in the UV-ozonation of methanol (Figure 68). The application of UV irradiation to enhance organic removal was not at all effective.

To eliminate possible leaching of organics from the reactor, an all-glass reactor will be used in the later study. Ozonation and UV-ozonation of methanol, formaldehyde, and formic acid will be examined in greater detail to determine the effect of UV irradiation and the ozonation course.

Ozonation and UV-Ozonation of N,N-Diethyl-m-Toluamide

Ozonation of N,N-diethyl-m-toluamide (DEET) was conducted at 25°C and a pH of 9. No DEET and other aromatic compounds were detected after 15 minutes of ozonation (Figure 69). Formic, acetic, and oxalic acids were formed during the course of ozonation. The formation of formic and oxalic acids is believed to be because of the breakdown of the benzene ring. In addition, further ozonation of acetic acid will produce oxalic acids. The breakdown of amide and/or amine seems the major cause of forming acetic acid. Acetic acid could also be formed because of the ozonation of a-keto-propionic acid, which is very likely present in the reaction mixture.

A similar result was observed for UV-ozonation of DEET (Figure 70), but acetic and oxalic acids were further oxidized toward the end of ozonation period, causing their concentrations to decrease. The fact that a valley was observed for formic acid at 90 minutes indicates that the mechanism for formic acid formation is rather complicated. It might involve two pathways. One route is predominant during the early stage of ozonation. It, however, becomes immaterial and the other route becomes predominant during the later stage of ozonation. The total organic carbon (TOC) can be fully accounted for after 105 minutes of UV-ozonation.

Nitrate nitrogen was also determined. The result shows that 45% of DEET nitrogen was oxidized to nitrate at the end of UV-ozonation. The nitrogen not accounted for was probably stripped off as NH_3. It was also found that 46% of DEET nitrogen was converted to nitrate at the end of ozonation. In addition to the stripped off nitrogen, the nitrogen not accounted for is probably present as organic nitrogen because there was still 12.5% of TOC unaccounted for after 2 hours of ozonation.

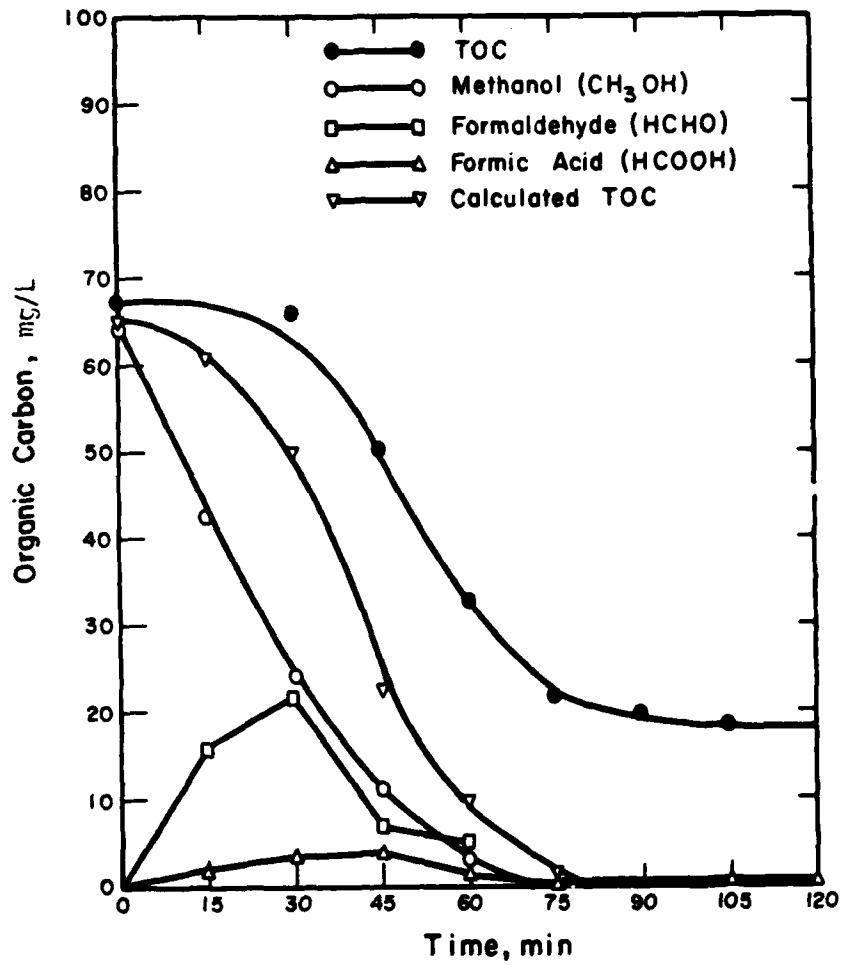

Figure 67. Ozonation of Methanol.

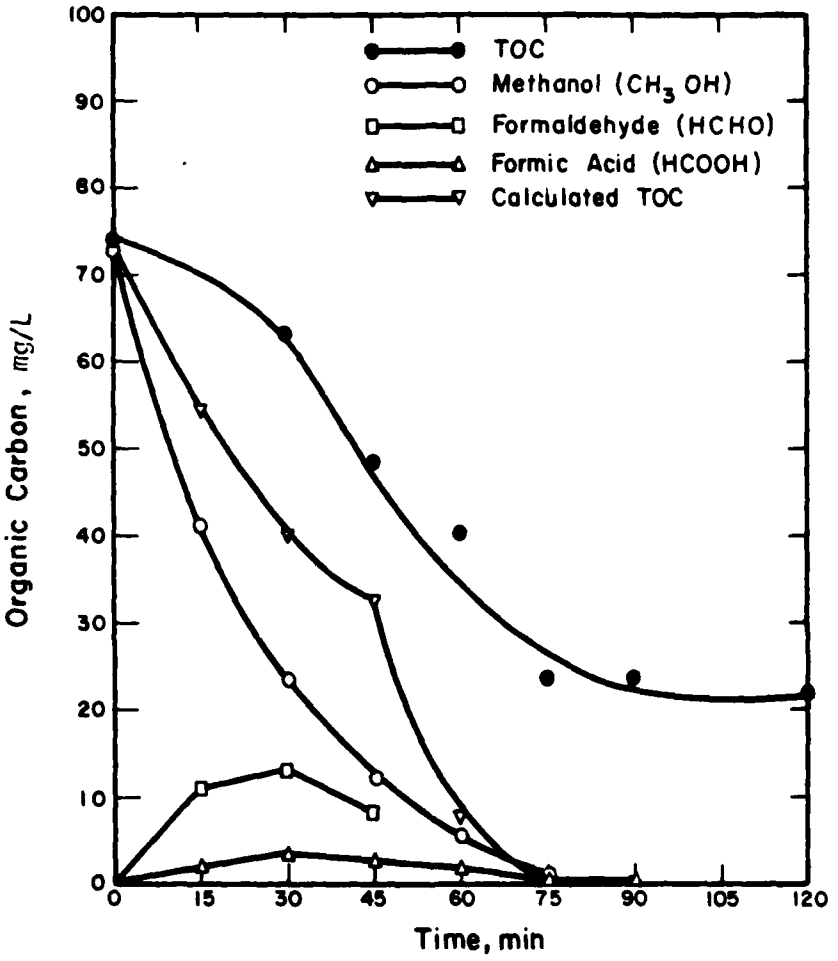

Figure 68. UV-Ozonation of Methanol.

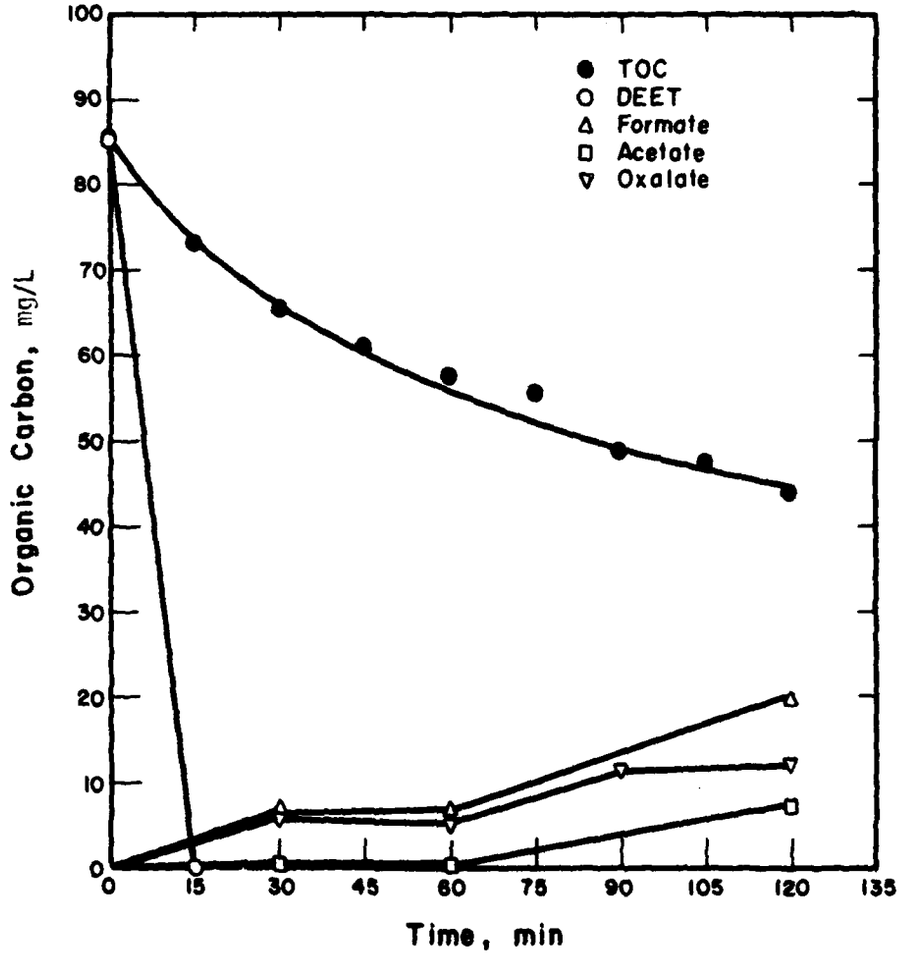

Figure 69. Ozonation of N,N-Diethyl-m-Toluamide.

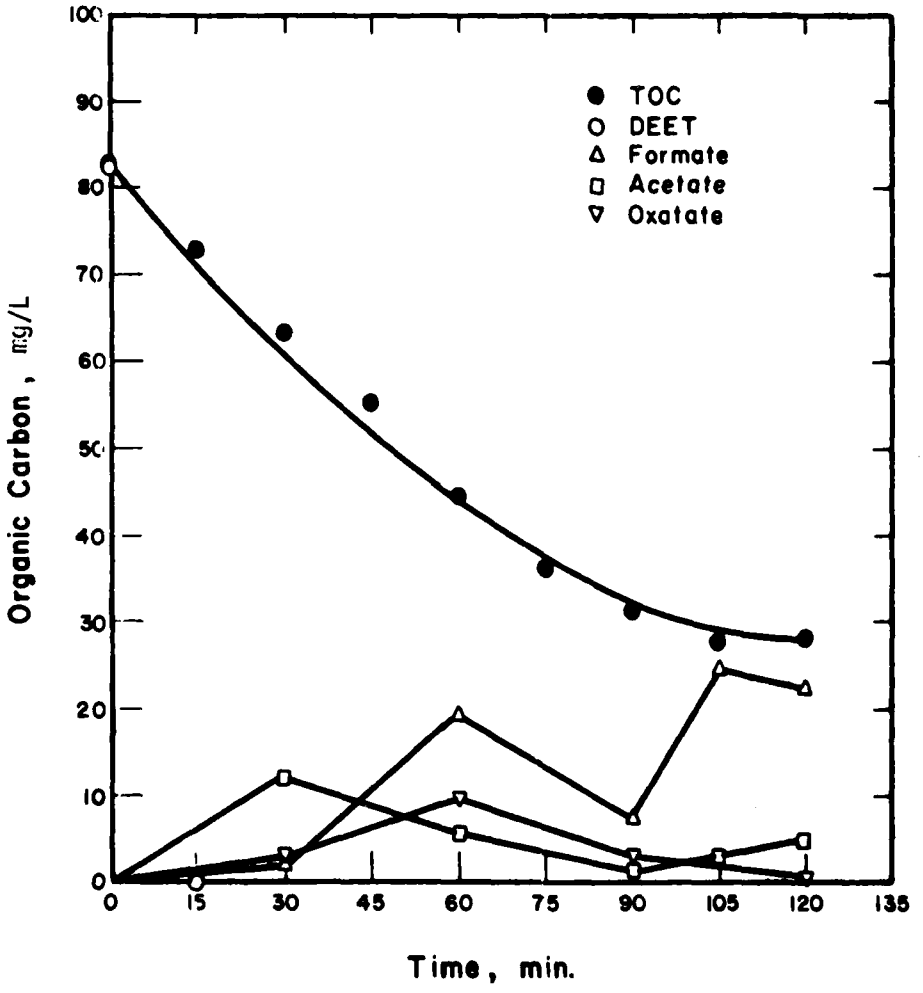

Figure 70. UV-Ozonation of N,N-Diethyl-m-Toluamide.

Summary

Ozonation products for the nine model compounds studied are listed in Table 49. Formic, glyoxylic, oxalic, and acetic acids were found to be the major end products. The oxidation of the first three acids to carbon dioxide is believed to be responsible for the organic removal by ozonation. Also, organic carbon might be removed through the direct formation of carbonate ions during the cleavage of molecules. Acetic acid was oxidized through ω-oxidation to yield glyoxylic acid, and further ozonation of glyoxylic acid caused either direct oxidation to carbon dioxide or the formation of oxalic acid (Gilbert, 1975). The depletion rate of glyoxylic acid appeared to be very rapid because no substantial amounts of glyoxylic acid were detected in any of the ozonation mixtures. Glyoxylic and oxalic acids can be formed directly through the breakdown of large molecules, particularly in the ozonation of aromatic compounds (Gould and Weber, 1976). Acetaldehyde, ethanol, ethyl acetate, diethyl ether, and MEK were found to be the precursors of acetic acid. Formation of formic acid occurs through the breakdown of large molecules as well as from oxidation of formaldehyde and methanol. The ozonation of o-toluidine and DEET produced a very complex mixture. In fact, only acetic and oxalic acids were detected. The cleavage of the benzene ring was very rapid even without UV irradiation, as was observed in this study and by Gould and Weber (1976). Reaction products derived from the ozonation of diethyl ether can be reasonably predicted according to the mechanism proposed by Price and Tumolo (1964).

An attempt was made to determine the reaction order and rate constant for the removal of organics and reactants by ozonation, but without correction for stripping effect. The results are presented in Table 50. As for reactant removal, only the initial reaction order and rate constant were estimated. The reaction rate can be determined from the product of the rate constant and the substrate concentration for first-order reaction kinetics and from the rate constant for the zero-order reaction kinetics. As can be noticed from Table 50, the reactant removal rate is faster under UV irradiation for MEK and acetic acid. This result might indicate that UV light enhances ozonation reactions by exciting the carbonyl group, resulting in easy oxidation of α-carbon. Methanol and diethyl ether exhibited reactant removal rates of approximately the same magnitude, but without apparent UV enhancement. For 2-propanol, the UV effect on the reactant removal rate was slightly better than for diethyl ether.

The removal of organic carbon by ozonation followed either pseudo first- or zero-order reaction kinetics with respect to the substrate concentration. Applying UV light during ozonation increased the first-order reaction rate constant by approximately one order of magnitude compared to the rate without UV irradiation, which is on the order of -3. It was observed that ozonation of diethyl ether, o-toluidine, and methanol followed multiple reaction rates, illustrating the existence of different removal steps by the ozonation process. In such cases, later ones usually proceeded at a slower rate with the exception of methanol, which started at a slower rate for the first

TABLE 49. OZONATION PRODUCTS

Reactant	Ozonation Products[a]	
	Major	Minor
n-Propanol	Propionaldehyde	
Propionic Acid[b]		
2-Propanol	Acetone	
Methyl Ethyl Ketone (MEK)	Acetate	Acetone, Ethanol
Acetic Acid	Oxalic Acid	Glyoxylic Acid
Diethyl Ether	Ethyl Acetate, Acetate	Acetaldehyde, Methyl Formate, Ethanol, Acetone, Ethyl Formate
o-Toluidine	Acetic Acid, Oxalic Acid	
Methanol	Formaldehyde, Formic Acid	
N,N-Diethyl-m-Toluamide (DEET)	Formic Acid, Acetic Acid, Oxalic Acid	

a. Ozonation products were monitored during the 2-hr ozonation period.
b. No attempts were made to determine ozonation products except for acetic acid and alcohols.

TABLE 50. ORGANIC REMOVAL BY OZONATION[a]

Reactant	Ozonation Time pH	hr	UV	Initial Concentration Organic Carbon (mg/L)	Percent Organic Removal[b]	Organic Removal Order	Period (min)	Rate Constant[c,d]	Reactant Removal Order	Period (min)	Rate Constant[e]
n-Propanol[f]	9	1	no	254	8						
			yes	255	12						
Propionic Acid[f]	9	2	no	233	15						
			yes	235	22						
2-Propanol	7	2	no	114	17	1st	0-120	1.66×10^{-3}	1st	0-90	1.35×10^{-2}
			yes	116	82	1st	30-105	1.29×10^{-2}	0	0-15	5.00
MEK	7	2	no	140	40	1st	0-120	3.50×10^{-3}	1st	0-120	2.72×10^{-3}
			yes	156	91	1st	0-75	1.34×10^{-2}	1st	0-90	2.46×10^{-2}
Acetic Acid	7[g]	2	no	84	14	1st	0-120	1.52×10^{-3}	1st	0-120	3.23×10^{-3}
			yes	83	92	0	0-60	0.892	0	0-60	1.17
Diethyl Ether	9	2	no	52	61	1st	0-30	1.82×10^{-2}			
						1st	30-120	4.23×10^{-3}	1st	0-30	7.37×10^{-2}
			yes	48	94	0	0-30	0.583			
						0	30-90	0.383	1st	0-30	9.68×10^{-2}
o-Toluidine	9	2	no	92	42	0	0-15	1.11			
						0	15-60	0.411			
						0	60-120	0.075			
			yes	94	91	0	0-75	1.10			
						0	75-120	0.056			
Methanol	9	2	no	66	72	1st	0-30	2.02×10^{-4}			
						1st	30-75	2.32×10^{-2}	1st	15-45	4.64×10^{-2}
						1st	75-105	7.91×10^{-3}			
			yes	74	71	1st	0-30	3.91×10^{-3}			
						1st	30-90	1.72×10^{-2}	1st	0-60	4.05×10^{-2}
						1st	90-120	2.20×10^{-3}			
DEET	9	2	no	83	48	1st	0-90	5.86×10^{-2}			
			yes	87	66	1st	0-90	1.11×10^{-2}			

a. Ozonation was performed at a constant 25°C, and the dissolved ozone concentration was about 4 mg/L.
b. Percent organic removal was calculated for the entire ozonation period.
c. First-order rate constant is in min^{-1}; zero order rate constant is in (mg org. carbon)/ (L x min).
d. The reaction rate is equal to the rate constant in zero order reactions and to the product of the rate constant and the reactant concentration in first-order reactions regardless of sign.
e. Initial reaction rate constant.
f. Reactions were mass-transfer limited.
g. Initial pH.

AD-A111 391 ILLINOIS UNIV AT URBANA F/G 13/2
FUNDAMENTAL STUDY ON THE OZONE POSTTREATMENT OF REVERSE OSMOSIS--ETC(U)
MAR 81 E S CHIAN, P P KUO, B J CHANG DAMD17-75-C-5006
UNCLASSIFIED NL

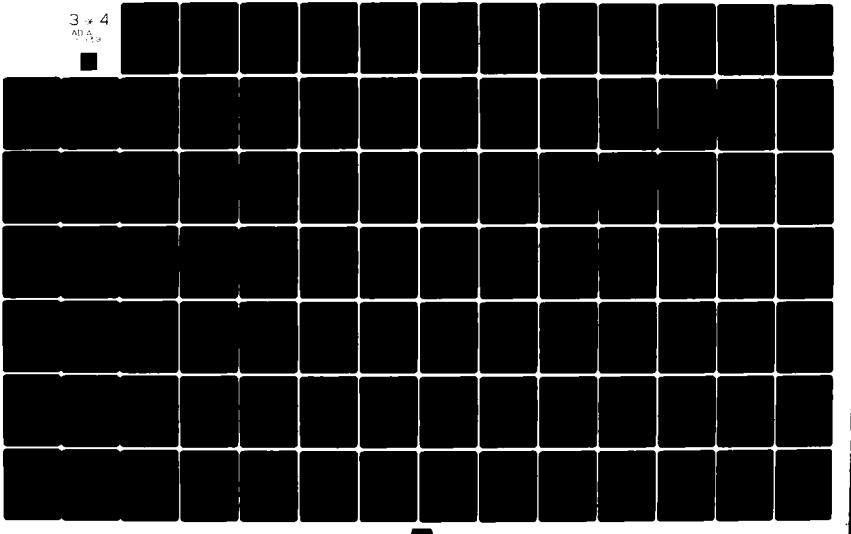

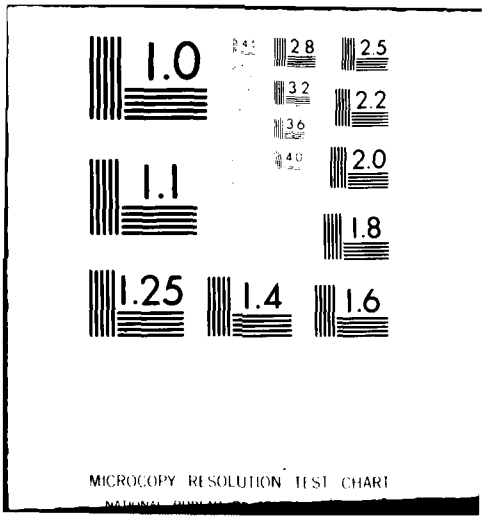
1.0
2.8
2.5
3.2
2.2
3.6
4.0
2.0
1.1
1.8
1.25
1.4
1.6
MICROCOPY RESOLUTION TEST CHART

30 minutes. The fact that formaldehyde and formic acid were formed to a maximum after 30 minutes of ozonation and are removed more easily than methanol may explain the slow start. The effect of UV irradiation on the organic removal rate during the ozonation of o-toluidine was not apparent for the first 15 minutes and last 45 minutes of ozonation. In the case of diethyl ether, the reaction rates with and without UV light were approximately the same for the first 30 minutes of ozonation. After that period, however, the rate was faster with UV irradiation.

In conclusion, it will be necessary to study further the effect of UV irradiation on the ozonation of model compounds of various functional groups and of different carbon numbers within each functional group if UV energy is to be used efficiently. In addition, ozonation of formic, glyoxylic, and oxalic acids should be performed to provide a better understanding of their fates and organic removal.

OZONATION AND UV-OZONATION OF OXALIC ACID AND pH EFFECT

Because oxalic acid is toxic (Gleason et al., 1969) and is a common end product of the ozonation of many organic compounds, as described in the Summary and reported by many investigators (Gould and Weber, 1976; Dobinson, 1959; Gilbert, 1975; Ahmed and Kinney, 1950), the ozonation of this compound was subjected to thorough study under various pH conditions. The rate of removal of oxalic acid was improved substantially under UV irradiation (Figures 71 and 72, Table 51); at a constant pH of 5, the initial removal rate was enhanced by a factor of 11. It was also observed that the removal of oxalic acid was more rapid under an acidic condition (Table 51). Accumulation of inorganic carbon in reaction mixtures at a high pH appeared to retard the ozonation reaction of oxalic acid to carbon dioxide. This finding is supported by the high concentration of inorganic carbon detected in the reaction mixture at a pH of 9 (Figure 73). The reaction rate did not vary significantly when the pH of the solution was controlled between 7 and 9 because of the stability of the bicarbonate species present within this pH range. If, however, the pH of solution is lowered to less than the pH value of 6.3 (e.g., to 5), most of the bicarbonate will be present in the unstable carbonic acid, resulting in a substantial improvement in the reaction rate. The pseudo first-order reaction rate constant was increased by a factor of 4 because of the removal of carbon dioxide by ozone gas stripping under an acidic condition. Thus, for efficient removal of TOC from water using UV-ozonation, the pH of the solution should be adjusted to less than 6.3 at the end of the reaction period when oxalic acid is the predominant species in the reaction mixture.

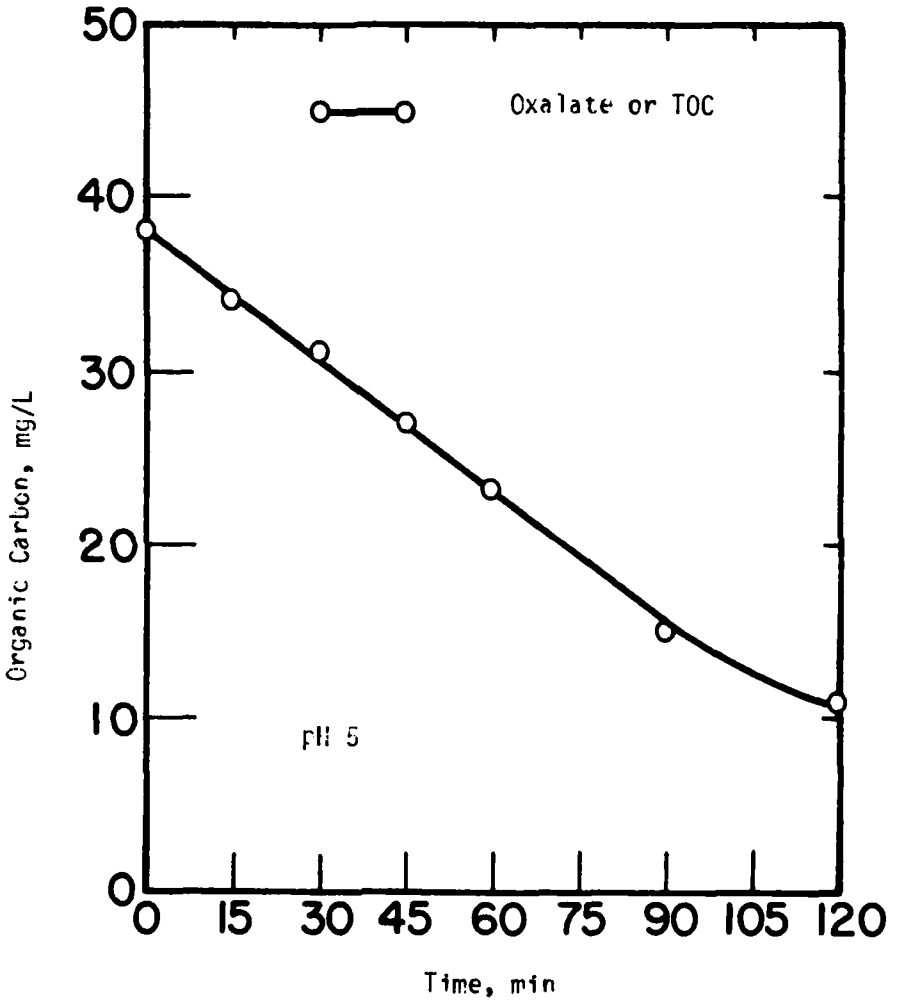

Figure 71. UV-Ozonation of Oxalic Acid.

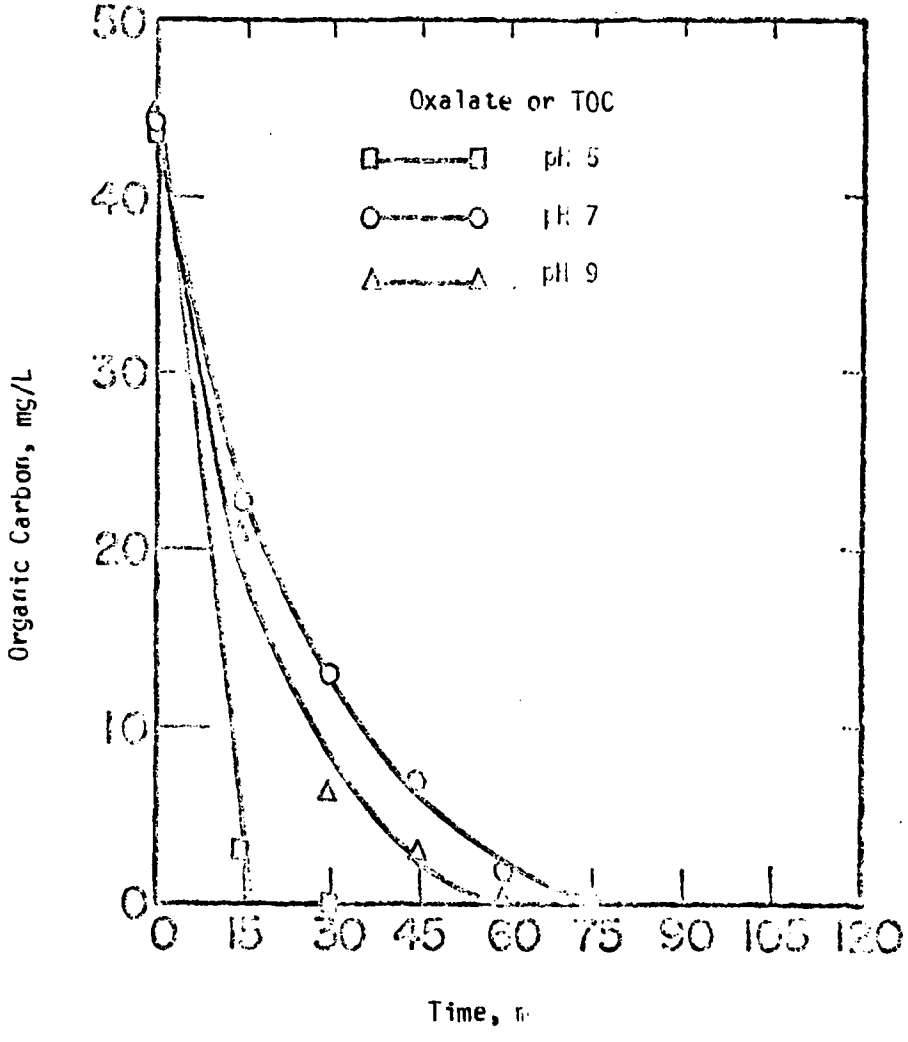

Figure 72. UV-Ozonation of Oxalic Acid.

TABLE 51. ORGANIC REMOVAL BY OZONATION AND UV-OZONATION OF OXALIC ACID AT VARIOUS pH

pH	5	7	9	5
UV[a]	yes	yes	yes	no
Initial TOC, mg/L	44	44	44	38
% TOC Removal				
1-hr ozonation	100	95	98	39
2-hr ozonation	100	100	100	71
Oxalic or TOC Removal[b]				
Order	1st	1st	1st	0
Period, min	0-30	0-45	0-60	0-90
Rate Constant	0.179 min^{-1}	4.09×10^{-2} min^{-1}	6.15×10^{-2} min^{-1}	0.250 mg/L-min

a. New UV lamp.
b. Organic carbon of reaction mixtures was fully accounted for by oxalic acid.

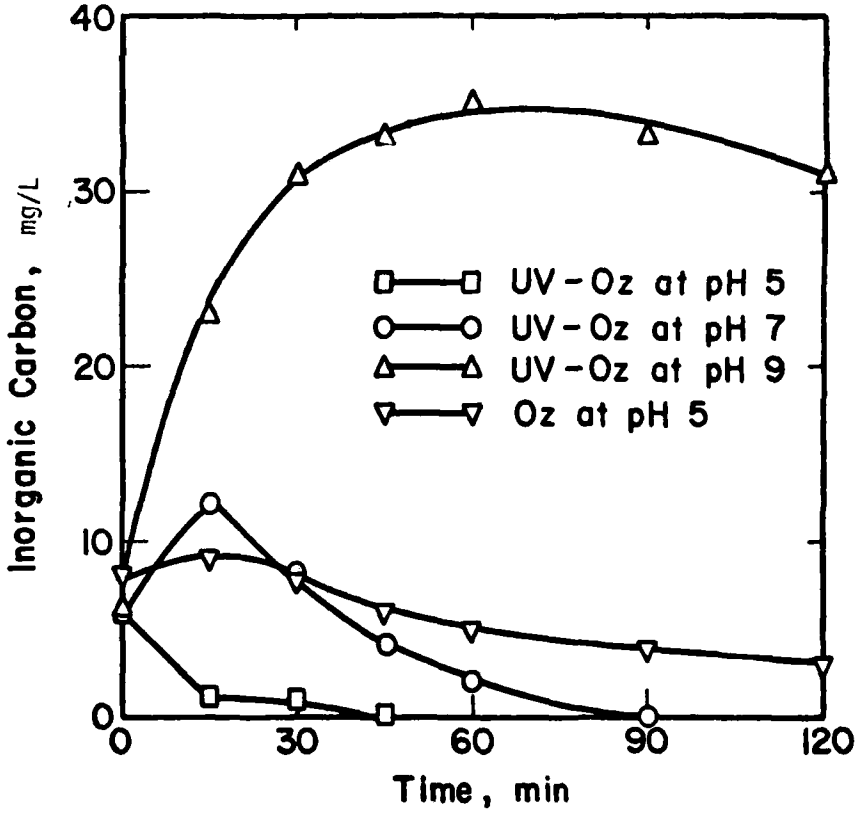

Figure 73. Inorganic Carbon in Reaction Mixtures Resulting from Ozonation and UV-Ozonation of Oxalic Acid.

OZONATION AND CHLORINATION OF ULTRAFILTRATION AND REVERSE OSMOSIS RETENTATES OF SECONDARY EFFLUENT

Introduction

Since the detection of halogenated organics in drinking water (Dowty et al., 1975a; Symons et al., 1975), much research effort has been directed toward finding water treatment processes to remove such organics or their precursors and toward finding disinfectants other than chlorine. Great interest has been focused upon ozonation because both disinfection and organic removal can be accomplished with this process.

Ultrafiltration (UF) and reverse osmosis (RO) retentates of municipal secondary effluent samples were subjected to both chlorination and ozonation to examine the formation of volatile halogenated organics. The application of ozonation to drinking water treatment is also discussed.

Experimental

Wastewater was collected from a Champaign-Urbana sewage main and treated, producing a secondary effluent that was then fractionated into three components by membrane ultrafiltration and reverse osmosis: the UF retentate, RO retentate, and RO permeate. The detailed experimental procedures have been described elsewhere (Chian et al., 1976). The UF and RO retentates were subjected to ozonation and chlorination after their concentrations were adjusted to 5 ppm of TOC.

The retentates were ozonated with the unit described previously. A constant temperature of 25°C was maintained, and the stirring speed was set at 355 rpm. The pH of the solution was not controlled. The ozonated mixture was sampled after 2, 10, and 20 minutes of ozonation. The dissolved ozone concentration increased from 0 to 5 ppm as ozonation time increased from 0 to 20 minutes. Control mixtures were obtained by the same procedures but without the ozonation step. Both the ozonated and the control mixtures were analyzed for volatile halogenated organics by a gas-stripping-GC and GC/MS method. A total of 125 mL of solution was stripped at 60°C and the stripped volatile organics were adsorbed in a Tenax-GC column. The adsorbed organics were thermally released and injected into the GC for quantitation and into the GC/MS for identification. A detailed description of the procedures has been given previously (Adsorption and Desorption Efficiencies) and described by Chian et al. (1976). For GC determinations of volatile organics, a 6-ft x 1/8-inch outside diameter, stainless steel column packed with 0.4% Carbowax 1500 on 80/100 Carbopack A was used. The column was conditioned at 200°C. A 12-ft x 1/4-inch outside diameter glass column was used for GC/MS determinations, which were performed on a Varian-2700 GC using a two-stage Watson-Biemann sample enricher.

The UF and RO retentates were dosed with sodium hypochlorite and mixed for 30 minutes. The reaction mixtures were then transferred into 125-mL glass bottles leaving no headspace volume, topped with Teflon-lined rubber septa, sealed with crimped-on aluminum caps, and stored in a dark place at

room temperature. Three bottles were removed for chemical analyses after storage for 1 day, three more were removed after 3 days, and three after 7 days. Sodium thiosulfate was added to two of the samples to remove residual chlorine before the stripping-GC and GC/MS determinations. At the same time, one bottle was used for determining residual chlorine by the DPD method (Standard Methods, 1971). Control samples (without chlorine dosage) were treated and analyzed similarly.

Results and Discussion

Ozonation and Chlorination of UF and RO Retentates of Secondary Effluent

It has been found that UF and RO retentates contain primarily humic acid-like and fulvic acid-like materials, respectively (DeWalle and Chian, 1974). The molecular weight distribution of soluble organics in these retentates was determined by fractionation on Sephadex gel permeation columns (Chian et al., 1976). The UF retentate contained two major molecular weight peaks, i.e., >50,000 and 2,000 to 5,000; the RO retentate had only one major peak at an apparent molecular weight of approximately 250. The formation of volatile halogenated organics as a result of ozonation and chlorination was tested on these retentates.

Table 52 shows that the concentrations of free chlorine and combined chlorine decrease with storage time, indicating that chlorination still proceeded 1 week after chlorine dosage. It was also observed that chlorine was consumed more rapidly in the RO retentate than in the UF retentate (Table 52). The rapid rate of chlorine uptake in the RO retentate can be attributed to the higher density of organic functional groups present in this fraction than in the UF retentate, as reported by DeWalle and Chian (1974). Since RO itself also concentrates inorganics (Fang and Chian, 1975), higher concentrations of chlorine oxidizable salts, such as bromide, in the RO retentate may also contribute to the higher chlorine demand. The latter possibility is supported by the finding of an appreciable amount of brominated compounds in the chlorinated RO retentate. These compounds are not found in appreciable amount in the chlorinated UF retentate, even after 7 days of storage (Table 53).

Using the gas stripping technique, volatile halogenated organics were detected in the chlorinated UF and RO retentates and their concentrations were determined. The results are summarized in Table 53. These compounds were identified by GC/MS and quantitated by GC. The data shown in Table 53 have been corrected for blank concentrations, which were obtained from control determinations and were generally less than 2 ppb. Figures 74 and 75 show, respectively, the reconstructed gas chromatograms of the chlorinated and the nonchlorinated RO retentates. The latter serves as a control. All of them were stored for 7 days. Some of the peaks in Figure 74 that were marked by the question marks were unable to be identified positively because of the sensitivity limit of the GC/MS and the overlapping of the peaks. The concentrations of most of the compounds in the samples increased upon storage. Chloroform was present in both retentates at concentrations higher than those of other halogenated compounds. It should be noted that a small amount of

TABLE 52. CHLORINATION OF UF AND RO RETENTATES UPON STORAGE

Retentate	Time (day)	pH	Concentration of Chlorine (mg/L)[a]	
			Free Chlorine	Combined Chlorine
UF	0	7.6	1.30	0.10
	1	7.4	0.60	0.10
	3	7.5	0.28	0.08
	7	7.5	0.09	0.08
RO	0	8.2	1.32	0.24
	1	8.1	0.32	0.23
	3	8.1	0.00	0.18
	7	8.0	0.00	0.09

a. Chlorine determination by DPD method.

TABLE 53. CONCENTRATIONS OF VOLATILE HALOGENATED ORGANICS IN CHLORINATED UF AND RO RETENTATES

Retentate	Day	Concentration (ppb)					
		CH_2Cl_2	$CHCl_3$	CCl_4	$CHCl_2Br$	$CHClBr_2$	$CHBr_3$
UF	1	15	35		2		
	3	18	42				
	7	23	61			?	
RO	1	4	28		2	12	7
	3		43		2	17	16
	7		50	5	26	25	21

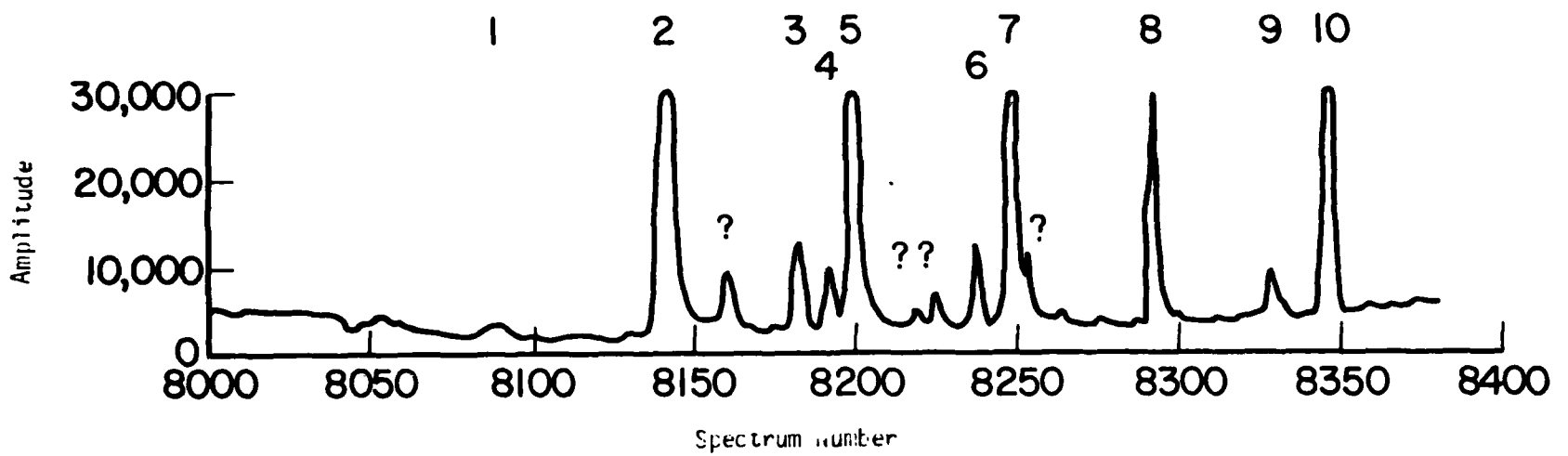

Figure 74. Reconstructed Gas Chromatogram of Chlorinated RO Retentate Stored for 7 Days.

Footnote to the Figure: The compounds identified were: (1) dimethoxy methane; (2) chloroform; (3) carbon tetrachloride; (4) dioxane; (5) bromodichloromethane; (6) benzene; (7) chlorodibromomethane; (8) bromoform; (9) bleed, and (10) bleed and toluene.

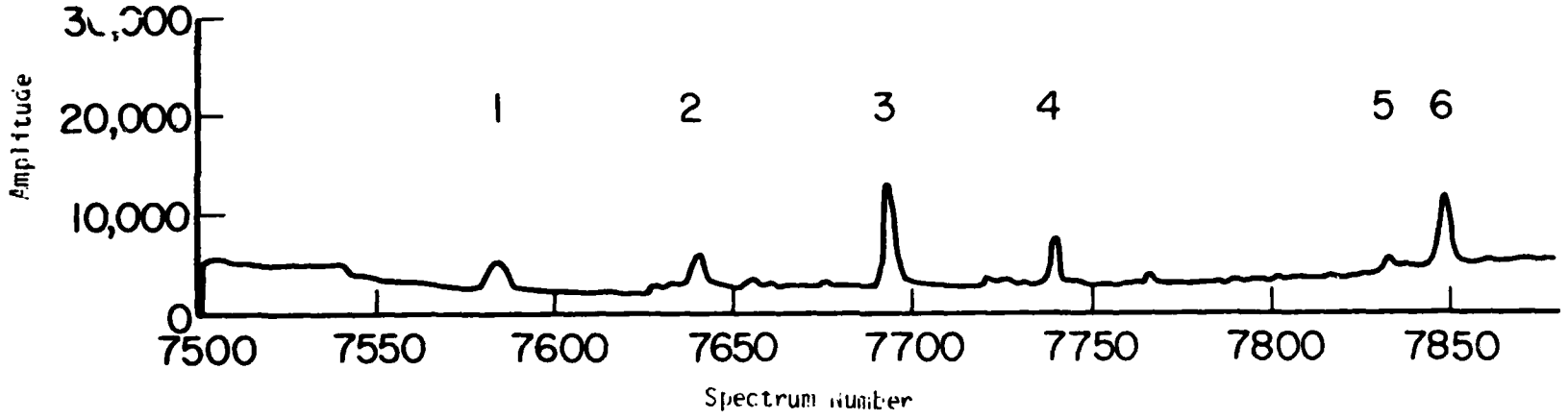

Figure 75. Reconstructed Gas Chromatogram of Nonchlorinated RO Retentate Stored for 7 Days (Control).

Footnote to the Figure: The compounds identified were: (1) dimethoxy methane; (2) chloroform; (3) dioxane; (4) benzene; (5) tetrachloroethylene; and (6) bleed.

carbon tetrachloride (e.g., 5 ppb) was detected in the RO retentate only after 7 days of storage. This shows that carbon tetrachloride also results from chlorination of humic substances (e.g., fulvic acid). Although Symons et al. (1975) have detected this compound in a survey of drinking water from 80 selected cities, they were unable to draw such a conclusion. Brominated organics were found in appreciable amounts only in the RO retentate, because bromide is diluted in the UV process and is concentrated by the RO process. Bromide can be oxidized by hypochlorite to form hypobromite, a compound with bromination can take place to produce brominated compounds (Bunn et al., 1975). A material balance for chlorine has shown that approximately 5 to 6% and 3 to 4% of the chlorine consumed ended up in the volatile chlorinated compounds in the UF and the RO retentates, respectively. Approximately 1 to 2% of the chlorine ended up in the volatile brominated compounds present in the RO retentate. It was also shown that approximately 0.2% of the organic carbon was converted to volatile halogenated organic compounds in both chlorinated retentates after they were stored 1 week. This result agrees very well with that reported by Rook (1976).

Ozonation, on the other hand, did not result in the formation of any of these volatile halogenated compounds. The concentration of these compounds actually decreased during ozonation, possibly resulting from both stripping and oxidation of these compounds by the ozone.

Application of Ozonation in Drinking Water Treatment

The use of chlorine for disinfection in drinking water treatment processes could result in the formation of volatile halogenated organics, as observed in the present study as well as by other investigators (Symons et al., 1975; Rook, 1976; Bunn et al., 1975; Kopfler et al., 1976; Bellar et al., 1974b). Stevens et al. (1976) found that the extent of the formation of trihalomethanes as a result of chlorination was governed by many factors, such as the types of precursors present, the pH of the water, the temperature of the water, the presence of particulates, the presence of ammonia, and chlorination time. The precursors of these halogenated compounds may be either humic acid-like or fulvic acid-like materials, as observed in this study. Rook (1976) found that m-dihydroxy aromatic compounds and methyl ketones as well as aliphatic compounds having a 1,3-dione configuration were precursors of haloforms. The results of these studies are supported by a nationwide survey in which six volatile halogenated organic compounds were detected in finished drinking water (Symons et al., 1975).

To minimize the formation of such potentially toxic halogenated compounds, an advanced water treatment process could be employed to remove haloform precursors prior to chlorine disinfection. The ozonation process appears to be a good candidate, as it provides disinfection and prevents the formation of halogenated compounds. To protect against postcontamination in the distribution system, chlorine could be applied after ozonation treatment at much lower dosages than would be required in a conventional treatment system.

The use of ozone should be fully investigated, however, to determine the toxicity of the ozonation products, such as ozonides, epoxides, and oxalic acid. The chlorinated ozonation products, resulting from subsequent chlorination of ozonated effluent to provide chlorine residuals for disinfection, should also be determined. For example, it has been found in cytotoxicology tests that the syntheses of proteins in tissue cells cultured in treated hospital wastewater effluents that were ozonated for various periods of time decreased and then increased slightly to the normal level as the time of ozonation increased (Kinman et al., 1976). This initial inhibition of cellular protein syntheses may be attributed to the accumulation of the toxic intermediates and/or oxalic acid, which were, in turn, removed gradually as the ozonation process proceeded. Oxalic acid is known to be one of the competitive inhibitors that inhibit succinate dehydrogenase in the Krebs tricarboxylic acid cycle. To avoid the possible formation of toxic halogenated compounds in ozonated effluents, chlorine dioxide may be used as a chlorine substitute to provide residual disinfection power.

Chemical coagulation followed by activated carbon or resin adsorption is an alternative for removing the precursor humic substances prior to chlorine disinfection (Love et al., 1975). The effectiveness of these processes in removing precursors varies with the properties of those compounds as well as with the types of coagulants and adsorbents. Carbon adsorption columns must be regenerated frequently because breakthrough of precursor compounds has been observed after a few weeks of operation (Rook, 1976; Stevens et al., 1976). The cost associated with the regeneration of adsorbents and the disposal of sludges and regenerants should also be evaluated when considering the coagulation and adsorption process.

With the ozonation process, organic compounds can ultimately be converted to harmless carbon dioxide by intensive ozonation of water. Cost, however, appears to be the major obstacle to the wide application of ozonation. Effective coagulation and sedimentation in the early stages of water treatment would tend to decrease ozone demand; incorporating UV irradiation and catalysts would enhance organic removal. These approaches would lower the ozonation cost. Further cost reductions can be realized through the development of efficient ozone generators and contactors and by obtaining knowledge about optimal conditions for ozonation reactions including such factors as reactor design, pH adjustment, temperature control, and application of UV. Future studies should therefore be directed toward minimizing costs by optimizing ozonation processes and toward assessing the health hazards associated with ozonation.

ULTRAVIOLET-OZONATION OF COMPOSITE REVERSE OSMOSIS PERMEATE

Ultraviolet-Ozonation of Mixture of Methanol and Acetone

UV-ozonation studies of a mixture of methanol and acetone were performed to investigate if there is any competitive or preferential ozonation between these two compounds. Of equal importance and interest in this study is to determine whether the TOC can be removed below the 5-ppm level and whether all the TOC of the ozonation mixtures can be accounted for from the ozonation products so determined.

The concentrations of methanol and acetone were 160 and 20 ppm, respectively (corresponding to 63 and 12.4 ppm of TOC), to simulate their composition ratio in the laboratory reverse osmosis (RO) permeate. The use of such low levels of methanol and acetone is to avoid the ozonation process from being operated under the conditions of ozone mass-transfer limiting condition. Four liters of the mixture were prepared and ozonated in a 5-liter New Brunswick fermentor (New Brunswick Scientific, New Brunswick, NJ) operated at a constant pH of 9 and a constant temperature of 25°C. The speed of the stirring impellers was 695 rpm. Ozone was generated from dried oxygen by a Welsback Model T-408 ozone generator (Philadelphia, PA). The feed gas to the fermentor had an ozone concentration of 25 mg/L and a flow rate of 4 L/minute. The fermentor was also equipped with a 15-watt, low-pressure mercury germicidal lamp (General Electric, Schenectady, NY) for the UV-ozonation study. The dissolved ozone concentration was determined by the Shechter's iodometric method (1973); and was found to increase from 0.3 to 2.3 ppm as the ozonation time increased from 15 to 120 minutes. The analytical methods used in determining the ozonation products were described previously.

Figure 76 shows the results of removal of methanol and acetone as well as their ozonation products. It was found that methanol was removed rather rapidly during the early stage of the UV-ozonation run. This is to be expected because the removal of methanol follows the first-order kinetics (Summary), and the initial concentration of methanol is relatively large. Methanol was completely removed after 90 minutes of ozonation. The removal of acetone appeared to follow a zero-order kinetics and was not complete at the end of 120 minutes of ozonation. It was observed, however, in the ozonation of 2-propanol that resulted in the formation of acetone (Figure 54), which was then removed within 1 hour. Therefore, it shows that the removal of acetone was somehow retarded in the UV-ozonation of a mixture of methanol and acetone at a weight ratio of 8.4 to 1 under the prevailing experimental conditions. This may be attributed to the presence at high concentrations of methanol and formaldehyde, an ozonation product of methanol. Interference arises probably because of competition for ozone rather than interaction between organic compounds. Ozonation of methanol and acetone should be individually studied under experimental conditions identical to those in this study so that parallel results can be compared to enable us to draw definite conclusions.

As shown in Figure 76, acetone was slowly removed with the accumulation of a very small amount of acetic acid and a negligible amount of oxalic acid. Formic acid appeared to be oxonated at a very rapid rate under the experimental conditions because only a small amount of it could be detected. Since a larger accumulation of formaldehyde than formic acid was observed, the rate

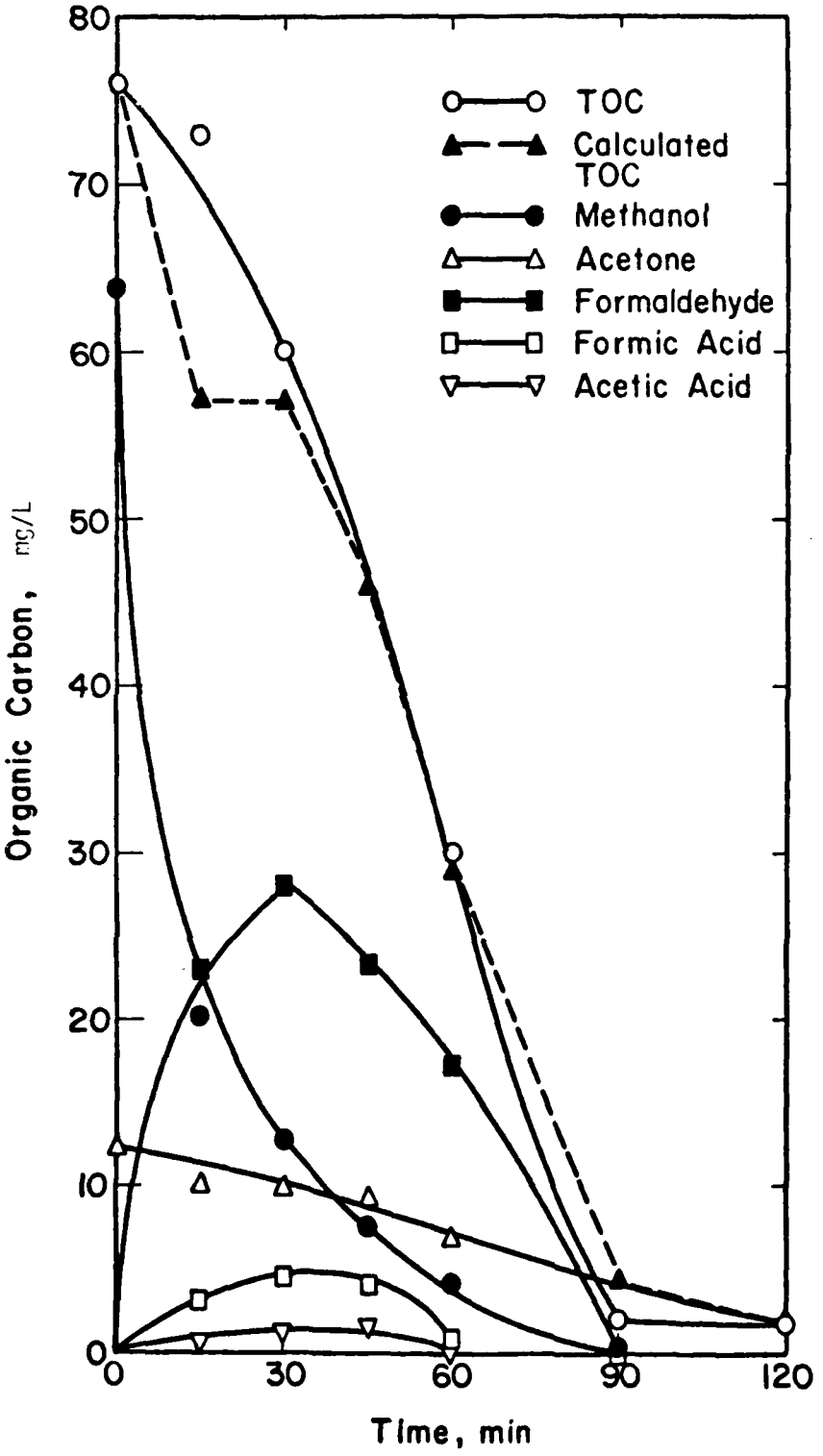

Figure 7C. UV-Ozonation of Mixture of Methanol and Acetone.

of ozonation of formaldehyde must be slower than that of formic acid. Except for the TOC data on various constituents determined during the first 15 minutes, all of the TOC of the ozonation mixtures can be accounted for (Figure 76). The final TOC of the ozonation mixture dropped to 2 ppm after 2 hours of UV-ozonation. The results indicate that under the ozonation conditions studied here, the laboratory RO permeate and, therefore, the composite RO permeate can be treated by UV-ozonation to meet the Army's criteria for reuse.

UV-Ozonation of Composite RO Permeate

Comparable studies on the analysis of the intermediates formed in the UV-ozonation of a composite RO permeate should be conducted as suggested in the recommendation section.

SCALE-UP OF OZONE-SPARGED VESSELS

Introduction

The treatment of water by ozonation is a dual-purpose unit process in that it accomplishes both the removal of organics and disinfection. Ozonation has been used as a final polishing step for wastewater renovation and as a disinfection process in the treatment of drinking water and wastewater.

The gas-sparged vessel has been demonstrated to be an efficient device for bringing ozone into contact with water and wastewater for the removal of organics through liquid-phase oxidation reactions. In its simplest form, the ozone-sparged unit is a vertical vessel in which porous diffusers are installed at the bottom. No stirrers or other moving parts are used. The gas bubbles containing ozone travel upward through a concurrent or countercurrent flow of liquid. The reaction proceeds in the liquid phase with ozone transferred from the gas phase. An ozone contactor may consist of a series of ozone-sparged vessels or stages.

The Torricelli ozone contactor (Torricelli, 1958) is a specific type of sparged ozone contactor reported to have a high ozone utilization efficiency. In the Torricelli device, shown in Figure 77, the liquid moves countercurrently and concurrently with respect to the gas flow in alternate stages. A modified design was developed by Life Systems, Inc., for the water processing element used in the Army Medical Unit, Self-Contained, Transportable (MUST) complex. The purpose of the ozonation process in that application is to reduce the concentration of residual organic compounds present in the permeate from an RO system in order to meet a specific criterion for reuse of the treated water.

While a sparged vessel is usually designed with a large ratio of height to diameter and is agitated only by the sparging gas, an agitated vessel normally has a depth comparable to its diameter and is equipped with a motor-driven stirrer and a gas sparger. The sparger may be a pipe ring with many holes or a single tube delivering the gas under the stirrer. The

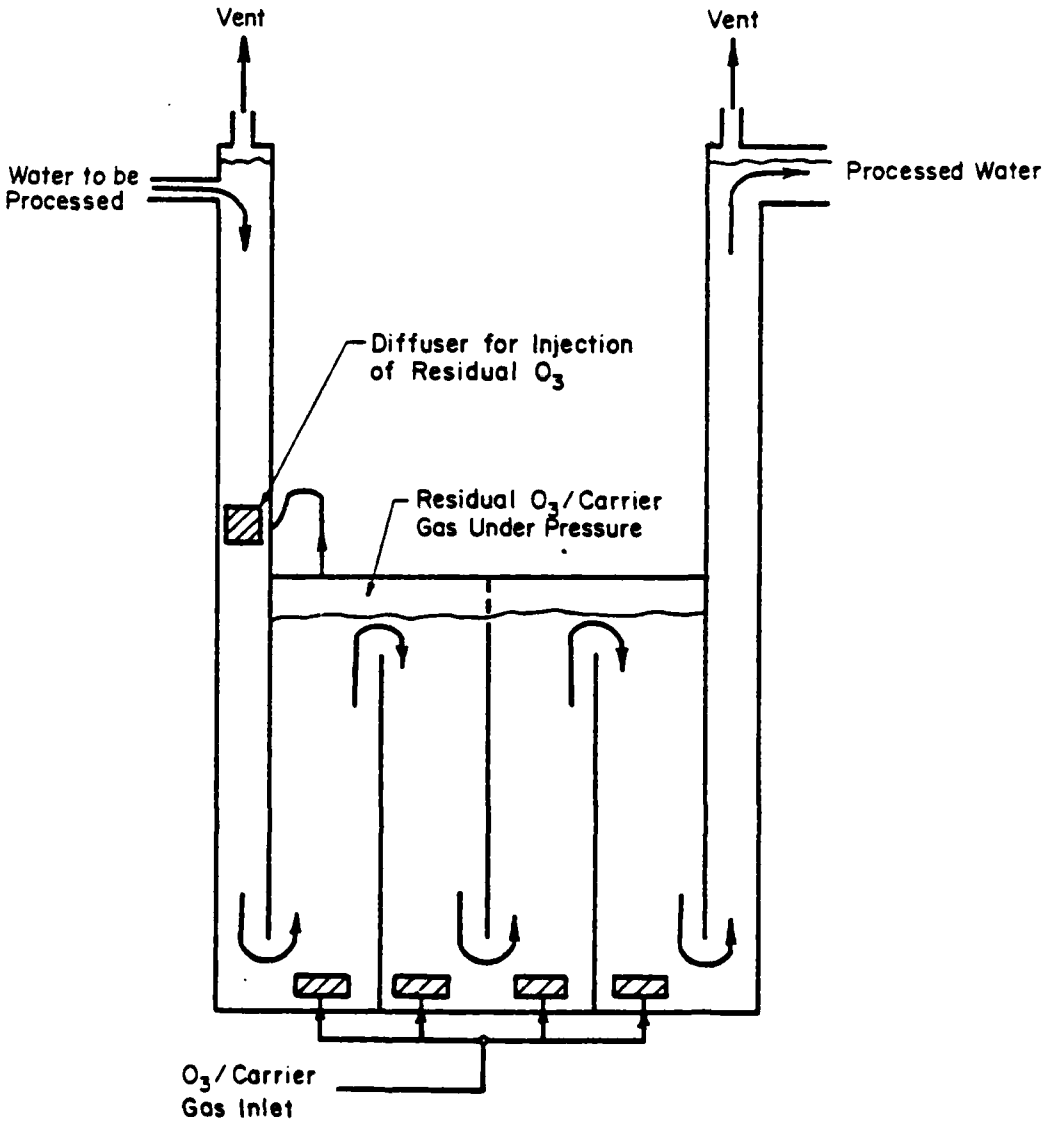

Figure 77. Schematic of Torricelli Ozone Contactor.

agitated vessel is widely used in the chemical industry for batch oxidations, chlorinations, and hydrogenations, with the chemical reaction occurring in the liquid phase. An agitated vessel may be used as an alternative to a sparged vessel in ozonation systems.

Literature Search

A gas-sparged vessel (or bubble column) is a relatively simple device for bringing gases into contact with liquids. It has been reported that gas-sparged vessels exhibit mass transfer rates on the same order of magnitude as packed columns at low liquid throughput rates. At high liquid throughput rates, where packed columns are ineffective, they exhibit much higher mass transfer rates (Shulman and Molstad, 1950). However, the pressure drop across sparged vessels is much greater than that across packed columns of the same height. It has also been reported that the transfer capacity level that can be achieved in agitated vessels by power stirring can be nearly equaled in sparged vessels through proper design and the use of high gas-flow rates and liquid heights; an economic limit would be reached at which the power required to compress and circulate the gas for sparged vessels would equal that required to operate a stirrer.

Mass Transfer Characteristics of Gas-Sparged Vessels

Research on mass transfer properties of sparged vessels for the absorption or desorption of sparingly soluble gases have centered on four characteristics; namely, the average gas bubble diameter, d; the average fractional gas holdup, h; the average interfacial area, a; and the liquid-phase mass transfer coefficient, k_L. The three parameters d, h, and a are interrelated by the following equation:

$$a = \frac{6h}{d} \tag{1}$$

Each of these characteristics is discussed in the following sections.

Average Gas Bubble Diameter. The shape of gas bubbles in a given liquid can vary from that of a sphere, an oblate sphere, or an ellipsoid to a spherical cap, depending on the gas-flow rate (Calderbank et al., 1970). Regardless of the shape, however, the size of the bubbles is reported in terms of the diameter of a sphere of equivalent surface area. The average diameter (surface-volume mean diameter) is defined as:

$$d \frac{\Sigma\ nd_B^3}{\Sigma\ nd_B^2} \tag{2}$$

where d_B is the diameter of the bubble in centimeters. The average bubble diameter can be evaluated directly by a statistical analysis of photomicrographs or high-speed flash photographs (Calderbank, 1967).

At low gas-flow rates, the size of the bubbles produced is determined by a balance between the buoyant force separating the bubble from the orifice and the shearing force necessary to break the surface tension across the orifice. At gas-flow rates above a certain level, the average diameter of the bubbles is a function of the gas-flow rate only and is independent of the orifice diameter (Akita and Yoshida, 1974). Shulman and Molstad (1950) reported that bubble size was not affected by the pore size when a porous plate was used instead of a single orifice in bubble contactors. They suggested that the coarsest grade of porous plate be used to minimize the pressure drop because there is no advantage to be gained from the use of fine porous plates for gas. In general, most researchers agree that the type of sparger used has little or no effect on bubble size at high gas-flow rates.

Reporting data from aeration in a laboratory column using several types of air-diffusing devices, Pasveer (1955) showed that the mean diameter of the bubble is an exponential function of the volumetric gas-flow rate, G_o; that is, $d \sim G_o^n$.

The theory of the interdispersion of immiscible fluid phases by turbulent forces has been given by Hinze (1955). Generally, the size of gas bubbles produced in a gas-liquid dispersion is determined by the balancing of the surface tension force with the force due to turbulent fluctuations. The above arguments lead to the result:

$$d = k' \frac{\gamma^{0.6}}{(P/V)^{0.4} \rho^{0.2}} \tag{3}$$

where d is the bubble diameter, γ is the surface tension, P is the power input, V is the liquid volume, ρ is the liquid density, and k' is a proportionality constant. A correlation was developed for gas-liquid contact in mechanically agitated tanks by Calderbank (1958):

$$d = 4.15 \left[\frac{\gamma^{0.6}}{(P/V)^{0.4} \rho^{0.2}} \right] h^{0.5} + 0.09 \tag{4}$$

where the expression in square brackets is in CGS units. Towell et al. (1965) reported that the bubble size data obtained in large-diameter bubble columns corresponds quite well with Equation (4) if the dissipation of power is related to the superficial gas velocity, U_G, in ft/second (defined as the volumetric gas-flow rate divided by the cross-sectional area of the vessel) by:

$$\frac{P}{V} = U_G \rho \frac{g}{g_c} \tag{5}$$

where P/V is the power supplied per volume of liquid (ft-lb_f/sec ft^3), g is the gravitational constant, and g_c is a conversion factor.

Akita and Yoshida (1974) reported a dimensionless correlation for the average bubble diameter:

$$\frac{d}{D} = 26\ (g\ D^2\ \rho/\gamma)^{-0.50}\ (g\ D^3/\nu^2)^{-0.12}(U_G/\sqrt{gD})^{-0.12} \tag{6}$$

or

$$\frac{d}{D} = 26(N_{BO})^{-0.50}\ (N_{Ga})^{-0.12}\ (N_{Fr})^{-0.12} \tag{7}$$

where D is the diameter of the vessel, ν is the kinematic viscosity, N_{Bo} is the Bond number, N_{Ga} is the Galilei number, and N_{Fr} is the Froude number.

Lehrer (1971) recommended that the geometric mean between bubble diameters at the sparger orifice, d_{BO}, and stable bubble diameters, d_{BE}, be used to characterize gas-sparged systems.

$$d_{BM} = (d_{BO}d_{BE})^{1/2} \tag{8}$$

where d_{BM} is the characteristic mean diameter of the system. For chain bubbling, d_{BO} is given as follows:

$$d_{BO} = 2.05 \left(\frac{G_o}{\pi\ N_o'}\right)^{0.4} \left(\frac{3\ C_D}{4\ g}\right)^{0.2} \tag{9}$$

where $C_D = 8/3$ for turbulent chain bubbling and $C_D = 24/N_{Re}$ for laminar chair bubbling. N_o' incorporates a correction for coalescence due to the overlapping of bubbles at the sparger. If $d_{BO}/0.75$ is less than the spacing between sparger holes, X, N_o' equals N_o, the actual number of holes. If $d_{BO}/0.75 \geq X$, N_o' for a perforated pipe sparger is

$$N_o' = \frac{(N_o-1)X + d_{BO}/0.75}{d_{BO}/0.75} \tag{10}$$

For a perforated plate design, Equation (10) applies in squared form. The stable bubble diameter is

$$d_{BE} = 3.48\, C_D^{-0.6} \left(\frac{\gamma^{0.6}}{(P/V)^{0.4}\, \rho^{0.2}} \right) \qquad (11)$$

Attainment of d_{BE} is presumed to require high turbulence in the immediate vicinity of a bubble, for which $C_D = 8/3$.

It should be noted that the above correlations do not take into consideration the fact that the presence of surface active materials or ionic materials would reduce the coalescence rate and result in more rigid and smaller bubbles (Calderbank, 1958). A correlation with limited practical use has been proposed by Marrucci and Nicodemo (1967) in an attempt to relate the average bubble diameter to the gas-flow rate and to a group of the electrolyte properties.

Average Fractional Gas Holdup. The holdup of gas in a sparged contactor is important in determining the residence time and interfacial area of gas bubbles, two parameters that affect mass transfer. If H_l is the clear liquid height and H_f is the expanded height of the bubbled liquid, the gas holdup, H_g, is:

$$H_g = H_f - H_l \qquad (12)$$

The fractional gas holdup, h, is the fraction of gas-liquid dispersion occupied by gas in the vessel:

$$h = \frac{H_f - H_l}{H_f} \qquad (13)$$

The fractional gas holdup has been determined by sampling the dispersion into an evacuated receiver or by measuring the volume of the dispersion and that of the liquid after phase separation. Although local values of h can be determined using methods such as pressure measurement and gamma-ray transmission (Calderbank, 1968), only the average value of h is of interest because it can be related to d and a according to Equation (1).

Towell et al. (1965) reported that columns with larger diameters exhibit lower fractional holdups than smaller columns. The higher fractional holdup in the latter columns results from the absence of liquid circulation patterns. Ellis and Jones' data (1965) indicate that wall effects increase the fractional gas holdup at diameters up to 3 inches. For diameters greater than 3 inches, the fractional gas holdup is independent of the diameter. This effect of vessel diameter on h for a small diameter tube was also reported by Argo and Cova (1965).

Braulick et al. (1965) found that the holdup increases with gas rates and with submergence-to-diameter ratios. On the other hand, Yoshida and Akita (1965) reported that gas holdup is independent of liquid height. They argued that although end effects are expected in shorter columns, these effects are masked in tall columns by experimental errors. Towell et al. (1965) also reported that as far as holdup is concerned the gas rate is the only pertinent parameter in large bubble columns because the initial conditions do not control the performance of the column.

Hughmark (1967) indicated that the holdup of gas in a bubble column can be correlated with the term $U_G \times (1/\rho + 72/\gamma)^{1/3}$. The holdup so given is at a liquid flow rate of zero. The correlation applies to a concurrent-flow liquid system if the holdup is defined by:

$$h = \frac{U_G}{U_S} \tag{14}$$

where U_S is the slip velocity between the bubbles and the liquid:

$$U_S = \frac{U_G}{h'} - \frac{U_L}{1-h'} \tag{15}$$

Here h' refers to the holdup of gas under liquid flow, and U_L is the superficial liquid velocity. The negative sign for $U_L/1-h'$ corresponds to concurrent flow; a positive sign would be used for countercurrent flow. Towell et al. (1965) found that the holdup in a concurrent-flow system was related to the gas-flow rate by:

$$\frac{1}{h'} - \frac{U_L/U_G}{1-h'} = \frac{U_T}{U_G} + 2 \tag{16}$$

which, when U_L/U_G is small (as is often the case in bubble contactors), reduces to

$$h' = \frac{U_G}{U_t + 2U_G} \tag{16a}$$

Akita and Yoshida (1973) reported that the effect of the liquid rate on the gas holdup was negligible for superficial liquid velocities up to 160 m/hour in gas/liquid operations with either countercurrent or concurrent flow. Likewise, Tadaki and Maeda (1964), Bischoff and Phillips (1966), Reith et al. (1968), and Eissa et al. (1971) all reported that the liquid flow had no

effect on gas holdup. Bischoff and Phillips (1966) indicated that the design of the perforated plate seemed to affect holdup, whereas the data of Towell et al. (1965) showed that different types of spargers exhibited the same gas holdup.

Akita and Yoshida (1973) proposed the following empirical correlation based on their experimental data:

$$\frac{h}{(1-h)^4} = 0.20\ (g\ D^2\ \rho/\gamma)^{1/8}\ (g\ D^3/\nu^2)^{1/12}\ (U_G/\sqrt{gD})^{1.0} \tag{17}$$

For an electrolyte solution, it is suggested that a constant of 0.25 be used instead of 0.20.

According to Miller (1974), gas holdup can be estimated from

$$h' = \frac{U_G}{U_t + U_G} \tag{18}$$

The terminal velocity at which the bubbles rise, U_t, can be predicted using Mendelson's wave equation,

$$U_t = \left(\frac{2\gamma}{\rho d} + \frac{gd}{2} \right)^{0.5} \tag{19}$$

Average Interfacial Area. Average interfacial area can be deduced from Equation (1) if d and h are known. It can also be determined directly using optical or chemical methods (Calderbank, 1967). It has been found that power dissipation increases the interfacial area and thus increases the mass transfer rate, although little effect on the mass transfer coefficient, k_L, can be realized (Calderbank and Moo-Young, 1961).

Sharma and Mashelka (1968) studied bubble columns with a liquid containing a dissolved electrolyte and concluded that the specific interfacial area a varies with $U_G^{0.7}$. The value of a was found to be unaffected by the ratio of the height to diameter, provided that this ratio lay between 3 and 12. Akita and Yoshida (1974) proposed the following correlation for a:

$$a\ D = 1/3 \left(\frac{gD^2\rho}{\gamma} \right)^{0.5} \left(\frac{gD^3}{\nu^2} \right)^{0.1} h^{1.13} \tag{20}$$

It should be noted that a is proportional to $D^{0.3}$ and $h^{1.13}$, the latter, in turn, being proportional to U_G.

Liquid-Phase Mass Transfer Coefficient. It has been shown that in the case of transferring into water sparingly soluble gases such as O_2 and O_3, the controlling resistance to mass transfer occurs in the liquid film; the gas film resistance can be neglected (Treybal, 1968).

The liquid-phase mass transfer coefficient denoted by k_L is actually an average value of k_L since the local value of k_L should vary even on the surface of one bubble and would depend on the bubble size. Some researchers have used a combined mass transfer coefficient $k_L a$ (or $k_G a$) to express the mass transfer rate in order to avoid evaluating a. These correlations for $k_L a$ (or $k_G a$) will also be given in the following presentations along with those for k_L. It should be noted that $k_L a$ and k_L are often calculated from mass transfer rates using a model that assumes a completely mixed liquid phase and a plug flow of the gas. However, this model may not accurately represent what happens in a sparged vessel.

Early work on evaluating the liquid-phase mass transfer coefficient, k_L, has been largely confined to studying the dissolution rates of single, well-defined bubbles rising freely. The results of such experiments, if applied to bubble swarms, would not account for the possible influence of interactions between bubbles. In general, sparged vessels operate with swarms of bubbles rather than single bubbles. Calderbank and Moo-Young (1961) combined the results of their experiments on gas-liquid dispersions with other published data for heat and mass transfer in liquid-liquid and solid-gas dispersions and reported a correlation for bubble swarms having an average bubble diameter greater than about 2.5 mm, such as those produced when pure liquid are aerated in mixing vessels and sieve plate columns:

$$k_L (N_{Sc})^{1/2} = 0.42 \left(\frac{\Delta \rho \mu g}{\rho^2} \right)^{1/3} \tag{21}$$

where N_{Sc} is the Schmidt number and $\Delta\rho$ is the density difference between the gas and the liquid. For bubble swarms having an average bubble diameter less than about 2.5 mm, such as those produced when aqueous solutions of hydrophilic solutes are aerated in mixing vessels, or when liquids in general are aerated with sintered plates or with plates containing very small perforations, the following correlation was given:

$$k_L (N_{Sc})^{2/3} = 0.31 \left(\frac{\Delta \rho \mu g}{\rho^2} \right)^{1/3} \tag{22}$$

Both correlations show that the liquid-phase mass transfer coefficients are independent of bubble size and slip velocity (free-rising velocity) and depend only on the physical properties of the system. It follows that in mixing vessels the liquid film mass transfer coefficients, k_L, are independent of the power dissipated by the agitator, and in sieve-plate columns they are

also independent of the fluid-flow rates. Those authors therefore conclude that the only reason for the differences in performance between various types of gas-liquid bubbling devices is the difference in the interfacial areas produced.

Towell et al. (1965), on the basis of their experiments on mass transfer in bubble columns with large diameters, reported that k_L is correlated quite well at high gas rates by Equation (21) and at low gas rates by Bowmann and Johnson's (1962) single bubble correlation:

$$\frac{k_L d}{D_L} = 2\sqrt{\frac{U_t d}{\pi D_L}} \tag{23}$$

where D_L is the diffusivity of the dissolved gas in liquid. These authors also confirmed that a large portion of the increase in volumetric mass transfer coefficient, $k_L a$, with increasing gas superficial rate is due to the increase in interfacial area. Hughmark (1967), however, proposed a correlation on the basis of the data of Towell et al. (1965):

$$N_{Sh} = 2 + 0.0187\left[(N_{Re})^{0.484}(N_{Sc})^{0.339}\left(\frac{dg^{1/3}}{D_L^{2/3}}\right)^{0.072}\right]^{1.61} \tag{24}$$

where the velocity in the Reynolds number, N_{Re}, is represented by the slip velocity. The Boussinesq equation (Boussinesq, 1905) has also been used to characterize mass transfer in gas-liquid contacting:

$$N_{Sh} = \sqrt{\frac{4}{\pi}}\, N_{Pe}^{1/2} \tag{25}$$

where N_{Pe} is the Peclet number.

Based on the data of Pasveer (1955) as well as Ippen and Carver (1955), k_L has been correlated by Eckenfelder (1959) as follows:

$$\frac{k_L d}{D_L} H^{1/3} = C' N_{Re} (N_{Sc})^{1/2} \tag{26}$$

or

$$k_L = \frac{C' U_t}{H^{1/3}} \frac{1}{N_{Sc}^{1/2}} \tag{27}$$

where C' is a constant. The effect of submergence depth, H, on k_L as indicated in Equation (27) was also reported by Shulman and Molstad (1950). Braulick et al. (1965) found that $K_G a$ varies with submergence-to-diameter ratio, H/D, to a 0.3 power:

$$K_G a = (2.5 \times 10^{-4} G_o - 0.002) (H/D)^{0.3} \quad (28)$$

Sharma and Mashelka (1968), however, found that $k_L a$ and $k_G a$ are unaffected by H/D if that ratio is between 3 and 12.

Yoshida and Akita (1965) found that $k_L a$ is practically independent of the liquid height. They also reported that the effect of the liquid rate on $k_L a$, studied using continuous countercurrent and concurrent sulfite oxidation experiments, was negligible. This finding is contradictory to the results of Shulman and Molstad (1950), in which mass transfer rates were found to be a function of liquid rate. These two pairs of authors also reported different results in studies of the effect of column diameter on the mass transfer rate. Shulman and Molstad (1950) reported that the mass transfer rate is independent of the column diameter, whereas Akita and Yoshida (1973), in their experimental correlation for $k_L a$, indicated a dependence on column diameter according to the following relationship:

$$k_L a = 0.6 D_L^{0.5} \nu^{-0.12} (\gamma/\rho)^{-0.62} D^{0.17} g^{0.93} h^{1.1} \quad (29)$$

or

$$N_{Sh} (aD) = k_L a D^2/D_L = 0.6 N_{Sc}^{0.5} N_{Bo}^{0.62} N_{Ga}^{0.31} h^{1.1} \quad (30)$$

Their correlation for the liquid-phase mass transfer coefficient can be written as:

$$k_L = 0.5 g^{5/8} D_L^{1/2} \rho^{3/8} \gamma^{-3/8} d^{1/2} \quad (30a)$$

It should be pointed out that Equations (23), (27), and (30a) show that k_L is not only a function of the physical properties of the system, but also a function of d or U_t.

For bubble aeration, $k_L a$ has been correlated as follows:

Eckenfelder Equation (1959)

$$k_L a = \frac{C'' G_o^{n} H^{0.67}}{V} \quad (31)$$

Boussinesq Equation (Aiba et al., 1973)

$$k_L a = \frac{C''' G_o^{n} H}{V} \tag{32}$$

where C'' and C''' are constants.

These two correlations are identical except that the exponent of H is 0.67 in one and unity in the other.

Mixing in Gas-Sparged Vessels

Extensive studies have been carried out on the mixing in the liquid phase in sparged vessels. It has been found that sparged vessels exhibit more intense mixing than that obtained with single-phase liquid flow and thus do not closely approach plug-flow conditions. The mixing in sparged vessels is usually characterized by an axial dispersion coefficient based on a one-dimensional diffusion model. The axial dispersion coefficient has been correlated with the superficial gas velocity (Tadaki and Maeda, 1964). Correlations using the Peclet number have also been attempted by Argo and Cova (1965) and by Reith et al. (1968).

Argo and Cova (1965) and Bischoff and Phillips (1966) found that liquid velocity has no noticeable effect on the dispersion coefficient. Thus, the mixing seems to be caused primarily by the gas flow. Reith et al. (1968) reported that when a sparged column was first under countercurrent and then concurrent flow conditions there was no difference in axial dispersion. A significant effect of column diameter on the dispersion coefficient has been reported by Argo and Cova (1965) and can be seen from the following correlation for the bubble flow condition as proposed by Ohki and Inoue (1970):

$$E_\ell = 0.30\, D^2\, U_G^{1.2} + 170\, d_h \tag{33}$$

where E_ℓ is the dispersion coefficient and d_h is the diameter of the sparger holes. For the coalesced bubble-slug flow condition, these authors give

$$E_\ell = \frac{14D}{(1-h)^2} \tag{34}$$

Deckwer et al. (1973) found that two regions of different mixing exist in a bubble column at a superficial gas velocity of 0.4 and 2.92 cm/sec. In the lower region of the column, they proposed the following empirical correlation for their axial mixing data:

$$E_\ell = (1.2 \pm 0.12)\, D^{1.5}\, U_G^{0.5} \tag{35}$$

whereas in the upper region the coefficient was greater:

$$E_{\ell} = (2.4 \pm 0.18)\, D^{1.5}\, U_G^{0.5} \tag{36}$$

and if no splitting into different back-mixing zones occurs (e.g., at a U_G value of 0.24 cm/sec):

$$E_{\ell} = (2 \pm 0.15)\, D^{1.5}\, U_G^{0.5} \tag{37}$$

Reith et al. (1968) found that the addition of inorganic ions to the water has a marked effect on the axial dispersion coefficient.

Little has been published on radial dispersion. The values that have been determined for the radial dispersion coefficient are much smaller than those for the corresponding axial coefficient, indicating that radial dispersion is of minor importance (Reith et al., 1968; Eissa et al., 1971).

Ozone Absorption and Simultaneous Chemical Reactions

The absorption of gases in a liquid with which they react is known to occur at a faster rate than purely physical absorption in many cases. The following sections review the simultaneous chemical reactions that occur when ozone is absorbed in water. Also discussed are the theoretical aspects of ozone absorption and simultaneous chemical reactions as they apply to an ozone-sparged vessel.

Ozone Decomposition Reaction in Water. Ozone decomposition in water has been studied by many investigators. Their findings, however, are conflicting, especially regarding the order of reaction. The decomposition has been reported to follow first-order, three-halves-order, and second-order kinetics. Table 54 summarizes the range of variables covered by various investigators and their conclusions concerning the reaction order relative to ozone.

Reactions Between Ozone and Organics Dissolved in Water. Ozone is a potent oxidant that reacts with many organic groupings. Of the organic groupings, compounds with carbon-carbon double bonds are usually the most reactive toward ozone. Substances with carbon-hydrogen and silicon-hydrogen bonds are usually the least reactive, but they do react with ozone provided that more reactive groupings are not present. Although many studies on the reaction of ozone with organics in nonaqueous media have been conducted, limited research has been directed toward the kinetics of ozone reactions with organics in aqueous solution (Bailey, 1972).

Products of the ozonation of methanol, formaldehyde, and formic acid have long been identified (Fischer, 1929; Long, 1940; Taube, 1941). The kinetics of these reactions were studied only recently by Kuo and Wen (1976).

TABLE 54. SUMMARY OF RESEARCH ON OZONE DECOMPOSITION IN WATER

Researcher	pH Range	Temperature Range (°C)	Reaction Order with Respect to Ozone
Alder and Hill, 1950	1-2.8	0-27	1
Czapski et al., 1968	10-13	25	1
Hewes and Davison, 1971	2-4,6,8	30-60,10-50,10-20	2,3/2-2,1
Kilpatrick et al., 1956	0-6.8,13	25	3/2,2
Kuo et al., 1975	2.2-11.0	15-35	3/2
Merkulova et al., 1971	0.22-1.9	5-40	1,2
Raukas et al., 1962	5.4-8.5	5-25	3/2
Rothmund and Burgstaller, 1913	2-4	0	2
Sennewald, 1933	5.3-8	0	2
Shambaugh and Melnyk, 1970	9.0	25	1
Stumm, 1954	7.6-10.4	1.2-19.8	1
Weiss, 1935	2-8	0	3/2

Ozonation of municipal wastewater effluents (Hewes and Davison, 1971; Kirk et al., 1972) and industrial wastewaters such as photographic processing wastes (Bober and Dagon, 1975) and dye wastes (Snider and Porter, 1974) were studied with total organic carbon (TOC), chemical oxygen demand (COD), and/or color being the parameters monitored. Kirk et al. (1972) reported that the organic removal rate appeared to follow both first-order and second-order kinetics. The first-order rate is represented by the following equation:

$$\frac{d(COD)}{dt} = -K_1(COD) \tag{38}$$

where K_1 is the pseudo first-order rate constant, and (COD) is the concentration of COD at time t. The second-order rate expression is the following:

$$\frac{d(COD)}{dt} = -K_2(O_3)\ \ (COD) \tag{39}$$

where K_2 is the second-order rate constant, (O_3) is the dissolved ozone concentration at time t, and (COD) is the same as in the first-order expression. Figure 78 shows a semilogarithmic plot of K_1 and K_2 against the percentage of influent COD remaining, as reported by Kirk et al. (1972). Both reaction rate constants nearly fall on a straight line. This gross change in reaction rate constants reflects the spectrum of reactivities of the wastewater organics with ozone.

Models for Ozone Absorption and Simultaneous Chemical Reactions. Kuo et al. (1975) used the film theory in developing the following model to describe the batch absorption and decomposition of ozone in water that is well mixed:

$$\frac{d^2(O_3)_f}{dx^2} = \frac{k_r}{D_{O_3}}(O_3)_f^{3/2}, \quad 0 < x < \delta \tag{40}$$

Boundary conditions:

$$x = 0, \quad (O_3)_f = (O_3)^*$$

$$x = \delta, \quad (O_3)_f = (O_3)(t)$$

$$V\frac{d(O_3)}{dt} = -A\,D_{O_3}\left.\frac{d(O_3)_f}{dx}\right|_{x=\delta} - Vk_r(O_3)^{3/2}, \quad x \geq \delta \tag{41}$$

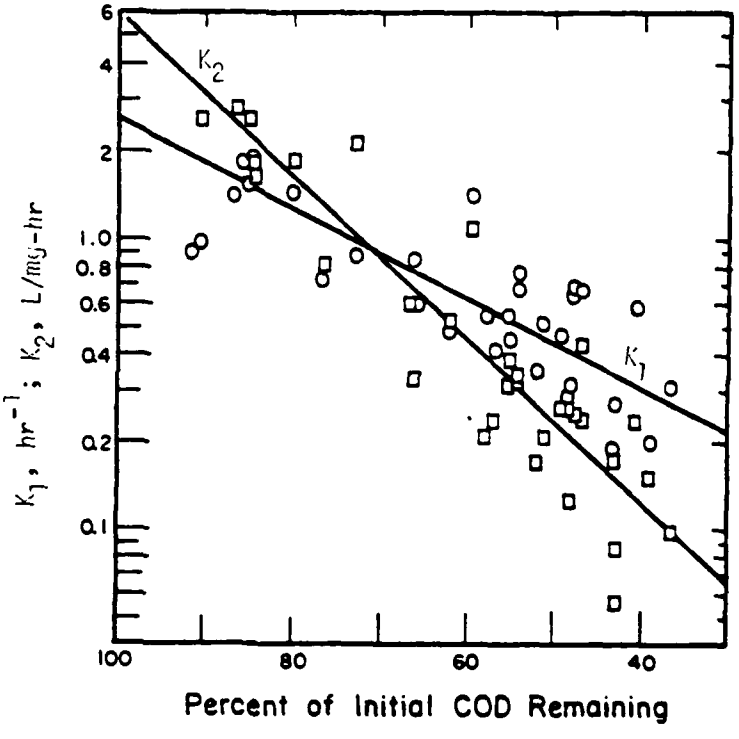

Figure 78. Variation of First-Order (K_1) and Second-Order (K_2) Reaction Rate Constants Calculated from COD Data for Lime-Clarified Raw Wastewater at a pH of 9.0 $\pm$ 0.3 (Kirk et al., 1972).

F Initial condition:

$$t = 0, \quad (O_3) = 0$$

where $(O_3)_f$ is the ozone concentration in the liquid film, (O_3) is the ozone concentration in the bulk liquid, $(O_3)^*$ is the concentration of ozone at the interface in equilibrium with gaseous ozone, A is the total interfacial area, and k_r is the decomposition rate constant for dissolved ozone. Because the above mathematical system is nonlinear, numerical solutions were obtained using the finite difference technique.

Dang and Steinberg (1976) used the following two-dimensional transient diffusion equation with a first-order chemical reaction for swarms of bubbles moving at low Reynolds numbers in a batch system:

$$\frac{\partial b}{\partial t} + V_r \frac{\partial b}{r} + \frac{V_\theta}{r} \frac{\partial b}{\partial \theta} = D_b \frac{\partial^2 b}{\partial r^2} - k_1 b \tag{42}$$

The initial conditions and boundary conditions are

$$b(0, r, \theta) = b_0$$

$$b(t, \infty, \theta) = b_0 e^{-k_1 t}$$

$$b(t, a, \theta) = b^*$$

where b is the concentration of the dissolved species. The velocity profiles for swarms of bubbles were established by Gal-Or and Yaron (1973). After solving the concentration distribution in the liquid phase, these authors evaluated the Sherwood number (N_{Sh}). They then continued to analyze the macroscopic absorption process by means of a quasi-steady-state approximation. The mass transfer coefficient, k_l, was obtained from the expression for N_{Sh} by allowing t to increase to infinity.

The general equation for absorption accompanied by chemical reactions based on Higbie's model (1935) may be written as:

$$D_b \frac{\partial^2 b}{\partial x^2} = \frac{\partial b}{\partial t} + \gamma(x,t) \tag{43}$$

$$D_c \frac{\partial^2 c}{\partial x^2} = \frac{\partial c}{\partial t} + \gamma(x,t) \tag{44}$$

where c is the concentration of the reacting species present in the liquid. For either flow or batch absorbers, a macroscopic material balance must be calculated based on the assumption that the chemical reactions are either slow or fast (Danckwerts, 1970).

The above discussion summarizes the possible approaches to solving theoretically the problem of ozone absorption and simultaneous chemical reactions. To use the model of Kuo et al. (1975) and that of Dang and Steinberg (1976), however, a different macroscopic material balance for flow absorbers is needed.

Mass Transfer Characteristics of Agitated Vessels

The basics of the four parameters characterizing mass transfer in sparged vessels hold true for agitated vessels as well. A brief review of the various correlations for d, h, a, and k_L in agitated vessels is presented in the following paragraphs.

Equation (4) was originally developed by Calderbank (1958) for correlating the bubble diameter in agitated vessels. The correlation for gas holdup, h, was presented by Calderbank (1958) as:

$$h = \left(\frac{hU_G}{U_G + U_t}\right)0.5 + 0.0216\left[\frac{(P/V)^{0.4}\rho^{0.2}}{\gamma^{0.6}}\right]\left(\frac{U_G}{U_t}\right)0.5 \qquad (45)$$

The interfacial area per unit volume of dispersion, a', is related to the power dissipated by the stirrer when operated at moderate speeds by the following expression (Calderbank, 1958):

$$a' = 1.44\left[\frac{(P/V)^{0.4}\rho^{0.2}}{0.6}\right]\left(\frac{U_G}{U_t}\right)0.5 \qquad (46)$$

To convert a' to interfacial area per unit volume of liquid, a, the following relationship can be used:

$$a = \frac{a'}{1 - h} \qquad (47)$$

To use the above correlations, it is necessary to know the power dissipated. The mechanical power input in a sparged, agitated system can be calculated from (Michel and Miller, 1962):

$$P/V = \frac{0.706}{V}\left(\frac{P_o^0 N D_s^3}{G_o^{0.56}}\right)0.45 \qquad (48)$$

where N is the impeller speed in revolutions per second; D_s is the impeller diameter in centimeters; and P_o is the ungassed power requirement, which can be obtained from

$$P_o = f \frac{N^3 D_s^5 \rho}{g_c} \tag{49}$$

The power factor f is available from the work of Rushton et al. (1950).

Westerterp et al. (1963) found that they could correlate their extensive data for a for turbine impellers by

$$\frac{aH_l}{1 - h} = 0.79\mu(N - n_0) D_s \left(\frac{\rho D}{\gamma}\right)^{1/2} \tag{50}$$

where

$$n_0 = \left(\frac{1.22}{D_s} + 1.25 \frac{D}{D_s^2}\right) \left(\frac{\gamma g}{\rho}\right)^{1/4} \tag{51}$$

The mass transfer coefficient k_L may be obtained from Equations (21) and (22). Miller (1974) has used a penetration theory expression to calculate k_L in his scale-up study:

$$k_L = \sqrt{\frac{4D_L}{\pi t_e}} \tag{52}$$

where t_e is assumed equal to the time it takes a bubble to rise one bubble diameter. A correction factor was incorporated into the calculated k_L to fit the experimentally determined k_L as given in Equation (42).

Objectives

It can be seen from the literature search that the various researchers disagree on the method of correlating the mass transfer characteristics of sparged vessels. It is difficult to justify choosing any one correlation over the others for use in the design of a sparged vessel. Moreover, because the physical properties of the system have a profound effect on the mass transfer characteristics, these quantities are difficult to predict by means of general formulas. Therefore, in designing sparged vessels for the ozonation process, it is desirable to first construct a small-scale model using the same gas-liquid system. A reliable method is then needed to scale up the results of measurements on the small-scale ozone-sparged vessel so that they can be used to predict the performance of a full-scale one. The typical approach to scaling up data on a heterogeneous reactor such as an ozone-sparged vessel is to formulate a suitably simplified mathematical model to represent the system, collect a body of laboratory data, and finally develop a scale-up method based on the model.

For a sparged vessel with fixed geometry and a fixed mean liquid residence time, the only major operational variables are the partial pressure of the reacting gas species and the superficial gas velocity. Both variables are important parameters to be considered in the design of a sparged vessel. Since no systematic studies of the effects of these two parameters on the performance of ozone-sparged vessels for organic removal have been reported in the literature, model experiments with ozone-sparged vessels should include studies of the effects of ozone partial pressure and superficial gas velocity on organic removal rates.

Since both sparged and agitated vessels are commonly used as the gas-liquid contacting equipment for dispersing sparingly soluble gases, a comparison of the performance of these two types of vessels would be of great interest to design engineers in selecting proper equipment for practical ozonation applications.

The model study reported here was undertaken to obtain information useful in the design of ozone-sparged vessels for the removal of organics from aqueous solutions. The specific objectives were: (1) to formulate a mathematical model for ozone-sparged vessels; (2) to determine the effects of the partial pressure of ozone and the superficial gas velocity on the performance of the sparged vessels; (3) to find a scale-up method for such vessels; and (4) to compare the performance of sparged vessels with that of agitated vessels.

Scope of Work

Ozone-sparged vessels used to treat an aqueous methanol solution were studied in the present work. The aqueous methanol solution was selected as the model compound for this ozonation study because: (1) methanol represents a common contaminant in the wastewaters from plastic and pharmaceutical industries; (2) methanol is likely to be found in wastewater treated by physical-chemical methods (such as the Army MUST hospital wastewater treatment process) since it is not effectively removed by either the activated carbon or the reverse-osmosis process; and (3) the reaction pathway of ozonating methanol in aqueous solution is well understood.

It has been reported that gaseous ozone is decomposed to a significant extent while passing through the diffuser (Perrich et al., 1975). Four different types of diffuser materials were therefore evaluated in this study to assess the degree of ozone decomposition through each of them. The most efficient diffuser was then selected for use in the rest of the experiments to facilitate data analysis.

A mathematical model was formulated for ozone-sparged vessels treating an aqueous methanol solution. The kinetics of the ozone decomposition reaction and the kinetics of the ozonation of methanol, formaldehyde, and formic acid in aqueous solutions were studied for use in the mathematical model. The latter two compounds are the intermediates resulting from the ozonation of methanol.

A laboratory-scale ozone-sparged column having a circular cross section was used in the experiments conducted to verify the model. The effect of the partial pressure of ozone and the superficial gas velocity on the performance of ozone-sparged vessels was determined using the same column.

A method for scaling up data on the performance of ozone-sparged vessels was developed through the use of the mathematical model. Experiments with two other columns of larger sizes were subsequently conducted to test the method developed for scaling up ozone contactors. Experiments were also conducted to confirm the results with different sizes of single-stage modified Torricelli ozone contactors having rectangular cross sections.

A comparison of the performance of sparged versus agitated vessels was made using a small sparged column and a laboratory-scale fermentor equipped with a stirrer.

Materials and Methods

Evaluation of Diffuser Materials

Four different diffuser materials, namely fritted glass, porous stainless steel, porous Teflon, and fused alumina, were evaluated in the laboratory to determine the percentage of ozone decomposition through each type of diffuser. Since the diffusers were obtained from different manufacturers, each one had a unique pore size. The fused alumina diffuser (Norton Co., Worcester, MA) had a pore size of 60 microns. The stainless steel diffuser (Paul Trinity Micro Co., Cortland, NY) had a pore size of 5 microns. The Teflon diffuser was made of 3/8-inch TB62 Gore-Tex tubing (W.L. Gore & Associates, Elkton, MD), which had a nominal pore size in the 1- to 2-micron range. The fritted glass diffuser was an ordinary laboratory diffuser with fine pores of undetermined size.

The percent of ozone decomposition through a diffuser can be determined by establishing a material balance around an ozone contactor in which the diffuser is used to disperse ozone into the liquid, providing that the ozone concentrations in the influent and effluent gas streams and in the liquid phase within the contactor are known. Since the liquid-phase ozone decomposition rate is slow at acidic and neutral pHs, the ozone decomposition percentages reported in this study were based on the difference between the influent and the effluent gaseous ozone concentrations only.

The experimental setup consisted mainly of an ozone contactor with gas lines leading from an ozone generator to the contactor and from the contactor to a vent. Relief valves were installed in both lines; the vent line also contained potassium iodide (KI) traps to remove ozone from the off gas prior to venting. All of the tubing, valves, and fittings were made of ozone-resistant materials, such as glass, Teflon, and stainless steel. The entire system was checked for leaks before it was put into operation.

The ozone contactor employed was a 4-liter fermentor (New Brunswick Scientific, New Brunswick, NJ). It was modified by sealing the stainless steel tubing leading to the sparger and installing a new gas line to fit the various diffusers. The pH of the aqueous solution was not adjusted during the experiment, nor was the solution in the contactor agitated. All experiments were conducted at room temperature, i.e., 23.5°C ± 1.0°C.

Experimental runs were conducted with the ozone reactor filled with distilled water, which was purged with purified N_2 at high temperature. While evaluating the different diffusers, the contactor was operated in a fashion similar to that of a bubble column.

Ozone was produced in a Welsback Model T-408 ozone generator (Philadelphia, PA) from tank oxygen. A trap using dry ice in 2-propanol was employed to remove moisture from the oxygen. Various nominal flow rates, as indicated by the built-in rotameter in the ozone generator, were set by using a needle valve to produce various ozone concentrations ranging from approximately 30 to 100 mg/L.

Two methods were used to determine ozone concentrations in the gas samples. An absolute physical method was tried first; it involved weighing a known volume of the gas at atmospheric pressure. A glass bulb was made for collecting and weighing the samples. The volume of the glass bulb was determined in the following manner: The average weight of the bulb when filled, in turn, with pure He, N_2, and O_2 was determined from at least three measurements for each gas. An equation based on the ideal gas law was then used to calculate the bulb volume from any two average weights. The He and N_2 pair and the He and O_2 pair gave very close results because of their greater difference in molecular weights. The average of these two results was taken as the volume of the glass bulb.

The glass bulb was made from a 300-mL boiling flask to which two side arms and valves were fused to facilitate operations. The weights were measured with a Sartorius Type 2403 analytical balance (Westbury, NY).

To use the absolute method for evaluating the diffusers, one glass bulb was placed in the influent line and one in the effluent line. A trap containing dry ice and 2-propanol was included in the effluent line prior to the glass bulb to remove moisture carried over from the contactor. A pressure gage was installed in front of each glass bulb to indicate the pressure in the bulb.

A chemical method was also used to determine ozone concentrations in the gas phase. The iodometric method employed involved the absorption of ozone into a 2% KI solution and titration with sodium thiosulfate (Standard Methods, 1971). The sodium thiosulfate titrant was standardized against potassium biniodate daily. In this experiment, the gas sample was introduced into two KI absorbers connected in series by means of a three-way valve, and a wet test meter was used to record the sample volume. Both the influent and the effluent gas samples were taken while evaluating the

diffusers. Duplicate tests were run for each diffuser. It was found that the first KI absorber absorbed more than 99% of the ozone present in the sample; the amount of sodium thiosulfate titrant needed for titrating the second KI absorber was negligible compared with that for the first one. As a result, the data were reported on the basis of the amount of titrant used in the first absorber only.

Kinetics of Ozonation of Methanol and Its Degradation Products in Aqueous Solution

Approach to Kinetic Study. The ozonation of an aqueous methanol solution results in the formation of formaldehyde, which, in turn, is oxidized to formic acid and finally to carbon dioxide. In the meantime, dissolved ozone undergoes decomposition via a reaction which is catalyzed by hydroxide ions in the aqueous solution. These reactions may be expressed as follows:

$$O_3 + CH_3OH \xrightarrow{k_{22}} HCHO + H_2O\ O_2 \tag{53}$$

$$O_3 + HCHO \xrightarrow{k_{22}} HCOOH + O_2 \tag{54}$$

$$O_3 + HCOOH \xrightarrow{k_{23}} CO_2 + H_2O + O_2 \tag{55}$$

$$2O_3 \xrightarrow{k_r} 3O_2 \tag{56}$$

The kinetics of the ozone decomposition reaction were studied by following the disappearance of dissolved ozone in ozone-demand-free water initially saturated with ozone. The ozone-demand-free water was prepared by ozonating distilled, deionized water for 15 minutes to oxidize any trace organic matter and then boiling it to dissipate the ozone residual.

Dissolved ozone concentrations were determined at selected intervals during batch ozonation of methanol. A number of runs were made using different initial methanol concentrations. Since only a small amount of methanol was depleted, the methanol concentration could be considered constant. The rate of disappearance of ozone may be expressed as:

$$\frac{d(O_3)}{dt} = - k_{21}\ (CH_3OH)^p(O_3)^q - k_r(O_3)^r$$

$$= - k_{21}'\ (O_3)^q - k_r(O_3)^r \tag{57}$$

Integration was then used to determine the values for k_{21}' and q with the known values of k_r and r obtained from the study of the ozone decomposition reaction. A plot of the apparent rate constant, k_{21}', versus methanol concentration on log-log graph paper was used to determine the reaction order, p, and the rate constant, k_{21}. A similar technique was employed to analyze the experimental results of batch ozonation of a formaldehyde solution to determine the kinetics of the reaction between ozone and formaldehyde.

Since the rate of the reaction between ozone and formic acid is greater than for the former two reactions, the kinetics of this reaction were studied using semi-batch ozonation of formic acid; i.e., ozone was fed continuously into an initial charge of aqueous formic acid solution. Samples withdrawn at 4-minute intervals were analyzed for dissolved ozone and TOC. The latter measurement was used to monitor the concentration of formic acid. Samples for TOC analysis were collected in test tubes containing one drop of a 5% KI solution to quench the dissolved ozone. A rate expression that is first order with respect to both ozone and formic acid was assumed in determining the rate constant using a trial-and-error curve-fitting method. The following set of ordinary differential equations was used in the data-fitting step. It was assumed in developing these equations that both the gas and liquid phases were well mixed.

$$\frac{d(HCOOH)}{dt} = - k_{23}(HCOOH)\ (O_3) \tag{58}$$

$$\frac{d\ C_{gout}}{dt} = \left(\frac{1-h}{h}\right)\frac{G_o}{V}\left(C_{goin}-C_{gout}\right) - \left(\frac{1-h}{h}\right) k_L a \left(D_i x C_{gout}-(O_3)\right) \tag{59}$$

$$\frac{d(O_3)}{dt} = k_L a \left(D_i x C_{gout}-(O_3)\right) - 4\ R_{HCOOH} - R_{O_3} \tag{60}$$

Initial conditions:

when $t = 0$, $(HCOOH) = (HCOOH)_0$, $C_{gout} = 0$, $(O_3) = 0$

where (HCOOH) is the concentration of formic acid in mg/L as carbon, (O_3) is the concentration of dissolved ozone in mg/L, k_{23} is the second-order rate constant in L/mg/minute, C_{gout} is the ozone concentration in the effluent gas at 1 atm in mg/L, C_{goin} is the ozone concentration in the influent gas at 1 atm in mg/L, G_o is the gas-flow rate at 1 atm in L/minute, V is the liquid volume in the reactors in liters, R_{HCOOH} is the rate of reaction between formic acid and ozone in mg of carbon/L/minute, R_{O_3} is the rate of the ozone decomposition reaction in mg/L/minute, and D_i is the distribution coefficient, which is defined as the ratio of the concentration of ozone in

water at a given temperature and pressure to the concentration of ozone in gas at the same temperature and pressure. The gas-flow rate can be considered constant because the amount of oxygen and ozone absorbed by the liquid was negligible compared with the total amount of gas flowing through the system. The $k_L a$ value was determined using the steady-state absorption data for the vessel in continuous operation. The D_i value used was 0.24, as reported in the literature (Manely and Niegowski, 1967). A subroutine, BLCKDQ, using a predictor-corrector formula of eighth order and a starting scheme based on Picard's method of successive substitution was called from the Math Science Library to solve the above three ordinary differential equations on the Cyber 175 (see Appendix IV).

Semi-batch ozonation of an aqueous methanol solution was conducted to check the kinetic data. Every 15 or 30 minutes during the course of ozonation, 20 mL of the solution were drawn for organic analysis. The experimental results were compared with the results predicted from the following set of differential equations using the kinetic information obtained previously:

$$\frac{d(CH_3OH)}{dt} = - R_{CH_3OH} \tag{61}$$

$$\frac{d(HCHO)}{dt} = R_{CH_3OH} - R_{HCHO} \tag{62}$$

$$\frac{d(HCOOH)}{dt} = - R_{HCOOH} + R_{HCHO} \tag{63}$$

$$\frac{d\, C_{gout}}{dt} = \frac{1-h}{h}\, G_o\, (C_{goin} - C_{gout}) - \frac{1-h}{}\, k_L a\, (D_i x C_{gout} - (O_3) \tag{64}$$

$$\frac{d(O_3)}{dt} = k_L a \left(D_i x C_{gout} - (O_3) \right) - 4 \left(R_{CH_3OH} + R_{HCHO} + R_{HCOOH} \right) - R_{O_3} \tag{65}$$

Initial Conditions:

when $t = 0$, $(CH_3OH) = (CH_3OH)_0$, $(HCHO) = 0$, $(HCOOH) = 0$, $C_{gout} = 0$, $(O_3) = 0$

where R_{CH_3OH} is the rate of reaction between methanol and ozone in mg of carbon/L/minute and R_{HCHO} is the rate of reaction between formaldehyde and ozone expressed in the same units. The gas phase and the liquid phase were assumed to be well mixed. The subroutine mentioned earlier was also used in solving these equations (see Appendix D).

Experimental. The kinetic studies for all reactions were performed in the 4-liter fermentor. The fermentor envelope was constructed of Pyrex glass; the top plate and interiors were constructed of stainless steel. The stirrer had three turbine wheels mounted on a central shaft, and each wheel contained six flat blades. The stirrer was driven by a 1/2-horsepower, variable-speed AC motor. Four equally spaced hollow baffles extended vertically down the inside walls of the fermentor. A constant liquid temperature of 25°C was maintained by circulating water through two of the interconnected hollow baffles from a separate water bath maintained at a constant temperature by a controller. Ozone gas produced from the Welsbach generator was introduced through a third hollow baffle via a single-orifice sparger below the bottom turbine. All experiments were conducted at a pH of 9 with a boric acid (0.05 M) and sodium hydroxide buffer system. The aqueous solutions were prepared using distilled, deionized water and reagent-grade chemicals. The stock formaldehyde solution was prepared using paraformaldehyde.

The gas-phase ozone concentration was determined by the iodometric method. The dissolved ozone concentration was determined by a UV spectrophotometric method (Shechter, 1973). Samples for dissolved ozone determinations were taken using a syringe partially filled with a neutral potassium iodide solution, and the absorbance of the liberated triiodide ion was measured at 352 nm using cells with a 1-cm light path in a Bausch & Lomb Spectronic 20 Colorimeter (Rochester, NY). A Beckman Model 915 TOC Analyzer (Fullerton, CA) was used for TOC determinations. Gas chromatographic (GC) analyses were performed on a HP 5750B gas chromatograph (Hewlett Packard, Palo Alto, CA) equipped with dual flame ionization detectors. A 6-ft x 1/4-inch outside diameter glass column packed with 0.2% Carbowax 1500 on 80/100 Carbopack C (Supelco, Bellefonte, PA) was used for determining methanol. The chromotropic acid method (Houle et al., 1970) was used to determine formaldehyde. The derivative-GC procedures of Bethge and Lindstroom (1974) were followed to determine formic acid. The benzyl ester from formic acid was determined on a 6-ft x 1/4-inch outside diameter glass column packed with 3% butane-1,4 diol succinate polyester on 100/120 AW Chromosorb W (Supelco).

Mathematical Model for Ozone-Sparged Vessel

Development of Mathematical Model. Several simplifying assumptions were made in developing the mathematical model for an ozone-sparged vessel treating a methanol solution. The justifications for these assumptions are discussed in this section and in the following chapter along with the experimental results.

Most researchers studying gas-sparged vessels have assumed a plug flow for the gas phase and a well-mixed condition for the liquid phase. Towell et al. (1965) have used the tracer technique to substantiate these assumptions for the sparged vessels operated at superficial gas velocities greater than those employed in this investigation. According to Yoshida and Akita (1965), liquid back-mixing is rapid in sparged columns. In the

liquid phase, a nearly uniform concentration from top to bottom was maintained at a superficial gas velocity of 0.661 cm/sec, which is lower than that used in the present study. Therefore, the same assumptions (plug flow of the gas phase and a well-mixed liquid phase) were used in the following treatment.

When an ozone-sparged vessel is used in treating a feed stream consisting of an aqueous methanol solution, the reaction mixture in the vessel is composed of methanol and its degradation products, namely, formaldehyde and formic acid. If the ozone decomposition reaction and the reactions between ozone and the three organic species are slow, only negligible amounts of ozone and organics may react in the liquid film; i.e., ozone absorption is not enhanced significantly by the simultaneous chemical reactions. Under these circumstances, the steady-state macroscopic material balances around a sparged vessel for each organic species, gaseous ozone, and dissolved ozone may be expressed by the following equations:

$$\frac{1}{\tau}(CH_3OH)_0 - R_{CH_3OH} - \frac{1}{\tau}(CH_3OH) = 0 \tag{66}$$

$$R_{CH_3OH} - R_{HCHO} - \frac{1}{\tau}(HCHO) = 0 \tag{67}$$

$$R_{HCHO} - R_{HCOOH} - \frac{1}{\tau}(HCOOH) = 0 \tag{68}$$

$$\frac{G_o}{V}(C_{goin}-C_{gout}) - k_L a \frac{D_i x(C^*_{goin}-C_{gout})}{\ln\left\{\frac{D_i xC^*_{goin}-(O_3)}{D_i xC_{gout}-(O_3)}\right\}} = 0 \tag{69}$$

$$k_L a \frac{D_i x(C^*_{goin}-C_{gout})}{\ln\left\{\frac{D_i xC^*_{goin}-(O_3)}{D_i xC_{gout}-(O_3)}\right\}} - A\,(R_{CH_3OH} + R_{HCHO} + R_{HCOOH})$$

$$- R_{C_3} - \frac{1}{\tau}(O_3) = 0 \tag{70}$$

where $(CH_3OH)_0$ is the methanol concentration in the feed solution in mg/L as carbon and C^*_{goin} is the ozone concentration in the influent gas at operating pressure in mg/L.

The rate of ozone decomposition reaction and the reaction rates of ozone with all organic species obtained from the kinetic study were used in these equations. The $k_L a$ value was determined from Equation (69) using the absorption data including C_{goin}, C_{gout}, and (O_3) determined in a separate run.

Once $k_L a$ was determined for a particular column operated at a fixed superficial gas velocity, the mathematical model represented by Equations (66) to (70) could be solved for (CH_3OH), (HCHO), (HCOOH), C_{gout}, and (O_3) under steady-state conditions. A subroutine, QNWT, from the Math Science Library based on a quasi-Newton algorithm was run on the Cyber 175 for this purpose (see Appendix B).

Laboratory experiments were conducted to test the mathematical model. Since only the concentration of the total organics in the effluent was of concern, the experimentally determined value for the percentage of TOC removal-instead of the percentage removals of the individual organic species-was compared with the predicted value from the mathematical model.

Effect of Chemical Reaction on Ozone Absorption. To verify the assumption that the mass transfer rate is not enhanced by the simultaneous chemical reactions, the following two equations based on the film theory were used to compute the concentration profiles and concentration gradients of dissolved ozone and TOC in the film.

$$D_{O_3} \frac{d^2 (O_3)_f}{dx^2} = R_{O_3} + R_{TOC} \tag{71}$$

$$D_{TOC} \frac{d^2 (TOC)_f}{dx^2} = SC \times R_{TOC} \tag{72}$$

Boundary conditions:

$$(O_3)_f = (O_3)^*, \; x = 0; \; (O_3)_f = (O_3), \; x = \delta$$

$$\frac{d(TOC)_f}{dx} = 0, \quad x = 0; \; (TOC)_f = (TOC), \; x = \delta$$

where R_{TOC} is the reaction rate between TOC and ozone, SC is the stoichiometric coefficient for ozone for the TOC and ozone reaction, and δ is the film thickness. R_{TOC} and SC were determined from the experimental results using a second-order expression, $R_{TOC} = k_2(TOC)\,(O_3)$. A subroutine, BVP,

for nonlinear boundary value problems in ordinary differential equations, which combines an initial value problem solver with a nonlinear-equation-solving program, was called from the Math Science Library to solve Equations (71) and (72). The enhancement factor 'E', defined as the ratio of the ozone concentration gradient at the surface to that at the inner boundary of the film, was also determined (see Appendix C).

Experimental. The experimental details are given in the following paragraphs. Methods for conducting tracer studies and $k_L a$ determinations are also discussed.

An ozone-sparged column with a liquid height-to-diameter ratio of 4 was constructed from Plexiglas with provisions for operating it with either concurrent or countercurrent flow. However, almost all of the experiments were conducted with countercurrent flows, for reasons to be given later. The inside diameter of the column was 4 inches, and the liquid capacity was 3.3 liters. A stainless steel porous plate with a pore size of 5 microns was installed at the bottom of the column. The column was operated at ambient temperature, i.e., 23.5° ± 2°C.

Large batches of methanol solution were prepared before each run using deionized water and reagent-grade methanol. Boric acid was added to the batch to give a concentration of 0.05 M, and the pH was adjusted to 9 by adding sodium hydroxide. This buffer system proved very effective in maintaining the reaction mixture at a constant pH of 9. Various concentrations of methanol ranging from 15 to 35 mg/L as carbon were used. At least two runs were made for each feed concentration.

The methanol solution was fed into the column using a Cole Parmer tubing pump (Chicago, IL), whereas the effluent from the column flowed by gravity. The flow rates were registered by two rotameters (Matheson Co., Inc., East Rutherford, NJ). A constant liquid residence time of 20 minutes was employed for all the experiments.

The Welsbach generator was used to supply ozone to the column. Tank oxygen passed through a molecular sieve column supplied the feed gas to the generator. Gas-flow rates were regulated by a built-in rotameter in the generator. A constant gaseous ozone concentration of 13.1 mg/L and a constant superficial gas velocity of 0.762 cm/sec were maintained for all runs.

An equilibrium period of four retention times was allowed to establish steady-state conditions before testing of the ozone-sparged column's performance was initiated. The performance of the column was monitored by measuring the gas-phase and liquid-phase ozone concentrations as well as the concentrations of TOC in the influent and effluent streams.

A rectangular vessel with dimensions of 5 cm x 60.5 cm x 78.6 cm was constructed from Plexiglas. The volume of this vessel was scaled on a 1:2.5 ratio from that of the modified Torricelli ozone contactor designed for the MUST project. The same type of porous stainless steel was installed at the bottom of the vessel. The vessel has a liquid volume of 22.09 liters. Similar experiments were conducted with this vessel as with the column.

Tracer studies in the liquid phase of the column were performed to demonstrate that the liquid phase was close to being well mixed. Sodium chloride was used as the tracer. A YSI Model 31 conductivity bridge (Yellow Spring, OH) was used to determine the salt concentration. The residence time distribution curves of the column were determined with step- and pulse-tracer inputs.

The overall mass transfer coefficient, $k_L a$, for ozone absorption was determined not only from the absorption data, but also from the overall oxygen transfer coefficient using the following relationship:

$$\frac{(k_L a)_{O_2}}{(k_L a)_{O_3}} \quad \frac{\text{Molecular Weight of } O_3}{\text{Molecular Weight of } O_2}^{1/2}$$

The unsteady-state method was employed for determining the overall oxygen transfer coefficient. A YSI Model 54 oxygen meter and a Sargent Model SRG strip-chart recorder (Skokie, IL) were used for this purpose.

Effect of Operational Variables on Performance of Ozone-Sparged Vessel

The operational variables investigated were the partial pressure of ozone and superficial gas velocity. The effect of the direction of flow and the liquid residence time were also examined.

The 3.3-liter column was used for this portion of the experiment. An aqueous methanol solution at a concentration of 30 mg/L as carbon was used as the feed to the column. The liquid residence time was maintained at 20 minutes.

Various gas-phase ozone concentrations at a superficial gas velocity of 0.762 cm/sec were obtained by adjusting the power input to the Welsbach generator or a W.R. Grace LG-2-L2 (Baltimore, MD) ozone generator. Different superficial gas velocities at a gas-phase ozone concentration of 13.1 mg/L were realized by varying the gas-flow rates with suitable power inputs.

The same parameters as mentioned in the previous section were monitored. The experimental results were compared with those predicted by the mathematical model. A power relationship between $k_L a$ and superficial gas velocity was determined from the experimental data.

Scaling-Up of Ozone-Sparged Vessel

Following the development of the mathematical model and the acquisition of the laboratory data, the problem of scaling-up the results was addressed.

Similarities in system geometry and fluid properties were adhered to while studying the scaling-up of ozone-sparged vessels. In addition to the 3.3-liter column, a column with a diameter of 5.5 inches and one with a diameter of 7.5 inches, having liquid capacities of 8.55 and 21.69 liters, respectively, were used in conducting these experiments. The same liquid residence time-20 minutes-was maintained in experiments with these columns.

For ozone-sparged vessels operated at a fixed partial pressure of ozone, the scale-up process is a matter of determining the gas-flow rate and thus the superficial gas velocity required in the larger vessel to achieve the same performance as in the smaller vessel. The scale-up procedure with the three columns was first tested based on an equal superficial gas velocity, as suggested by Sharma and Mashelka (1968). Based on the mathematical model formulated in this study, a computer program taking into consideration the relationship between $k_L a$ and superficial gas velocity was used to calculate the required superficial gas velocity for the scaled-up columns. Experiments were performed with the two larger columns at the calculated superficial gas velocities to examine this scale-up method.

Another vessel scaled on a 1:2.15 volume ratio from the modified Torricelli ozone contactor was constructed and used to further test the validity of the scale-up method. The vessel had a liquid capacity of 35.34 liters.

Comparison of Ozone-Sparged Vessel with Agitated Vessel

In this comparison, the 4-liter fermentor was used as the agitated vessel. Different levels of power input to the fermentor were achieved by varying the rotational speed of the impellers, which was measured with a hand tachometer (James G. Biddle Co., Plymouth Meeting, PA). The feed to the agitated vessel was a methanol solution with a concentration of 30 mg/L as carbon. The values of liquid volume, liquid mean residence time, and gas-flow rate maintained for the agitated vessel were equivalent to those for the 3.3-liter sparged column. Since the cross-sectional areas of the two vessels were different, different superficial gas velocities resulted even at the same gas-flow rate per unit liquid volume.

The performance of the agitated vessel at different power inputs was compared with that of the sparged vessel. A modification of the mathematical model for the sparged vessel was used to fit the experimental results obtained from the agitated vessel.

RESULTS AND DISCUSSIONS

Evaluation of Diffuser Materials

The absolute method for ozone determination was employed when testing the fritted glass diffuser. The experimental results were erratic, perhaps because a small variation in the weight measurement can introduce a significant error in the calculation of the ozone concentration, especially when the gas samples contain a low level of ozone-e.g., 1 to 4% ozone by weight.

The accuracy of the absolute method may be improved if the ozone concentration is increased. However, the ozone decomposition results thus obtained may not be extrapolated to the low ozone concentrations commonly used in practical ozonation applications.

It was further found that the ozone concentration in the influent gas determined by the absolute method was higher than that determined by the iodometric method, as shown in Table 55. The flow rates reported in column 2 of Table 55 are nominal flow rates read from the built-in rotameter on the ozone generator. The obvious overestimation of the ozone concentrations with the absolute method led to a switch to the iodometric method.

TABLE 55. COMPARISON OF ABSOLUTE METHOD AND IODOMETRIC METHOD

Pressure (psi)	Flow Rate (L/min)	Weight Percent	
		Absolute Method	Iodometric Method
5.5	2.5	5.89	2.09
5.0	0.5	9.58	4.41

In the iodometric method, the absorption of O_3 is usually accomplished by dispersing the gas sample through a sintered glass diffuser to a KI solution in a fritted gas-washing bottle. Since this method of absorption involves the use of a diffuser, the question of whether that device would introduce any unidentifiable errors was raised. Therefore, a Dreschel gas-washing bottle was substituted for the fritted gas-washing bottle. The Dreschel bottle has essentially the same features as the fritted bottle except that it uses as the gas bubbler a straight length of glass tubing with an inside diameter of 4 mm.

The O_3 concentrations in the influent gases from the ozone generator at various flow rates determined using the two different gas-washing bottles are shown in Table 56. There is only a slight difference between the two sets of measurements, probably due to experimental errors. These results indicate that ozone does not decompose when it passes through the glass diffuser. Nevertheless, the Dreschel gas-washing bottles were adopted for the later experiments.

TABLE 56. COMPARISON OF FRITTED GAS-WASHING BOTTLE AND DRESCHEL GAS-WASHING BOTTLE USING IODOMETRIC METHOD

Ozone Concentration (mg/L)	
Fritted Gas-Washing Bottle	Dreschel Gas-Washing Bottle
32.18	31.32
32.78	39.75
44.38	53.42
47.76	57.25
86.27	83.24
85.50	85.02
101.50	102.46
91.89	104.58

Since more gaseous-phase ozone could be decomposed catalytically by the diffuser material at low flow rates when the contact time and the ozone concentration are greater, the evaluation of stainless steel, Teflon, and fused alumina diffusers was conducted at a flow rate of only 0.5 L/min. The results are shown in Table 57. The observed 2 to 5% differences in ozone concentration between the influent and the effluent gas samples may result from liquid-phase ozone decomposition.

This study indicates that none of the diffusers decompose the gas-phase ozone to a significant extent. Because of its physical strength and machinability, the stainless steel diffuser was chosen for use in the sparged column for the later experiments.

Kinetics of Ozonation of Methanol and Its Degradation Products in Aqueous Solution

The decomposition of dissolved ozone clearly follows first-order reaction kinetics, as can be seen in Figure 79. The rate constant was found to be 0.01006 sec^{-1}, and the half-life was 68.9 seconds at a pH of 9 and a temperature of 25°C. These results are identical to the data extrapolated from the work of Czapski et al. (1968) and are close to those of Shambaugh and Melnyk (1976).

TABLE 57. RESULTS OF EVALUATION OF STAINLESS STEEL, TEFLON, AND FUSED ALUMINA DIFFUSERS AT HIGH OZONE CONCENTRATION

Type of Diffuser	Influent Concentration (mg/L)	Effluent Concentration (mg/L)	Percent Decomposition
Stainless steef diffuser	87.50	82.84	5.3
Stainless steel diffuser	85.30	82.66	3.1
Teflon diffuser	77.67	74.79	3.7
Teflon diffuser	79.09	76.44	3.4
Fused alumina diffuser	78.74	76.65	2.7
Fused alumina diffuser	79.99	78.22	2.2

Dissolved ozone concentrations as a function of time in batch ozonation for four different levels of methanol concentrations are plotted on a semi-logarithmic scale in Figure 80. The straight-line fit indicates that the reaction between ozone and methanol is first order with respect to ozone. In Figure 81, the logarithms of apparent rate constants (k_{21}'s) are plotted against the logarithms of the corresponding methanol concentrations. The slope, which represents the order of reaction with respect to methanol, is 1. The rate constant, k_{21}, was found to be 7.58×10^3 L/mole/minute.

Results obtained from the ozonation of formaldehyde at various concentrations are presented in Figures 82 and 83. It appears that a first-order kinetic with respect to ozone and a first-order kinetic with respect to formaldehyde adequately describe the reaction between ozone and formaldehyde. The rate constant, k_{22}, for this reaction was determined to be 8.4×10^3 L/mole/minute.

An attempt to follow ozone concentrations during batch ozonation of formic acid failed because of the large rate constant for this reaction. Figure 84 shows the results of semi-batch ozonation of formic acid. The curves in Figure 84 are concentration profiles predicted by solving equations (58) to (60) with a second-order rate constant, k_{23}, of 5.26×10^4 L/mole/minute; the symbols represent the experimental data points.

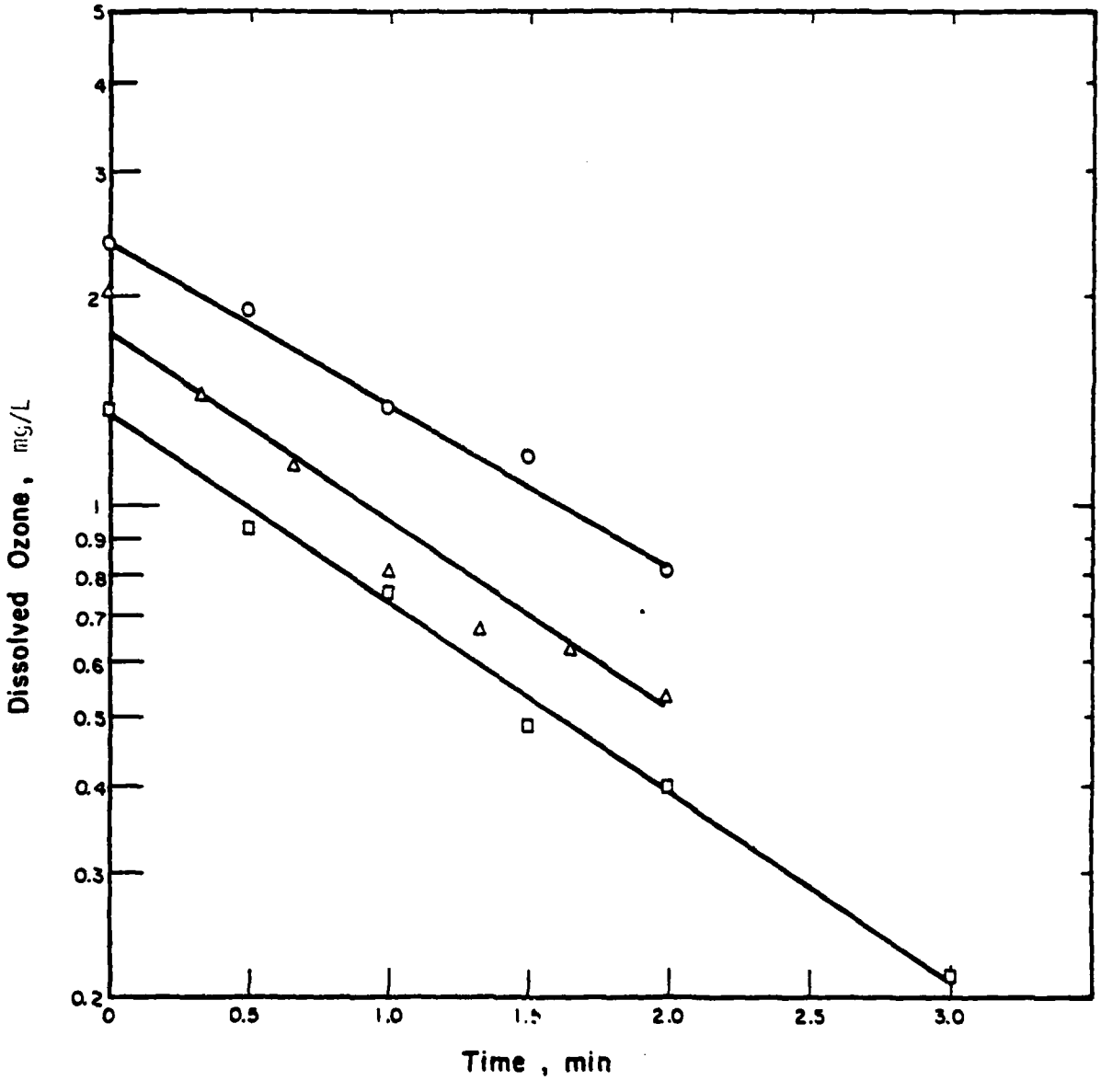

Figure 79. Ozone Decomposition as Function of Time (25°C, pH 9).

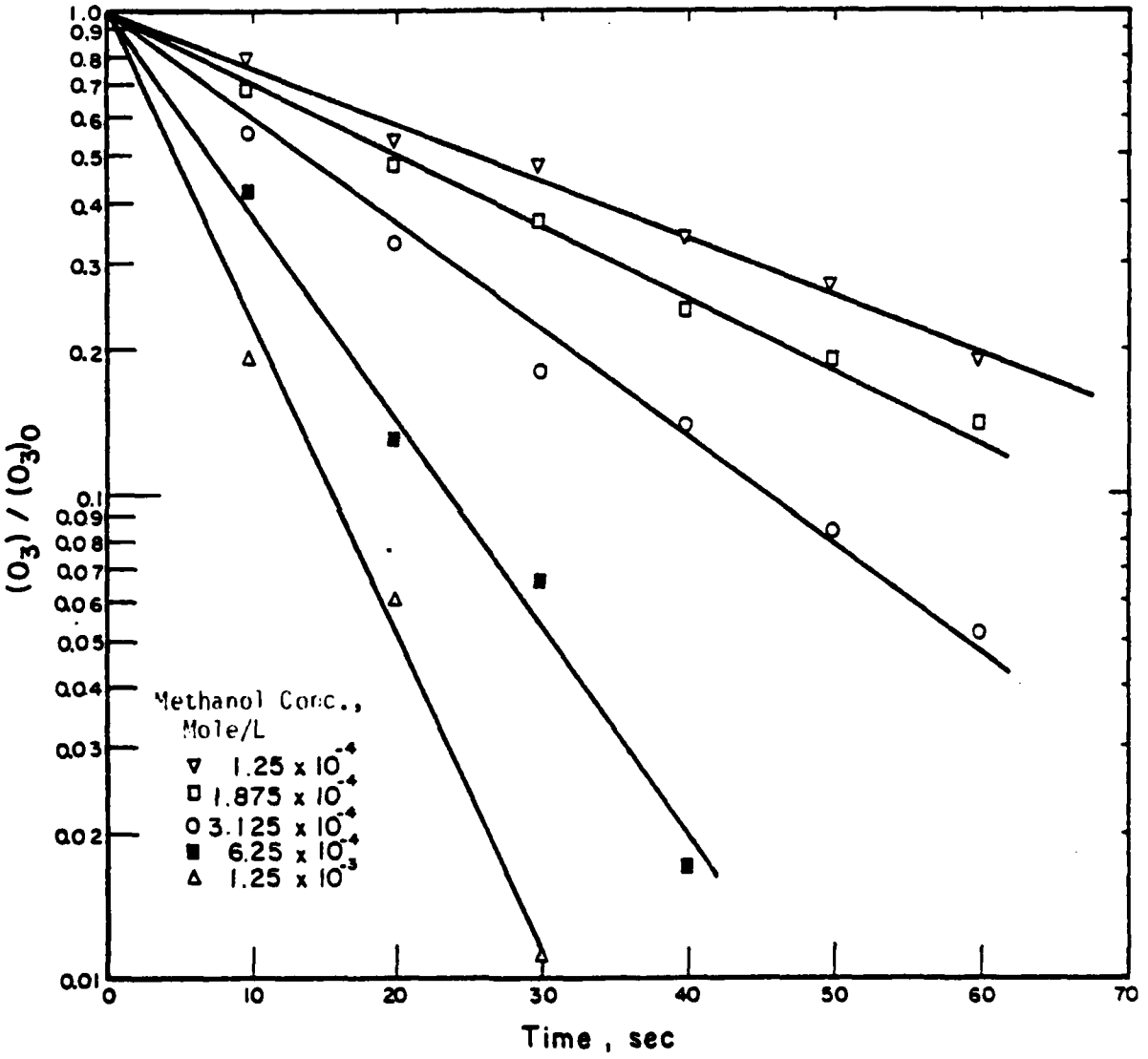

Figure 80. Determination of Reaction Order with Respect to Ozone for Ozone-Methanol Reaction (25°C, pH 9).

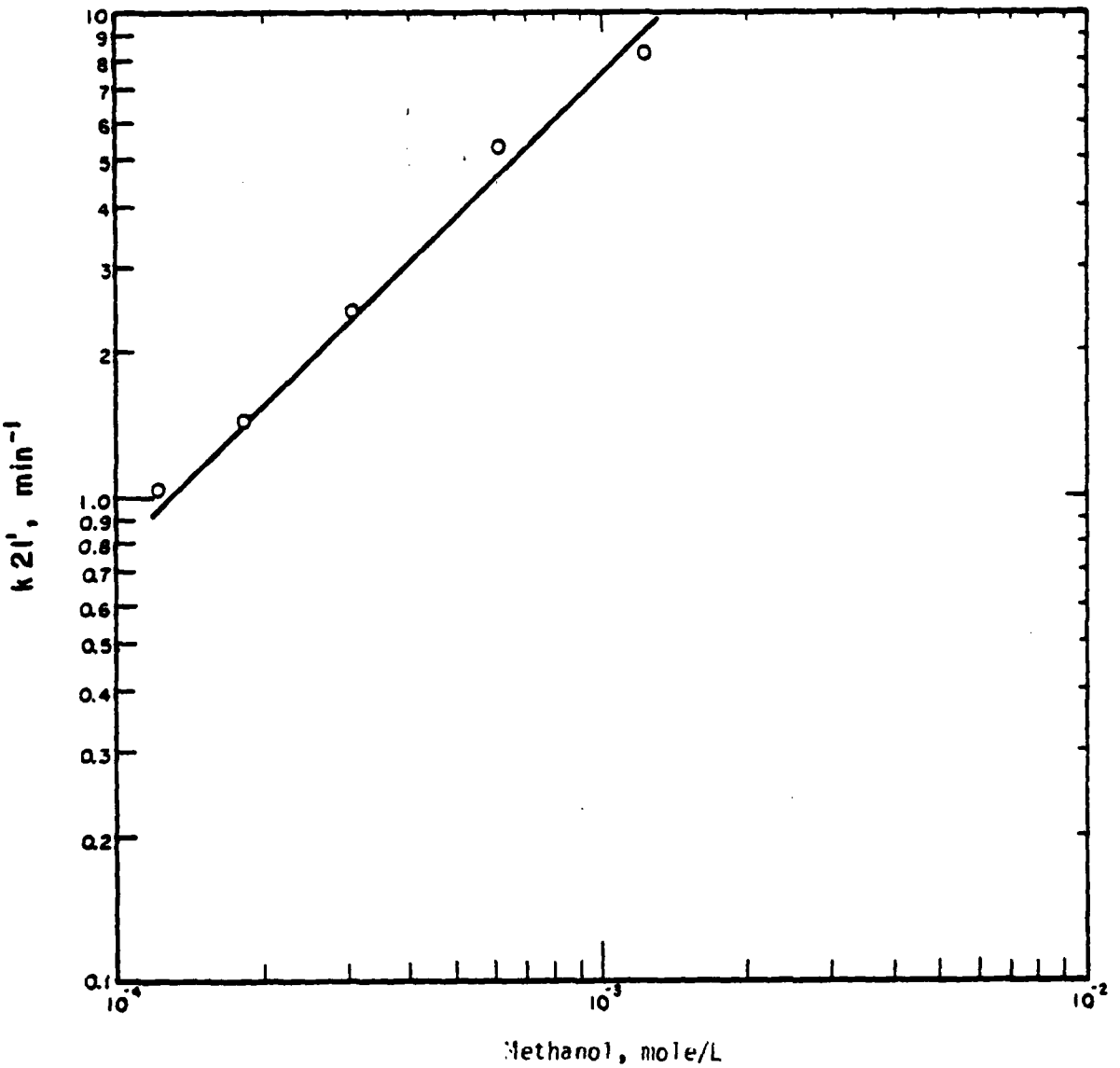

Figure 81. Determination of Reaction Order with Respect to Methanol (25°C, pH 9).

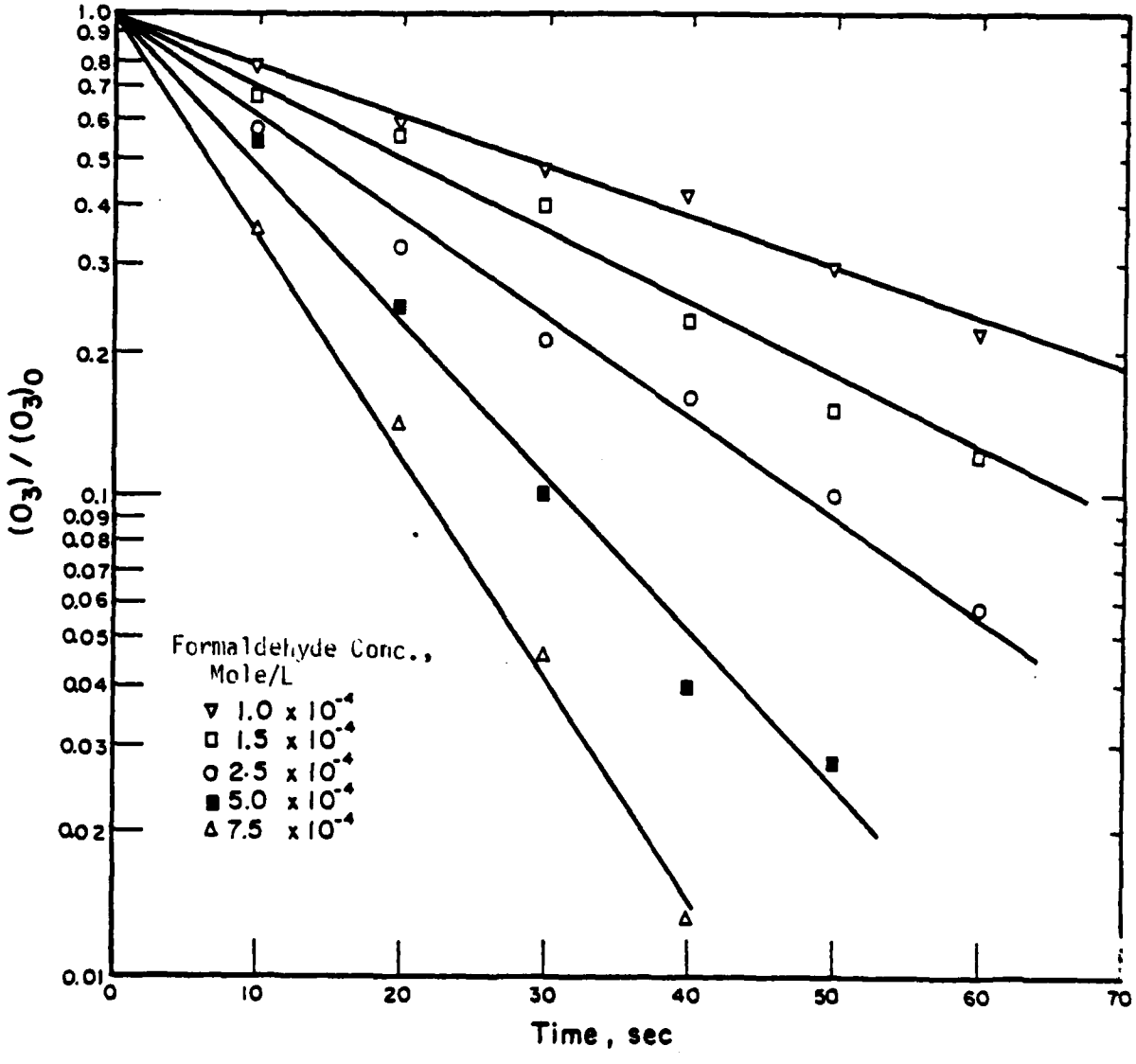

Figure 62. Determination of Reaction Order with Respect to Ozone for Ozone-Formaldehyde Reaction (25°C, pH 9).

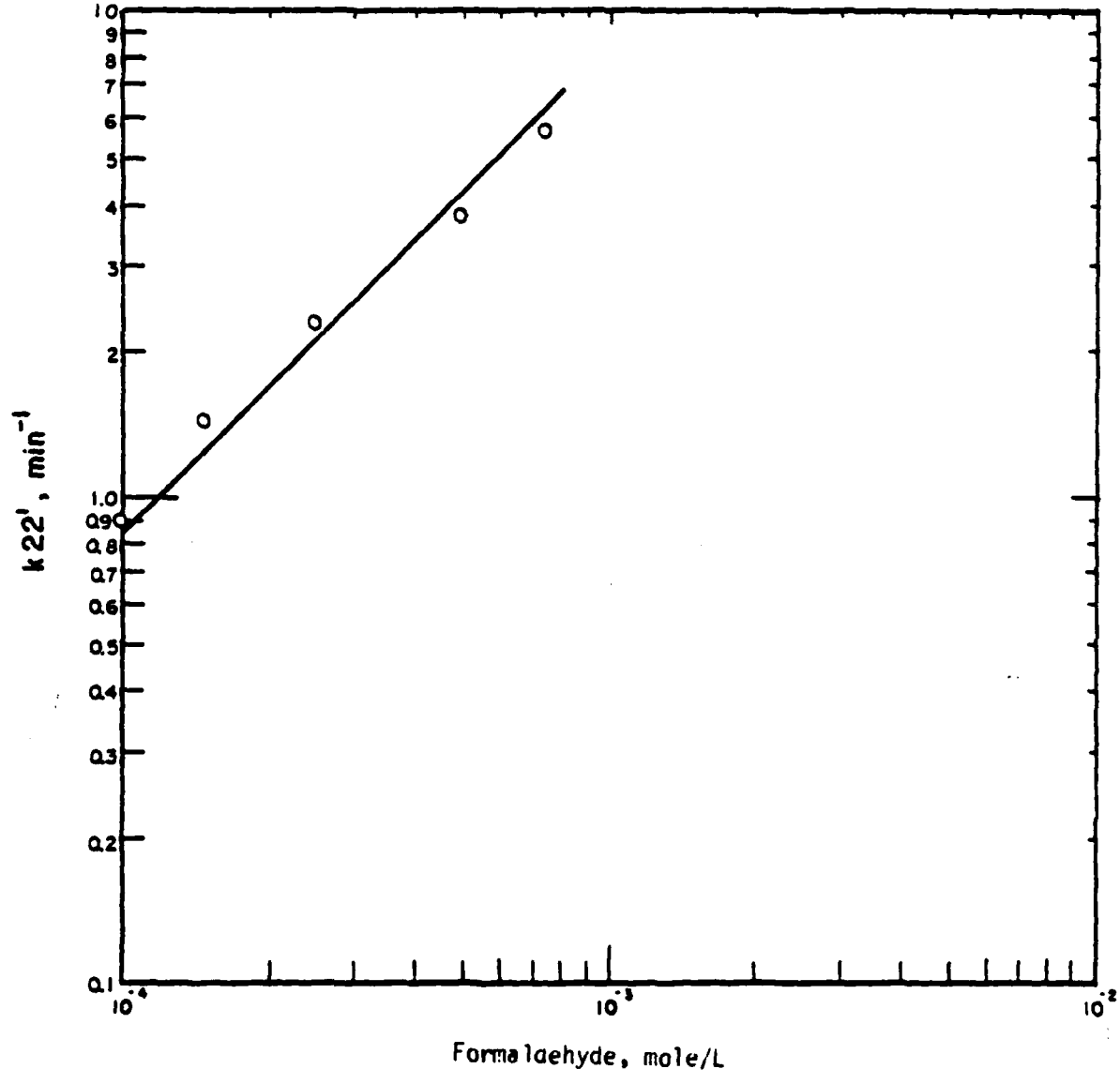

Figure 83. Determination of Reaction Order with Respect to Formaldehyde (25°C, pH 9).

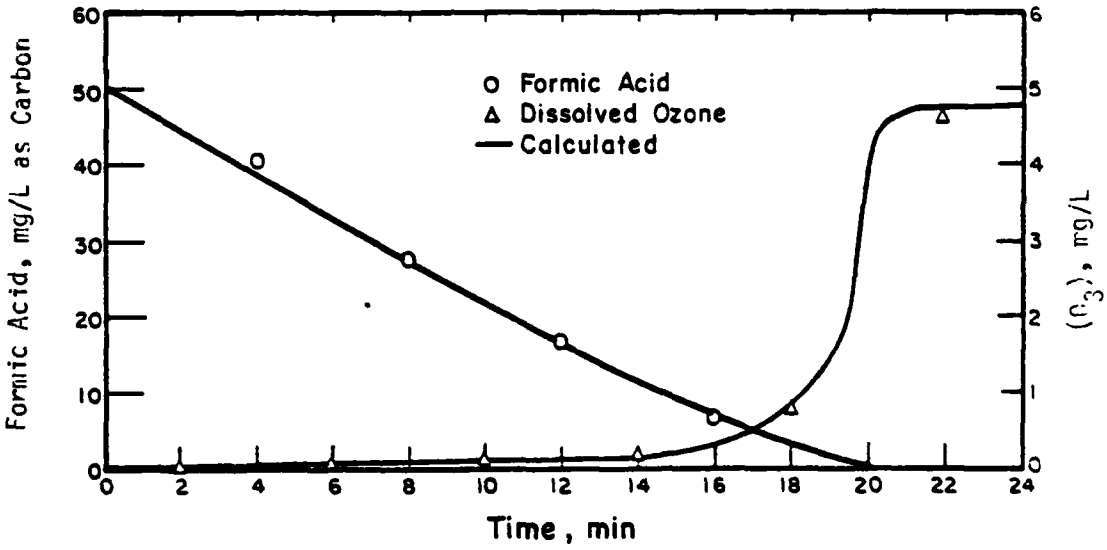

Figure 84. Semi-Batch Ozonation of Formic Acid in Aqueous Solution (25°C, pH 9).

The results of the semi-batch ozonation of a methanol solution are shown in Figure 85. The predicted concentrations of each organic species and that of TOC calculated using the previously obtained rate expressions seem to be in good agreement with the experimental data.

It is difficult to compare the kinetic results of the ozonation of methanol, formaldehyde, and formic acid obtained in this study with those of Kuo and Wen (1976) because those authors did not conduct their experiments at a pH of 9. The kinetic results reported by Kuo and Wen (1976) may be summarized as follows: The reaction between ozone and methanol follows first-order kinetics with respect to methanol and three-halves- to one-half-order kinetics with respect to ozone as pH values of the aqueous solutions increase from 7.2 to 11.0; the kinetics of the reaction between ozone and formaldehyde are one-half order with respect to ozone and first order with respect to formaldehyde; the kinetics of the ozonation of formic acid are first order with respect to formic acid, but the order with respect to formic acid changes from 1.2 to 0.74 as the pH varies from 2.7 to 11.0. Therefore, the reaction orders determined in this study are comparable to those reported by Kuo and Wen (1976) with the exception that the kinetics of the reaction between ozone and formaldehyde is first order in ozone in this study. The rate constants in the two studies cannot be compared because of the difference in units caused by the slightly different reaction orders reported. However, both studies agree that the ozonation of formic acid is the fastest among all of these reactions and that the rate of ozonation of methanol is on the same order of magnitude as that of formaldehyde. Consequently, the second-order rate constant for TOC removal would gradually increase with time in the ozonation of a methanol solution when the reaction mixture shifts toward more oxidized forms. This behavior is different from that which would be experienced in ozonating wastewater containing assorted organics. There the rate constant would decrease with time because the easily oxidized organics would be removed first and the refractory ones would be left at the end.

Mathematical Model for Ozone-Sparged Vessel

Verification of Mathematical Model. The effluent responses to the step- and pulse-tracer inputs are shown in Figures 86 and 87, respectively, for the 3.3-liter column operated at a superficial gas velocity of 0.762 cm/sec. The assumption that the liquid is well mixed seems justified. This assumption is further supported by the later findings that the mathematical model gives a satisfactory fit to the data obtained from operating the column.

It is likely that some degree of mixing in the gas phase may exist. The error introduced by using the logarithmic mean driving force in this study should be only a few percent since the mole fraction of ozone in the effluent gas was always over 50% and was about 70% of that in the influent gas in most cases.

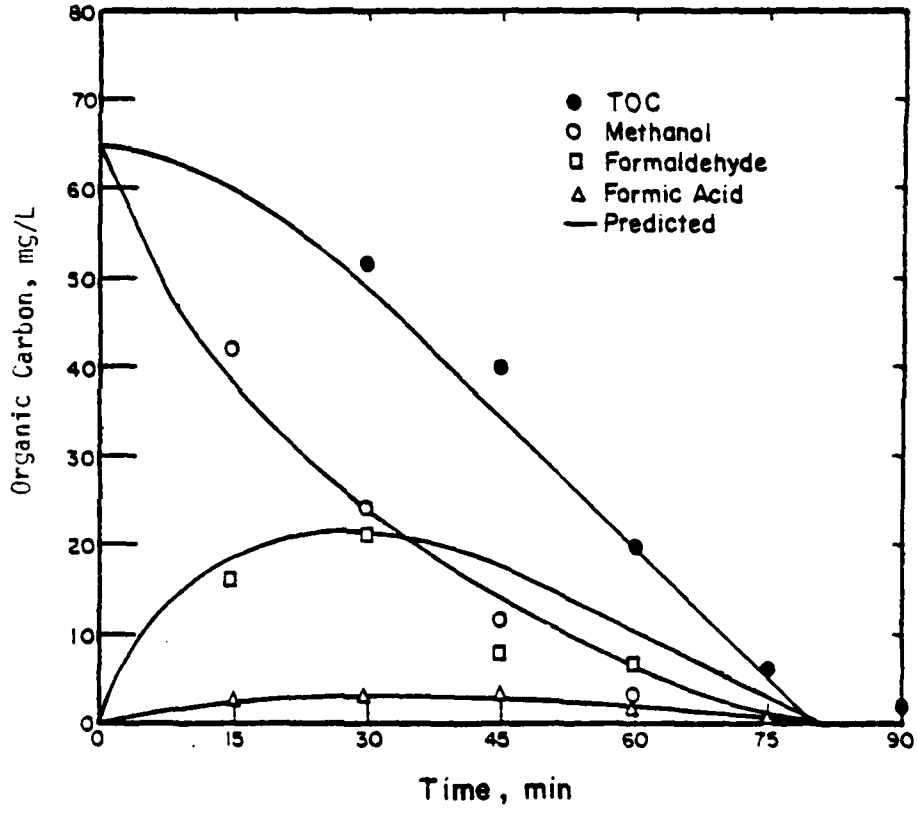

Figure 85. Semi-Batch Ozonation of Methanol in Aqueous Solution (25°C, pH 9).

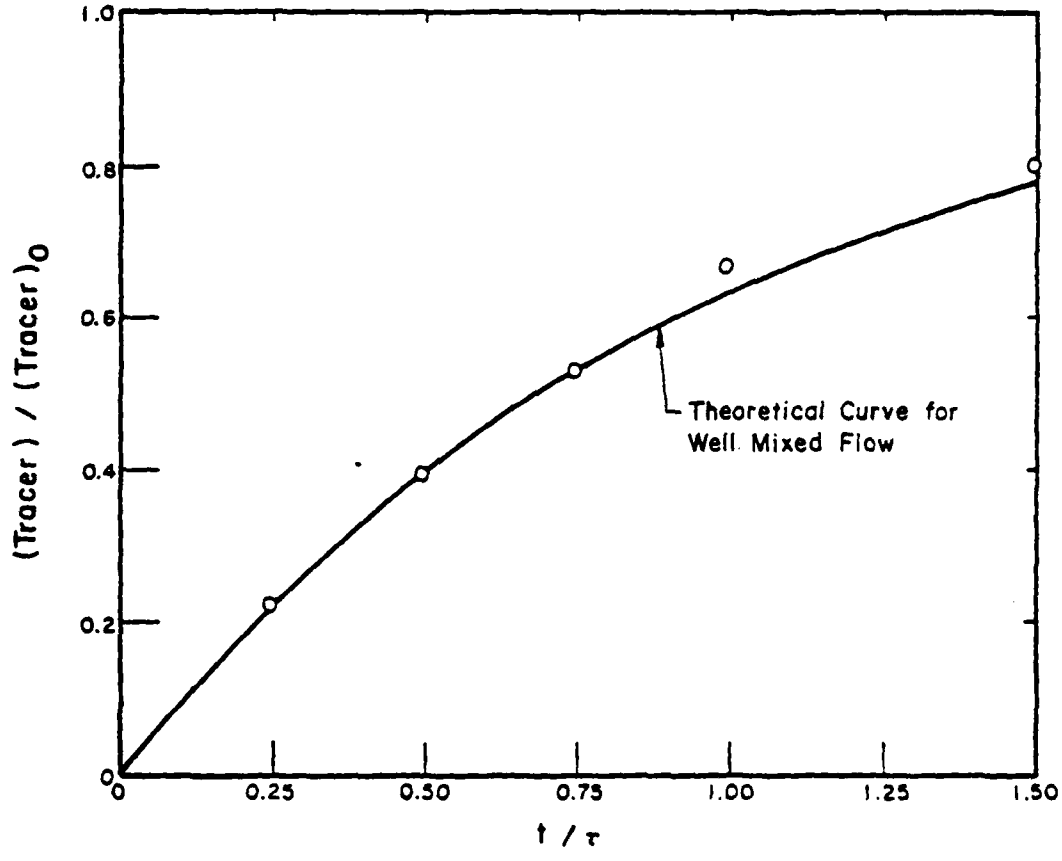

Figure 86. Response to Step-Tracer Input.

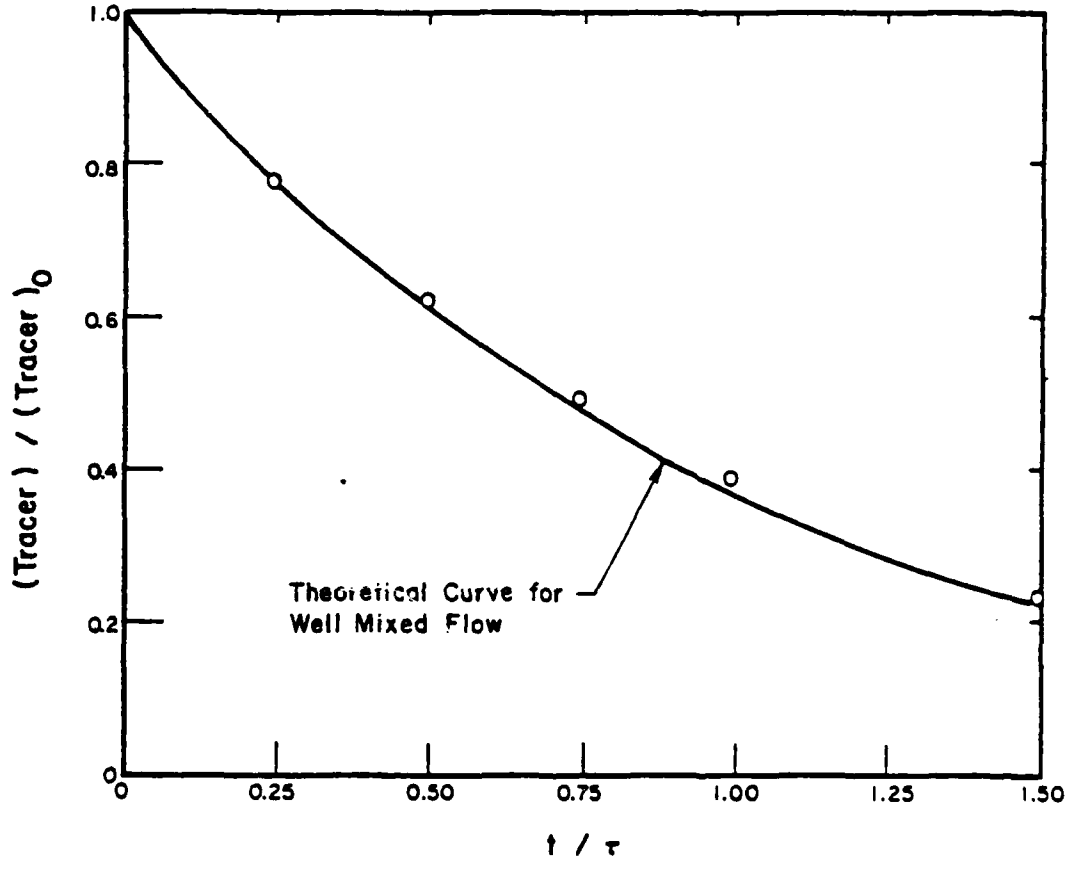

Figure 87. Response to Pulse-Tracer Input.

Figure 88 shows the percentage of TOC removal of a countercurrent run at various times after the onset of the operation of the column. It is apparent that a steady state is reached after four liquid residence times. In another test, the steady-state TOC removal of a concurrent run showed that no differences could be discerned between the two modes. This result was not unexpected because the liquid may be considered well mixed in the range of superficial gas velocities used in this study. This observation is also consistent with the report that the direction of liquid has no bearing on the mass transfer characteristics of a sparged vessel (Akita and Yoshida, 1973). As a result, all later runs were operated only with countercurrent flows.

The steady-state percentage TOC removals, percentage gas-phase ozone absorptions, and dissolved ozone concentrations are shown in Figures 89, 90, and 91, respectively, as a function of the concentrations of methanol in the feed solution. It can be seen from the predicted curves that the mathematical model satisfactorily describes the performance of an ozone-sparged column used to treat a methanol solution. Moreover, an examination of the composition of the effluent in one test gave the following results: methanol, 15.8 mg/L as carbon; formaldehyde, 7.2 mg/L as carbon; formic acid, 0.7 mg/L as carbon, which compares favorably with the corresponding concentrations of each organic species as predicted by the model, i.e., 16.3, 6.6, and 0.9 mg/L. It should be pointed out that the formic acid concentration was obtained by subtracting the concentrations of methanol and formaldehyde from the TOC concentration.

Measurements of percentage TOC removal in a similar test conducted with the 22.09-liter vessel having a rectangular cross section are shown in Figure 92. The mathematical model again gave satisfactory predictions in this case.

Effect of Chemical Reaction on Ozone Absorption. The second-order rate constant, k_2, and the stoichiometric coefficient for the reaction between TOC and ozone was determined to be 2.017×10^3 L/mole/minute and 4.36, respectively, for the case where the concentration of the methanol solution fed to the column was 30 mg/L as carbon. This rate expression was used in Equations (71) and (72) to find the concentration profiles and gradients of dissolved ozone and TOC in the liquid film at the bottom of the column where the driving force for mass transfer is the greatest. The results are shown in Table 58. The interesting fact is that the TOC concentration is constant within the film, and the ozone concentration gradients change very little from the gas-liquid interface to the interface between the liquid film and bulk liquid. Since the ozone concentration profile in the film is almost a straight line, the rate at which the unreacted ozone diffuses out of the film into the bulk is essentially the same as the rate at which it diffuses into the film from the gas-liquid interface. This result implies that the absorbed ozone is transferred unreacted to the bulk and that all reactions occur in the main body of the liquid. The enhancement factor is calculated to be 1.004, which indicates that the ozone absorption in this study can be described as a purely physical process where the liquid film provides resistance to the transfer of ozone.

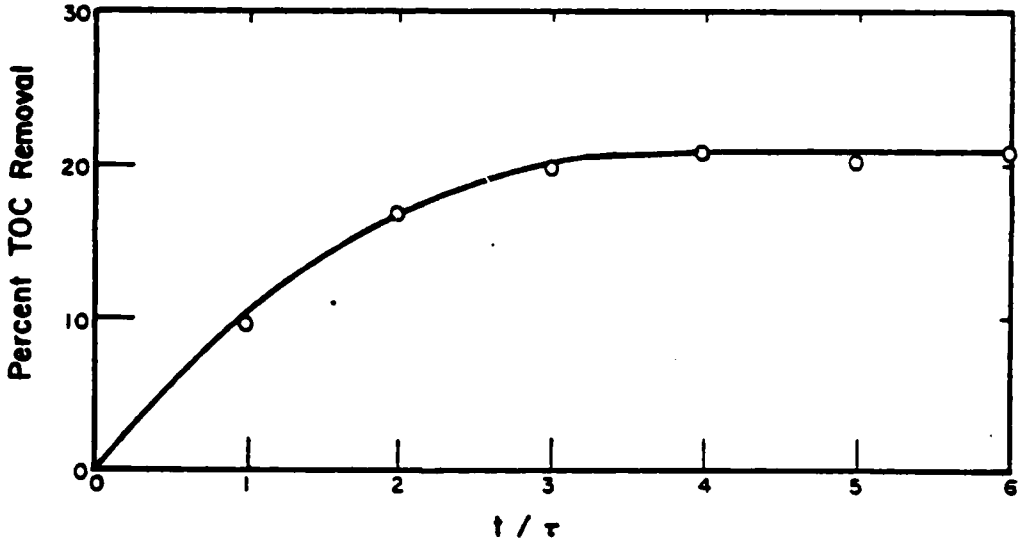

Figure 88. Determination of Steady State.

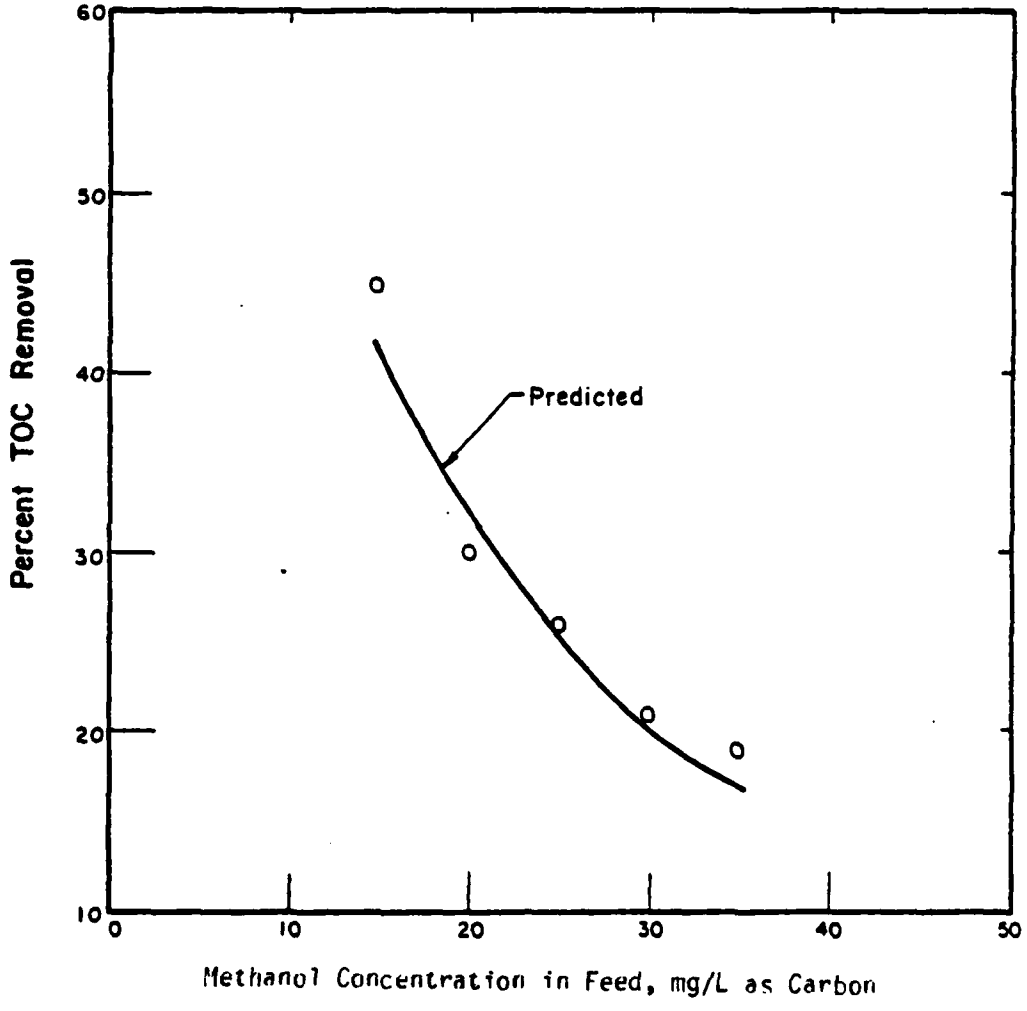

Figure 89. Percent TOC Removal vs. Methanol Concentration in Feed.

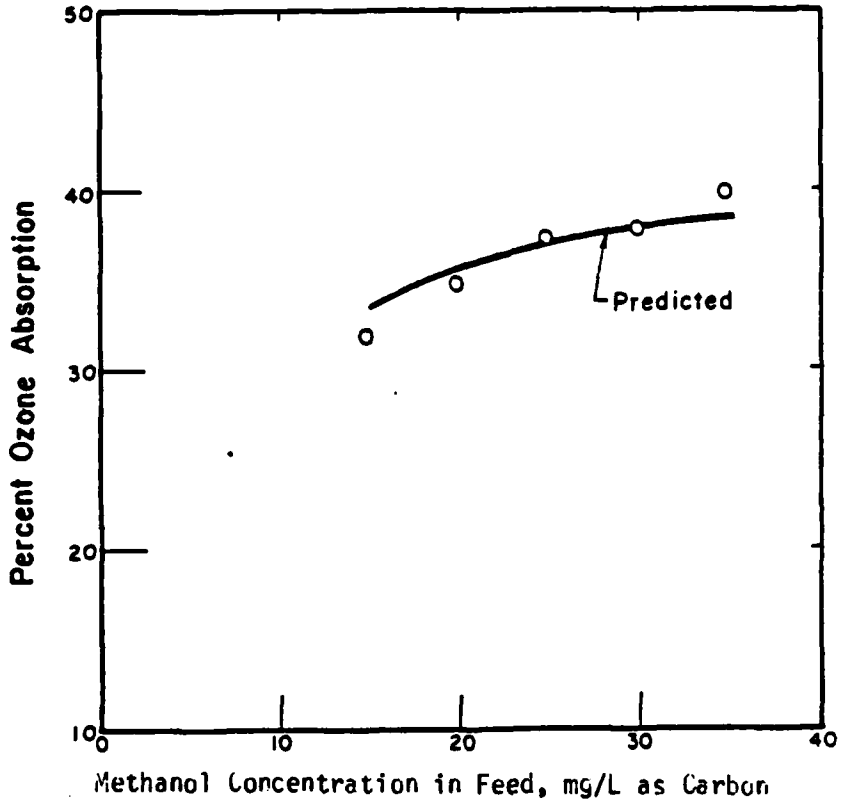

Figure 90. Percent Ozone Absorption vs. Methanol Concentration in Feed.

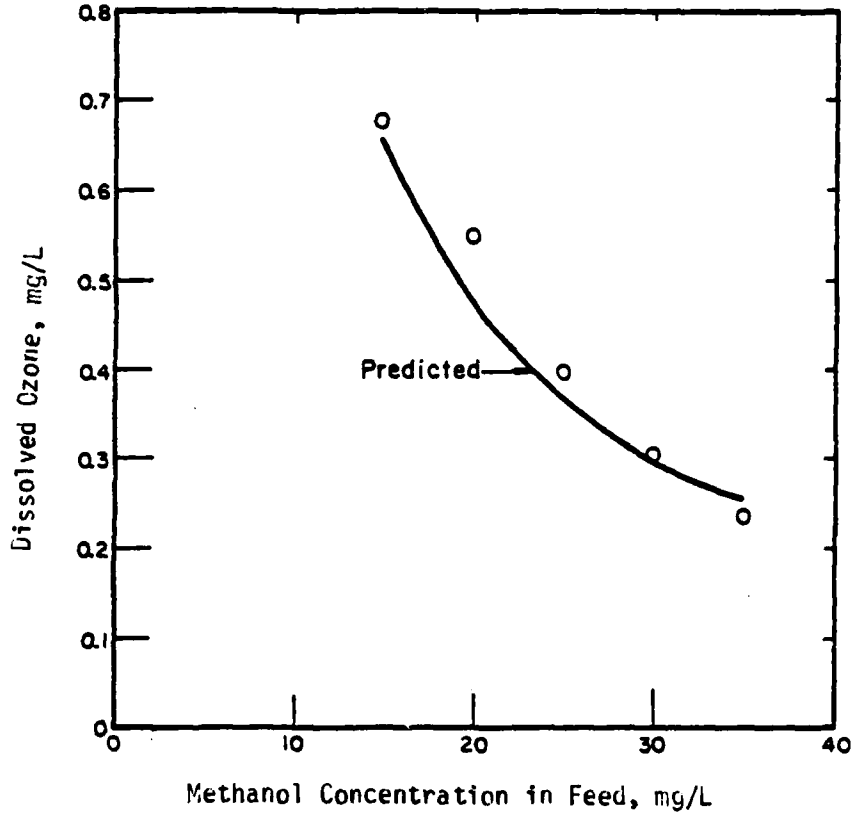

Figure 91. Dissolved Ozone vs. Methanol Concentration in Feed.

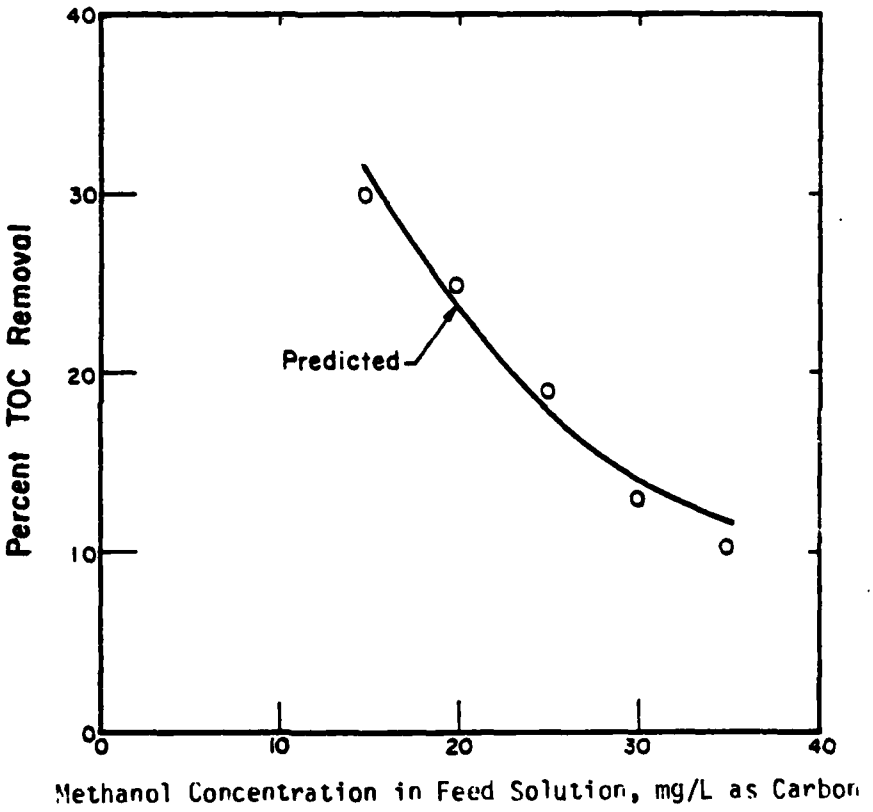

Figure 92. Performance of 22.09-Liter Vessel.

TABLE 58. CONCENTRATION PROFILES AND GRADIENTS OF DISSOLVED OZONE AND TOC IN LIQUID FILM[a]

$\bar{x}$	0	0.2	0.4	0.6	0.8	1.0
B	10.54	8.629	6.720	4.812	2.906	1.000
$\frac{dB}{d\bar{x}}$	-9.563	-9.551	-9.542	-9.535	-9.530	-9.527
C	1.000	1.000	1.000	1.000	1.000	1.000
$\frac{dC}{d\bar{x}}$	3.03×10^{-20}	1.038×10^{-5}	1.869×10^{-5}	2.493×10^{-5}	2.911×10^{-5}	3.122×10^{-5}

a. All quantities are dimensionless. As defined in Appendix III, $\bar{x} = x/\delta$, $B = (O_3)_f/(O_3)$, and $C = (TOC)_f/(TOC)$.

A necessary and usually sufficient condition for ensuring that no reaction occurs within the film for an irreversible and first-order reaction is

$$\frac{D_L k_1}{k_L^2} \ll 1 \qquad (73)$$

as proposed by Danckwerts (1970). The ozone decomposition and the TOC reduction reactions were individually tested for this condition. For the TOC reduction reaction, the effluent TOC concentration was used to obtain the pseudo-first-order reaction rate constant. It was found that the value of the expression on the left-hand side of the inequality is on the order of 10^{-4} and 10^{-3} for the ozone decomposition and the TOC reduction reactions, respectively. Since both reactions satisfy this condition, it is possible that the combination of these two is still a slow overall reaction in the sense that it results in no significant amount of reaction within the film. This possibility is in good agreement with the computed results.

In most chemical processes, it would be unusual for the gas species absorbed to be transferred unreacted to the bulk and for all reactions to occur in the main body of liquid (Levenspiel, 1972). However, it is likely that the ozonation of most organic pollutants in water falls into this category because the concentrations of these pollutants are low and the uncatalytic reactions are generally slow at ambient temperatures. The latter supposition is substantiated by the results of semi-batch ozonation of acetic acid and oxalic acid, which are the two common degradation products found in ozonation mixtures (Kuo et al., 1977a).

Comparison of Overall Mass Transfer Coefficients. Table 59 compares the $k_L a$ values determined from the absorption data with those calculated from the various correlations. The apparent discrepancy may be explained as follows.

It is known that the bubble size is determined by both the orifice diameter and the hydrodynamic field in which the bubble finds its way. For a given amount of gas sparged, the intensity of turbulence in the liquid phase is certainly greater when a smaller orifice diameter is used because the energy dissipation, observed as pressure drop, increases with decreasing orifice diameter. It was noted that all of the previous investigators who proposed the various correlations used perforated spargers with relatively large holes.* The use of a diffuser with a 5-micron pore size in this study resulted in an average bubble diameter of less than 0.2 cm as observed visually. This diameter is appreciably smaller than the 0.599- to 0.767-cm diameters calculated from the correlations developed by the other investigators. The fractional gas holdup, h, determined to be 0.0431, is also

* The only exception was the work of Akita and Yoshita (1974), who used a porous plate of the same fineness as used in this study for the purpose of obtaining a uniform bubble distribution at a very low superficial gas velocity. None of these low flow rate data were incorporated in their correlations.

TABLE 59. COMPARISON OF $k_L a$ DETERMINED FROM EXPERIMENT AND CORRELATIONS

$k_L a$ (hr^{-1})	Method or Equations
150.0	Experiment
19.3	(29)
18.5	(23),(20)
9.9	(24),(20)
24.4	(23),(4),(18),(19),(1)
13.1	(24),(4),(18),(19),(1)

greater than that calculated from the correlations-approximately 0.03. Because the interfacial area a is inversely proportional to the bubble diameter and is proportional to the fractional gas holdup, a larger $k_L a$ is expected for the column used in this study.* In view of the fact that the various correlations are for pure liquids only, the presence of electrolytes in the solution in this study may also be responsible for the smaller bubble size, which may explain why the various correlations failed to predict the values of $k_L a$, d, and h accurately.

The $k_L a$ determined from the overall oxygen transfer coefficient using the unsteady-state method along with an oxygen meter is 127 hr^{-1}. This value is 84% of that determined from the ozone absorption data. A possible explanation for this difference is that the oxygen probe has some "delay" in measuring the dissolved oxygen. The delay in response, which would be significant at high mass transfer rates, would result in a $k_L a$ value lower than the true value. Nevertheless, this result seems to support the finding that the various correlations are not reliable under the conditions used in this study. The widely used steady-state sodium sulfite oxidation method for determining the overall oxygen transfer coefficient was not used because of the controversy over that technique (Benedek et al., 1975).

* The liquid-phase mass transfer coefficient, k_L, is likely to assume a smaller value when the bubble size becomes smaller. However, the value of k_L is relatively insensitive to the bubble diameter, as seen in Equation (30a).

Effect of Operational Variables on Performance of Ozone-Sparged Vessel

The percentage TOC removal and percentage gas-phase ozone absorption at a superficial gas velocity of 0.762 cm/sec are presented in Figures 93 and 94, respectively. They are plotted as a function of the ozone partial pressure, i.e., the volume percent of ozone in the gas. The curves are the results predicted by the mathematical model. The validity of the model is again demonstrated in this case.

The $k_L a$ values at various superficial gas velocities are plotted on a log-log scale in Figure 95. The straight line has a slope of 0.7, indicating that the value of $k_L a$ varies with the superficial gas velocity raised to the 0.7 power, which is identical to that reported in the literature (Sharma and Mashelkar, 1968; Kuo et al., 1975).

The performance of the sparged column operated at various superficial gas velocities and a constant gaseous ozone concentration of 13.1 mg/L is illustrated in Figures 96 and 97. The curves are the predicted results based on the mathematical model using $k_L a$ values determined from Figure 95. The good agreement between the experimentally determined results and the theoretically predicted ones is obvious.

Raising either the partial pressure of ozone or the superficial gas velocity increases the TOC removal efficiency. However, the underlying mechanisms for achieving better TOC removal are different for the two cases; in the former, the improvement is due to a larger driving force for mass transfer, whereas in the latter it is the result of a higher $k_L a$ value. In either case, there is an increase in ozone supply to the reactor.

The percentage of ozone absorption is less sensitive to the changes in the ozone partial pressure and the superficial gas velocity than is the percentage TOC removal. In addition to better TOC removal at higher partial pressures and velocities, there is an increasing amount of unreacted ozone escaping from the ozone-sparged vessel. Therefore, optimum operating conditions may exist for each practical ozonation system.

As reported previously, there was little or no difference in the performance of the column when operated with concurrent vs. countercurrent flow because the mass transfer characteristics of the column are not affected by the direction of the liquid flow and the liquid may be considered well mixed within the ranges of the superficial gas velocities used in this study. Although the liquid residence time was not studied in the present work, its effect may be deduced from the mathematical model. Figure 98 presents the theoretically predicted TOC removals at various residence times when the methanol feed concentration, partial pressure of ozone, and superficial gas velocity are maintained at 30 mg/L, 1% by volume, and 0.762 cm/sec, respectively.

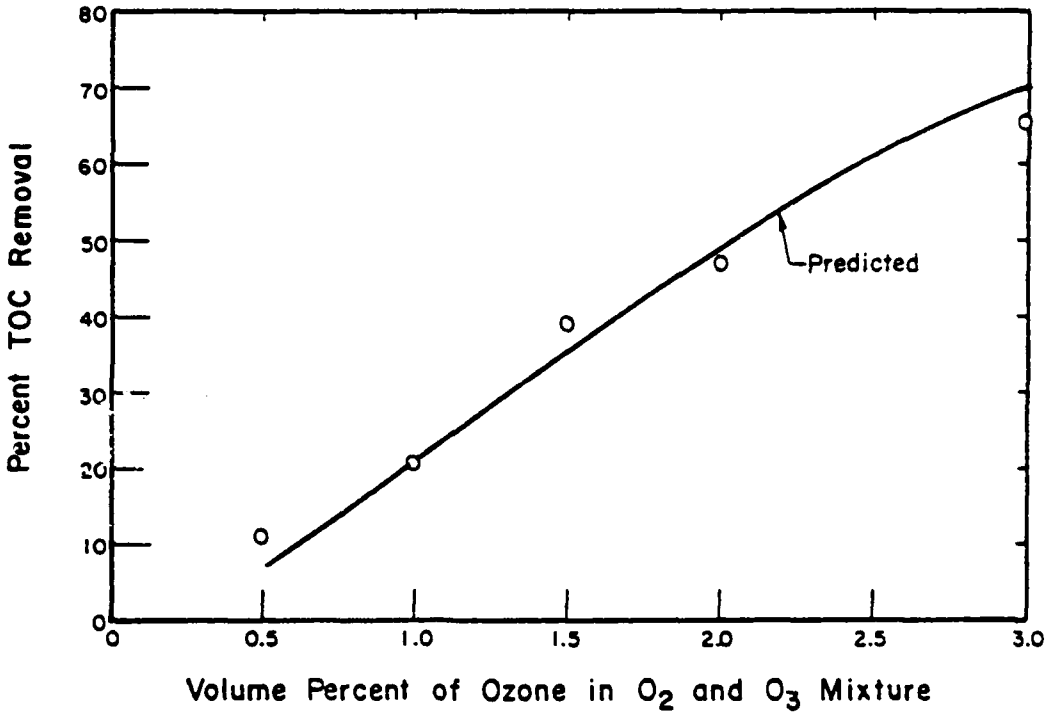

Figure 93. Percent TOC Removal vs. Partial Pressure of Ozone.

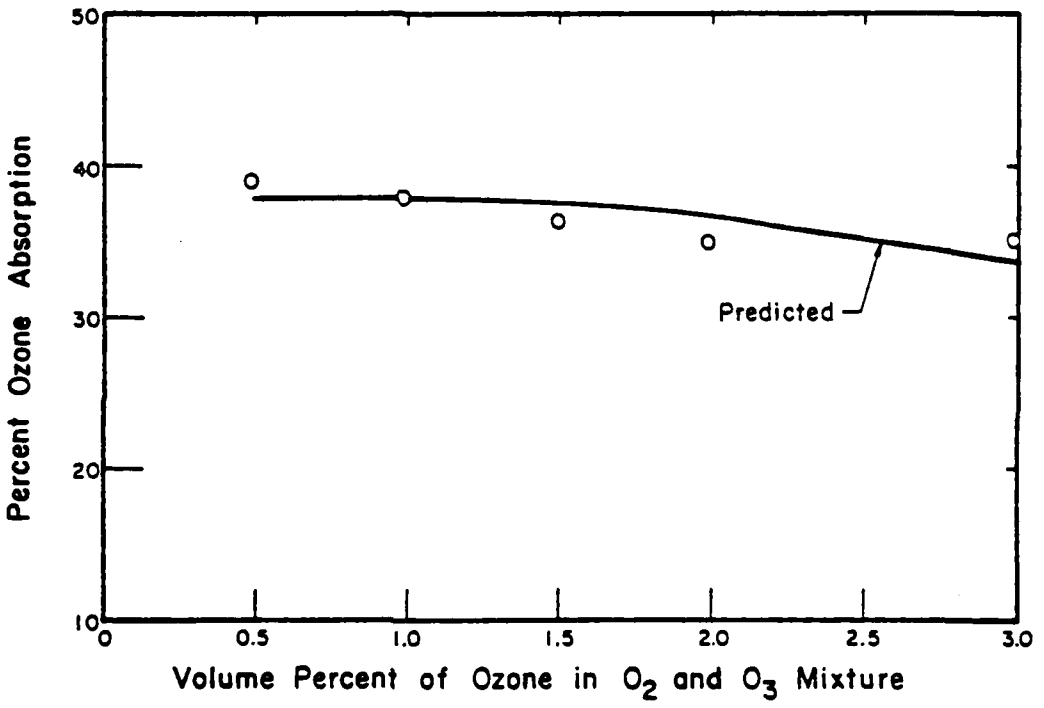

Figure 94. Percent Ozone Absorption vs. Partial Pressure of Ozone.

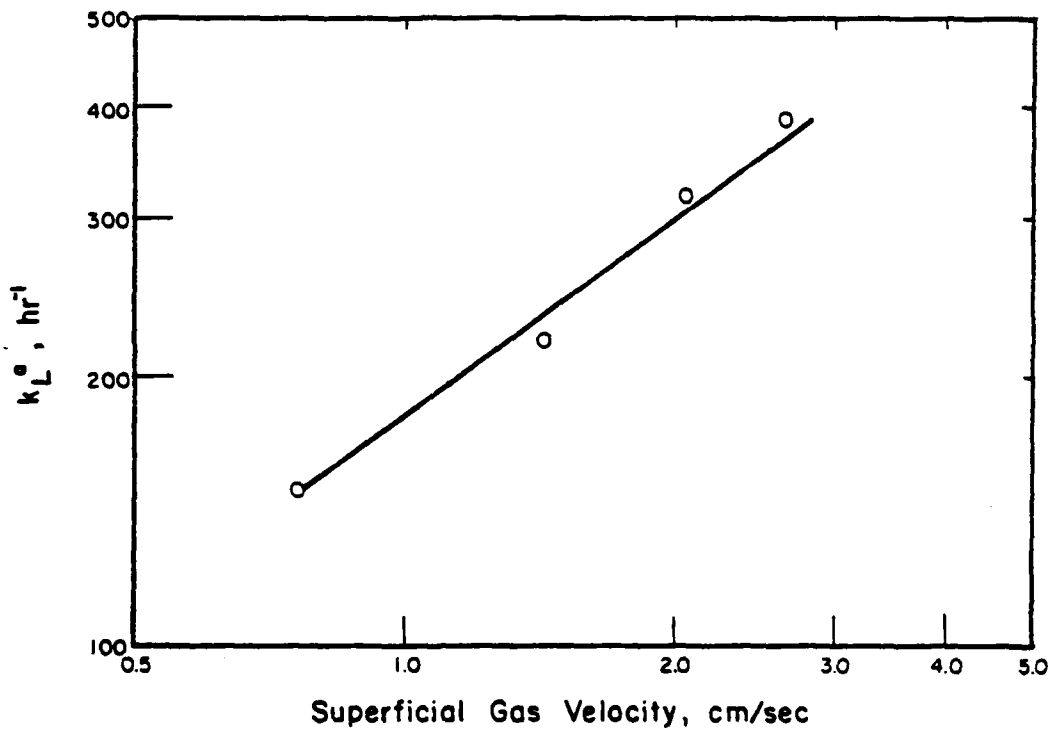

Figure 95. Overall Mass Transfer Coefficient vs. Superficial Gas Velocity.

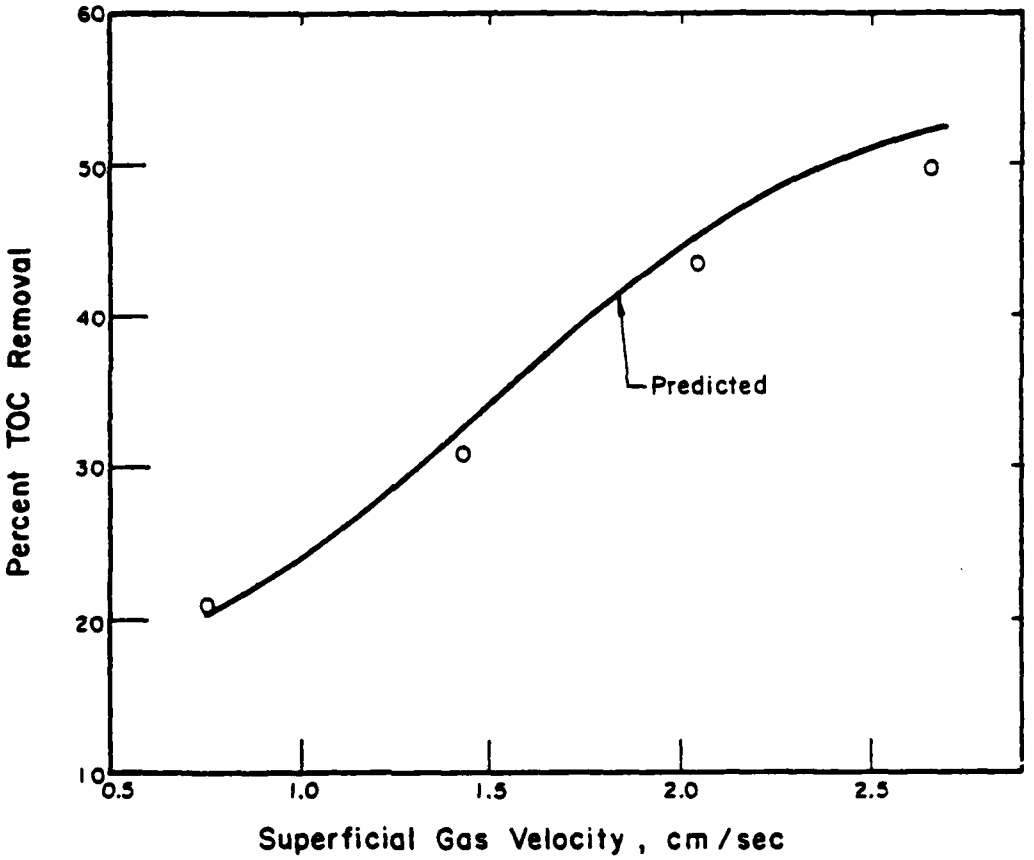

Figure 96. Percent TOC Removal vs. Superficial Gas Velocity.

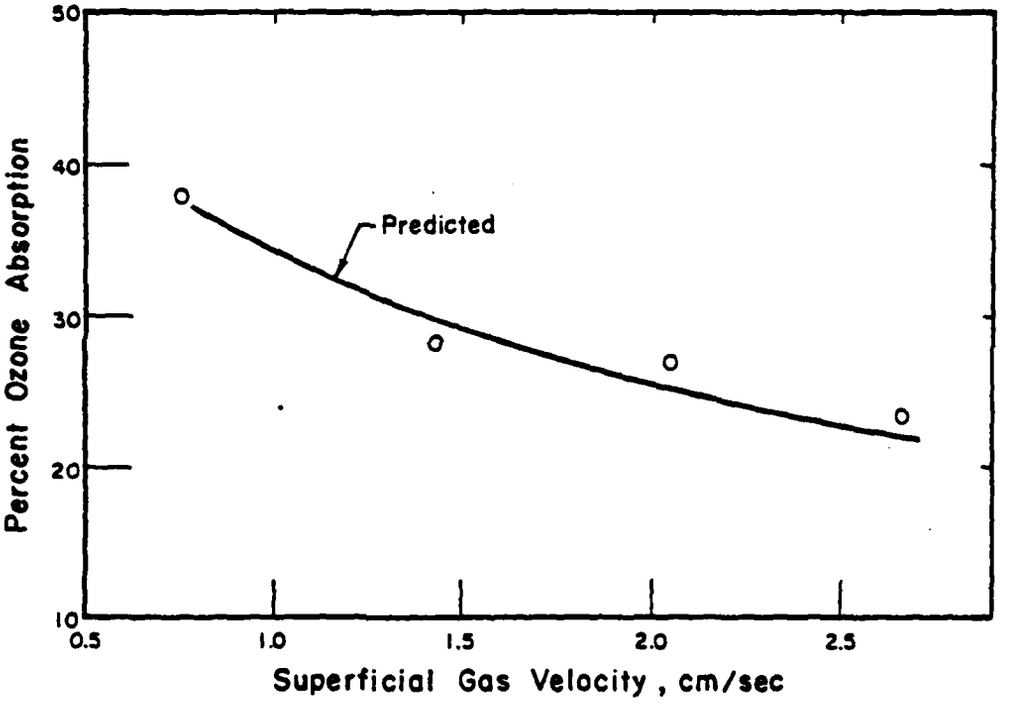

Figure 97. Percent Ozone Absorption vs. Superficial Gas Velocity.

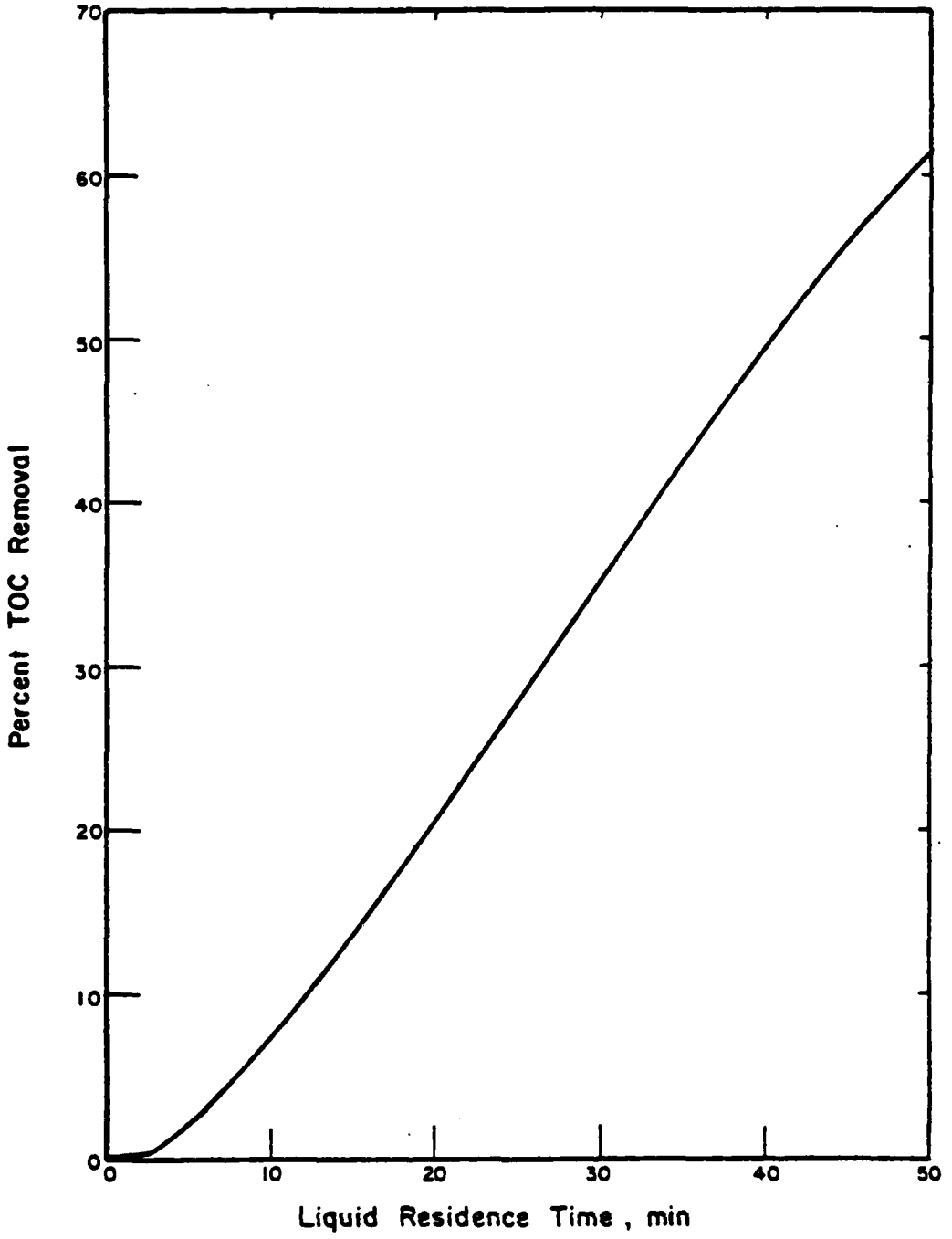

Figure 98. Predicted Effect of Liquid Residence Time on Performance of Sparged Vessel.

Scaling-Up of Ozone-Sparged Vessel

The residence time distribution curves were determined for the 8.55- and 21.69-liter columns at a superficial gas velocity of 0.762 cm/sec. Results similar to those in Figure 86 were obtained, indicating that the liquid in these two columns could be considered well mixed.

The TOC removals for the 3.3-, 8.55-, and 21.69-liter columns, when operated at a superficial gas velocity of 0.762 cm/sec and fed with a methanol concentration of 30 mg/L, were 21, 17.5, and 15%, respectively. It was found that $k_L a$ values for all columns were maintained at more or less the same level. The latter result is consistent with the results given in the literature in that $k_L a$ is mainly a function of the superficial gas velocity. It was also found that these TOC removal percentages can be predicted with accuracy from the mathematical model using a constant $k_L a$ of 150 hr^{-1}. The decrease in TOC removal efficiency with an increase in the size of the sparged vessel can be recognized from the mathematical model. If a constant $k_L a$ is maintained, the ratio of G_o/V becomes smaller and so does the dissolved ozone concentration as the column becomes larger.

To achieve the same TOC removal efficiency in the larger column as in the small one, the superficial gas velocity must be increased while the same level of ozone partial pressure is maintained. The required superficial gas velocity can be calculated using the mathematical model, taking into consideration the relationship between the $k_L a$ and the superficial gas velocity by a factor of twice the percentage difference between the calculated TOC and the desired TOC would give fast convergence to the latter. The coding of a program written for this purpose is given in Table 60. The calculated superficial gas velocities for the 8.55- and 21.69-liter columns are 0.863 and 0.982 cm/sec, respectively. Experiments conducted with the columns operated at these superficial gas velocities resulted in TOC removal efficiencies close to the 21% value obtained with the 3.3-liter column. A similar test was conducted with the 35.34-liter sparged vessel having rectangular cross section, and the validity of this scale-up method was again demonstrated.

It may be concluded that in applying data obtained from a small sparged vessel to a large one, the superficial gas velocity and therefore the $k_L a$ must be increased. The computer program given in Table 60 can be used for calculating the superficial gas velocity required to attain the same percentage of TOC removal. A similar procedure may be developed if the superficial gas velocity is to remain constant while the partial pressure is allowed to increase for a large column.

Comparison of Ozone-Sparged Vessel with Agitated Vessel

The TOC removal percentage for the agitated vessel operated at a superficial gas velocity of 0.349 cm/sec is shown in Figure 99 as a function of the impeller speed, which is directly related to the power input. The

TABLE 60. COMPUTER CODE USED TO CALCULATE REQUIRED SUPERFICIAL GAS VELOCITY IN LARGE OZONE-SPARGED VESSEL TREATING METHANOL SOLUTION

```
      PROGRAM SCALEUP (INPUT,OUTPUT,TAPE5=INPUT,TAPE6=OUTPUT)
C  THIS PROGRAM COMPUTES THE REQUIRED SUPERFICIAL GAS VELOCITY
C  FOR A SCALED-UP OZONE-SPARGED VESSEL TREATING METHANOL
C  SOLUTION.
C  THE SUBROUTINE QNWT IN THE MATH SCIENCE LIBRARY IS USD
C  IN THIS PROGRAM.
C  THE USER MUST SUPPLY VALUES OF KLA, KR, K21, K22, K23, DTOC,
C  XINV, DI, CH3CHO, CGOIN, GO, V, XT, OG, AND AREA.
C  SOME OF THE INPUT AND OUTPUT PARAMETERS ARE DEFINED
C  IN THE WRITE-UP OF QNWT ON PAGES 8-119 TO 8-126 OF
C  THE MATH SCIENCE LIBRARY.
C  DEFINITION OF TERMS AND THEIR UNITS:
C  KLA=OVERALL MASS TRANSFER COEFFICIENT,MIN**-1.
C  KR=FIRST-ORDER RATE CONSTANT FOR OZONE DECOMPOSITION REACTION,
C     MIN**-1.
C  K21=SECOND-ORDER RATE CONSTANT FOR REACTION BETWEEN OZONE AND
C      METHANOL,L/MG/MIN.
C  K22=SECOND-ORDER RATE CONSTANT FOR REACTION BETWEEN OZONE AND
C      FORMALDEHYDE,L/MG/MIN.
C  K23=SECOND-ORDER RATE CONSTANT FOR REACTION BETWEEN OZONE AND
C      FORMIC ACID,L/MG/MIN.
C  DTOC=DESIRED TOC;EFFLUENT TOC CONCENTRATION OBTAIN IN SMALL
C       OZONE-SPARGED VESSEL,MG/L.
C  XINV=INVERT OF LIQUID RESIDENCE TIME,MIN**-1.
C  DI=DISTRIBUTION COEFFICIENT,DIMENSIONLESS.
C  CH3OHO=METHANOL CONCENTRATION IN FEED SOLUTION,MG/L AS CARBON.
C  CGOIN=OZONE CONCENTRATION IN INFLUENT GAS AT 1 ATM.,MG/L.
C  GO=GAS FLOW RATE AT 1 ATM.,L/MIN.
C  V=LIQUID VOLUME,L.
C  XL=LIQUID HEIGHT,CM.
C  UG=SUPERFICIAL GAS VELOCITY,CM/MIN.
C  AREA=CROSS-SECTIONAL AREA OF OZONE-SPARGED VESSEL,CM**2
C  ACGOIN=OZONE CONCENTRATION IN INFLUENT GAS AT OPERATING PRESSURE,MG/L.
C  CH3OH=METHANOL CONCENTRATION IN EFFLUENT,MG/L AS CARBON.
C  HCHO=FORMALDEHYDE CONCENTRATION IN EFFLUENT,MG/L AS CARBON.
C  HCOOH=FORMIC ACID CONCENTRATION IN EFFLUENT,MG/L AS CARBON.
C  CGOUT=OZONE CONCENTRATION IN EFFLUENT GAS,MG/L.
C  O3=DISSOLVED OZONE CONCENTRATION IN EFFLUENT,MG/L.
C  TOC=TOC CONCENTRATION IN EFFLUENT,MG/L.
C  TEST=ABSOLUTE VALUE OF DIFFERENCE BETWEEN CALCULATED TOC AND
C       DESIRED TOC,MG/L.
C  X=AT ENTRY:INITIAL ESTIMATE VECTOR; AT RETURN:SOLUTION VECTOR
C    ESTIMATED FROM LAST ITERATION,MG/L.
        COMMON KLA,KR,K21,K22,K23,XINV,DI,CH3OHO,
       $CGOIN,GO,V,XL,ACQOIN
        REAL KLA,KR,K21,K22,K23
        READ (5, 100) KLA,KR,K21,K22,K23,DTOC,XINV,DI,CH3OHO,
       $CGOIN,GO,V,KL,UG,AREA
        WRITE (6,606)
        WRITE (6,200) KLA,KR,K21,K22,K23,DTOC,XINV,DI,CH3OHO,
```

```
      $CGOIN,GO,V,KL,UG,AREA
       ACQOIN=CGOIN*(XL/1033.27+1.)
       DO 50 LIJ=4,10
       WRITE (6, 707)KLA,UG,GO
       CALL MODELC (TOC)
       TEST=ABS(TOC-DTOC)
       IF (TEST.LT.0.004) GO TO 60
       UG=UG* (1+2* (TOC-DTOC)/DTOC)
       KLA=KLA*(1+2*(TOC-DTOC)/DTOC)**.7
       GO=UG*AREA/1000.
    50 CONTINUE
   100 FORMAT (5F7.4/3F7.4/6F7.4,F8.4)
   200 FORMAT (//2X, 15F8.4)
   606 FORMAT (//7X,3HKLA,6X,2HKR,5X,3HK21,5X,3HK22,5X,3HK23,
      $4X,4HDTOC,4X,4HXINV,6X,2HDI,2X,6HCH3OHO,3X,5HCGOIN,
      $6X,2HGO,7X,1HV,6X,2HXL,6X,2HUG,4X,4HAREA)
   707 FORMAT (//7X,4HKLA=,F10.4,7X,3HUG=,F10.4,7X,3HGO=,F10.4)
    60 STOP
       END
       SUBROUTINE MODELC (TOC)
C X(1) =CH3OH, X(2)=HCHO,X(3)=HCOOH,X(4)=CGOUT,X(5)=O3
       DIMENSION X(5),R(5),AJ(5,5),B(5,7),IP(6)
       EXTERNAL FUN
       REAL KLA,KR,K21,K22,K23
       COMMON KLA,KR,K21,K22,K23,XINV,DI,CH3OHO,
      $CGOIN,GO,V,XL,ACGOIN
C GIVE INITIAL ESTIMATE VECTOR.
       X(1)=16.
       X(2)=7.
       X(3)=1.
       X(4)=6.
       X(5)=.4
       P=0
C NO PRINT-OUT WAS USED AS THE PRINT OPTION.
       IP(1)=-55
C THE TERMINATION CRITERION FOR NONCONVERGENT ITERATIONS
C WAS USED.
       CALL QNWT(X,5,5,FUN,P,.1E-8,IP,0,R,RMS,AJ,B)
C THE TOLERANCE LEVEL FOR RESIDUAL NORM WAS SET AT .1E-8.
C NO JACOBIAN MATRIX WAS GIVEN.
       TOC=X(1)+X(2)+X(3)
       WRITE (6,808)
       WRITE (6,300)P,X,TOC
   300 FORMAT (/F3.1//5X,6F10.2)
   808 FORMAT (//2X,1HP,7X,5HCH3OH,6X,4HHCHO,5X,5HHCOOH,5X,
      $5HCGOUT,8X,2HO3,7X,3HTOC)
       RETURN
       END
       SUBROUTINE FUN (X,N,K,R,P)
       REAL KLA,KR,K21,K22,K23
       COMMON KLA,KR,K21,K22,K23,XINV,DI,CH3OHO,
      $CGOIN,GC,V,XL,ACGOIN
       DIMENSION X(5),R(5)
       R(1)=-K21*X(1)*X(5)+XINV*(CH3OHO-X(1))
```

```
      R(2)=K21*X(1)*X(5)-K22*X(2)*X(5)-XINV*X(2)
      R(3)=K22*X(2)*X(5)-K23*X(3)*X(5)-XINV*X(3)
      R(4)=GO*(CGOIN-X(4))/V-
     $KLA*DI*(ACQOIN-X(4))
     $/ALOG((DI*ACGOIN-X(5))/(DI*X(4)-X(5)))
      R(5)-KLA*DI*(ACGOIN-X(4))
     $/ALOG((DI*ACGOIN-X(5))/(DI*X(4)-X(5)))
     $-(4.,*(K21*X(1)*K22*X(2)+K23*X(3))+KR+XINV)*X(5)
      RETURN
      END
```

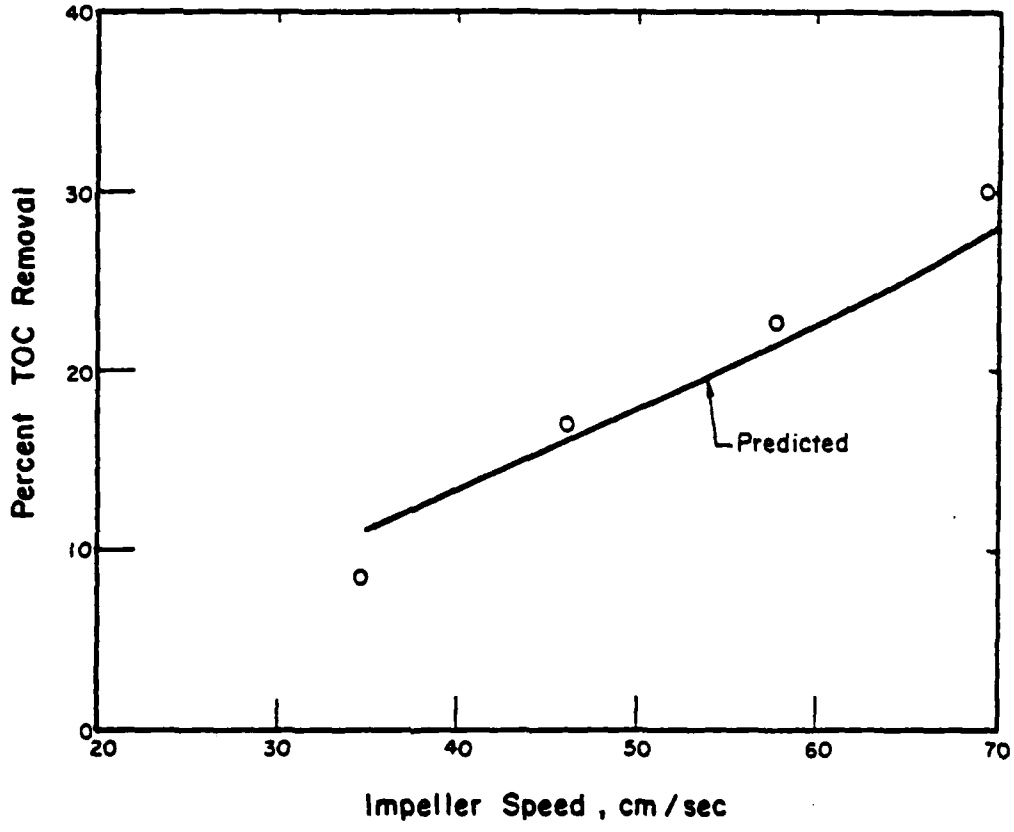

Figure 99. Percent TOC Removal vs. Impeller Speed for Agitated Vessel.

curve was obtained from the mathematical model for a sparged vessel modified to assume that the gas phase is also well mixed. It can be seen that reasonably good agreement exists beteen the experimental results and the predicted ones.

It appears that the same $k_L a$ value would result in somewhat different TOC removal efficiencies in the sparged vessel and the agitated vessel. For instance, the agitated vessel when operating at a $k_L a$ value of 149 hr^{-1} gave a TOC removal efficiency of 17% compared to the 21% efficiency of the sparged vessel operated at a comparable $k_L a$ value. This discrepancy probably resulted from the difference between the logarithmic mass transfer driving force and the driving force based on the effluent gas composition. It should be pointed out that in the above example the amount of ozone absorbed was greater in the sparged vessel than in the agitated vessel.

The $k_L a$ in the sparged vessel is a function of the superficial gas velocity alone, whereas in the agitated vessel it is related to both the power input and the superficial gas velocity, as indicated by Equations (45), (46), (50), (51), and (52). However, these correlations for k_L and a in agitated vessels cannot be used indiscriminately; a scrutiny of the correlations shows that they apply only to a particular vessel and pure liquids. As a result, no comparison was made between the $k_L a$ determined from the absorption data and the ones calculated using the various correlations.

ENGINEERING SIGNIFICANCE

The ozonation of wastewater containing a complex mixture of organic compounds can be modeled by the method presented in this study. In practice, it probably would not be feasible to determine the kinetics for each organic species present in wastewater. If a model were constructed in which a TOC material balance replaced all of the material balances for individual organic species, it would be necessary to have a priori knowledge of the second-order rate constant and the stoichiometric coefficient for the reaction between TOC and ozone. Because the rate constant and the stoichiometric coefficient change as the ozonation reaction proceeds, it would not be possible to use such a model directly to predict the performance of practical ozone-sparged vessels.

A model based on a TOC material balance, however, seems feasible for use in scaling up data on the performance of ozone-sparged vessels. The rate constant and the stoichiometric coefficient for the TOC reduction reaction can be determined from a laboratory-scale column. These data can then be used in a program similar to that given in Table 60 to calculate the superficial gas velocity for a larger column in which it is desired to achieve the same performance as in the laboratory-scale column. For instance, suppose that the 3.3-liter column is operated under the following conditions:

a methanol feed concentration of 30 mg/L as carbon, a superficial gas velocity of 0.762 cm/sec, a gaseous ozone concentration of 13.1 mg/L, and a liquid residence time of 20 minutes. The second-order rate constant and the stoichiometric coefficient for the TOC reduction reaction are then determined to be 2.017×10^3 L/mole/minute and 4.36, respectively. Using the above approach, the required superficial gas velocities are calculated to be 0.870 and 0.990 cm/sec for the 8.55 and 21.69-L columns, respectively. These results are close to the values of 0.863 and 0.982 cm/sec calculated previously from the program in Table 60. Table 61 presents the coding of a program for the scale-up process using kinetic data of the TOC reduction reaction. In essence, it appears that this scale-up method for ozone-sparged vessels based on the model involving a TOC material balance may be usable in most practical ozonation applications.

CONCLUSIONS

Based on the results of this study, the following conclusions may be drawn:

(1) The performance of stainless steel, Teflon, fused alumina, and fritted glass diffusers is satisfactory because their use results in the decomposition of a negligible amount of gaseous ozone.

(2) Ozone decomposition in an aqueous solution at a pH of 9 follows first-order reaction kinetics with a rate constant of $0.01006\ sec^{-1}$ at 25°C. The ozone reactions with methanol, formaldehyde, and formic acid in aqueous solution at a pH of 9 and 25°C may be described as second-order reactions with the rate constants of 7.58×10^3, 8.4×10^3, and 5.26×10^4 L/mole/minute, respectively.

(3) The mathematical model developed in this study successfully describes an ozone-sparged vessel used to treat an aqueous methanol solution. The effect of the partial pressure and superficial gas velocity on the performance of the vessel can be predicted using the model.

(4) The scale-up method based on the mathematical model accurately predicts the superficial gas velocity required for a large vessel to achieve the same level of TOC removal obtained in a small vessel.

(5) The agitated vessel generally can be operated at a higher $k_L a$ value by increasing the power input to obtain the same performance as that of the sparged vessel when the gas-flow rates per unit liquid volume and other conditions are identical. However, the percentage of TOC removal is lower with the agitated vessel than with a sparged one operated at the same $k_L a$.

(6) The rate of mass transfer in most ozonation applications is probably not enhanced by the liquid-phase oxidation reaction and can be considered equivalent to the rate of a purely physical mass transfer.

TABLE 61. COMPUTER CODE FOR SCALE-UP OF OZONE-SPARGED VESSEL

```
      PROGRAM TOCSUP (INPUT,OUTPUT,TAPE5=INPUT,TAPE6=OUTPUT)
C THIS PROGRAM COMPUTES THE REQUIRED SUPERFICIAL GAS VELOCITY
C FOR A SCALED-UP OZONE-SPARGED VESSEL TREATING WASTEWATER
C CONTAINING A COMPLEX MIXTURE OF ORGANIC COMPOUNDS.
C THE SUBROUTINE QNWT IN THE MATH SCIENCE LIBRARY IS USED
C IN THIS PROGRAM.
C THE USER MUST SUPPLY VALUES OF KLA,KR,K2,SC,DTOC,XINV,
C DI,TOCO,CGOIN,GO,V,XL,UG,AND AREA.
C SOME OF THE INPUT AND OUTPUT PARAMETERS ARE DEFINED IN THE
C WRITE-UP OF QNWT ON PAGES 8-119 TO 8-126 OF THE MATH
C SCIENCE LIBRARY.
C DEFINITION OF TERMS AND THEIR UNITS:
C KLA=OVERALL MASS TRANSFER COEFFICIENT,MIN**-1.
C KR=FIRST-ORDER RATE CONSTANT FOR OZONE DECOMPOSITION REACTION,
     MIN**-1.
C K2=SECOND-ORDER RATE CONSTANT FOR TOC REDUCTION REACTION,
     L/MG/MIN.
C SC=STOICHIOMETRIC COEFFICIENT FOR OZONE FOR TOC REDUCTION
C    REDUCTION,DIMENSIONLESS.
C DTOC=DESIRED TOC;EFFLUENT TOC CONCENTRATION OBTAINED IN SMALL
C      OZONE-SPARGED VESSEL,MG/L.
C XINV=INVERT OF LIQUID RESIDENCE TIME,MIN**-1.
C DI=DISTRIBUTION COEFFICIENT,DIMENSIONLESS.
C TOCO=TOC CONCENTRATION IN FEED SOLUTION,MG/L.
C CGOIN=OZONE CONCENTRATION IN INFLUENT GAS AT 1 ATM.,MG/L.
C GO=GAS FLOW RATE AT 1 ATM.,L/MIN.
C V=LIQUID VOLUME,L.
C XL=LIQUID HEIGHT,CM.
C UG=SUPERFICIAL GAS VELOCITY,CM/MIN.
C AREA=CROSS-SECTIONAL AREA OF OZONE-SPARGED VESSEL,CM**2.
C TOC=TOC CONCENTRATION IN EFFLUENT,MG/L.
C CGOUT=OZONE CONCENTRATION IN EFFLUENT GAS,MG/L.
C O3=DISSOLVED OZONE CONCENTRATION IN EFFLUENT,MG/L.
C ACGOIN=OZONE CONCENTRATION IN INFLUENT GAS AT OPERATING
C        PRESSURE,MG/L.
C TEST=ABSOLUTE VALUE OF DIFFERENCE BETWEEN CALCULATED TOC
C      AND DESIRED TOC,MG/L.
C X=AT ENTRY:INITIAL ESTIMATE VECTOR; AT RETURN:SOLUTION VECTOR
C   ESTIMATED FROM LAST ITERATION,MG/L.
      COMMON KLA,KR,K2,SC,XINV,DI,TOCO,CGOIN,
     $GO,V,XL,ACGOIN
      REAL KLA,KR,K2
      READ (5,100)KLA,KR,K2,SC,DTOC,XINV,DI,TOCO,CGOIN,
     $GO,V,XL,UG,AREA
      WRITE (6,101)
      WRITE (6,200)KLA,KR,K2,SC,DTOC,XINV,DI,TOCO,CGOIN,
     $GO,V,XL,UG,AREA
      ACGOIN=CGOIN*(XI/1033.27+1.)
      DO 50 LIJ=1,10
      WRITE (6,707)KLA,UG,GO
      CALL CTOC(TOC)
      TEST=ABS(TOC-DTOC)
```

```
      IF (TEST.LT.0.004) GO TO 60
      UG=UG* (1.+2.*(TCC-DTOC)/DTOC)
      KLA=KLA*(1.+2.*(TOC-DTOC)/DTOC)**.7
      GO=UG*AREA/1000.
   50 CONTINUE
  100 FORMAT (2F7.4,F7.5,F7.4/3F7.4/6F7.4,F8.4)
  200 FORMAT (//2X,14F9.5)
  101 FORMAT (//8X,3HKLA,7X,2HKR,7X,2HK2,7X,2HSC,5X,4HDTOC,
     $5X,4HXINV,7X,2HDI,5X,4HTOCO,4X,5HCGOIN,7X,2HGO,8X,1HV,
     $7X,2HXL,7X,2HUG,5X,4HAREA)
  707 FORMAT (//7X,4HKLA=,F10.4,7X,3HUG=,F10.4,7X,3HGO=,F10.4)
   60 STOP
      END
      SUBROUTINE CTOC (TOC)
C X(1)=TOC,X(2)-CGOUT,X(3)=03
      REAL KLA,KR,K2
      DIMENSION X(3),R(3),AJ(3,3) B(3,5),IP(4)
      EXTERNAL FUN
      COMMON KLA,KR,K2,SC,XINV,DI,TOCO,CGOIN,
     $GO,V,XL,ACGOIN
      P=0.
C NO PRINT-OUT WAS USED AS THE PRINT OPTION.
      IP(1)=-55
C THE TERMINATION CRITERION FOR NONCONVERGENT ITERATIONS
C WAS USED.
C GIVE INITIAL ESTIMATE VECTOR.
      X(1)=25.
      X(2)=6.
      X(3)=.4
      CALL QNWT (X,3,3,FUN,P,.1E-10,IP,0,R,RMS,AJ,B)
C THE TOLERANCE LEVEL FOR RESIDUAL NORM WAS SET AT .1E-8.
C NO JACOBIAN MATRIX WAS GIVEN.
      WRITE (6,808)
      WRITE (6,300)P,X
      TOC=X(1)
  300 FORMAT (//F5.1,3F12.2)
  808 FORMAT (//4X,1HP,9X,3HTOC,7X,5HCGOUT,10X,2HO3)
     RETURN
     END
     SUBROUTINE FUN (X,N,K,R,P)
     REAL KLA,KR,K2
     COMMON KLA,KR,K2,SC,XINV,DI,TOCO,CGOIN,
    $GO,V,XL,ACGOIN
     DIMENSION X(3),R(3)
     R(1)=XINV*TOCO-XINV*X(1)-K2*X(3)*X(1)
     R(2)=(CGOIN-X(2))*GO/V-KLA*DI*(ACGOIN-X(2))
    $/ALOG((DI*ACGOIN-X(3))/(DI*X(2)-X(3)))
     R(3)-KLA*DI8(ACGOIN-X(2))
    $/ALOG((DI*ACGOIN-X(3))/(DI*X(2)-X(3)))
    $-XINV*X(3)-KR*X(3)-4.*SC*K2*X(3)*X(1)
     RETURN
     END
```

(7) The ozonation of wastewater containing organics other than methanol may be modeled in the same way as was done in this study.

(8) A material balance using TOC values along with appropriate TOC removal kinetics can be used to replace the material balance for individual organic species in the mathematical model. Although such a model would be of little use in predicting the performance of a particular sparged vessel, it could be used satisfactorily in the scaling-up of an ozone-sparged vessel.

NOMENCLATURE

Symbol		Dimensions
A	Total interfacial area	L^2
a	Average interfacial area per unit volume of liquid	L^{-1}
a'	Average interfacial area per unit volume of dispersion	L^{-1}
b	Concentration of absorbed species	ML^{-3}
B	$(O_3)_f/(O_3)$	--
c	Concentration of reacting species	ML^{-3}
C	$(TOC)_f/(TOC)$	--
C_{goin}	Ozone concentration in influent gas at 1 atm	ML^{-3}
C_{gout}	Ozone concentration in effluent gas at 1 atm	ML^{-3}
C^*_{goin}	Ozone concentration in influent gas at operating pressure	ML^{-3}
C_D	Drag coefficient	--
(CH_3OH)	Methanol concentration	ML^{-3}
$(CH_3OH)_0$	Methanol concentration in feed solution	ML^{-3}
d	Average bubble diameter	L
d_{BE}	Stable bubble diameter	L
d_{BM}	Mean bubble diameter	L
d_{BO}	Orifice bubble diameter	L
d_h	Diameter of the sparge holes	L
D	Diameter of the column	L
D_b	Diffusivity of absorbed species b	L^2T^{-1}
D_c	Diffusivity of dissolved species c	L^2T^{-1}
D_i	Ozone distribution coefficient	--
D_L	Diffusivity of dissolved species	L^2T^{-1}

D_{O_3}	Diffusivity of dissolved ozone	L^2T^{-1}
D_{TOC}	Diffusivity of TOC	L^2T^{-1}
E	Mass transfer enhancement factor	--
E_l	Axial dispersion coefficient	L^2T^{-1}
G_o	Volumetric gas-flow rate	L^3T^{-1}
g	Gravitational constant	LT^{-2}
h	Average fractional gas holdup	--
h'	Average fractional gas holdup under liquid flow	--
H	Liquid height	L
H_f	Gassed liquid height	L
H_l	Ungassed liquid height	L
(HCHO)	Formaldehyde concentration	ML^{-3}
(HCOOH)	Formic acid concentration	ML^{-3}
k_1	First-order rate constant	T^{-1}
K_1	First-order rate constant for reaction between COD and ozone	T^{-1}
k_2	Second-order rate constant for reaction between TOC and ozone	$L^3M^{-1}T^{-1}$
K_2	Second-order rate constant for reaction between COD and ozone	$L^3M^{-1}T^{-1}$
k_{21}	Second-order rate constant for reaction between methanol and ozone	$L^3M^{-1}T^1$
k_{21}'	$k_{21}(CH_3OH)$	T^{-1}
k_{22}	Second-order rate constant for reaction between formaldehyde and ozone	$L^3M^{-1}T^{-1}$
k_{22}'	$k_{22}(HCHO)$	T^{-1}
k_{23}	Second-order rate constant for reaction between formic acid and ozone	$L^3M^{-1}T^{-1}$
k_Ga	Volumetric mass transfer coefficient based on gas phase concentration	T^{-1}

k_L	Liquid phase mass transfer coefficient	LT^{-1}
$k_L a$	Overall (or volumetric) mass transfer coefficient based on liquid phase concentration	T^{-1}
k_r	Ozone decomposition rate constant	T^{-1}
n	Number of bubbles in unit volume of dispersion	--
N	Impeller speed	T^{-1}
N_{Bo}	Bond No. = $gD^2\gamma$	--
N_{Fr}	Froude No. = $U_G/(gD)^{1/2}$	--
N_{Ga}	Galilei No. = gD^3/ν^2	--
N_{Pe}	Peclet No. = $U_t d/D_L$	--
N_{Re}	Reynolds No. = $U_t d/\nu$	--
N_{Se}	Schmidt No. = ν/D_L	--
N_{Sh}	Sherwood No. = $k_L d/D_L$	--
N_o	Number of sparger hole	--
N_o'	Equivalent number of sparger hole	--
(O_3)	Dissolved ozone concentration	ML^{-3}
$(O_3)^*$	Dissolved ozone concentration at interface equilibrium with gaseous ozone	ML^{-3}
$(O_3)_f$	Dissolved ozone concentration in liquid film	ML^{-3}
p, q, r	Exponents	--
P	Power input in aerated liquid	ML^2T^{-3}
P_o	Power dissipated by impeller in unaerated liquid	ML^2T^{-3}
R_{CH_3OH}	Rate of reaction between methanol and ozone	$ML^{-3}T^{-1}$
R_{HCHO}	Rate of reaction between formaldehyde and ozone	$ML^{-3}T^{-1}$
R_{HCOOH}	Rate of reaction between formic acid and ozone	$ML^{-3}T^{-1}$
R_{O_3}	Rate of ozone decomposition reaction	$ML^{-3}T^{-1}$

SC	Stoichiometric coefficient for ozone for TOC reduction reaction	--
(TOC)	TOC concentration	ML^{-3}
$(TOC)_f$	TOC concentration in liquid film	ML^{-3}
U_G	Superficial gas velocity	LT^{-1}
U_L	Superficial liquid velocity	LT^{-1}
U_S	Slip velocity	LT^{-1}
U_t	Bubble terminal velocity	LT^{-1}
V	Liquid volume	L^3
X	Sparger hole spacing	L
x	x/δ	--
γ	Interfacial tension	MT^{-2}
δ	Thickness of liquid film	L
μ	Viscosity of liquid	$ML^{-1}T^{-1}$
ν	Kinematic viscosity of liquid	L^2T^{-1}
ρ	Density of liquid	ML^{-3}
$\Delta\rho$	Density difference between liquid and gas	ML^{-3}
τ	Liquid residence time	T

RECOMMENDATIONS

Based on the results of this study, the following recommendations may be made for future work:

(1) A detailed analysis of organics present in the composite RO permeates obtained from pilot-scale runs should be conducted in order to verify the results of this study using model compounds.

(2) An in-depth study on the composition of UV-ozonated composite RO permeates should be made using the analytical procedures developed in this study. This involves the analysis of UV-ozonated samples obtained at various times of ozonation.

(3) The toxicity tests of the concentrates of the UV-ozonated RO permeates should be carried out to ensure suitability of the treated wastewater for potable purpose.

(4) The mathematical model developed in this study for scale-up of ozone-sparged vessels should be verified with the composite RO permeates using TOC values as a parameter for scale-up instead of the specific compounds as used in this study.

REFERENCES

Ackman, R.G. 1972. J. Chromatogr. Sci. 10:560.

ACS. 1972. No. 111, American Chemistry Society, Washington, DC.

Ahlstrom, D.H., Kilgrou, R.J., and Liebman, S.A. 1975. Anal. Chem. 47:1411.

Ahmed, M.D. and Kinney, C.R. 1950. J. Am. Chem. Soc. 72:559.

Aiba, S., Humphrey, A.E., and Millis, N.F. 1973. Biochemical Engineering, Academic Press, New York.

Akita, K. and Yoshida, F. 1973. Ind. Eng. Chem. Process Des. Dev. 12:76.

Akita, K. and Yoshida, F. 1974. Ind. Eng. Chem. Process Des. Dev. 13:84.

Alder, M.G. and Hill, G.R. 1950. J. Am. Chem. Soc. 72:1884.

Alley, C.D., Brooks, J.B., and Choudhary, G. 1976. Anal. Chem. 48:387.

Argo, W.B. and Cova, D.R. 1965. Ind. Eng. Chem. Process Des. Dev. 4:352.

Austern, B.M., Dobbs, R.A., and Cohne, J.M. 1975. Environ. Sci. Technol. 9(6):588.

Bailey, P.S. 1972. Ozone in Water and Wastewater Treatment, F.L. Evans, ed., Ann Arbor Science Publishers, Inc., Ann Arbor, MI.

Baker, R.A. 1965. J. Water Pollut. Control Fed. 37:1164.

Baker, R.A. 1967a. Water Res. 1:61.

Baker, R.A. 1967b. Water Res. 1:97.

Baker, R.A. 1969. Water Res. 3:717.

Baker, R.A. 1970. Water Res. 4:559.

Baker, R.A. and Malo, B.A. 1967. J. Sanit Eng. Div., Am. Soc. Civ. Engr. 93:41.

Bassette, R., Ozeris, S., and Whitnah, C.H. 1962. Anal. Chem. 34:1540.

Becka, J. and Feltl, L. 1977. J. Chromatogr. 131:179.

Bellar, T.A. and Lichtenberg, J.J. 1974a. EPA Report 670/4-74-009.

Bellar, T.A. and Lichtenberg, J.J. 1974b. J. Am. Water Works Assoc. 66:739.

Bellar, T.A., Lichtenberg, J.J., and Eichelberger, J.W. 1976. Environ. Sci. Technol. 10:926.

Bellar, T.A., Lichtenberg, J.J., and Kroner, R.C. 1974a. EPA Report 670/4-74-008.

Bellar, T.A., Lichtenberg, J.J., and Kroner, R.C. 1974b. J. Am. Water Works Assoc. 66:703.

Benedek, A., Bennett, G.F., and Ho, K.W.A. 1974. AIChE Symp. Series 145: 190.

Bertsch, W., Anderson, E., and Holzer, G. 1975. J. Chromatogr. 112:701-718.

Bertsch, W., Chang, R.C., and Zlatkis, A. 1974. J. Chromatogr. Sci. 12:175.

Bethge, P.O. and Lindstrom, K. 1974. Analyst 99:137.

Bhatia, K. 1973. Anal. Chem. 45:1344.

Bischoff, K.B. and Phillips, J.B. 1966. Ind. Eng. Chem. Process Des. Dev. 5:416.

Bober, T.W. and Dagon, T.J. 1975. J. Water Pollut. Control Fed. 47:2128.

Boussinesq, J. 1905. J. Math. Phys. Appl. 6:285.

Bowmann, C.W. and Johnson, A.I. 1962. Can. J. Chem. Eng. 4:139.

Braulick, W.J., Fair, J.R., and Lerner, B.J. 1965. AIChE J. 11:73.

Bunn, W.W., Haas, B.B., Deane, E.R., and Kleopfler, R.D. 1975. Environ. Lett. 10:205.

Burnham, A.K., Calder, G.V., Fritz, J.S., Junk, G.A., Svec, H.J., and Willis, R. 1972. Anal. Chem. 44:139.

Calderbank, P.H. 1958. Trans. Inst. Chem. Eng. 36:443.

Calderbank, P.H. 1959. Trans. Inst. Chem. Eng. 37:173.

Calderbank, P.H. 1967. Mixing, V.W. Uhl and J.B. Gray, eds., Academic Press, New York.

Calderbank, A. 1968.

Calderbank, P.H. and Moo-Young, M.B. 1961. Chem. Eng. Sci. 16:39.

Calderbank, P.H., Johnson, D.S.L., and Loudon, J. 1970. Chem. Eng. Sci. 25:235.

Campbell, K. and Palmer, J.M. 1971. Chem. Ind. 35:992.

Carpenter, A.P., Siggia, S., and Carter, S. 1976. Anal. Chem. 48:225.

Carter, M.K. and Moore, M. 1975. Anal. Chem. 47:1489.

Casteele, K.V., DePooter, H., and Van Sumere, C.F. 1976. J. Chromatogr. 121:49.

Chalmers, R.A. and Watts, R.W.E. 1972. Analyst (London) 97:951.

Chan, M.L., Whetseel, C., and McChesney, J.D. 1974. J. Chromatogr. Sci. 12:512.

Chian, E.S.K. and DeWalle, F.B. 1976. J. Water Pollut. Control Fed. 48:1042.

Chian, E.S.K. and Fang, H.H.P. 1974. Evaluation of New Reverse Osmosis Membranes for the Separation of Toxic Compounds from Water. Water-1973, AIChE Symposium Series

Chian, E.S.K. and Kuo, P.P.K. 1975. Fundamental Study on the Post Treatment of Reverse Osmosis Permeates from Army Wastewaters. First Annual Report to the U.S. Army Medical Research & Development Command, Contract No. DAMD 17-75-C-5006.

Chian, E.S.K. and Kuo, P.P.K. 1976. 2nd Annual Report, U.S. Army Contract No. DAMD 17-75-C-5006.

Chian, E.S.K. et al. 1976. Final Reports, U.S. Environmental Protection Agency, Contract No. 68-01-3234.

Chian, E.S.K., Cheng, S.S., DeWalle, F.B., and Kuo, P.P.K. 1977a. Prog. Water Technol. 9:761.

Chian, E.S.K., Kuo, P.P.K., Cooper, W.J., Cowen, W.F., and Fuentes, R.C. 1977b. Environ. Sci. Technol. 11:282-285.

Christian, R.T. 1973. University of Cincinnati Third Quarterly Progress Report, DADA 17-73-C-3013.

Chriswell, C.D. 1977. J. Chromatogr. 132:537.

Chriswell, C.D., Chang, R.C., and Fritz, J.S. 1975. Anal. Chem. 47:1325.

Cooper, A.R., Johnson, J.F., and Porter, R.S. 1973. Am. Lab. 5(5):12.

Corcia, A.D. 1973a. Anal. Chem. 45:492.

Corcia, A.D. 1973b. J. Chromatogr. 80:69.

Corcia, A.D., Liberti, A., and Samperi, R. 1973. Anal. Chem. 45:1228.

Coughlin, R.W. and Ezra, F.S. 1968. Environ. Sci. Technol. 2:291.

Cowen, W.F. and Cooper, W.J. 1975. Environmental Laboratory Research Branch, U.S. Army Bioengineering Research and Development Laboratory, Fort Detrick, Frederick, MD 21701, Interim Report, Dec. 4.

Cowen, W.F., Cooper, W.J., and Highfill, J.W. 1975. Anal. Chem. 47:2483.

Cunningham, K.M., Goldberg, M.C., and Weiner, E.R. 1977. Anal. Chem. 49:70.

Czapski, G., Samuni, A., and Yellin, R. 1968. Israel J. Chem. 6:969.

Danckwerts, P.V. 1970. Gas-Liquid Reactions, McGraw-Hill Book Co., New York.

Dang, V.D. and Steinberg, M. 1976. AIChE J. 22:925.

Deckwer, W., Graeser, U., Langemann, H., and Serpemen, Y. 1973. Chem. Eng. Sci. 28:1223.

Deguchi, T., Hisanaga, A., and Nagai, H. 1977. J. Chromatogr. 134:173.

DeWalle, F.B. and Chian, E.S.K. 1974. J. Environ. Eng. Div., ASCE, 100:EE5, Proc. Paper 10867.

Dilling, W.L., Tefertiller, N.B., and Kallos, G.J. 1975. Environ. Sci. Technol. 9:833.

Dilling, W.L., Tefertiller, N.B., and Kallos, G.J. 1977. Environ. Sci. Technol. 11:405.

Dobinson, F. 1959. Chem. Ind. 853.

Dowty, B. and Laseter, J.L. 1975. Anal. Lett. 8(1):25.

Dowty, B.J., Charlisle, D.R., Laseter, J.L., and Storer, J.S. 1975a. Environ. Sci. Tech. 9:762.

Dowty, B.J., Charlisle, D.R., Laseter, J.L., and Storer, J.S. 1975b. Science 187:75.

Dowty, B.J., Green, L.E., and Laseter, J.L. 1976a. Anal. Chem. 48:946.

Dowty, B., Green, L., and Laseter, J.L. 1976b. J. Chromatogr. Sci. 14:187.

Drarnuks, A., Krotoszynski, B.K., Whitfield, J., O'Donnell, A., and Burgwald, T. 1971. Environ. Sci. Technol. 5:1220.

Drawert, F. and Leupold, G. 1976. Chromatographia 9:605.

Dressman, R.C. and McFarren, E.F. 1977. J. Chromatogr. Sci. 15:69.

Dunges, W. 1977. Anal. Chem. 49:442.

Durst, H.D. et al. 1975. Anal. Chem. 47:1797.

Eckenfelder. 1959.

Eichelberger, J.W., Dressman, R.C., and Longbottom, J.E. 1970. Environ. Sci. Technol. 4:576.

Eisenhauer, H.R. 1971. J. Water Pollut. Control Fed. 43:200.

Eissa, S.H., El-Halwagi, M.M., and Saleh, M.A. 1971. Ind. Eng. Chem. Process Des. Dev. 10:31.

Ellis, J.E. and Jones, E.L. 1967. Two Phase Flow Symposium, Exeter, England.

EPA. 1971. NERC, EPA, Cincinnati, OH 45268.

EPA. 1973. EPA-R2-73-277, NERC, EPA, Corvallis, OR 97330.

EPA. 1974. EPA-904/10-74-002, U.S. EPA, Dallas, TX.

EPA. 1975. Interim Report WO-1/75, Organic Section, Chemical Services Branch, Region IV, EPA, Athens, GA.

Errst, G.R. and Van Lierop, J.B.H. 1975. J. Chromatogr. 109:439.

Fang, H.H.P. and Chian, E.S.K. 1975. J. Appl. Polymer Sci. 19:2889.

Fang, H.H.P. and Chian, E.S.K. 1976. Environ. Sci. Technol. 10:364.

Farrington, J.W. and Quinn, J.G. 1973. J. Water Pollut. Control Fed. 45:704.

Feigl, F. and Anger, V. 1966. Spot Tests in Organic Analysis, Elsevier Publishing Co., New York.

Fell, V. and Lee, C.R. 1976. J. Chromatogr. 121:41.

Fieser, L.F. and Fieser, M. 1967. Reagents for Organic Synthesis, p. 413, John Wiley and Sons, New York.

Fischer, F.G. 1929. Ann. Chem. 476:233.

Fochtman, E.G. and Huff, J.E. 1975. Presented at Second International Ozone Symposium, Montreal, Canada.

Ford, J.H., McDaniel, C.A., White, F.C., Vest, R.E., and Roberts, R.E. 1975. J. Chromatogr. Sci. 13:291.

Fritz, J.S. and Tateda, A. 1968. Anal. Chem. 40:2115.

Funasaka, W., Hani, T., and Fujimura, K. 1974. J. Chromatogr. Sci. 12:517.

Gabriel, T.F. and Michalewsky, J.E. 1973. Am. Lab. 5(10):8.

Gales, M.E., Jr. and Booth, R.L. 1976. J. Am. Water Works Assoc. 68:540.

Gal-Or, B. and Yaron, I. 1973. AIChE J. 19:200.

Gilbert, E. 1975. Presented at Second International Ozone Symposium, Montreal, Canada.

Glaze, W.H., Henderson, J.E., Bell, J.E., and Wheeler, V.A. 1973. J. Chromatogr. Sci. 11:580.

Gleason, M.N., Gosselin, R.E., Hodge, H.C., and Smith, R.P. 1969. Clinical Toxicity of Commercial Products, 3rd Ed., Williams and Wilkins Co., Baltimore, MD.

Gloor, R. and Leidner, H. 1976. Chromatographia 9:618.

Goldberg, M.C., DeLong, L., and Kahn, L. 1971. Environ. Sci. Technol. 5:161.

Goldberg, M.C., DeLong, L., and Sinclair, M. 1973. Anal. Chem. 45:89.

Gollan, A.A. et al. 1976. Final Report to the U.S. Army Medical R&D Command, Contract No. DAMD 17-74-C-4066.

Gorbenko-Germanov, D.S. and Kozlova, I.V. 1973. Dokl. Akad. Nauk. SSSR 210:851.

Goren-Strul, S., Kleijn, H.F.W., and Mostaert, R.E. 1966. Anal. Chem. Acta 34:322.

Gould, J.P. and Weber, W., Jr. 1976. J. Water Pollut. Control Fed. 48:47.

Grieser, M.D. and Pietrzyk, D.J. 1973. Anal. Chem. 45:1348.

Grob, K. 1973. J. Chromatogr. 84:225.

Grob, K. and Zurcher, F. 1976. J. Chromatogr. 117:285.

Grob, K., Grob, K., Jr., and Grob, G. 1975. J. Chromatogr. 106:299-315.

Grote, J.O. 1975. Am. Lab. 7(7):47.

Harris, L.E., Budde, W.L., and Eichelberger, J.W. 1974. Anal. Chem. 46:1912.

Harris, W.E. 1975. J. Chromatogr. Sci. 13:514.

Hewes, C.G. and Davison, R.R. 1971. AIChE J. 17:141.

Hewes, C.G., Prengle, H.W., Mauk, C.E., and Sparkman, O.D. 1974. Final Report No. 7184 for U.S. Army Mobility Equipment, Research and Development Center.

Higbie. 1935.

Hites, R.A. and Biemann, K. 1972. Science 178:158.

Hinze, J.O. 1955. AIChE J. 1:289.

Hoak, R.D. 1962. Int. J. Air Water Pollut. 6:521.

Hoigne, J. and Bader, H. 1975. Presented at Second International Ozone Symposium, Montreal, Canada.

Hoigne, J. and Bader, H. 1976. Water Res. 10:377.

Horning, M.G., Boucher, E.A., Moss, A.M., and Horning, E.C. 1968. Anal. Lett. 1:713.

Houle, M.J., Long, D.E., and Smette, D. 1970. Anal. Lett. 3:401.

Hrutfiord, B.F. and Christman, R.F. 1972. Presented at Boston ACS Meeting.

Hughmark, G.A. 1967. Ind. Eng. Chem. Process Des. Dev. 6:218.

Ippen, A.T. and Carver, E. 1955. M.I.T., Hydrodynamics Lab. Tech. Report No. 14.

Ishitoya, Y., Itoh, C., Osawa, N., Hashimoto, I., Iwanaga, T., and Nambara, T. 1970. Clin. Chim. Acta 27:233.

Janak, J., Ruzickova, J., and Novak, J. 1974. J. Chromatogr. 99:689.

Junk, G.A. et al. 1974. J. Chromatogr. 99:745-762.

Junk, G.A., Richard, J.J., Svec, H.J., and Fritz, J.S. 1976. J. Am. Water Works Assoc. 68:218.

Kahn, L. and Wayman, C.H. 1964. Anal. Chem. 36:1340.

Kaiser, K.L.E. and Oliver, B.G. 1976. Anal. Chem. 48:2207.

Kallio, h. and Linko, R.R. 1973. J. Chromatogr. 76:229.

Kammerer, P.A. and Lee, F.G. 1969. Environ. Sci. Technol. 3:276.

Kasai, Y., Tanimura, T., and Tamura, Z. 1975. Anal. Chem. 47:34.

Kasai, Y., Tanimura, T., Tamura, Z., and Ozawa, Y. 1977. Anal. Chem. 49:655.

Kawahora, F. 1971. Environ. Sci. Technol. 5:235.

Keith, L.H. 1976. Identification and Analysis of Organic Pollutants in Water, Ann Arbor Science Publishers, Inc., Ann Arbor, MI.

Kennedy, D.C. 1973. Environ. Sci. Technol. 7:138.

Kepner, R.E., Maarse, H., and Strating, J. 1964. Anal. Chem. 36:77.

Kilpatrick, M.L., Herrick, C.C., and Kilpatrick, M. 1956. J. Am. Chem. Soc. 78:1784.

AD-A111 391 ILLINOIS UNIV AT URBANA F/G 13/2
FUNDAMENTAL STUDY ON THE OZONE POSTTREATMENT OF REVERSE OSMOSIS--ETC(U)
MAR 81 E S CHIAN, P P KUO, B J CHANG DAMD17-75-C-5006
UNCLASSIFIED NL

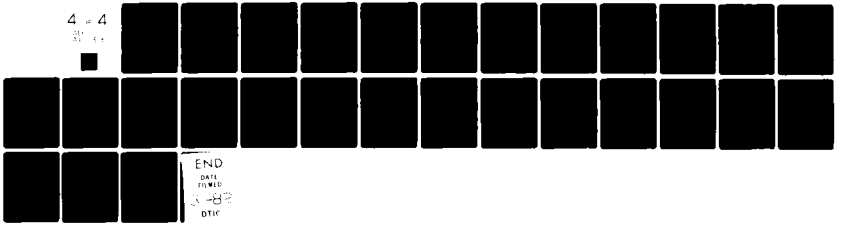

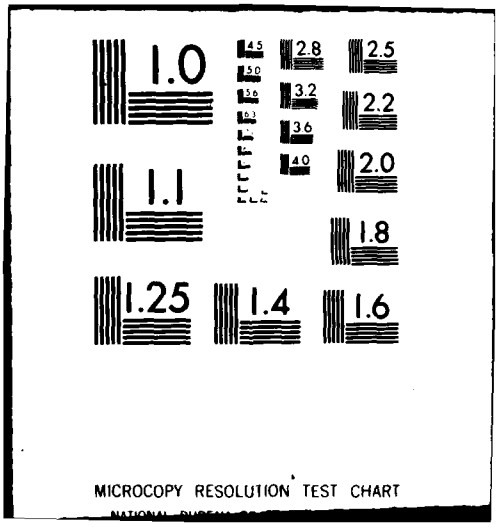
1.0
1.1
1.25
1.4
1.6
1.8
2.0
2.2
2.5
2.8
3.2
3.6
4.0
4.5
5.0
5.6
6.3
MICROCOPY RESOLUTION TEST CHART

Kinman, R., Rickabaugh, J., Elia, V., McGinnis, K., Cody, T., Clark, S., and Christian, R. 1976. Presented at International Ozone Institute Workshop: Ozone/Chlorine Dioxide Oxidation Products of Organic Materials, Cincinnati, OH.

Kirk, B.S., McNabney, R., and Wynn, C.S. 1972. Ozone in Water and Wastewater Treatment, F.L. Evans, ed., Ann Arbor Science Publishers, Inc., Ann Arbor, MI.

Kirkland, J.J. 1971. Anal. Chem. 43(12):36A.

Kissinger, L.D. and Fritz, J.S. 1976. J. Am. Water Works Assoc. 68:435.

Kleopfer, R.D. and Fairless, B.J. 1972. Environ. Sci. Technol. 6:1036.

Kobayashi, S. and Lee, G.F. 1964. Anal. Chem. 36:2197.

Kolb, B. 1975. J. Chromatogr. 112:287.

Kolb, B. 1976. J. Chromatogr. 122:553.

Komers, R. and Sir, Z. 1976. J. Chromatogr. 119:251.

Kopfler, F.C., Melton, R.G., Lingg, R.D., and Coleman, W.E. 1976. Chapter 6, ed. by L.H. Keith, Ann Arbor Science Publishers, Inc., Ann Arbor, MI.

Kramer, D.N., Klein, N., and Baselice, R.A. 1959. Anal. Chem. 31:250.

Kunin, R. 1974. Personal communication (Rohm & Haas).

Kuo, C.H. and Wen, C.P. 1976. Paper presented at AIChE 69th Meeting, Chicago, IL.

Kuo, C.H., Li, K.Y., Wen, C.P., and Weeks, J.L., Jr. 1975. Paper presented at AIChE 68th Annual Meeting, Los Angeles, CA.

Kuo, P.P.K., Chian, E.S.K., and Chang, B.J. 1977a. Environ. Sci. Technol. 11:1177.

Kuo, P.P.K., Chian, E.S.K., Dewalle, F.B., and Kim, J.H. 1977b. Anal. Chem. 49:1023.

Lancaster, G., Lamm, P., Scriver, C.R. Tjoa, S.S., and Mamer, O.A. 1973. Clin. Chim. Acta 48:279.

Langenbeck, U., Hoinowski, A., Mantel, K., and Mohring, H.U. 1977. J. Chromatogr. 143:39.

Lee, G.F., Kumke, G.W., and Becker, S.L. 1965. Int. J. Air Water Pollut. 9:69.

Lehrer, I.H. 1971. Ind. Eng. Chem. Process Des. Dev. 10:37.

Leoni, V., Puccetti, G., and Grella, A. 1975. J. Chromatogr. 106:119.

Levadie, B. and MacAskill, S. 1975. Anal. Chem. 47:1851.

Levenspiel, O. 1972. Chemical Reaction Engineering, John Wiley & Sons, Inc., New York.

Liebman, S.A., Ahlstrom, D.H., and Sanders, C.I. 1975. Am. Lab. 7(9):21.

Ligon, W.V., Jr. and Johnson, R.L., Jr. 1976. Anal. Chem. 48:481.

Limpert, R.J., Cotter, R.L., and Dark, W.A. 1973. Am. Lab. 6(5):63.

Long, L., Jr. 1940. Chem. Rev. 27:437.

Love, O.T., Jr., Carswell, J.K., Stevens, A.A., and Symons, J.M. 1975. An EPA Progress Report, presented at the 95th Annual Conference AWWA, Minneapolis, MN.

Loy, E.W., Jr. 1973. Procedure for Water Soluble Volatile Organic Solvents in Effluents and Streams. Org. Lab., Chem. Services Br., Region 4, EPA, Athens, GA.

Lysyi, I. et al. 1966. Research and Development Progress Report #152, U.S. Dept. of the Interior, PB 178 525.

Manely, T.C. and Niegowski, S.J. 1967. Encyclopedia of Chemical Technology Vol. 14, Interscience-John Wiley, New York.

Marrucci, G. and Nicodemo, L. 1967. Chem. Eng. Sci. 22:1257.

Melpolder, F.W., Warfield, C.W., and Headington, C.E. 1953. Anal. Chem. 25:1453.

Merkulova, V.P., Lovchikov, V.S., and Ivanouskii, M.D. 1971. Izv. Vyssh. Uchebn. Zaved. Khim. Khim. Tekhnol. 14:818.

Michel, B.J. and Miller, S.A. 1962. AIChE J. 8:262.

Mieure, J.P. 1977. J. Am. Water Works Assoc. 69:60.

Mieure, J.P. and Dietrich, M.W. 1973. J. Chromatogr. Sci. 11:559.

Mieure, J.P., Mappes, G.W., Tucker, E.S., and Dietrich, M.W. 1976. Chapter 8, Identification and Analysis of Organic Pollutants in Water, ed. by L.H. Keith, Ann Arbor Science Publishers, Inc., Ann Arbor, MI.

Miller, D.N. 1974. AIChE J. 20:445.

Morris, R.L. and Johnson, L.G. 1976. J. Am. Water Works Assoc. 68:492.

Nakajima, M., Ozawa, Y., Tanimura, T., and Tamura, Z. 1976. J. Chromatogr. 123:129.

Neher, M.B. and Jones, P.W. 1977. Anal. Chem. 49:512.

Nojima, K., Fukaya, K., Fukui, S., and Kanno, S. 1974. Chemosphere No. 5:247-252.

Novak, J., Zluticky, J., Kubelka, V., and Mostecky, J. 1973. J. Chromatogr. 76:45.

Novotny, M., Lee, M.L., and Bartle, K.D. 1974. Chromatographia 7:333.

Ohki, Y. and Inoue, H. 1970. Chem. Eng. Sci. 25:1.

Ottenstein, D.M. and Bartley, D.A. 1971. J. Chromatogr. Sci. 9:673.

Ozeris, S. and Bassette, R. 1963. Anal. Chem. 35:1091.

Pasveer, I. 1955. Sewage Ind. Wastes 27:1130.

Peleg, M. 1976. Water Res. 10:361.

Pellizzari, E.D., Bunch, J.E., Carpenter, B.H., and Sawicki, E. 1975a. Environ. Sci. Technol. 9:552.

Pellizzari, E.D., Carpenter, B.H., Bunch, J.E., and Sawicki, E. 1975b. Environ. Sci. Technol. 9:556.

Perkin-Elmer. 1977. Instrumental News 27(1):12.

Perrich, J., McCammon, J., Cronholm, L., Fleischman, M., Pavoni, J., and Riesser, V. 1975. AIChE 68th Annual Meeting, Los Angeles, CA.

Perry's Chemical Engineer's Handbook. 1963. Ed. by Perry, J.H., p. 13-7. McGraw-Hill, New York.

Politzer, I.R., Githens, S., Dowty, B.J., and Laseter, J.L. 1975. J. Chromatogr. Sci. 13:378.

Popl, M., Stejskal, M., and Mostecky, J. 1975. Anal. Chem. 4.

Prengle, Jr., H.W., Mauk, C.E., and Payne, J.E. 1976. Presented at the International Ozone Institute Forum on Ozone Disinfection, Chicago, IL.

Price, C.C. and Tumolo, A.L. 1964. J. Am. Chem. Soc. 86:4691.

Price, C.C. and Tumolo, A.L. 1967. J. Polymer Sci., Part A-1 5:175.

Price, P. et al. 1975. Anal. Chem. 47:190.

Pryde, A. 1974. J. Chromatogr. Sci. 12:486.

Rapp, A. and Ziegler, A. 1976. Chromatographia 9:148.

Raukas, M.M., Siirode, E.K., and Kyulm, S.R. 1962. J. Tallin. Politekh. Inst., Ser. A 198:219.

Reith, T., Renken, S., and Israel, A. 1968. Chem. Eng. Sci. 23:619.

Renberg, L. 1974. Anal. Chem. 46:459.

Richard, J.J. and Junk, G.A. 1977. J. Am. Water Works Assoc. 69:62.

Rook, J.J. 1976. J. Am. Water Works Assoc. 68:168.

Rosen, A.A. and Middleton, F.M. 1955. Anal. Chem. 27:790.

Rosenquist, H., Kallio, H., and Nurmikko, V. 1972. Anal. Biochem. 46:224.

Rothmund, V. and Burgstaller, A. 1913. Monatsh. Chem. 34:665.

Rushton et al. 1950.

Schafer, M.L., Peeler, J.T., Gardner, W.S., and Campbell, J.E. 1969. Environ. Sci. Technol. 3:1261.

Sennewald, K. 1933. Z. Phys. Chem. 164:305.

Shambaugh, R.L. and Melnuk, P.B. 1976. Forum on Ozone Disinfection, International Ozone Institute.

Shapiro, J. 1961. Sciences 133:2063.

Sharma, M.M. and Mashelkar, R.A. 1968. Proc. Symp. Mass Transfer with Chemical Reaction, Inst. Chem. Eng.

Schechter, H. 1973. Water Res. 7:729.

Shulmar and Molstad. 1950.

Sierka, R.A. 1974. University of Arizona, Tucson, AZ.

Simmonds, P.G., Pettitt, B.C., and Zlatkis, A. 1967. Anal. Chem. 39:163.

Smith, M.S., Francis, A.J., and Duxbury, J.M. 1977. Environ. Sci. Technol. 11:51.

Snider, E.H. and Porter, J.J. 1974. J. Water Pollut. Control Fed. 46:886.

Sokol, H.A. 1977. Anal. Chim. Acta 89:407.

Standard Methods. 1971. Standard Methods for the Examination of Water and Wastewater, 13th Ed., American Public Health Assoc., Washington, DC.

Sternowsky, H.J., Roboz, J., Hutterer, F., and Gaull, G. 1973. Clin. Chim. Acta 47:371.

Stevens, A.A., Slocum, C.J., Seeger, D.R., and Robeck, G.G. 1976. J. Am. Water Works Assoc. 68:615.

Stuum, W. 1954. Helv. Chim. Acta 37:773.

Stuum, W. 1958. J. Boston Soc. Civ. Eng. 45(1):68.

Suffet, I.H. and Radziul, J.V. 1976. J. Am. Water Works Assoc. 68:520.

Suffet, I.H., Brenner, L., and Silver, B. 1976. Environ. Sci. Technol. 10:1273.

Suzuki, J. 1976. J. Appl. Polymer Sci. 20:93.

Swinnerton, J.W. and Linnenbom, V.J. 1967. J. Gas Chromatogr. 5:570.

Symons, J.M. et al. 1975. J. Am. Water Works Assoc. 67:634.

Tadaki, T. and Maeda, S. 1964. Kagaku Kogaku Chem. Eng. Jpn. 2:195.

Takahagi, H. and Setsuya, S. 1974. J. Chromatogr. Sci. 12:507.

Taube, H. 1941. J. Am. Chem. Soc. 63:2453.

Terada, H., Hayashi, T., Kawai, S., and Ohno, T. 1977. J. Chromatogr. 130:281.

Tomkins, B. 1974. School of Chemical Sciences, University of Illinois, Urbana, IL.

Torricelli, A. 1958. Ozone Chemistry and Technology, Advances in Chemistry Series, 21.

Towell, G.D., Strand, C.P., and Ackerman, G.H. 1965. AIChE - Ind. Chem. Eng. Symp. Series No. 10, 97.

Treybal, R.E. 1968. Mass Transfer Operations. 2nd ed., McGraw-Hill, New York.

Tyler, J.E. and Dibdin, G.H. 1975. J. Chromatogr. 105:71.

Versino, B., deGroot, M., and Geiss, F. 1974. Chromatographia 7:302.

Versino, B. et al. 1976. J. Chromatogr. 122:373.

Vitenberg, A.G. 1975. J. Chromatogr. 112:319.

Vitenberg, A.G., Butaeva, I.L., and St. Dimitrova, Z. 1975. Chromatographia 8:693.

Wauchope, R.D. 1975. Anal. Chem. 47:1879.

Webb, R.G. 1964. Interim Report. Southeast Environmental Research Laboratory, Athens, GA.

Webb, R.G. 1974. ROAP 16ADN Tast 37, Program Element 1BA027, SERL, National Environmental Research Center, Athens, GA.

Webb, R.G. 1975. Isolating Organic Water Pollutants: XAD Resins, Urethane Foams, Solvent Extraction, U.S. EPA Report 660/4-75-003, Washington, DC.

Webb, R.G., Garrison, A.W., Keith, L.H., and McGuire, J.J. 1973. U.S. EPA Report No. EPA-R2-73-277.

Weiss, J. 1935. Trans. Faraday Soc. 31:668.

Werner, A.E. and Waldichak, M. 1962. Anal. Chem. 34:1674.

Westerterp, K.R., van Dierendonck, L.L., and de Kraa, J.A. 1963. Chem. Eng. Sci. 18:157.

White, W.R. and Leenheer, J.A. 1975. J. Chromatogr. Sci. 13:386.

Wilkinson, P.K., Wagner, J.G., and Sedman, A.J. 1975. Anal. Chem. 47:1506.

Williams, F.W. and Unstead, M.E. 1968. Anal. Chem. 40:2232.

Williams, R.C., Barker, D.R., Larman, J.P., and Hudson, D.R. 1973. Am. Lab. 5(10):45.

Yoshida, F. and Akita, K. 1965. AIChE J. 11:9.

Zlatkis, A. and Liebrich, H.M. 1971. Clin. Chem. 17:592.

Zlatkis, A., Lichtenstein, H.A., and Fishbee, A. 1973a. Chromatographia 6:67.

Zlatkis, A. et al. 1973b. Anal. Chem. 45:763.

APPENDIX A

LIST OF PUBLICATIONS

P.P.K. Kuo, E.S.K. Chian, and F.B. DeWalle, "Determination of Trace Low-Molecular-Weight Volatile Polar Organics in Water by Gas Chromatography Using Distillation Methods," Water Res. 11(11):1005-1011 (1977).

E.S.K. Chian, P.P.K. Kuo, W.J. Cooper, W.F. Cowen, and R.C. Fuentes, "Distillation Headspace Gas Chromatographic Analysis for Volatile Polar Organics in Water at ppb Level," Environ. Sci. Technol. 11(2):282-285 (1977).

P.P.K. Kuo, E.S.K. Chian, F.B. DeWalle, and J.H. Kim, "Study of the Gas Stripping, Sorption, and Thermal Desorption Procedures for Preconcentrating Volatile Polar Organics from Water Samples for Analysis by Gas Chromatography," Anal. Chem. 49(7):1023-1028 (1977).

P.P.K. Kuo, E.S.K. Chian, and B.J. Chang, "Identification of End Products Resulting from Ozonation and Chlorination of Organic Compounds Commonly Found in Water," Environ. Sci. Technol. 11(12):1177-1181 (1977).

J.J. McCarthy, W.F. Cowen, E.S.K. Chian, and B.W. Peterman, "Evaluation of an Air Stripping Ozone Contactor System," Proc. 32nd Annual Purdue Ind. Waste Conf., Purdue University, West Lafayette, IN, pp. 310-324 (May 1977).

E.S.K. Chian, P.P.K. Kuo, W.J. Cooper, W.F. Cowen, and J.J. McCarthy, "Removal of Organics in Hospital Wastewaters with Various Physical-Chemical Treatment Processes," Paper presented at the Joint Am. Chem. Soc. and Can. Inst. of Chem, Conference, Montreal, Canada (May 30-June 3, 1977).

E.S.K. Chian, H.H.P. Fang, F.B. DeWalle, and J.W. Smith, "Physical-Chemical Treatment of Hospital Waste for Potential Reuse," Proc. 30th Annual Purdue Ind. Waste Conf. pp. 377-389 (May 1975).

E.S.K. Chian and D. Roy, "Advance Treatment of Secondary Effluent for Reuse," presented at the Water Reuse Symposium, AWWA and the U.S. Army, Washington, DC (March 1979).

E.S.K. Chian, F.B. DeWalle, and J.W. Smith, "Ozonation of Effluents from Various Biological Treatment Processes," Proc. Second Int. Ozone Symp., Montreal, Canada, pp. 566-585 (May 1975).

B.J. Chang and E.S.K. Chian, "A Model Study of Ozone-Sparged Vessels for the Removal of Organics from Water and Wastewater," Paper submitted to ASCE, Environmental Engineering Division for publication, 1979.

B.J. Chang and E.S.K. Chian, "Evaluation of Diffuser Materials for Ozonation in Sparged Tanks," Submitted to American Water Works Association for publication, 1979.

APPENDIX B

GC CHROMATOGRAPHS

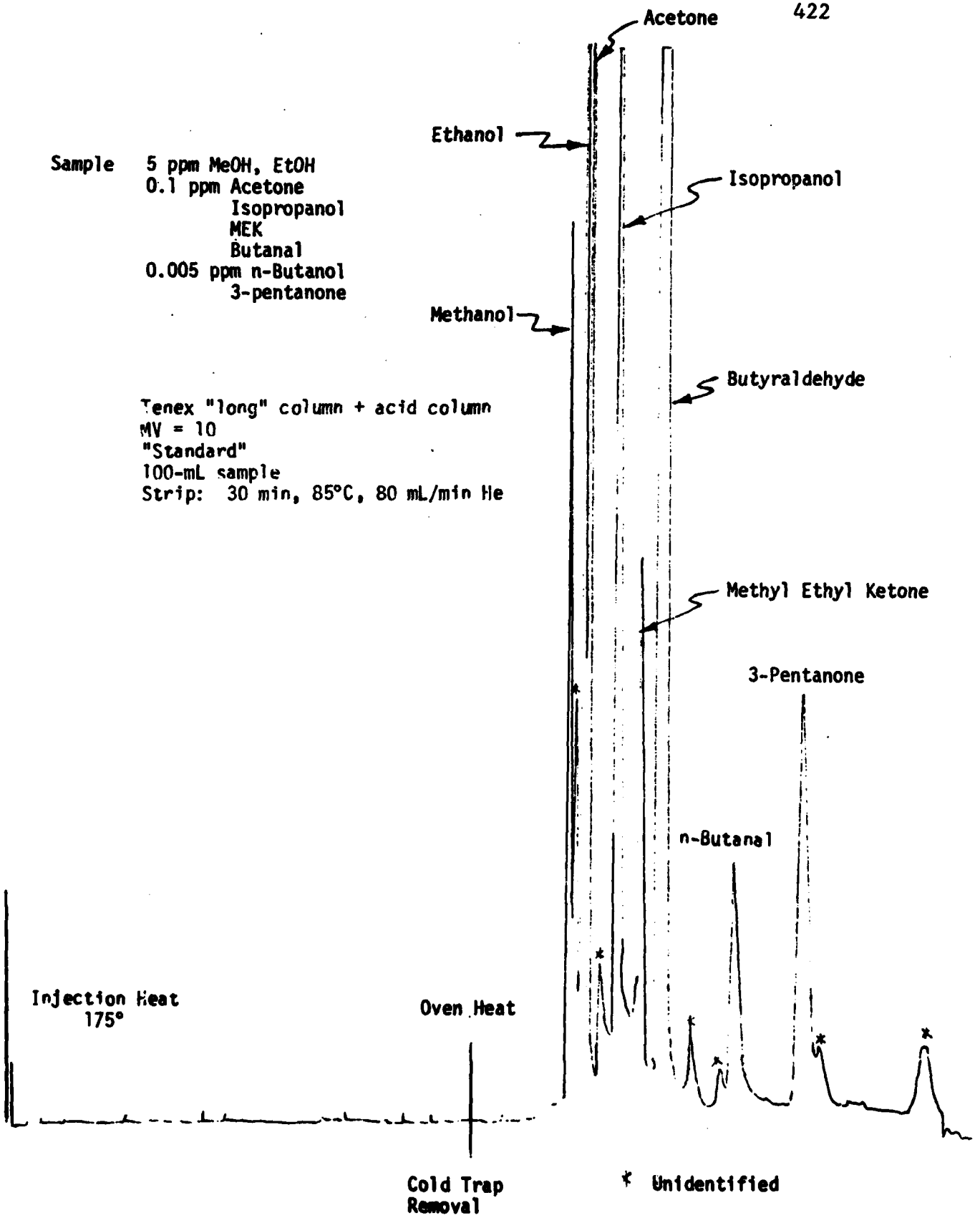

Sample 5 ppm MeOH, EtOH
0.1 ppm Acetone
Isopropanol
MEK
Butanal
0.005 ppm n-Butanol
3-pentanone

Tenex "long" column + acid column
MV = 10
"Standard"
100-mL sample
Strip: 30 min, 85°C, 80 mL/min He

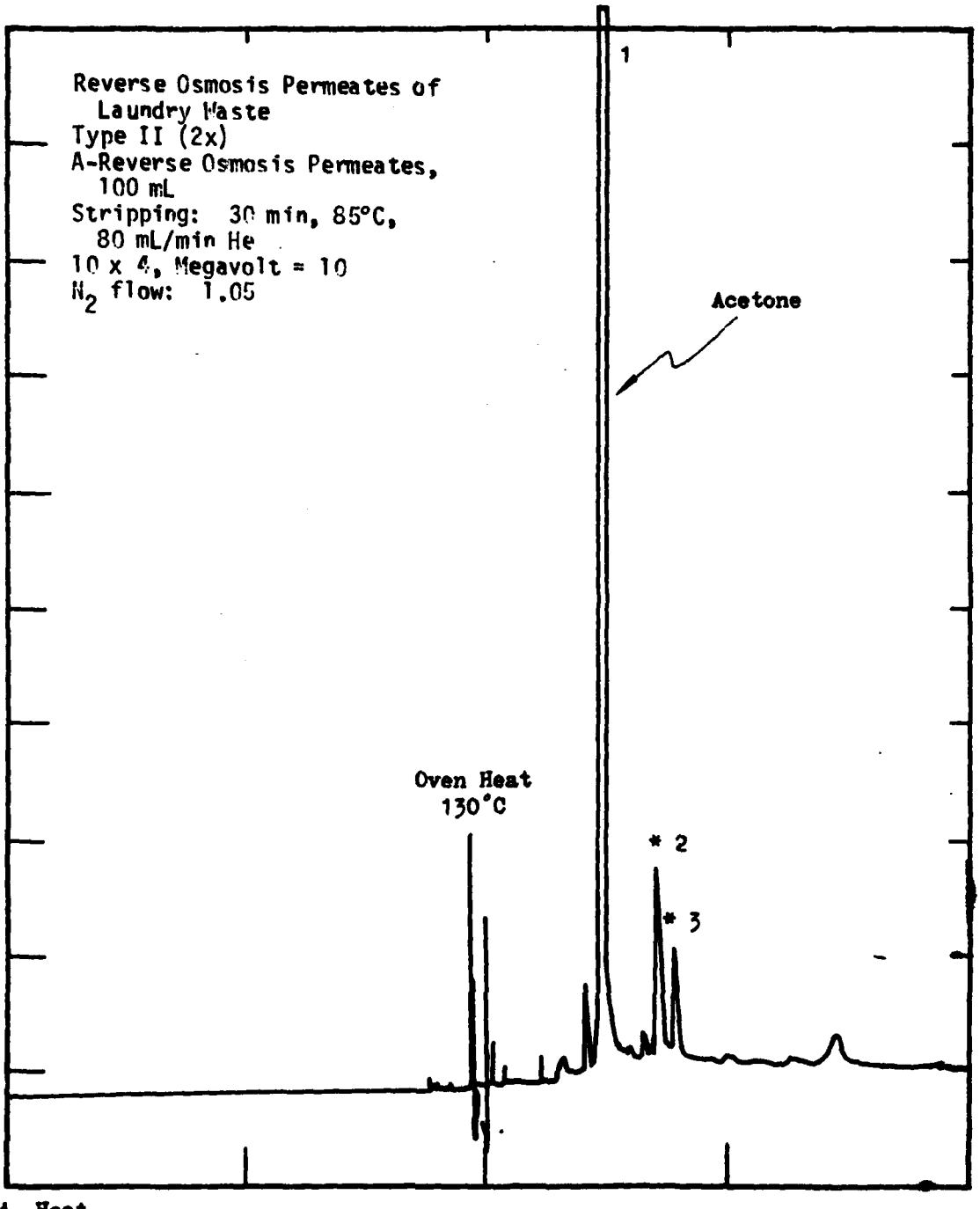
Reverse Osmosis Permeates of
Laundry Waste
Type II (2x)
A-Reverse Osmosis Permeates,
100 mL
Stripping: 30 min, 85°C,
80 mL/min He
10 x 4, Megavolt = 10
N_2 flow: 1.05
1
Acetone
Oven Heat
130°C
* 2
* 3
Inj. Heat
2 min/div

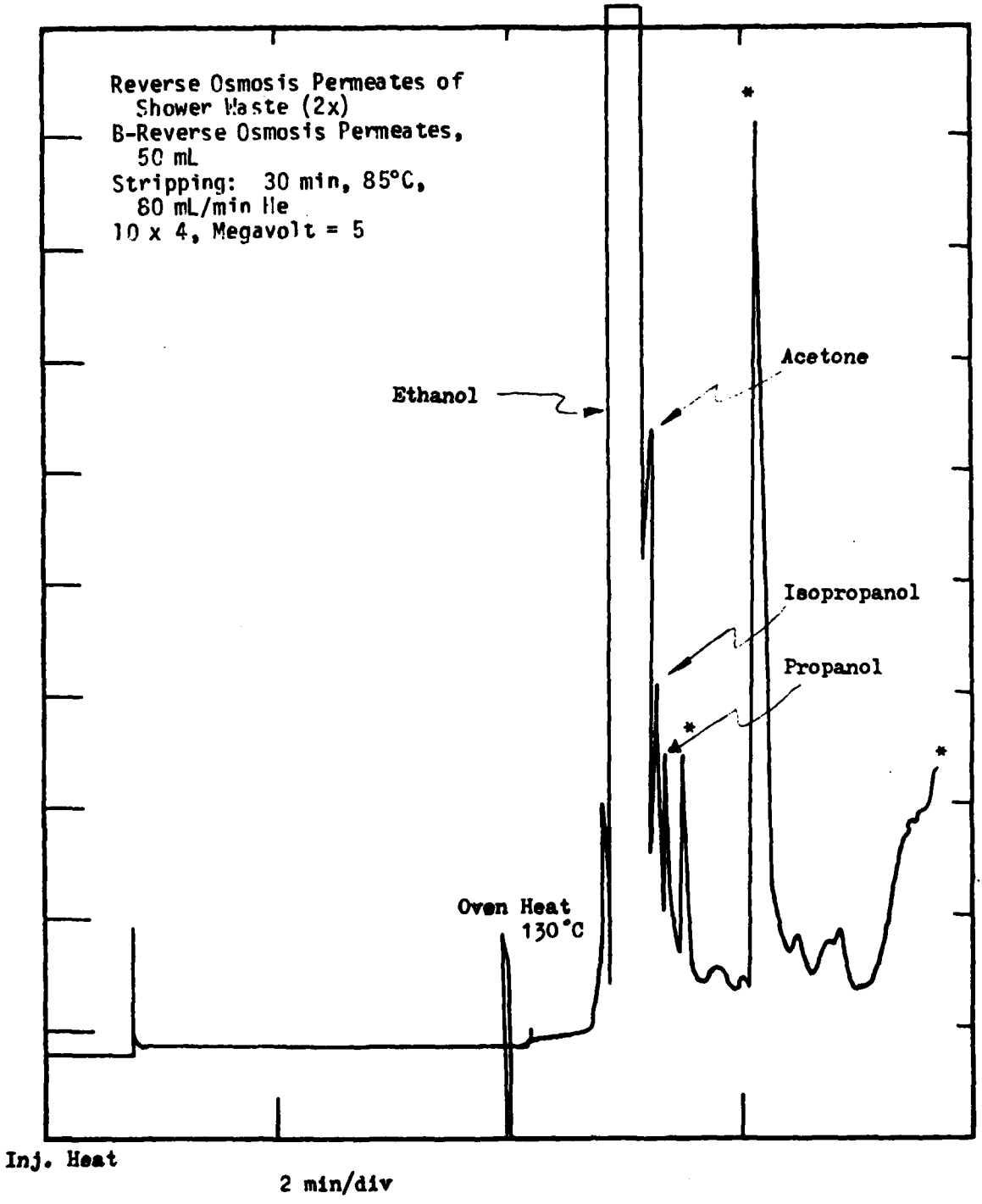
Reverse Osmosis Permeates of
Shower Waste (2x)
B-Reverse Osmosis Permeates,
50 mL
Stripping: 30 min, 85°C,
60 mL/min He
10 x 4, Megavolt = 5
Ethanol
Acetone
Isopropanol
Propanol
Oven Heat
130°C
Inj. Heat
2 min/div

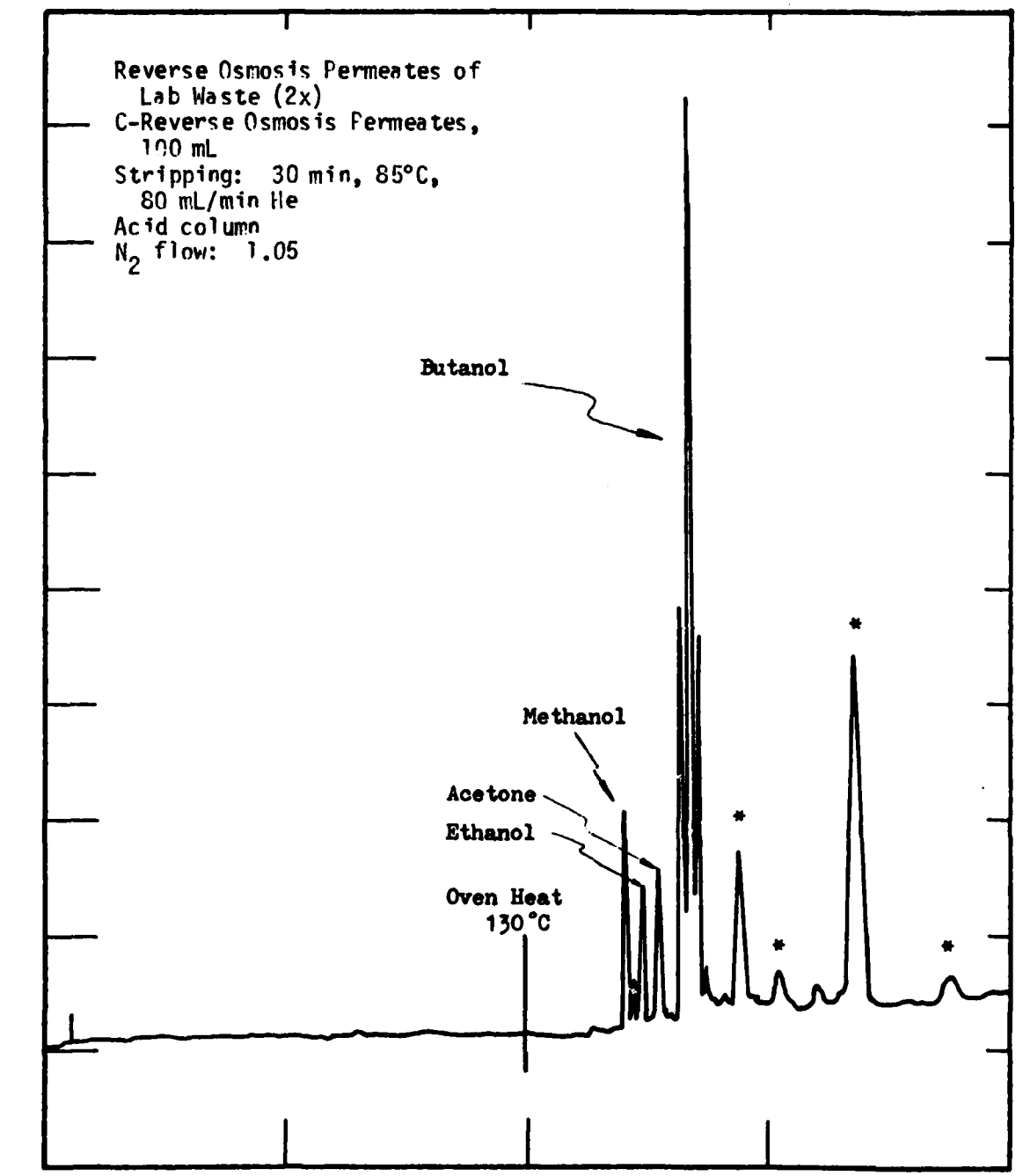
Reverse Osmosis Permeates of
Lab Waste (2x)
C-Reverse Osmosis Permeates,
100 mL
Stripping: 30 min, 85°C,
80 mL/min He
Acid column
N_2 flow: 1.05
Butanol
Methanol
Acetone
Ethanol
Oven Heat
130°C
Inj. Heat
2 min/div

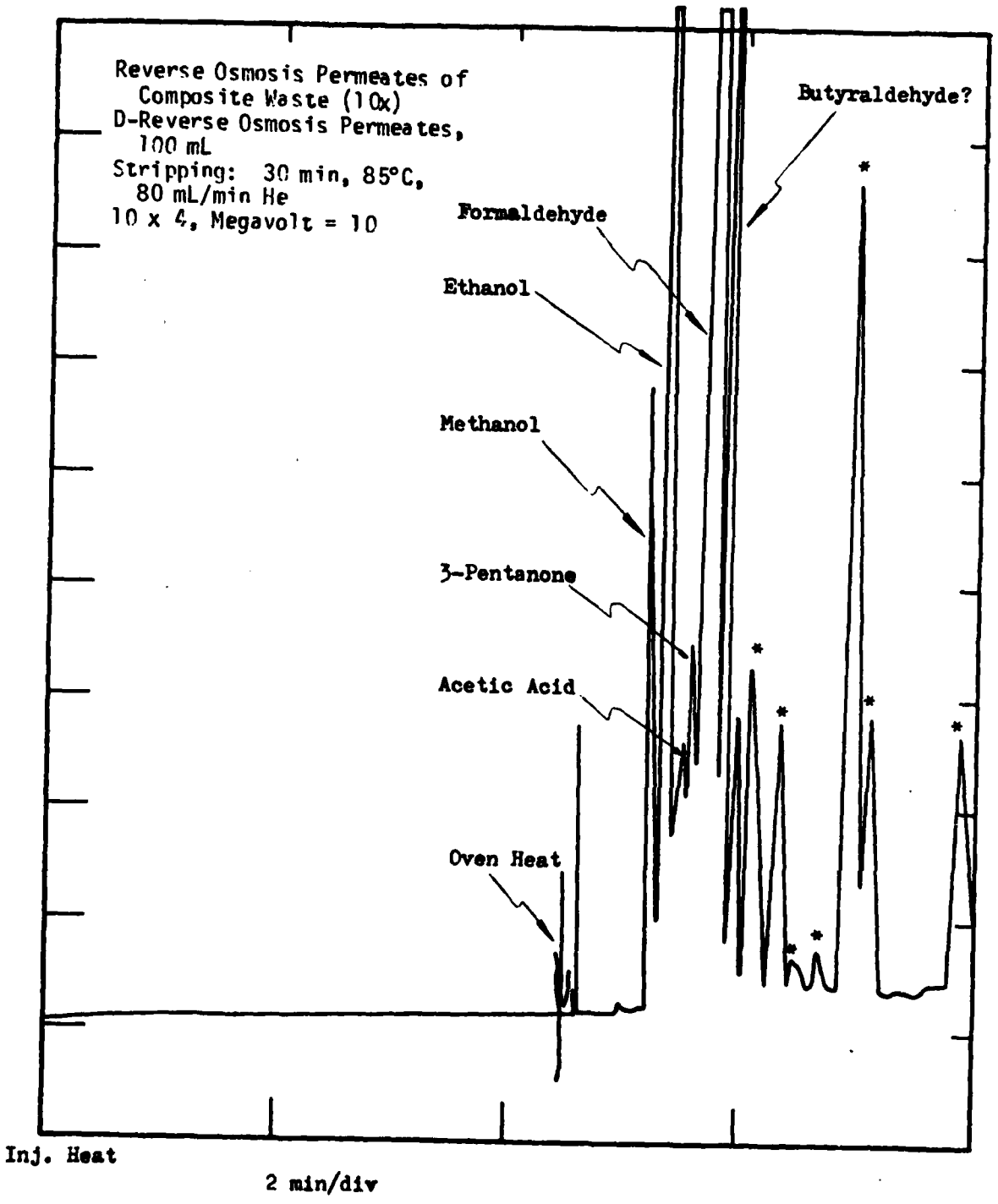
Reverse Osmosis Permeates of
Composite Waste (10x)
D-Reverse Osmosis Permeates,
100 mL
Stripping: 30 min, 85°C,
80 mL/min He
10 x 4, Megavolt = 10
Butyraldehyde?
Formaldehyde
Ethanol
Methanol
3-Pentanone
Acetic Acid
Oven Heat
Inj. Heat
2 min/div

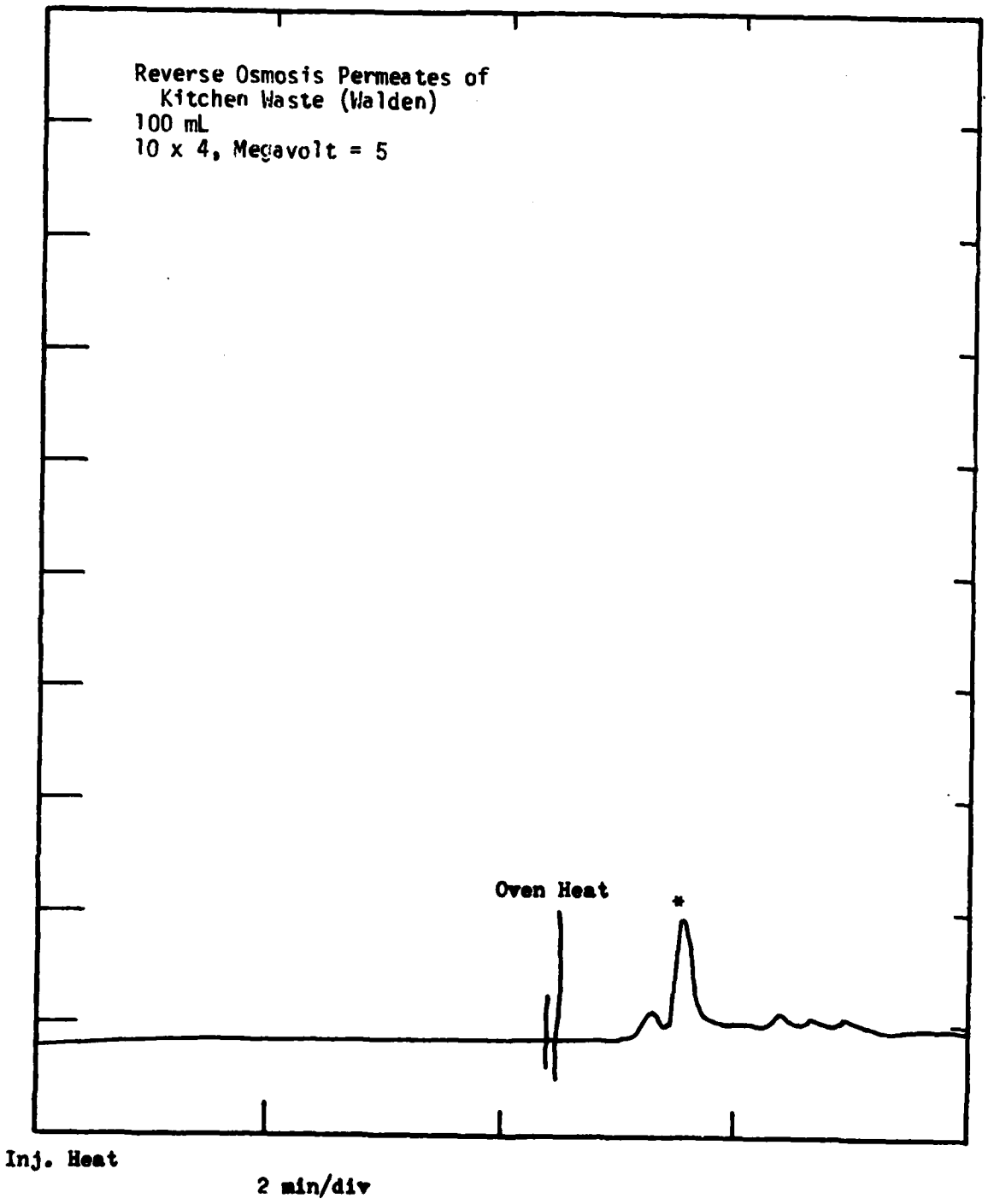
Reverse Osmosis Permeates of
Kitchen Waste (Walden)
100 mL
10 x 4, Megavolt = 5
Oven Heat
*
Inj. Heat
2 min/div

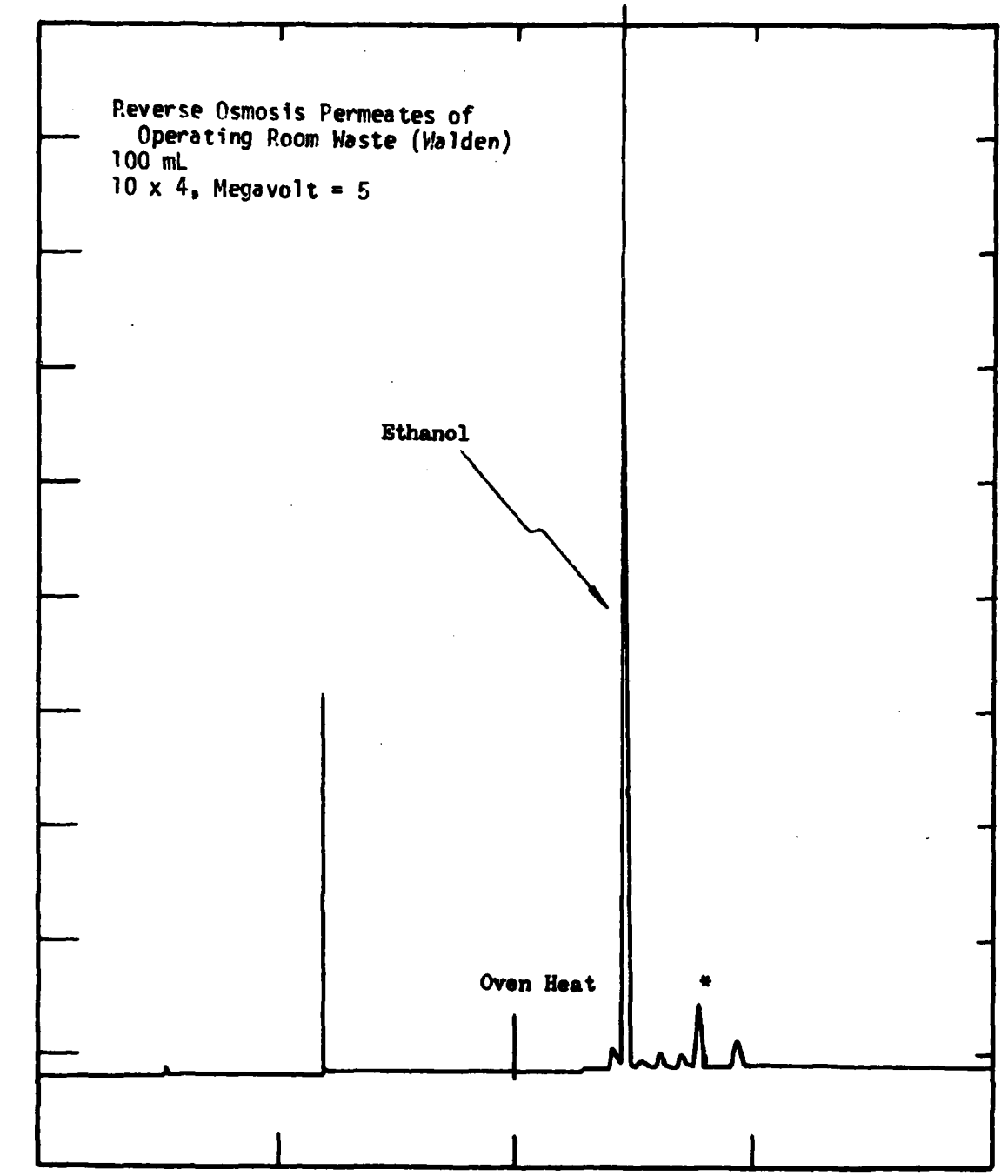
Reverse Osmosis Permeates of
Operating Room Waste (Walden)
100 mL
10 x 4, Megavolt = 5
Ethanol
Oven Heat
*
Inj. Heat
2 min/div

APPENDIX C

GC SEPTUM COOLER

To eliminate septum bleeding at high temperatures, a septum cooler was installed. Figure A shows the cooler, which consists of three pieces -- a septum holder, a water-cooling jacket, and a tightening nut, all fabricated from brass. The exact dimensions are not critical. However, the septum holder should be able to hold a GC septum and fit into the GC injection port properly. Figure B is a detailed drawing of the septum holder. The septum swinger from Varian Associates functions in the same manner as the septum cooler to eliminate the bleeding problem.

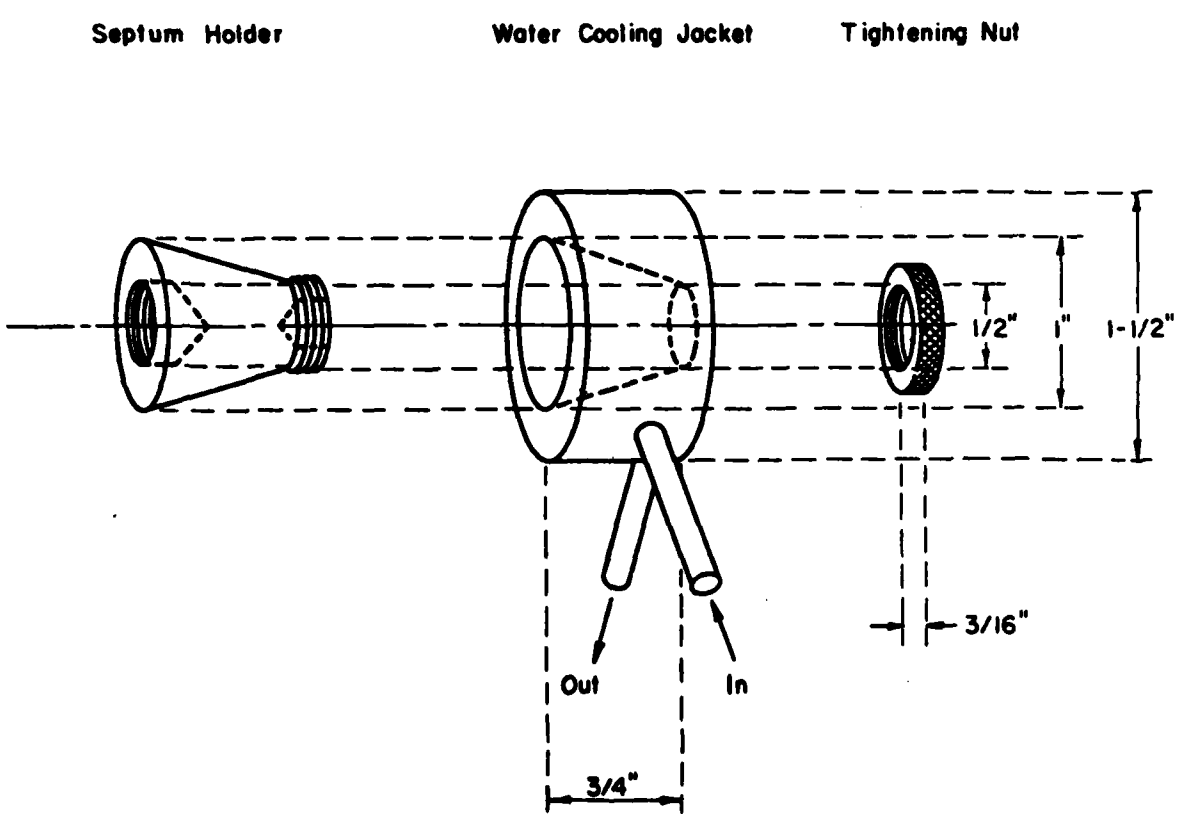

Figure C-1. GC Septum Cooler.

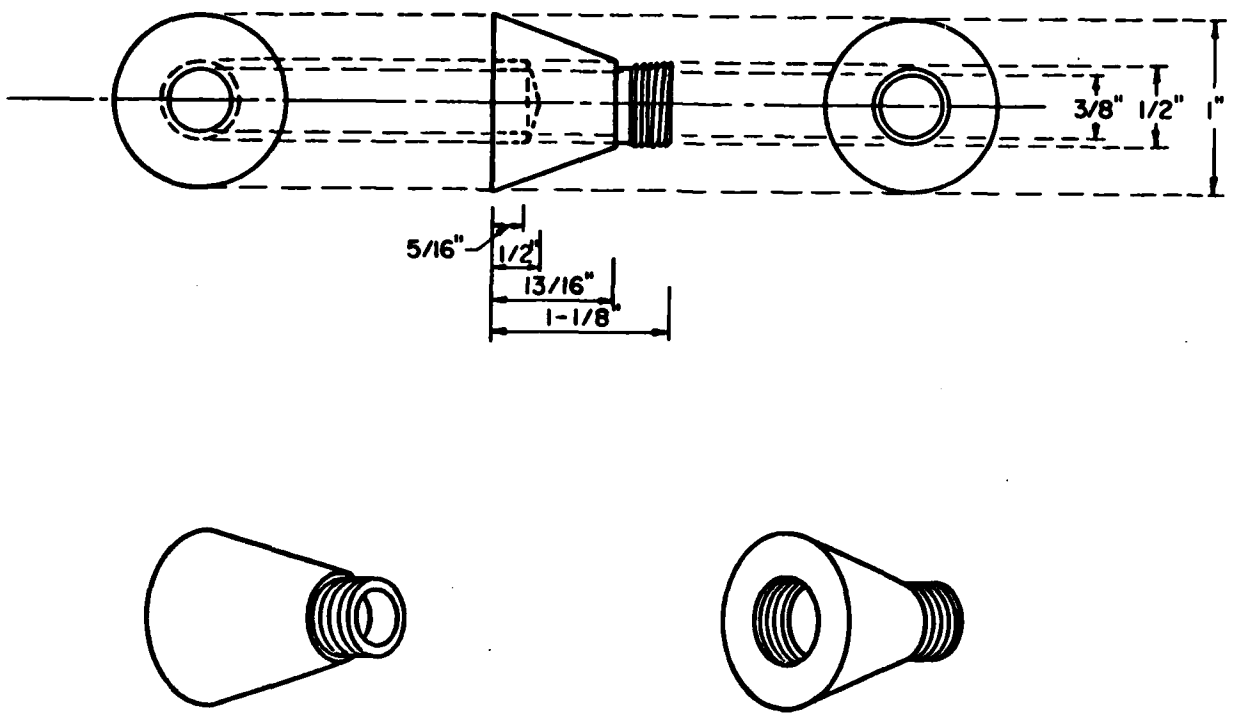

Figure C-2. Detailed Drawing of Septum Holder.

APPENDIX D

COMPUTER PROGRAM FOR COMPUTATIONS OF KINETICS OF SEMI-BATCH OZONATION OF METHANOL AND ITS DEGRADATION PRODUCTS

```
      PROGRAM KINETIC (INPUT,OUTPUT,TAPE5=INPUT,TAPE6=OUTPUT)
C THIS PROGRAM COMPUTES THE CONCENTRATION OF OZONE IN THE
C EFFLUENT GAS AS WELL AS THE CONCENTRATIONS OF METHANOL,
C FORMALDEHYDE, FORMIC ACID, AND DISSOLVED OZONE IN THE REACTION
C MIXTURE AS A FUNCTION OF TIME FOR SEMI-BATCH OZONATION OF
C METHANOL AND IST DEGRADATION PRODUCTS.
C THE SUBROUTINE BLCKDQ IN THE MATH SCIENCE LIBRARY IS USED
C IN THIS PROGRAM.
C THE USER MUST SUPPLY VALUES OF KLA, KR, K21,K22,K23,XLM,XINV
C YS,XINV,DI,H,CGOIN,GO,V,AND XL.
C SOME OF THE INPUT AND OUTPUT PARAMETERS ARE DEFINED IN THE
C WRITE-UP OF BLCKDQ ON PAGES 4-55 TO 4-64 OF THE MATH
C SCIENCE LIBRARY.
C DEFINITION OF TERMS AND THEIR UNITS:
C KLA=OVERALL MASS TRANSFER COEFFICIENT,MIN**-1.
C KR=FIRST-ORDER RATE CONSTANT FOR OZONE DECOMPOSITION
C    REACTION,MIN**-1
C K21=SECOND-ORDER RATE CONSTANT FOR REACTION BETWEEN OZONE AND
C    METHANOL,L/MG/MIN.
C K22=SECOND-ORDER RATE CONSTANT FOR REACTION BETWEEN OZONE AND
C    FORMALDEHYDE,L/MG/MIN.
C K23=SECOND-ORDER RATE CONSTANT FOR REACTION BETWEEN OZONE AND
C     FORMIC ACID,L/MG/MIN.
C LM=NUMBER OF POINTS WHERE DATA ARE TO BE TABULATED,
C    DIMENSIONLESS.
C YS=AT ENTRY:ARRAY CONTAINING INITIAL VALUES OF THE
C    DEPENDENT VARIABLES; AT RETURN:ARRAY CONTAINING SOLUTION
C    AT X=XOUT,MG/L.
C XINV=INVERT OF LIQUID RESIDENCE TIME,MIN**-1.
C DI=DISTRIBUTION COEFFICIENT,DIMENSIONLESS.
C H=FRACTIONAL GAS HOLDUP, DIMENSIONLESS.
C CGOIN=OZONE CONCENTRATION IN INFLUENT GAS,MG/L.
C GO=GAS FLOW RATE AT 1 ATM.,L/MIN.
C V=LIQUID VOLUME,L.
C XL-LIQUID HEIGHT,CM.
C ACGOIN=OZONE CONCENTRATION IN INFLUENT GAS AT OPERATING
C        PRESSURE,MG/L.
C Y=ARRAY CONTAINING CURRENT VALUE OF DEPENDENT VARIABLES,MG/L.
C CH3OH=METHANOL CONCENTRATION,MG/L AS CARBON.
C HCHO=FORMALDEHYDE CONCENTRATION,MG/L AS CARBON.
C HCOOH=FORMIC ACID CONCENTRATION,MG/L AS CARBON.
C CGOUT=OZONE CONCENTRATION IN EFFLUENT GAS,MG/L.
C O3=DISSOLVED OZONE CONCENTRATION,MG/L.
C Y(1)=CH3OH,Y(2)=HCHO,Y(3)=HCOOH,Y(4)=CGOUT,Y(5)=O3
      DIMENSIONYS(5),X(12),Y(5,12),F(5,12),ALWNC(5),ALLOW(5)
     $,SIZE(5)
      EXTERNALFCN
      COMMON KLA,KR,K21,K22,K23,XINV,DI,H,
```


REPRODUCED FROM BEST AVAILABLE COPY

```
     $CGOIN,GO,V,XL,ACGOIN
      REAL KLA,KR,K21,K22,K23
      READ (5,100) KLA,KR,K21,K22,K23,XINC,LM,YS,XINV,DI,
     $H,CGOIN,GO,V,XL
      WRITE (6,101)
      WRITE (6,200) KLA,KR,K21,K22,K23,XINC,LM
      WRITE (6,202)
      WRITE (6,300) YS,XINV,DI
      WRITE (6,303)
      WRITE (6,200) H,CGOIN,GO,V,XL
      ACGOIN=CGOIN*(XL/1033.27+1.)
      NEQ=5
      ND=5
      XIN=0
C INITIALIZE XOUT.
      XOUT=0.
C GIVE STEPSIZE ESTIMATE.
      HEST=.001
C SET POINTS WHERE DATA TO BE TABULATED.
      DO 2 IJK=1,5
    2 ALWNC(IJK=.1E-6
      IBLCK=-1
C NO SIZE ESTIMATES WERE GIVEN
      WRITE (6,404)
      DO 20 IJ=1,LM
      XOUT=XOUT+XINC
      CALL BLCKDQ (FCN,NEQ,ND,XIN,XOUT,YS,X,Y,
     $F,ALWNC,ALLOW,HEST,SIZE,IBICK)
      TOC=YS(1)+YS(2)+YS(3)
      WRITE (6,500) XOUT,YS,TOC
   20 CONTINUE
  100 FORMAT (6F7.4,I7/7F7.4/5F7.4)
  200 FORMAT (6F12.4I12)
  300 FORMAT (7F12.4)
  101 FORMAT (9X,3HKLA,10X,2HKR,9X,3HK21,9X,3HK22.
     $9X,3HK23,8X,4HXINC,10X,2HLM)
  202 FORMAT (/9X,3HYS1,9X,3HYS2,9X,3HYS3,
     $9X,3HYS4,9X,3HYS5,8X,4HXINV
     $,10X,2HDI)
  303 FORMAT (/11X,1HH,7X,5HCGOIN,
     $10X,2HGO,11X,1HV,10X,2HYL)
  404 FORMAT (/3X,4HYOUT,6X,3HYS1,7X,3HYS2,
     $7X,3HYS3,7X,3HYS4,7X,3HYS5,7X,3HTOC)
  505 FORMAT (F7.3/6X,6F10.2)
      STOP
      END
      SUBROUTINE FCN (X,Y,F)
      COMMON KLA,K4,K21,K22,K23,XINV,DI,H,
     $CGOIN,GO,V,XL,ACGOIN
      DIMENSION Y(5),F(5)
      REAL KLA,KR,K21,K22,K23
      F(1)=-K21*Y(1)*Y(5)
      F(2)=K21*Y(1)*Y(5)-K22*Y(2)*Y(5)
      F(3)=K22*Y(2)*Y(5)-K23*Y(3)*Y(5)
```

```
      F(4)=(CGOIN-Y(4))*GO*(1-H)/V/H
     $-KLA*(DI*Y(4)-Y(5))*(1-H)/H
      F(5)=-(4.*(K21*Y(1)+K22*Y(2)
     $+K23*Y(3))+KR)*Y(5)
     $+KLA*(DI*Y(4)-Y(5))
      RETURN
      END
```

APPENDIX E

COMPUTER PROGRAM FOR SOLVING MATHEMATICAL MODELS FOR OZONE-SPARGED VESSEL TREATING AN AQUEOUS METHANOL SOLUTION

```
      PROGRAM SPARGE (INPUT,OUTPUT,TAPE5=INPUT,TAPE6=OUTPUT)
C THIS PROGRAM COMPUTES THE STEADY-STATE CONCENTRATIONS OF
C METHANOL, FORMALDEHYDE, FORMIC ACID, GAS-PHASE AND LIQUID-PHASE
C OZONE IN THE EFFLUENT STREAMS FROM AN OZONE-SPARGED VESSEL
C TREATING A METHANOL FEED SOLUTION.  IT ALSO COMPUTES PERCENT
C TOC REMOVAL,PERCENT OZONE ABSORPTION, AND SECOND-ORDER RATE
C CONSTANT AND STOICHIOMETRIC COEFFICIENT FOR OZONE FOR THE
C TOC REDUCTION REACTION.
C THE SUBROUTINE QNWT IN THE MATH SCIENCE LIBRARY IS USED
C IN THIS PROGRAM.
C THE USER MUST SUPPLY VALUES OF KLA,KR,K21,K22,K23,X,XINV,DI,
C CH3OHO,CGOIN,GO,V,AND XL.
C SOME OF THE INPUT AND OUTPUT PARAMETERS ARE DEFINED IN THE
C WRITE-UP OF QNWT ON PAGES 8-119 TO 8-126 OF THE MATH
C SCIENCE LIBRARY.
C DEFINITION OF TERMS AND THEIR UNITS:
C KLA=OVERALL MASS TRANSFER COEFFICIENT,MIN**-1.
C KR=FIRST-ORDER RATE CONSTANT FOR OZONE DECOMPOSITION REACTION,
C    MIN**-1.
C K21=SECOND-ORDER RATE CONSTANT FOR REACTION BETWEEN OZONE AND
C     METHANOL,L/MG/MIN.
C K22=SECOND-ORDER RATE CONSTANT FOR REACTION BETWEEN OZONE AND
C     FORMALDEHYDE, L/MG/MIN.
C K23=SECOND-ORDER RATE CONSTANT FOR REACTION BETWEEN OZONE AND
C     FORMIC ACID,L/MG/MIN.
C X=AT ENTRY:INITIAL ESTIMATE VECTOR; AT RETURN:SOLUTION VECTOR
C   ESTIMATED FROM LAST ITERATION,MG/L.
C XINV=INVERT OF LIQUID RESIDENCE TIME,MIN**-1.
C DI=DISTRIBUTION COEFFICIENT,DIMENSIONLESS.
C CH3OHO=METHANOL CONCENTRATION IN FEED SOLUTION,MG/L AS CARBON.
C CGOIN=OZONE CONCENTRATION IN INFLUENT GAS AT 1 ATM.,MG/L.
C GO=GAS FLOW RATE AT 1 ATM.,L/MIN.
C V=LIQUID VOLUME,L.
C XL=LIQUID HEIGHT,CM.
C ACGOIN=OZONE CONCENTRATION IN INFLUENT GAS AT OPERATING
C        PRESSURE,MG/L.
C CH3OH=METHANOL CONCENTRATION IN EFFLUENT,MG/L AS CARBON.
C HCHO=FORMALDEHYDE CONCENTRATION IN EFFLUENT,MG/L AS CARBON.
C HCOOH=FORMIC ACID CONCENTRATION IN EFFLUENT,MG/L AS CARBON.
C CGOUT=OZONE CONCENTRATION IN EFFLUENT GAS,MG/L.
C O3=DISSOLVED OZONE CONCENTRATION IN EFFLUENT,MG/L.
C TOC=TOC CONCENTRATION IN EFFLUENT,MG/L.
C REM=PERCENT TOC REMOVAL, DIMENSIONLESS.
C PRE=PERCENT TOC REMAINING, DIMENSIONLESS.
C XK2=SECOND ORDER RATE CONSTANT FOR TOC REDUCTION REACTION,
C     L/MG/MIN.
C SO=STOICHIOMETRIC COEFFICIENT FOR OZONE FOR TOC REDUCTION
C    REACTION, DIMENSIONLESS.
```

```
C ABSORP=PERCENT GASEOUS OZONE ABSORPTION.
C X(1)=CH3OH, X(2)=HCHO,X(3)=HCOOH,X(4)=CGOUT,X(5)=03
      DIMENSION X(5),R(5),AJ(5,5),B(5,7),IP(6)
      EXTERNAL FUN
      REAL KLA,KR,K21,K22,K23
      COMMON KLA,KR,K21,K22,K23,XINV,DI,CH3OHO,
     $CGOIN,GO,V,XL,ACGOIN
      READ (5,100) KLA,KR,K21,K22,K23,X,XINV,DI,CH3OHO,
     $CGOIN,GO,V,XL
C INITIAL ESTIMATE VECTOR WAS FURNISHED.
      WRITE (6,101)
      WRITE (6,200) KLA,KR,K21,K22,K23
      WRITE (6,303)
      WRITE (6,200) CH3OHO,CGOIN,GO,V,XL
      ACGOIN=CGOIN*(XL/1033.27+1.)
      P=0.
C NO PRINT-OUT WAS USED AS THE PRINT OPTION.
      IP-(1)=-55
C THE TERMINATION CRITERION FOR NONCONVERGENT ITERATIONS
C WAS USED.
      CALL QNWT(X,5,5,FUN,P,.1E-8,IP,0,R,RMS,AJ,B)
C THE TOLERANCE LEVEL FOR RESIDUAL NORM WAS SET AT .1E-8.
C NO JACOBIAN MATRIX WAS GIVEN.
      TOC=X(1)+X(2)+X(3)
      REM=(CH3OHO-TOC)/CH3OHO
      PRE=1.-REM
      XK2=K23*X(3)/TOC
      SC=(K21*X(1)+K22*X(2)+K23*X(3))/TOC/XK2
      ABSORP=(CGOIN-X(4))/CGOIN
      WRITE (6,404)
      WRITE (6,300)P,X,TOC,REM,PRE,ABSORP,XK2,SC
  100 FORMAT (5F7.4/7F7.4/5F7.4)
  200 FORMAT (7F12.4)
  101 FORMAT (/9X,3HKLA,10X,2HKR,9X,3HK21,9X,3HK22,9X,3HK23)
  202 FORMAT (/10X,2HX1,10X,2HX2,10X,2HX3,10X,2HX4,
     $10X,2HX5,8X,4HXINV,10X,2HDI)
  303 FORMAT (//6X,6HCH3OHO,7X,5HCGOIN,10X,2HGO,11X,1HV,10X,2HXL)
  300 FORMAT (/F3.0//5X,6F10.2,3F10.3,E15.4,F9.2)
  404 FORMAT (//2X,1HP,7X,5HCH3OH,6X,4HHCHO,5X,5HHCOOH,5X,
     $5HCGOUT,8X,2H03,7X,3HTOC,7X,3HREM,7X,3HPRE,7X,3HABS,12X,
     $3HXK2,7X,2HSC)
      STOP
      END
      SUBROUTINE FUN (X,N,K,R,P)
      REAL KLA,KR,K21,K22,K23
      COMMON KLA,KR,K21,K22,K23,XINV,DI,CH3OHO,
     $CGOIN,GO,V,XL,ACGOIN
      DIMENSION X(5),R(5)
      R(1)=-K21*X(1)*X(5)+XINV*(CH3OHO-X(1))
      R(2)=K21*X(1)*X(5)-K22*X(2)*X(5)-XINV*X(2)
      R(3)=K22*X(2)*X(5)-K23*X(3)*X(5)-XINV*X(3)
      R(4)=GO*(CGOIN-X(4))/V-
     $KLA*DI*(ACGOIN-X(4))
     $/ALOG((DI*ACGOIN-X(5))/DI*X(4)-X(5)))
```

```
 R(5)=KLA*DI*(ACGOIN-X(4))
$/ALOG((DI*ACGOIN-X(5))/(DI*X(4)-X(5)))
$-(4.*(K21*X(1)+K22*X(2)+K23*X(3))+KR+XINV)*X(5)
 RETURN
 END
```

APPENDIX F

COMPUTER PROGRAM FOR COMPUTATIONS OF CONCENTRATIONS AND CONCENTRATION GRADIENTS OF OZONE AND TOC IN THE LIQUID FILM

Equations (71) and (72) are rewritten in terms of dimensionless variables including ozone concentration, $B = (O_3)_f/(O_3)$, TOC concentration, $C = (TOC)_f/(TOC)$, and distance, $\bar{x} = x/\delta$. By defining the dimensionless groups, $PM1 = k_r\delta^2/D_{O_3}$, $PM2 = SC \times k_2(TOC)\delta^2/D_{O_3}$, $PN2 = k_2(O_3)\delta^2/D_{TOC}$, the restated equations are:

$$\frac{d^2B}{d\bar{x}^2} = PM1 \times B + PM2 \times B \times C \qquad (74)$$

$$\frac{d^2C}{d\bar{x}^2} = PN2 \times B \times C \qquad (75)$$

The following program is used to compute the dimensionless concentrations and concentration gradients from equations (74) and (75).

```
            PROGRAM FILM (INPUT,OUTPUT,TAPE5=INPUT,TAPE6=OUTPUT)
C THIS PROGRAM COMPUTES THE CONCENTRATION PROFILES
C AND THE CONCENTRATION GRADIENTS OF DISSOLVED OZONE AND TOC
C WITHIN THE LIQUID FILM.
C THE SUBROUTINE BVP IN THE MATH SCIENCE LIBRARY IS USED
C IN THIS PROGRAM.
C THE USER MUST SUPPLY VALUES OF O3,TOC,CGOIN,XL,DELTA,K4,K2,
C AND SC.
C SOME OF THE INPUT AND OUTPUT PARAMETERS ARE DEFINED IN
C THE WRITE-UP OF BVP ON PAGES 4-65 TO 4-74 OF THE
C MATH SCIENCE LIBRARY.
C CGS SYSTEM IS USED THROUGHOUT; ALL CONCENTRATIONS ARE IN
C GRAM MOLE/CC.
C DEFINITION OF TERMS:
C TOC=TOC CONCENTRATION IN BULK SOLUTION.
C O3=DISSOLVED OZONE IN BULK SOLUTION.
C CGOIN-GASEOUS OZONE IN INFLUENT GAS.
C XL=LIQUID HEIGHT.
C DELTA=FILM THICKNESS.
C KR=FIRST-ORDER RATE CONSTANT FOR OZONE DECOMPOSITION REACTION.
C K2=SECOND ORDER RATE CONSTANT FOR TOC REDUCTION REACTION.
C SC=STOICHIOMETRIC COEFFICIENT FOR OZONE FOR TOC REDUCTION
C    REACTION.
C DO3=DIFFERSIVITY OF OZONEI IN WATER.
C DTOC=DIFFUSIVITY OF TCC IN WATER.
C DI=DISTRIBUTION COEFFICIENT.
C INCRE=INCREMENT.
      EXTERNAL FCN,BCOND
      COMMON/EQPRMT/PM1,PM2,PN2
      COMMON/BCPRMT/C1,C2,C3,C4
      DIMENSION XB(2),XMESH(12),S(270),YOUT(4,11)
      REAL INCRE,K4,K2
C GIVEN VALUES FOR THE PARAMETERS APPEARED IN THE
C DIFFERENTIAL EQUATIONS.
      O3=6.4583E-9
      TOC=1.9853-6
      CGOIN=2.729E-7
      XL=4.064E1
      DELTA=6.3165E-4
      KR=1.006E-2
      K2=3.3617E4
      SC=4.36
      DO3=1.960E-5
      DTOC=1.600E-5
      DI=.24
C GIVE BOUNDARY CONDITIONS.
      C1=DI*CGOIN*(XL/1033.27+1.)/O3
      C2=1.
      C3=0.
      C4=1.
C CALCULATE THE THREE DIMENSIONLESS GROUPS.
      PM1=KR*DELTA*DELTA/DO3
      PM2=SC*K2*TOC*DELTA*DELTA/DO3
      PN2=K2*O3*DELTA*DELTA/DTOC
```

```
      NP=2
      XB(1)=0.
      XB(2)=1.
      NEQ=4
      ND=4
      NX=11
C SET THE ABSCISSAE AT WHICH TO TABULATE THE SOLUTION.
      INCRE=-.1
      DO 5 IJ=1,11
      INCRE=INCRE+.1
      XMESH(IJ)=INCRE
    5 CONTINUE
C SET TOLERANCE, MAXIMUM ITERATIONS, AND MAXIMUM NUMBER OF
C ATTEMPTS WITHOUT IMPROVEMENT.
      TOL=.1E-8
      MXITER=9
      MXFAIL=6
      IPR=0
C GIVE GUESSES FOR THE MAGNITUDE OF THE SOLUTION, GUESSES FOR
C THE SOLUTION AT X=XB(1) AND ESTIMATES FOR HOW GOOD THESE
C GUESSES ARE.
      S(1)=2.
      S(2)=-1.
      S(3)=1.
      S(4)=.1E-2
      S(5)=2.
      S(6)=-1.
      S(7)=1.
      S(8)=0.
      S(9)=.1
      S(10)=.1
      S(11)=.1
      S(12)=.1E-4
      CALL BVP(FCN,BCOND,NP,XB,NEQ,ND,NX,XMESH,TOL,
     $MXITER,MXFAIL,S,IPR,ATOL,YOUT,IRR)
      WRITE (6,101) IRR,ATOL
      WRITE (6,202) ((YOUT(I,J),J=1,11),I=1.4)
  101 FORMAT (//I2,9X,E10.4)
  202 FORMAT (///11E12.4)
      STOP
      END
      SUBROUTINE FCN (X,Y,F)
      COMMON/EQPRMT/PM1,PM2,PN2
      DIMENSION Y(4),F(4)
      F(1)=Y(2)
      F(2)=PM1*Y(1)+PM2*Y(1)+Y(3)
      F(3)=Y(4)
      F(4)=PN2*Y(1)*Y(3)
      RETURN
      END
      SUBROUTINE BCOND (YTRIAL,FOUT,ND)
      COMMON/BCPRMT/C1,C2,C3,C4
      DIMENSION YTRIAL (ND,2),FOUT(4)
      FOUT(1)=C1-YTRIAL(1,1)
```

```
FOUT(2)=C2-YTRIAL(1,2)
FOUT(3)=C3-YTRIAL(4,1)
FOUT(4)=C4-YTRIAL(3,2)
RETURN
END
```

DISTRIBUTION LIST

No. of Copies	
25	Commander US Army Medical Bioengineering Research and Development Laboratory ATTN: SGRD-UBG Fort Detrick, Frederick, MD 21701
4	US Army Medical Research and Development Command ATTN: SGRD-RMS Fort Detrick, Frederick, MD 21701
12	Defense Technical Information Center (DTIC) ATTN: DTIC-DDA Cameron Station Alexandria, VA 22314
1	Dean School of Medicine Uniformed Services University of the Health Sciences 4301 Jones Bridge Road Bethesda, MD 20014
1	Commandant Academy of Health Sciences, US Army ATTN: AHS-COM Fort Sam Houston, TX 78234
1	Commander US Army Medical Bioengineering Research and Development Laboratory ATTN: SGRD-UBD-A/Librarian Fort Detrick Frederick, MD 21701